

Sheffield Hallam University

Post-translational processing of proteins implicated in the pathogenesis of Alzheimer's disease.

CAMPBELL, Emma.

Available from the Sheffield Hallam University Research Archive (SHURA) at:

<http://shura.shu.ac.uk/19422/>

A Sheffield Hallam University thesis

This thesis is protected by copyright which belongs to the author.

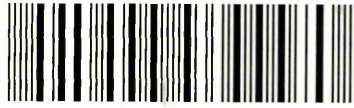
The content must not be changed in any way or sold commercially in any format or medium without the formal permission of the author.

When referring to this work, full bibliographic details including the author, title, awarding institution and date of the thesis must be given.

Please visit <http://shura.shu.ac.uk/19422/> and <http://shura.shu.ac.uk/information.html> for further details about copyright and re-use permissions.

LEARNING CENTRE
CITY CAMPUS, HOWARD STREET
SHEFFIELD S1 1WB

101 688 298 X



19772

Fines are charged at 50p per hour

16 AUG 2002

4.03pm

20 AUG 2002 4.18

18 SEP 2002

4.19

06 APR 2004 4.22

27 MAR 2007 5.00pm

28 JUL 2007

9/6/08 5pm

REFERENCE

ProQuest Number: 10694303

All rights reserved

INFORMATION TO ALL USERS

The quality of this reproduction is dependent upon the quality of the copy submitted.

In the unlikely event that the author did not send a complete manuscript and there are missing pages, these will be noted. Also, if material had to be removed, a note will indicate the deletion.



ProQuest 10694303

Published by ProQuest LLC (2017). Copyright of the Dissertation is held by the Author.

All rights reserved.

This work is protected against unauthorized copying under Title 17, United States Code
Microform Edition © ProQuest LLC.

ProQuest LLC.
789 East Eisenhower Parkway
P.O. Box 1346
Ann Arbor, MI 48106 – 1346

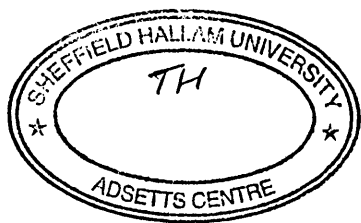
**Post-translational processing of proteins
implicated in the pathogenesis of
Alzheimer's disease**

Emma Campbell

A thesis submitted in partial fulfilment of the requirements of
Sheffield Hallam University
for the degree of Doctor of Philosophy

September 2001

Collaborating Organisation: University of Sheffield



ABSTRACT

The β -amyloid peptide characteristic of the lesions of Alzheimer's disease (AD) is derived from the amyloid precursor protein (APP), a single transmembrane-spanning protein with several alternatively-spliced variants, some of which contain a Kunitz protease inhibitory (KPI) domain. Although intracellular localisation of APP has been described in many cell types, it has not been characterised in NTera 2 (NT2) neurones, which are the best available model of human CNS neurones. Here, the subcellular distributions of APP and APLP2 (amyloid precursor-like protein 2) were demonstrated, by indirect immunocytochemistry, to be overlapping but not the same in both NT2 stem cells and neurones. No obvious differences were apparent when comparing the locations of either APP or APLP2 in stem cells versus neurones, APLP2 being restricted to the region of the Golgi apparatus, and APP extending into compartments approaching the cell membrane, including growth cones of neurones. Therefore, no clear differences in intracellular routing of these proteins were identified, immunocytochemically, in human CNS-type neurones compared with stem cells, which represent non-neuronal cells. This work emphasised the need to use antibodies that distinguish between APP and APLP2 (which does not contain the β -amyloid sequence) in studies of APP processing and amyloidogenesis, since only APP was concentrated in compartments beyond the Golgi apparatus. Heat-shock and no feeding had no immunocytochemically detectable effects on APP or APLP2 distributions or β -amyloid production in NT2 cells. Although a preliminary investigation to establish a protocol by which NT2 cells can be studied by electron microscopy produced only scant cellular material, more recent publications have shown that slight variations on methods tested here give a successful protocol.

The expression of KPI-containing APP in human brains has only been described previously in terms of its mRNA. The ratio of KPI-/non-KPI-APP mRNA appears to be elevated in AD (Tanaka *et al.*, 1989; Johnston *et al.*, 1996). A novel polyclonal antibody (Ab993), specific for the KPI-domain epitope, was characterised for use in immunohistochemistry using paraffin-embedded human brain sections. Immunohistochemical staining was enhanced significantly by reduction of sulphhydryl bonds with 2-mercaptoethanol, followed by alkylation of the reduced bonds with sodium iodoacetate. Microwaving of sections also enhanced immunolabelling, by a mechanism that was additive to reduction and alkylation. Incubation with 80% formic acid did not increase immunolabelling. KPI-containing protein distribution in normal and AD human brains was characterised by indirect immunohistochemistry. KPI-APP was concentrated mainly in pyramidal cells of the temporal and visual neocortex. In Alzheimer's disease there was a significantly increased incidence of cellular staining for KPI-APP. KPI-containing protein was closely related to the pathology of AD. It was found in association with the tangle-bearing population of neurones, blood vessels including those affected by cerebro-vascular amyloid, within the neuropil and in association with plaques. This evidence corroborates that supplied previously by mRNA data and studies of hAPP transgenic mice in highlighting the importance of this isoform of APP in the pathogenesis of AD.

The cytokine transforming growth factor- β 1 (TGF- β 1) is upregulated in AD brains, but its mRNA expression has not been characterised. TGF- β 1 and hAPP(V717F) bigenic

mice show accelerated development of AD-like pathology compared with hAPP(V717F) singly transgenic mice (Wyss-Coray *et al.*, 1997). It has been suggested that elevated TGF- β 1 could increase expression of KPI-containing APP isoforms in AD and/or upregulate CNS extracellular matrix proteins that may promote amyloid deposition. TGF- β 1 mRNA in AD and control frozen human brain sections was quantified by *in situ* hybridization histochemistry. A modest, significant increase in TGF- β 1 mRNA was found in AD temporal cortex and white matter compared to controls, supporting previous immunohistochemical studies.

CANDIDATE'S STATEMENT

The objectives of this research were to further present understanding of the sub-cellular processing of proteins that have been demonstrated to be involved in the pathogenesis of Alzheimer's disease. This work aimed to concentrate on the processing of these proteins in human brains as well as in cultured human cells that can be differentiated into a phenotype bearing close resemblance to human CNS-type neurones, thus providing evidence that is as relevant as currently possible to the *in vivo* processes of Alzheimer's disease.

Results of work included in this thesis, carried out by Dr. D. Parkinson at Sheffield Hallam University, are indicated in the text below. Dr. Parkinson was responsible for making the anti-KPI antibody used in this study and described below, and for the characterisation of this antibody by immunoprecipitation and Western blotting (Campbell *et al.*, 1999).

CONTENTS

ABSTRACT	2
CANDIDATE'S STATEMENT	4
CONTENTS	5
FIGURES	7
CHAPTER 1: INTRODUCTION	9
<i>Neuropathology of Alzheimer's disease</i>	<i>10</i>
<i>Processing of amyloid precursor protein and other proteins with potential roles in Alzheimer's disease</i>	<i>14</i>
<i>Functions of the amyloid precursor protein</i>	<i>27</i>
<i>The genetics of Alzheimer's disease</i>	<i>29</i>
<i>Sporadic Alzheimer's disease</i>	<i>32</i>
<i>The role of cellular stress in Alzheimer's disease</i>	<i>35</i>
<i>Investigation of APP processing in a model human CNS neuronal system</i>	<i>37</i>
<i>Summary</i>	<i>38</i>
CHAPTER 2: METHODS	40
<i>Cell culture</i>	<i>40</i>
<i>Immunocytochemistry</i>	<i>45</i>
<i>Localization of intracellular compartments using other markers</i>	<i>48</i>
<i>Purification and concentration of antibodies using protein G-agarose</i>	<i>49</i>
<i>ELISA</i>	<i>51</i>
<i>Electron Microscopy</i>	<i>52</i>
<i>In situ hybridization</i>	<i>60</i>
<i>Immunohistochemistry</i>	<i>69</i>
CHAPTER 3: LOCALISATION OF APP AND APLP2 IN NTERA 2 STEM CELLS AND NEURONES	76
INTRODUCTION	76
<i>NTera 2 cells as a model system for investigating APP processing</i>	<i>76</i>
<i>Identification of intracellular compartments in NT2 cells</i>	<i>77</i>
<i>Immunolocalisation of APP, APLP2 and β-amyloid in NT2 cells</i>	<i>77</i>
RESULTS	78
<i>Optimisation of cell culture</i>	<i>78</i>
<i>Optimisation of immunocytochemical labelling</i>	<i>79</i>
<i>Purification and concentration of antibodies and ELISA</i>	<i>80</i>
<i>Immunolocalisation of APP and APLP2 in NTERA 2 stem cells</i>	<i>83</i>
<i>Immunolocalisation of APP, APLP2 and β-amyloid in NTERA 2 neurones</i>	<i>87</i>
DISCUSSION	126
<i>Subcellular localisation of APP and APLP2</i>	<i>126</i>
<i>Discrimination between APP and APLP2</i>	<i>128</i>
<i>Routes of amyloidogenic and non-amyloidogenic processing of APP</i>	<i>129</i>
<i>The effects of stress on APP processing</i>	<i>132</i>
CHAPTER 4: DEVELOPMENT OF A PROTOCOL FOR ELECTRON MICROSCOPICAL EXAMINATION OF NTERA 2 CELLS	136
INTRODUCTION	136
METHODS	136
RESULTS	137
<i>Stem cells collected by centrifugation</i>	<i>137</i>
<i>Neurones collected by centrifugation</i>	<i>137</i>
<i>Neurones collected by scraping</i>	<i>138</i>
<i>Neurones processed in situ</i>	<i>138</i>
<i>Comparison of methods</i>	<i>139</i>
DISCUSSION	144
CHAPTER 5: KPI-CONTAINING APP IN THE HUMAN BRAIN	147

UNCOVERING OF A KPI DOMAIN EPIOTOPE OF ALZHEIMER'S AMYLOID PRECURSOR PROTEIN FOR IMMUNOHISTOCHEMISTRY IN HUMAN BRAIN.....	147
INTRODUCTION	147
METHODS.....	148
<i>Antibody production</i>	148
<i>Immunohistochemical staining of human brain sections</i>	148
RESULTS.....	150
<i>Western blots</i>	150
<i>Immunohistochemistry</i>	151
DISCUSSION	156
CHAPTER 6: KPI-CONTAINING AMYLOID PRECURSOR PROTEIN IN THE BRAIN IN NORMAL HUMANS AND IN ALZHEIMER'S DISEASE	159
INTRODUCTION	159
METHODS.....	162
<i>Immunolabelling of KPI-APP in AD and normal brains</i>	162
<i>Image analysis of KPI immunostaining</i>	163
<i>Immunolabelling of serial sections to localise KPI-APP in AD temporal cortex</i>	164
<i>Measurement of amyloid load of temporal cortex of AD brains</i>	164
RESULTS.....	168
<i>Results of image analysis of KPI immunohistochemistry</i>	168
<i>Distribution of KPI-containing APP in human brain by immunohistochemistry</i>	172
<i>Amyloid load of brains</i>	173
DISCUSSION	198
CHAPTER 7: TRANSFORMING GROWTH FACTOR-β1 <i>IN SITU</i> IN THE HUMAN BRAIN ...	203
INTRODUCTION	203
<i>In situ hybridization histochemistry</i>	205
<i>Results of in situ hybridization histochemistry</i>	206
DISCUSSION	212
CHAPTER 8: DISCUSSION.....	218
APPENDIX	229
<i>Tris-phosphate-buffered saline (TBS), 0.1M, pH7.4 – 7.8</i>	229
<i>Phosphate-buffered saline (PBS), 0.1M, pH7.4</i>	229
<i>Alkaline Phosphatase (AP) buffer, pH9.5</i>	229
<i>Anti-fade</i>	230
<i>20x Standard saline citrate (SSC)</i>	230
<i>Hybridization buffer</i>	230
ACKNOWLEDGEMENTS.....	233
REFERENCES.....	234

Figures

Figure 1	19
Figure 2	20
Figure 3	81
Figure 4	82
Figure 5	92
Figure 6	92
Figure 7	94
Figure 8	94
Figure 9	96
Figure 10	98
Figure 11	98
Figure 12	100
Figure 13	100
Figure 14	102
Figure 15	104
Figure 16	106
Figure 17	106
Figure 18	108
Figure 19	108
Figure 20	110
Figure 21	112
Figure 22	112
Figure 23	114
Figure 24	114
Figure 25	116
Figure 26	116
Figure 27	118
Figure 28	118
Figure 29	120
Figure 30	120
Figure 31	120
Figure 32	120
Figure 33	120
Figure 34	122
Figure 35	122
Figure 36	124
Figure 37	124
Figure 38	140
Figure 39	140
Figure 40	142
Figure 41	142
Figure 42	153
Figure 43	154
Figure 44	155
Figure 45	170

Figure 46	170
Figure 47	171
Figure 48	174
Figure 49	174
Figure 50	176
Figure 51	176
Figure 52	178
Figure 53	178
Figure 54	180
Figure 55	180
Figure 56	182
Figure 57	184
Figure 58	184
Figure 59	186
Figure 60	186
Figure 61	188
Figure 62	188
Figure 63	190
Figure 64	190
Figure 65	192
Figure 66	192
Figure 67	194
Figure 68	194
Figure 69	196

CHAPTER 1: INTRODUCTION

After heart disease, cancer and stroke, Alzheimer's disease (AD) is the fourth most prevalent cause of death in the developed world. It is the commonest cause of dementia, affecting an estimated 17–20 million people worldwide (Shastry and Giblin, 1999), including between 2 and 10 per cent of Europeans and North Americans over 65 years of age (Alloul *et al.*, 1998) and costing the US, for example, \$60 billion annually (Martin, 1999). AD is a progressive, age-related dementia that leads to premature death from associated complications such as pneumonia, the clinical course ranging typically from 5 to 7 years from onset until death (Perry, 1991). Better health care and healthier lifestyles mean that those at risk for AD will increasingly survive other diseases and live longer. Therefore both the social and financial burdens of this distressing illness are rising, and it is becoming an ever more pressing issue to uncover the causes of AD and to identify potential therapeutic mechanisms.

Age is the least disputed risk factor for AD. Also likely factors are family history of AD, presence of the apolipoprotein E ϵ 4 allele, history of depression, Down's syndrome, race and head trauma with loss of consciousness. Other suspected risk factors include lower education, aluminium absorption, gender, hypertension and vascular disease. Among factors generally identified to be protective against AD are cigarette smoking, non-steroidal anti-inflammatory drugs, oestrogen intake, arthritis and apolipoprotein E ϵ 2 allele (Alloul *et al.*, 1998). However, it is likely that there is a multitude of factors that contribute towards whether or not any individual develops this devastating disease.

At present AD cannot be diagnosed with certainty until post-mortem. The clinical diagnostic criteria include progressive dementia with characteristic signs and symptoms, notably failure of memory, disorientation and confusion (Corsellis, 1976), and exclusion of other diseases that cause dementia. However, the clinical diagnosis must be confirmed post-mortem by the presence of neuropathological lesions characteristic of AD: senile or neuritic plaques, congophilic angiopathy and neurofibrillary tangles in the cerebral tissue (Sanan *et al.*, 1994). Therefore studies of the cellular mechanisms underlying AD may identify a means of testing for the presence of the disease pre-mortem as well as finding potential targets for drug therapy.

Neuropathology of Alzheimer's disease

AD brains show marked atrophy of the cerebral cortex, particularly of the frontal and temporal lobes, with associated neurone loss (principally cholinergic) and astrocyte proliferation in affected areas (Perry, 1991). Senile plaques are the most prominent feature of the neuropathology of AD: they are found throughout the grey matter of the cerebral cortex, particularly in the hippocampus and entorhinal cortex, and in deep cerebral nuclei including the amygdala and corpus striatum (Selkoe, 1994b). Two distinct types of plaque have been described, the "diffuse" plaque and the "classical", "neuritic" or "mature" plaque. Both of these contain a 4kD peptide, beta-amyloid, a fragment of the amyloid precursor protein (APP). This varies in length from 39-42 amino acids, the 42 amino acid length peptide being the species that is deposited initially in plaques (Iwatsubo *et al.*, 1994). β -amyloid (29-42) exists exclusively in a β sheet conformation in solution, suggesting that this peptide may act as a "seed" for deposition of β -amyloid (1-42), followed by deposition of peptides terminating at amino acids 39-40 (Barrow and Zagorski, 1991). β -amyloid (40) may even inhibit

aggregation of β -amyloid (42) (Mucke *et al.*, 2000). The classical or neuritic plaque also contains dystrophic neurites that often surround the β -amyloid deposits, activated microglia, reactive fibrous astrocytes, and several other proteins such as heat-shock proteins, amyloid P component, α -1 antichymotrypsin, apolipoprotein E, α ₂-macroglobulin, presenilins 1 and 2, and heparan sulphate proteoglycans (Rosenberg, 2000). It has been demonstrated recently that senile plaques also contain mRNAs, predominantly neuronal ones, lending support to the notion that senile plaques form at sites where neurones degenerate (Ginsberg *et al.*, 1999).

Recently, the ultrastructure of β -amyloid fibrils has been examined *in situ* in human brain tissue (Inoue *et al.*, 1999). The 10nm-diameter fibrils were found to have a core composed of amyloid P component subunits and chondroitin sulphate proteoglycan (CSPG), surrounded by a layer of heparan sulphate proteoglycan (HSPG). β -amyloid filaments, 1nm wide, were associated with the surface of these fibrils. This is likely to be a more accurate reflection of the structure of fibrillar β -amyloid than had been described previously because the fibrils were examined *in situ*. Examination *in situ* avoided alteration of their structure by the process of extraction from the tissue, which may cause dissociation of β -amyloid and HSPG. HSPGs have been demonstrated to be an invariable component of all systemic amyloids in humans as well as being present in amyloid plaques, neurofibrillary tangles (NFTs) and cerebrovascular amyloid in AD brains (Young *et al.*, 1989; Verbeek *et al.*, 1999). This supports the notion of their being an integral part of β -amyloid fibrils, and emphasises their contribution to AD pathology. Heparan sulphate is found in cholinergic synaptosomes, suggesting that degeneration of axons of cholinergic neurones may result in deposition of HSPGs in

senile plaques (Young *et al.*, 1989). Furthermore, APP has been suggested to be an HSPG core protein (Schubert *et al.*, 1988).

The dystrophic neurites of mature plaques contain NFTs, which are paired helical filaments (PHF) in a double helix, consisting mainly of abnormally phosphorylated tau protein (Johnston *et al.*, 1994), and some studies have suggested that they contain β -amyloid among other components (Masters *et al.*, 1985; Perry *et al.*, 1992; Rosenblum, 1999). Subsequent death of these neurones may then leave “ghost” tangles in the neuropil due to the relatively high resistance of NFT to degradation. Although it is notable that, in some instances of dementia, neuritic plaques may be found in the absence of tangles (Duff and Hardy, 1995). Neuropil threads may also be seen forming a dense meshwork in the neuropil. These are recognised by antibodies to phosphorylated tau or PHF, and probably represent abnormal axons and dendrites of neurones that contain or will develop NFT (Esiri *et al.*, 1997).

Finally, β -amyloid is also deposited in other forms in AD such as long, ribbon-like amorphous deposits in the superficial subpial cortex, or fibrillar deposits in the walls of meningeal and intracerebral microvessels known as congophilic angiopathy or cerebral amyloid angiopathy (CAA) (Selkoe, 1994b). In capillaries of cerebral cortex, β -amyloid fibrils have been observed in association with the basement membrane (Miyakawa *et al.*, 1974; Inoue *et al.*, 1999). In Madin–Darby canine kidney (MDCK) cells, β -amyloid was secreted preferentially at the basolateral cell membrane, postulating a potential mechanism by which β -amyloid accumulates at the abluminal basement membrane of AD brain microvessels (Haass *et al.*, 1994). Examination of serial sections through senile plaques by electron microscopy indicated that amyloid fibrils were produced at the basement membranes of capillary endothelial cells, and projected into the

surrounding parenchyma, at least one degenerable capillary being found in each senile plaque (Miyakawa *et al.*, 1982).

β -amyloid is deposited in diffuse plaques and cerebral blood vessels only occasionally in normal ageing but is often present in mild dementia (Price, 1993), in the absence of neuritic plaques and NFT. β -amyloid deposits in non-demented aged individuals have been shown to lack accompanying cellular abnormalities, including NFT, astroglial and microglial reaction or proliferation (Coria *et al.*, 1993). It may be that this represents an early stage of AD, before neuronal death becomes widespread and cognitive deficit becomes more apparent. Furthermore, neuritic plaques are present only in AD, whereas NFT are present in normal ageing as well as being the result of neuronal injury in a variety of other neurodegenerative illnesses, such as Pick's disease, Lewy body dementia and Parkinson's disease (Schmechel *et al.*, 1993). The numbers of neuritic plaques or NFTs may correlate better than the number of amyloid plaques with degree of dementia, but neither plaque numbers nor NFT numbers correlate well with degree of dementia (Esiri *et al.*, 1997). In contrast, amyloid load and levels of extracted β -amyloid have been shown to correlate well with degree of dementia (Cummings and Cotman, 1995; Näslund *et al.*, 2000). It is therefore postulated that β -amyloid is the species initially responsible for causing neuronal damage, and that NFT and neuritic plaques develop subsequently. Further evidence in support of this will be discussed below. Increasing degree of cognitive impairment is associated also with diminishing levels of acetyl choline and synaptophysin, thought to reflect loss of cholinergic neurones and/or their synapses (Esiri *et al.*, 1997).

Before extracellular β -amyloid deposition occurs, there is gathering evidence of intracellular β -amyloid accumulation. This appears to be followed by appearance of a

“halo” of β -amyloid around dying and ghost neurones, several of which may result in the genesis of an amyloid plaque and its associated pathology (LaFerla *et al.*, 1997; Wilson *et al.*, 1999). Even prior to intracellular β -amyloid deposition, some studies have identified synaptic pathology that appears to either precipitate or result from accumulation of intracellular APP, finally resulting in cell death and extracellular β -amyloid deposition (Martin *et al.*, 1994; Masliah *et al.*, 1994; Games *et al.*, 1995). Alternatively, it has been postulated that elevated soluble intra- or extracellular β -amyloid produces the neurotoxic effects that result in synaptic pathology (Turner *et al.*, 1996; Lee *et al.*, 1998; Wilson *et al.*, 1999; Mucke *et al.*, 2000).

Processing of amyloid precursor protein and other proteins with potential roles in Alzheimer’s disease

Expression and roles of APP isoforms

APP is expressed by most cells of the human body. Differential splicing of the primary RNA transcript of APP generates eight protein products of differing length, APP-695 being the most abundant in brain, followed by APP-751 then APP-770, both of which contain a domain with considerable homology to the Kunitz protease inhibitors (KPI).

Evidence suggests that APP-751 mRNA has a higher abundance in neurones in regions of the human brain associated with neuritic plaque formation, in normal adults as well as in AD (Neve *et al.*, 1988; Johnson *et al.*, 1990), implying early involvement of this phenomenon in the pathogenesis of AD. In human AD brain there are elevated levels of cytokines, markers of the inflammatory response, and astrocytosis occurs. In primary cultures from foetal human cerebral cortex, astrocytes were shown to be the major

producers of β -amyloid (Busciglio *et al.*, 1993). Astrocytes produce a higher proportion of KPI-containing APP mRNA isoforms than APP-695 (Gray and Patel, 1993a). Interestingly, pyramidal neurones, in areas of human brains affected by AD pathology, also contain relatively more KPI-APP than APP-695 (Neve *et al.*, 1988).

The APP-751 isoform was shown to be up-regulated and the APP-695 isoform down-regulated in response to neuronal injury in rat brain (Iverfeldt *et al.*, 1993). It is possible that this effect was mediated via the products of microglia and macroglia that invade the sites of CNS lesions: cytokines such as interleukin-1 (IL-1), a mitogen for astrocytes, transforming growth factor- β 1 (TGF- β 1) and basic fibroblast growth factor (bFGF). These are found at the sites of lesions, including senile plaques, and have been shown to elevate the expression of all three APP isoforms, APP-751 and APP-770 more so than APP-695 (Gray and Patel, 1993a and b). In a normal human foetal astrocytic cell line, heat-shock led to an increase in KPI-APP mRNA, with no change in APP-695, reduced secreted APP and increased intracellular, possibly β -secretase, processing (Shepherd *et al.*, 2000). Stress, induced by serum deprivation, increased the proportion of APP mRNA that contained exons 7 and 8 but lacked exon 15 (adjacent to the β -amyloid N-terminus (König *et al.*, 1992)) in the C6 glioma cell line, suggesting a potential means by which elevated β -amyloid could be generated (Sudoh *et al.*, 1996). It has also been reported that higher expression of APP-751 suppresses the expression of APP-695 and APP-770 (Ramakrishna *et al.*, 1996).

Together, these findings raise the question of whether these KPI-containing APP isoforms release more β -amyloid, or β -amyloid that is more susceptible to aggregation, than that produced from the degradation of APP-695? These possibilities have been investigated *in vitro*. In human foetal astrocytic cells, increased KPI-APP expression

induced by heat-shock was accompanied by a shift from APP secretion towards intracellular processing, possibly via β -secretase cleavage (Shepherd *et al.*, 2000). Expression of APP-751 in mouse teratocarcinoma P19 cells and human embryonic kidney 293 cells resulted in increased secretion of β -amyloid (42) (Ho *et al.*, 1996). Much research has focussed on the metabolism of APP with the hope of identifying the pathways via which its various degradation products are formed, and the molecules and mechanisms that regulate the routing of APP along these pathways.

Transforming growth factor- β 1 and its association with KPI-APP in Alzheimer's disease

Immunoreactivity of the cytokine transforming growth factor- β 1 (TGF- β 1) has been demonstrated in capillaries of the hippocampus and entorhinal cortex of normal human brains (Van der Wal *et al.*, 1993) and in astrocytes, microglia and oligodendrocytes of frontal cortex from a single normal human brain (Da Cunha *et al.*, 1993). Increased immunoreactivity was present in AD brains, with TGF- β 1 immunolabelling in diffuse plaques, NFTs, glial cells and the neuritic element of senile plaques, as well as in blood vessels (Van der Wal *et al.*, 1993; Peress and Perillo, 1995).

It has been postulated that TGF- β 1 may be neuroprotective in response to β -amyloid toxicity and other cellular insults (Prehn *et al.*, 1993; Prehn *et al.*, 1996; Ren *et al.*, 1997), and its mRNA is upregulated in response to stress or injury (Klempt *et al.*, 1992; Logan *et al.*, 1992; Ata *et al.*, 1997).

TGF- β 1 has been shown to accelerate development of AD pathology in hAPP/TGF- β 1 bigenic mice, which overexpress particularly the KPI-containing isoforms of mutant hAPP (V717F) (Wyss-Coray *et al.*, 1997). TGF- β 1 elevates APP mRNA in astrocytes,

and mRNA and protein in microglia *in vitro* (Gray and Patel, 1993; Amara *et al.*, 1999; Mönning *et al.*, 1994), more so the KPI-containing isoforms than APP-695 in astrocytes (Gray and Patel, 1993). Thus overexpressed TGF- β 1 may potentially influence APP splicing, and/or production or deposition of β -amyloid.

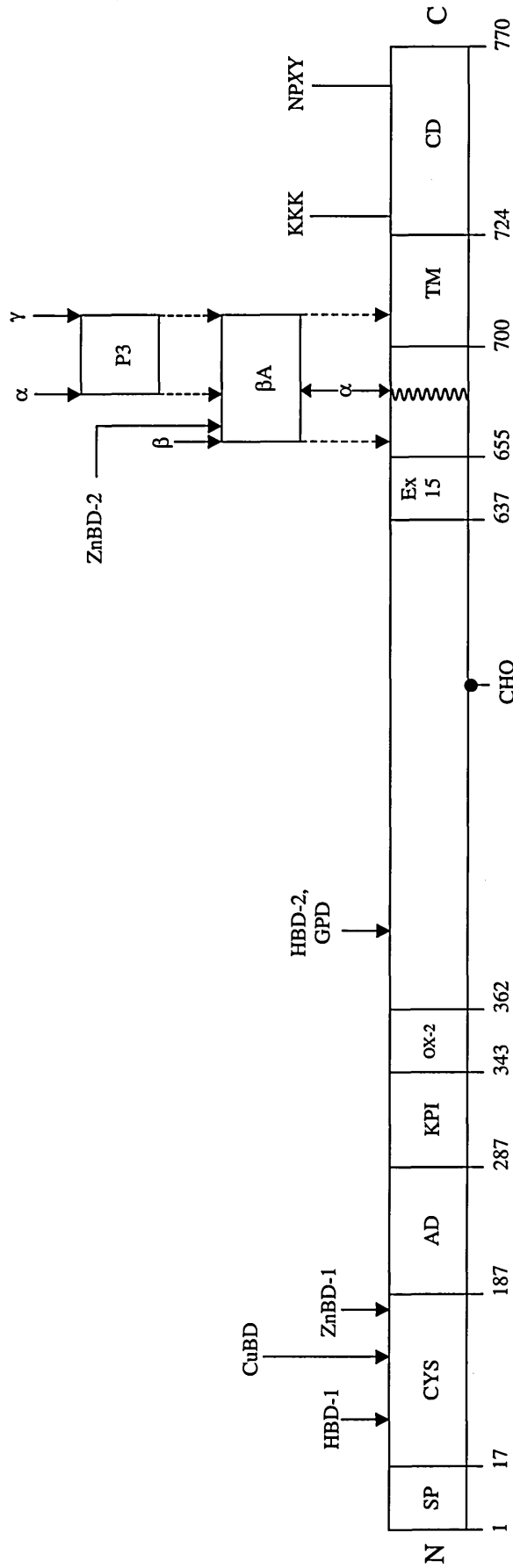
Subcellular processing of APP

Following translation, APP undergoes N- then O-linked glycosylation and tyrosine sulphation in the Golgi complex (Weidemann *et al.*, 1989), after which the mature protein is cleaved resulting in the generation of peptides of various lengths, some potentially amyloidogenic. Rab1b, a small GTP-binding protein that is an important regulatory protein in ER to Golgi transport, is necessary for trafficking of APP from the ER to the Golgi. Furthermore, Golgi maturation of APP and production of soluble α - and β -secretase cleaved APP (sAPP α and sAPP β) are dependent on correct functioning of Rab1b in cultured 293 cells (Dugan *et al.*, 1995). This raises the possibility that other members of the Rab family may be important in further steps of APP trafficking.

The enzymes that are responsible for APP cleavage are beginning to be identified. They were originally designated α -secretase, β -secretase and γ -secretase, cleaving APP between residues 16 and 17 of the β -amyloid sequence, at the N-terminus of β -amyloid and at the C-terminus of β -amyloid respectively, as shown in Figure 1. Some of these enzymes have now been identified, as described below. Five different length C-terminal fragments of APP have been identified, from human brain and APP-695-transfected human embryonic kidney (293) cells, of which two fragments included the β -amyloid sequence (Estus *et al.*, 1992). The larger, potentially amyloidogenic fragments were more abundant in brain (normal and AD) than in liver, kidney, small intestine or

muscle, indicating that a distinct pathway for APP processing exists in the brain, which may partly explain the selective deposition of β -amyloid in the brain in AD.

APP is illustrated in Figure 2. It is predicted to have a single transmembrane region, with the β -amyloid sequence partially embedded within this and extending into the extracellular domain. The intracellular C-terminus is relatively short, and contains a triplet of lysine residues that are important for correct membrane anchorage and consequently for normal α -secretase cleavage of APP within the β -amyloid sequence, just N-terminal to the transmembrane domain (Usami *et al.*, 1993). Another study showed that the precise amino acid sequence at and around the α -secretase site does not greatly affect the efficacy of proteolysis; rather it depends on the presence of an α -helical conformation and the distance (12–13 amino acids) of the cleavage site from the membrane (Sisodia, 1992). This provides further evidence that correct membrane anchorage of APP is essential for non-amyloidogenic processing, and implies that increased production of β -amyloid may result from incorrect membrane insertion, leading to β -amyloid deposition. The C-terminus also contains an NPTY motif that binds two neuronal proteins, X11 and FE65, and may be involved in internalisation of APP via clathrin-coated pits (Fiore *et al.*, 1995; McLoughlin *et al.*, 1996; Borg *et al.*, 1996). The amyloid precursor-like protein 2 (APLP2), a member of the APP family that does not contain β -amyloid, also includes an NPTY sequence in its cytoplasmic region that binds FE65 (Gu nette *et al.*, 1996), suggesting similarity in this aspect of its processing compared with APP. Point mutations in APP, found in familial AD, appear to have an adverse effect on its interaction with FE65 (Zambrano *et al.*, 1997), implying a role for the NPTY domain in AD.



Key:

- SP = signal peptide
- CYS = cysteine-rich domain
- AD = acidic domain
- KPI = Kunitz protease inhibitor-like domain
- OX-2 = OX-2 homology domain
- TM = transmembrane domain
- CD = cytoplasmic domain
- CHO = N-linked carbohydrate site
- HBD-1 / -2 = heparin-binding domain-1 / -2
- CuBD = copper-binding domain
- ZnBD-1 / -2 = zinc-binding domain-1 / -2
- GPD = growth promoting domain
- α, β, γ = secretase sites
- N, C = N-/C-terminus

Figure 1

The structure of APP, showing the position of the β-amyloid sequence, partially embedded in the transmembrane region and extending extracellularly. Depicted in the large, extracellular domain are the KPI region that is examined in this study, and binding sites, at which APP interacts with the various substances denoted. Beyond the single transmembrane-spanning region, are the triplet of lysine residues (KKK) that aid correct membrane anchorage of the protein, and the NPXY sequence that may act as a signal for APP internalisation. After Esiri et al. (1997), p. 182.

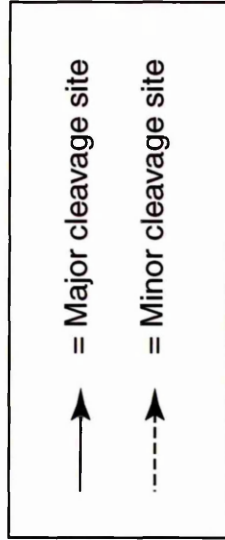
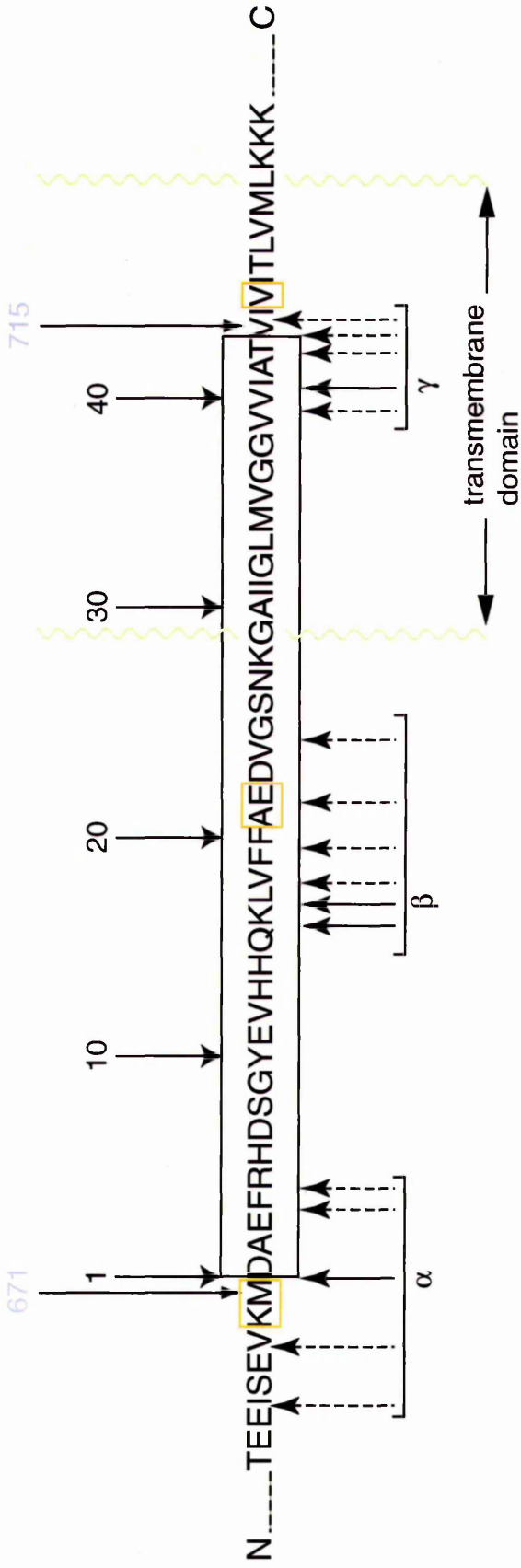


Figure 2

The β-amyloid sequence of APP (numbered in black, 1-40), and the adjacent regions of APP (APP-770 numbering shown in blue at the top of the figure). α, β and γ secretase cleavage sites are shown, demonstrating the intramembranous location of the γ secretase cleavage site. After Esiri et al. (1997), p. 181.

When APP is cleaved within the β -amyloid sequence a non-amyloidogenic N-terminal derivative, secreted APP α (sAPP α), containing residues 1–16 of β -amyloid, is released into the extracellular environment. However, sAPP found in the brain tissue and CSF of both normal and AD patients does not always include this truncated β -amyloid fragment (Weidemann *et al.*, 1989). Mixed human brain cell cultures were demonstrated to secrete truncated sAPP β , cleaved (by β -secretase) between residues Met 596 and Asp 597 of APP-695, the N-terminus of β -amyloid (Seubert *et al.*, 1993). β -secretase cleavage was subsequently demonstrated to occur prior to cleavage at the C-terminus of β -amyloid to generate soluble β -amyloid from the secretory pathway in cultured African green monkey kidney (COS) cells (Maruyama *et al.*, 1994).

However, alternative proteolytic processing pathways exist that yield β -amyloid. Both full-length, mature APP and various β -amyloid-containing fragments were detected in late endosomes/lysosomes in human umbilical vein endothelial cells (HUVECs), which express large amounts of APP-751 and APP-770 (Haass *et al.*, 1992b). It was demonstrated by cell surface antibody labelling and cell surface biotinylation that APP was re-internalized into these compartments from the plasma membrane; although the possibility that some APP may be targeted directly to endosomes/lysosomes, from the Golgi apparatus, was not ruled out. In human NTera 2 neurones β -amyloid was secreted into the culture medium with a 2 hour delay following metabolic labelling (Turner *et al.*, 1996). This β -amyloid could be detected intracellularly before it was recovered in the medium, and it was still produced following trypsin treatment of the intact cells but not after trypsin treatment of permeabilised cells. Thus, in this cell type, APP appears not to be re-internalized from the plasma membrane before intracellular β -amyloid is produced.

Full-length, mature APP and C-terminal fragments were then shown to be present in clathrin-coated vesicles (CCVs) in rat neuroendocrine PC12 cells (Norstedt *et al.*, 1993). CCVs are known to participate in two intracellular pathways: trafficking from the plasma membrane to early endosomes, and from the trans-Golgi network to late endosomes/lysosomes. This therefore supports the findings of Haass *et al.* (1992b). Furthermore, deletion of the cytoplasmic portion of APP or depletion of potassium in the medium of cultured transfected Chinese hamster ovary (CHO) cells (which decreased APP re-internalization via clathrin-coated vesicles) resulted in reduced secretion of labelled β -amyloid from the cells following cell surface radioiodination (Koo and Squazzo, 1994). However, sAPP production remained unaffected, suggesting that sAPP and β -amyloid were generated by different proteolytic pathways. The majority of sAPP secreted from the radiolabelled cells was recovered during the following 15 minutes, whereas β -amyloid was collected at relatively low levels over a course of 105 minutes, supporting the idea that β -amyloid was produced via the endocytic pathway.

APP secretase enzymes

Tumour necrosis factor- α converting enzyme (TACE), also known as ADAM (a disintegrin and metalloprotease) 17, and ADAM 10 have been identified to possess α -secretase activity (Buxbaum *et al.*, 1998; Lammich *et al.*, 1999). In cultured cells, TACE was responsible for regulated α -secretase cleavage, and ADAM 10 allowed both constitutive and regulated α -secretase cleavage of APP. Lammich *et al.* (1999) suggested that ADAM 10 may be activated *en route* to the plasma membrane by furin, which cycles between the Golgi and plasma membrane, thus allowing α -cleavage of APP either intracellularly or at the plasma membrane. Although TACE and ADAM 10

have just 21% amino acid identity, their catalytic domains may share more structural similarity (Lammich *et al.*, 1999).

β -secretase activity has been demonstrated in the endosomal/lysosomal, acidic protease, cathepsin D (Chevallier *et al.*, 1997). Cathepsin D cleaved a synthetic peptide bearing the Swedish double missense mutation, (KM \diamond NL) N-terminal to β -amyloid, preferentially to non-mutated APP analogue peptides. However, it has not been shown to increase β -amyloid production from full-length, cellular APP. β -secretase activity has been suggested to occur in detergent-insoluble membrane domains, enriched in glycosylphosphatidylinositol (GPI)-anchored aspartyl proteases and cholesterol (Lee *et al.*, 1998; Sambamurti *et al.*, 1999). A transmembrane aspartyl protease, Asp 2, BACE (β -site APP-cleaving enzyme), or memapsin 2, cloned and identified in human AD and age-matched, control brains, cleaves APP specifically at the β -secretase site (Hussain *et al.*, 1999; Sinha *et al.*, 1999; Vassar *et al.*, 1999; Yan *et al.*, 1999; Lin *et al.*, 2000). BACE was identified in the Golgi, trans-Golgi network (TGN), secretory vesicles and endosomes, and to a lesser extent in endoplasmic reticulum (ER) and lysosomes of transfected human embryonic kidney (HEK) 293 cells, and acted optimally at pH 4.5 (Vassar *et al.*, 1999). It was co-localised with APP in the ER and Golgi, but not further towards the cell periphery where only APP was present, in COS-7 cells (Hussain *et al.*, 1999). In rat brain, BACE was expressed at higher levels in neurones than in glia (Vassar *et al.*, 1999) and in human brain it was detected immunohistochemically only in neurones (Hussain *et al.*, 1999). It also had high activity levels in CNS-derived cell lines (Sinha *et al.*, 1999). β -secretase cleavage was increased *in vitro* by overexpression of BACE, and decreased by inhibition of endogenous BACE (Vassar *et al.*, 1999).

A second β -secretase enzyme, BACE2, was characterised recently, which cleaves APP both at the β -secretase site and within β -amyloid (Farzan *et al.*, 2000; Solans *et al.*, 2000). BACE2 has been suggested to contribute to excessive β -amyloid production in individuals bearing the Swedish double missense mutation adjacent to its cleavage site within β -amyloid (Farzan *et al.*, 2000). β -secretase cleavage appears to be the rate-limiting step in β -amyloid production, because total β -amyloid formation can be increased or decreased by mutations at the β -cleavage site, but is not altered by mutations at or near the γ -cleavage site (Sinha and Lieberburg, 1999).

A gene on chromosome 14, mutations in which account for approximately 80% of early-onset autosomal dominant AD (Sherrington *et al.*, 1995) encodes a putative seven transmembrane-spanning protein, S182 or presenilin 1 (PS1). This protein appears likely to contain the active site of the γ -secretase APP-cleaving enzyme, in its C-terminal fragment (Wolfe *et al.*, 1999; Esler *et al.*, 2000; Kimberly *et al.*, 2000; Li *et al.*, 2000). Another early-onset FAD locus on chromosome 1 (Levy-Lahad *et al.*, 1995a; Rogaev *et al.*, 1995) encodes a protein, STM2 (second seven transmembrane gene), or presenilin 2 (PS2). with 67% amino acid sequence identity to S182 (Levy-Lahad *et al.*, 1995b), suggesting a similar function to the S182 protein. Evidence suggests that PS2 also can function as a γ -APP-cleavage enzyme (Kimberley *et al.*, 2000; Li *et al.*, 2000). Furthermore, mouse embryonic stem cells lacking PS1 and PS2 have been shown to have no γ -secretase activity (Herreman *et al.*, 2000). Mutations in PS1 and PS2 are discussed below.

Manipulations *in vitro* of APP processing

The pathways of APP trafficking and proteolysis can be studied further by observing the outcomes of various biochemical manipulations of cellular events. For example, inhibition of endosomal–lysosomal proteolysis by ammonium chloride or leupeptin results in decreased production of the C–terminal derivatives of APP in HEK 293 cells (Golde *et al.*, 1992) supporting the role of these intracellular compartments in APP degradation that produces potentially amyloidogenic fragments.

Brefeldin A (BFA), a fungal metabolite, induces dissolution of the Golgi complex into pre– and post–Golgi compartments: the cis–, medial– and trans–Golgi compartments being redistributed to the ER, and the TGN fusing with early endosomes. Treatment of CHO cells and COS cells with BFA caused accumulation of APP in the ER and inhibition of APP secretion (Caporaso *et al.*, 1994), suggesting that secretory cleavage of APP occurs distal to the trans–Golgi. However, no APP immunoreactivity was found in the reticular TGN–endosomal structure formed upon BFA treatment, indicating that APP or APP fragments are not transported directly between the TGN and early endosomes. Another study, also using COS cells, showed that both BFA and monensin (which disrupts intra–Golgi transport and processing and inhibits lysosomal degradation) increased the production of an 11.5kD APP derivative which includes the β –amyloid sequence, and inhibited APP maturation and secretion of sAPP (Gabuzda *et al.*, 1994). This supported the observation made by Caporaso *et al.* (1994), that α –secretase cleavage of APP occurs in a later secretory compartment, and demonstrated that inhibition of APP maturation can lead to the formation of amyloidogenic derivatives in the ER or early Golgi compartments.

In N2a neuroblastoma cells, doubly transfected with human APP and PS1, and in primary rat cortical neurones, β -amyloid (x-42) was generated and retained, in an insoluble form, in the ER. Both β -amyloid (1-42) and (x-42) were produced in the TGN and packaged into post-TGN secretory vesicles. β -amyloid (1-40) and (x-40) were made only in the TGN and packaged into secretory vesicles (Greenfield *et al.*, 1999). Of the β -amyloid within the TGN, some was detergent-soluble and some detergent-insoluble.

However, in PC12 cells treated with the weak base chloroquine, which inhibits proteolytic enzymes within the normally acidic lysosomes and Golgi complex, APP and C-terminal APP fragments accumulated in lysosomes (where they were not easily detected prior to chloroquine treatment). However, they were not detected in Golgi compartments (Caporaso *et al.*, 1994). The same effect of chloroquine was observed in COS cells (Gabuzda *et al.*, 1994). It is therefore possible that lysosomal proteolysis of APP allows β -amyloid production.

When A-172 human glioblastoma cells are treated with phorbol 12-myristate 13-acetate (PMA), which activates protein kinase C (PKC), an increase in sAPP secretion results, and a decrease in intracellular amyloidogenic fragments is observed (Fukushima *et al.*, 1993). It thus seems possible that in AD aberrant regulation of the balance between APP processing in these two pathways could result in an increase in production of β -amyloid or of β -amyloid (42) relative to β -amyloid (40), and subsequently neurotoxicity and β -amyloid deposition.

However, α -secretase and amyloidogenic pathways are not necessarily mutually exclusive. For example, in SY5Y cells, α -secretase cleavage of APP is up-regulated by PKC activation while β -secretase cleavage remains unaffected, although regulation of

APP cleavage pathways appears to be controlled by different mechanisms in different cell types (Dyrks *et al.*, 1994).

On the whole the studies described above support each other and discrepancies between them can sometimes be explained by differences in experimental technique, or the use of different cell types that express varying levels of the different length APP isoforms and metabolise APP in different ways. However, the evidence provided by these studies, notably those on cultured cells and non-human brain cells, is not always necessarily a true representation of APP processing in human brain. This is primarily because of its complex environment as an organ, wherein interactions between its many cell types and surrounding tissues add complexity to the events described in isolated cell types. Therefore, as described in more detail below, this project made use of human CNS-type cultured neurones (NTERA 2 neurones) and human brain tissue.

Functions of the amyloid precursor protein

Many potential functions of APP and sAPP have been proposed, KPI-containing sAPP being identical to protease nexin-II, a serine protease inhibitor (Cunningham, 1993). Fibrillar β -amyloid was shown recently to bind KPI-APP, thus enhancing its inhibition of coagulation factor XIa, and potentially contributing to cerebral haemorrhage associated with CAA. The fibrillar β -amyloid bound to the N-terminal region of APP, where there are also binding sites for Zn^{2+} and heparin, which also stimulate inhibition of factor XIa by KPI-APP (Wagner *et al.*, 2000). APP and sAPP may be involved in neurite outgrowth, acting via binding with laminin (Kibbey *et al.*, 1993) and/or heparan sulphate proteoglycans (HSPG) via its heparin binding site (Snow *et al.*, 1990; Small *et al.*, 1994), and APP itself may be an HSPG core protein (Schubert *et al.*, 1988). Splicing

out of exon 15 of the APP gene creates a new consensus sequence for attachment of a chondroitin sulphate chain, resulting in production of appicans, which appear to be strong cell adhesion molecules and may participate in cell arborization (Pangalos *et al.*, 1995).

APP may function as a cell surface receptor (Ferreira *et al.*, 1993), possibly at synaptic terminals in neurones where it has been identified at the synaptic plasma membrane (Shimokawa *et al.*, 1993). It has been suggested that APP may bind and recycle substances such as histones, proteases and matrix proteins from the extracellular medium (Potempska *et al.*, 1993). The latter theory is supported by the particularly high expression of APP in cells that have a high membrane turnover and undergo endocytic and phagocytic retrieval and exocytosis (Beer *et al.*, 1995) implying a potential role for APP in tissue maintenance and repair. There is evidence that sAPP also protects against hypoglycaemia- and glutamate-induced excitotoxicity by lowering intracellular calcium concentration ($[Ca^{2+}]_i$) (Mattson *et al.*, 1993), and that the effect of sAPP on $[Ca^{2+}]_i$ is mediated via cyclic GMP (cGMP) (Barger *et al.*, 1995). In addition, sAPP can activate the p21^{ras}-dependent mitogen-activated protein kinase (MAPK) cascade, which enhances phosphorylation of intracellular substrates, including tau, which is hyperphosphorylated in AD (Selkoe, 1994a).

Aberrant processing of APP in AD may have effects upon the functions of sAPP as well as causing damage via β -amyloid, for example by production of sAPP that is less effective at regulating $[Ca^{2+}]_i$, or exhibits defective binding to extracellular matrix components.

The genetics of Alzheimer's disease

Chromosome 21

The linkage of some cases of autosomal dominant AD with missense mutations in the APP gene on chromosome 21 within or immediately adjacent to the β -amyloid sequence (Haass and Selkoe, 1993) supports a primary role for APP processing in the pathogenesis of AD. These mutations are associated with early onset familial AD (FAD). A double missense mutation, found in a Swedish pedigree, that alters the lysine-methionine, immediately N-terminal to β -amyloid residue 1, to asparagine-leucine, results in the secretion of approximately 7 times the normal amount of β -amyloid in transfected cell cultures (Johnston *et al.*, 1994). Three other FAD-linked mutations convert the valine, three residues C-terminal from β -amyloid residue 43, to isoleucine, phenylalanine or glycine. These mutations result in a 1.5-1.9-fold increase in the proportion of β -amyloid (1-42) over β -amyloid (1-40) released into conditioned medium of human neuroblastoma (M17) cells (Suzuki *et al.*, 1994) and produced by other cultured cell types (Selkoe, 1995). The APP717 valine to phenylalanine mutation has since been shown to produce AD-type pathology in transgenic mice (Games *et al.*, 1995). In addition, all people with Down's syndrome (trisomy 21) who live into their late thirties and beyond develop a neuropathology indistinguishable from that of AD (Ashall and Goate, 1994), the APP gene being normal but over-expressed. This indicates that overproduction of β -amyloid results ultimately in extracellular deposition of the peptide. However, mutations in APP itself only account for about 2-3% of FAD cases (Barinaga, 1995).

Chromosome 19

A gene on chromosome 19 that encodes apolipoprotein E (apo E) has been linked with some cases of late-onset AD. Apo E is a carrier molecule, produced predominantly by astrocytes, that binds soluble β -amyloid *in vitro* (Wisniewski *et al.*, 1993), and is transported into neurones by members of the low-density lipoprotein (LDL) receptor superfamily, predominantly the lipoprotein receptor related protein (LRP) (Martin, 1999; Rosenberg, 2000). The apo E ϵ 4 allele has the highest affinity for LRP, the ϵ 3 allele has intermediate affinity and the ϵ 2 allele binds least efficiently. Apo E ϵ 4 is strongly associated with late-onset familial and sporadic AD, although no mutations in apo E are associated with AD (Scott, 1993), indicating that possession of this allele increases AD susceptibility, while presence of the ϵ 2 allele decreases risk of AD and delays onset, these effects being dose-dependent. In addition, presence of the LRP C allele may be a risk factor for late-onset sporadic AD (Shastry and Giblin, 1999; Rosenberg, 2000). Apo E is found in senile plaques and has been shown *in vitro* to induce β -amyloid filament formation (Sanan *et al.*, 1994). It was subsequently demonstrated that, in AD brains, intracellular apo E correlates with β -amyloid immunoreactivity within the same cytoplasmic granules, suggesting that the hydrophobic β -amyloid is stabilised by this lipid (LaFerla *et al.*, 1997). These cells, which were found in clusters, also exhibited DNA fragmentation, were found in areas of extracellular β -amyloid deposition, and the extent of DNA damage correlated with intracellular β -amyloid immunoreactivity.

Chromosome 12

A further locus linked to late-onset AD is present on chromosome 12. On this chromosome a candidate gene, which may contain deletions in AD patients, encodes

α_2 -macroglobulin, a serum protease inhibitor, which also binds to β -amyloid and LRP (Martin, 1999; Rosenberg, 2000).

Chromosomes 14 and 1

Many mutations occur in a gene that was identified recently on chromosome 14 (Sherrington *et al.*, 1995), accounting for approximately 80% of early-onset autosomal dominant AD and resulting in very early and severe amyloidosis. The gene encodes a putative seven transmembrane-spanning protein, S182 or presenilin 1 (PS1). There is convincing evidence that this protein contains the active site of γ -secretase APP-cleaving enzyme, in its C-terminal fragment, and that this becomes active on PS1 endoproteolysis (Wolfe *et al.*, 1999; Esler *et al.*, 2000; Kimberley *et al.*, 2000; Li *et al.*, 2000). One of the PS1 mutations that is associated with familial AD, PS1 Δ E9, which lacks the cytoplasmic loop (encoded by exon 9) containing the PS1 endoproteolytic cleavage site, appears to result in a stable, single-chain protein with γ -secretase activity (Li *et al.*, 2000). PS1 and the two peptides produced following PS1 proteolysis have been localised within the cell bodies and dendrites of human NTera 2 neurones, and have been shown to reside in the ER and early Golgi in several cell types (Cook *et al.*, 1996; Parkinson, 1998; Wolfe *et al.*, 1999). Following the discovery of PS1, another early-onset FAD locus was identified on chromosome 1 (Levy-Lahad *et al.*, 1995a; Rogaev *et al.*, 1995). The protein encoded by this gene also is predicted to have seven transmembrane domains (and is hence named the second seven transmembrane gene associated with AD, STM2, or presenilin 2 (PS2)). It has a 67% identical amino acid sequence to S182 (Levy-Lahad *et al.*, 1995b), suggesting a similar function to the S182 protein, and there is evidence to suggest that it too can function as a γ -secretase enzyme (Kimberley *et al.*, 2000; Li *et al.*, 2000). Other evidence indicates that an

apoptosis-linked gene, ALG-3, the mouse homologue of PS2, may be protective against T cell receptor- and Fas-induced cell death (Vito *et al.*, 1996). Presenilin mutations that occur in some cases of familial AD have been shown to increase production of the more readily deposited 42-amino acid length β -amyloid in transfected cells and transgenic mice (Citron *et al.*, 1997), whereas a PS1 knockout reduced β -amyloid (40) and (42) production significantly (Steiner *et al.*, 1999).

Chromosome 10

A further susceptibility locus for AD has been identified recently, residing on chromosome 10. This locus appears to influence the risk of AD independently of apo E genotype (Myers *et al.*, 2000), and is associated with elevated levels of plasma β -amyloid (42) (Ertekin-Taner *et al.*, 2000). A further study found evidence for linkage of four further adjacent markers on chromosome 10q with AD, particularly late-onset (Bertram *et al.*, 2000). The locus of one of these markers is within 195 kb of the insulin degrading enzyme gene, which has been postulated to degrade β -amyloid in neurones and in microglia, implying that this chromosome 10 locus may influence, indirectly, intracellular β -amyloid metabolism.

Sporadic Alzheimer's disease

Most cases of AD are sporadic and occur with late-onset (over age 65). Some suggested causes of sporadic AD include toxic agents such as metal ions including aluminium, zinc and iron, which have been shown to promote aggregation of physiological concentrations of β -amyloid (Mantyh *et al.*, 1993; Bush *et al.*, 1994); infectious agents, although spongiform changes that are apparent in Creutzfeldt-Jakob and Gerstmann-Straussler disease are not part of the AD pathology; neurotransmitter

deficits, principally acetyl choline, demonstrated by a 90% drop in cortical choline acetyltransferase activity in AD; and selective death of the cells responsible for the neurotransmitter deficits (Perry, 1991). Given the genetic evidence for the importance of APP in AD, it can be postulated that abnormal processing of APP due to environmental factors may result in overproduction of β -amyloid or release of abnormal β -amyloid. This β -amyloid may be more prone to aggregation and/or might not be cleared as effectively as usual from the central nervous system (CNS), leading to plaque formation. There is evidence that β -amyloid promotes neurite extension in its soluble form but becomes increasingly neurotoxic upon aggregation (Pike *et al.*, 1991; Howlett *et al.*, 1995). β -amyloid has been demonstrated to interact with endothelial cells with the result of an excess of superoxide radical production, which could lead to neurodegeneration (Thomas *et al.*, 1996). Amyloid fibrils have been observed within the cytoplasm of endothelial cells in AD brain (Miyakawa *et al.*, 1974). A recent study using patch-clamp techniques has suggested that aggregated β -amyloid may produce neurotoxic effects by insertion into the cell membrane of NT2N neurones as a Ca^{2+} -carrying ionophore (Sanderson *et al.*, 1997). Abnormally processed APP may also give rise to other altered APP degradation products that have a detrimental effect on neurones (Mattson *et al.*, 1993).

Mitochondrial dysfunction has been implicated in sporadic AD (Davis *et al.*, 1997; Swerdlow *et al.*, 1997; Tanaka *et al.*, 1998; Beal, 2000). Cytoplasmic hybrid (cybrid) cell lines have been created, by replacing the mitochondrial DNA of NT2 cells or human neuroblastoma SH-SY5Y cells with mitochondrial DNA of sporadic AD subjects (Swerdlow *et al.*, 1997; Khan *et al.*, 2000). These AD cybrids displayed reduced cytochrome *c* oxidase (COX) activity, lowered mitochondrial membrane potential, elevated β -amyloid (40) and (42) secretion and intracellular β -amyloid (40),

and increased caspase-3 activity. Caspase enzymes, which participate in activation of cell death pathways, can cleave APP, resulting in increased β -amyloid production, and caspase-3 protein is elevated in AD brains (Gervais *et al.*, 1999). β -amyloid (40) secretion by cybrids was normalised by caspase-3 inhibition, and lowered with antioxidant treatment (Khan *et al.*, 2000).

It has been demonstrated that β -amyloid is produced by cultured cells during normal metabolism (Haass *et al.*, 1992a; Shoji *et al.*, 1992) and β -amyloid is present in both normal human brain and cerebro-spinal fluid (CSF) (Tabaton *et al.*, 1994). This peptide varies in length from 39 to 43 amino acids (β -amyloid (39)– β -amyloid (43)). It has been shown that all diffuse plaques, thought to represent an early stage of AD, contain β -amyloid (42/43) but not β -amyloid (40), and that all neuritic plaques contain β -amyloid (42/43) while only one third of them are β -amyloid (40)-positive (Iwatsubo *et al.*, 1994). Furthermore, the C-terminus of β -amyloid has been demonstrated to determine the rate of formation of amyloid deposits *in vitro*, β -amyloid species that terminate at residues 39–40 being nucleated by those that include the C-terminal residues 42–43 (Jarrett *et al.*, 1993). Hence these longer β -amyloid species are likely to be crucial to the initiation and/or acceleration of development of amyloid deposits in the central nervous system in AD. A further possibility is that higher than normal concentrations of unrelated globular proteins could effectively reduce the critical concentration required for β -amyloid fibrillization. For example, typical cytoplasm has a total protein concentration approaching 1M, so a burst of protein production associated with neuronal repair could result in fibrillization of β -amyloid when it is approaching its normal critical concentration (Lansbury, 1999).

Thus any genetic or environmental factor that affects the rate or manner of production or proteolysis of APP, or the aggregation state of β -amyloid in the brain, could result in amyloid deposition and/or neuronal injury.

Reduced cerebral blood flow and decreased oxidative glucose metabolism in AD brain indicate other factors that may contribute to development of AD. There is often a marked vascular component to AD pathology and alterations to cerebral blood vessels have been described. There are thickenings, fragmentations and irregularities of capillary basement membranes, with deposition of basement membrane proteoglycans, and β -amyloid fibrils that project into the neuropil (de la Torre and Mussivand, 1993; Inoue *et al.*, 1999). De la Torre and Mussivand suggested that alterations in the capillary basement membranes, along with reduced vessel elasticity, damage to vessels caused by amyloid deposits, or vessel degeneration due to genetic predisposition, may all contribute to abnormal blood flow patterns, and changes in shear stress and shear rate in vessel walls. This results in impaired blood flow and delivery of nutrients, such as oxygen and glucose, to the brain. Neurones in area CA1 of the hippocampus, which is affected severely in AD, are reported to be particularly susceptible to chronic cerebrovascular ischaemia. Affected neurones, when deprived of energy substrates, trigger release of diffusible glial mitogens that signal reactive astrocyte proliferation (de la Torre and Mussivand, 1993), and astrocytosis is indeed a feature of AD pathology.

The role of cellular stress in Alzheimer's disease

Factors that have been suggested to be involved in the pathogenesis of AD and APP metabolism include reduced cerebral glucose metabolism (Hoyer, 1993; Meier-Ruge *et al.*, 1994), oxidative stress and heat shock (Pappolla *et al.*, 1995), mitochondrial

dysfunction (Davis *et al.*, 1997; Swerdlow *et al.*, 1997; Tanaka *et al.*, 1998) and inflammatory activity (Schnabel, 1993). Inhibition of oxidative energy metabolism in COS cells by sodium azide or carbonyl cyanide, a mitochondrial uncoupler, has been shown to increase the production of potentially amyloidogenic C-terminal APP fragments, which accumulate in the Golgi complex (Gabuzda *et al.*, 1994). This indicates that energy-related metabolic stress may alter APP processing in a way that increases β -amyloid production or results in a change in mechanism of proteolysis that produces an abnormal β -amyloid species. Heat shock induces APP secretion from HUVECs, followed by upregulation of APP mRNA and protein synthesis (Ciallella *et al.*, 1994). APP accumulation following heat shock was reported to have a Golgi-like distribution in both HUVECs (Ciallella *et al.*, 1994) and in stably transfected C6 glioma cells (Pappolla *et al.*, 1995). Furthermore, glucocorticoids have been shown to enhance cell death caused by β -amyloid- and glutamate-induced oxidative stress in rat and mouse hippocampal neurones (Behl *et al.*, 1997). Glucocorticoid receptors may be dysfunctional or have a decreased level of expression in the hippocampus AD (Wetzel *et al.*, 1995), leading to an increase in glucocorticoid production in AD brain (Eber, 1996).

As mentioned above, it has been suggested that disturbance of brain microcirculation is responsible for the reduced cerebral blood flow and glucose and oxygen metabolism that have been described in AD (de la Torre and Mussivand, 1993; de la Torre, 1997). An alternative explanation of the reduction in oxidative glucose metabolism is that the neuronal insulin receptors of the brain become desensitized, perhaps by increased levels of stress factors such as cortisol and catecholamines (Henneberg and Hoyer, 1995). Insulin receptors are found with the highest density in the olfactory bulb, hypothalamus, cerebral cortex and hippocampus, while insulin mRNA has been detected mostly in

hippocampal pyramidal cells, followed by medial prefrontal cortex, entorhinal cortex, perirhinal cortex, thalamus and the olfactory bulb granule cell layer. Stimulation of neuronal insulin receptors in rats, with intracerebroventricularly administered insulin, increased brain energy metabolism, while experimental desensitisation of neuronal insulin receptors resulted in decreased oxidative glucose metabolism, reduced energy formation and impairment of learning and memory (Henneberg and Hoyer, 1995).

Investigation of APP processing in a model human CNS neuronal system

In this study processing of APP and the effects of cellular stress were investigated in a system that bears a closer resemblance to neurones of the human CNS. The cell line NTera 2/D1 (NT2) is a pluripotent human embryonal carcinoma cell line which can be induced by treatment with retinoic acid to terminally differentiate into a neuronal phenotype (NT2N) (Andrews *et al.*, 1984; Andrews, 1984). These neurones express many markers of human CNS neurones, such as CNS neurofilament proteins, but not peripherin, a peripheral nervous system (PNS) neurofilament protein; several neuronal microtubule associated proteins (MAPs), including tau, but not a PNS isoform of tau; and many other neuronal markers such as NCAM and synaptophysin (Pleasure *et al.*, 1992). NT2 neurones also possess axons and functional dendrites (Pleasure *et al.*, 1992).

Undifferentiated NT2 stem cells can be studied alongside NT2N neurones as comparative models of the processing of APP in non-CNS cells versus CNS-type neurones. In this investigation, the intracellular localization of APP has been demonstrated in stem cells and neurones by indirect immunocytochemical techniques,

with the aim of providing a means of comparing APP processing in neurones versus equivalent non-neuronal cells. As discussed above, the effects of metabolic stresses, implicated in AD, were studied in relation to APP localization in both the stem cells and neurones. The aim of this was to identify any differences in the responses of the two different cell types to stress, and thus suggest reasons why the characteristic pathology of AD is restricted to the brain and not other tissues and organs. However, it has to be taken into account that the evidence provided by previous studies may sometimes be complicated by the subsequent discovery that commonly used antibodies to APP also recognise other members of the APP family, the amyloid precursor-like proteins 1 and 2 (APLP1 and 2). These proteins do not contain the β -amyloid sequence but otherwise show great homology to APP (Webster *et al.*, 1995). APLP2 is present in normal and AD human brain, in neurones, astrocytes, neuritic plaques and dystrophic neurites (Crain *et al.*, 1996), and is expressed by NT2 cells. Therefore great care must be taken in the selection of antibodies to APP when studying its intracellular distribution, as discussed above. The distribution of APLP2 in NT2 cells was therefore compared with that of APP under all experimental conditions that were employed to investigate APP.

Summary

This work focussed on clarification of differences in processing and distribution of various members of the family of amyloid precursor and amyloid precursor-like proteins in cultured neurones and/or human brains. Expression of TGF- β 1 mRNA in human brains was also quantified, following its recent association, when expressed in combination with hAPP (V717F), with AD pathology in transgenic mice (Wyss-Coray *et al.*, 1997).

APP was examined, in comparison with APLP2, in cultured NTERA 2 cells, which share more similarities with CNS neurones than any other type of cultured cell currently available. The effects of cellular stresses were investigated on immunolocalisation of APP, APLP2 and β -amyloid. The potential for electron microscopical examination of APP distribution and processing in these cells was investigated briefly.

There is accumulating evidence for the importance of KPI-APP in the development of AD pathology, as is discussed in detail elsewhere. Although KPI-APP mRNA has been examined in normal and AD human brains, KPI-APP protein has not. Therefore a protocol was established for examining KPI-APP protein in paraffin-embedded human brain sections by indirect immunohistochemistry, using a new anti-KPI antibody, and a study was carried out to investigate the expression and distribution of this protein in normal and AD human brains.

Although TGF- β 1 protein has been localised immunohistochemically in normal and AD human brains, its mRNA has not been studied. Therefore TGF- β 1 mRNA was examined in human brains by *in situ* hybridization histochemistry, with the aim of characterising its expression levels and cellular distribution in normal aged controls versus AD individuals.

CHAPTER 2: METHODS

Cell culture

NTera2 (NT2) stem cells were derived from an original P30 passage of clone NT2/D1 from the laboratory of P. W. Andrews (University of Sheffield). Cells were cultured in Dulbecco's Modified Eagle's Medium (DMEM) with 10% foetal bovine serum (FBS), 1% L-glutamine and 1% penicillin-streptomycin (cDMEM (complete DMEM)), at 37°C under a humidified atmosphere containing 10% CO₂ in air. Tissue culture plastic flasks with ventilated caps were used. FBS was heat-inactivated at 50°C for 30 minutes before use. Cells were passaged 1:3 every 3 to 4 days, when confluent, by scraping gently with sterile glass beads. This technique of removing the cells from the flask detaches them in small clusters without damaging them greatly. Cells were replated at a density above 5×10^6 cells per 75-cm² flask. All contaminated waste material was disposed of in bleach or by autoclaving.

Freezing NT2 stem cells

At every passage of the stem cells, any cells that were not needed for differentiation or to maintain the stem cell cultures were frozen in liquid nitrogen. This allowed a stock of low passage (P) number (between P30 and P50) stem cells to be collected. These were recovered whenever the stem cell cultures became infected or passed beyond P50.

Freezing medium was made with 90% foetal calf serum (FCS) and 10% dimethyl sulphoxide (DMSO).

Cells were removed from the flask by scraping with sterile glass beads.

Cells were spun down at 1500 rpm for 5 minutes and the supernatant was removed.

Cells were resuspended in freezing medium. The cells from two 75-cm² flasks were resuspended in 9ml freezing medium, and this suspension was frozen in 1ml aliquots at -70°C. The vials in which the cells were frozen were placed in an insulated container at room temperature so that the freezing process occurred over several hours. This minimised damage to the cells that would be caused by more rapid freezing.

After three to four days the cells were transferred from -70°C to liquid nitrogen.

Recovering NT2 stem cells

Stem cells that had been stored in liquid nitrogen were recovered to replace cultures that had passed beyond P50 or become infected. Stem cells were only kept until they reached P50 because each passage of cells created a sub-culture of the original stem cells. Therefore the cells become progressively less similar to the original phenotype with every successive passage. P50 was selected as the cut-off point because beyond this passage a lower yield of neurones was obtained on differentiation of the stem cells.

Cells were removed from liquid nitrogen and thawed immediately in a water bath (Gallenkamp) at 37°C.

Complete DMEM was added dropwise, washing out the DMSO slowly so that the cells were not shocked by a sudden addition of medium.

Cells were centrifuged at 1500 rpm for 5 minutes.

The supernatant was removed and cells were resuspended in cDMEM.

The cell suspension was added to a 25-cm² flask and placed in the incubator.

Differentiation of NT2 stem cells to produce neuronal cultures

NT2 stem cells were harvested by incubation with $0.5\mu\text{gml}^{-1}$ trypsin containing 0.53mM ethylene–diaminetetraacetic acid (trypsin–EDTA) or cell dissociation solution (Sigma Chemical Co) for 5 minutes at 37°C . This yields a single cell suspension rather than the clumps of cells obtained by scraping with glass beads. To obtain 99% pure neuronal cultures, these cells were replated at a density of 10^6 per 75-cm^2 flask and fed weekly with 10^{-5}M retinoic acid in cDMEM for 21 days.

Cells again were removed from the flasks with trypsin–EDTA or cell dissociation solution, split 1:2 and fed with cDMEM.

After 2 days cells were harvested using trypsin–EDTA or cell dissociation solution and replated at a density of $3\text{--}9\times 10^6$ per 25-cm^2 flask in cDMEM with mitotic inhibitors. The inhibitors used were uridine, fluorodeoxyuridine (both used at $10\mu\text{M}$), and cytosine arabinoside (used at $1\mu\text{M}$). The mitotic inhibitors prevented any non–neuronal cells from replicating. The neuronal cells, which were terminally differentiated and had therefore dropped out of the cell cycle, remained unaffected by the mitotic inhibitors. Once the non–neuronal cells had been prevented from dividing by the mitotic inhibitors, the neurones formed a layer on top of the other cell types.

Cells were fed with cDMEM and inhibitors twice per week for 2 to 3 weeks. Then the neurones, which formed the top layer of cells, were removed with trypsin–EDTA, cell dissociation solution, or mechanically, by striking the side of the flask firmly. They were replated in flaskette chambers. Some of these were not coated, some were coated with just poly–D–lysine, and others were coated with poly–D–lysine and matrigel

(Collaborative Research). The neurones were fed twice per week with cDMEM and inhibitors.

Coating coverslips and chamber slides with poly-D-lysine and matrigel

This procedure was carried out in a sterile hood. 12mm diameter glass coverslips were used. These were etched in 6M hydrochloric acid, rinsed several times with distilled water, then sterilised with 70% ethanol (BDH) before use, then placed in the wells of a 24-well plate in a sterile hood and allowed to dry. The chamber slides consisted of glass slides with 1, 2, 4 or 8 plastic chambers attached by a silicone seal. The coverslips and slides had to be coated with poly-D-lysine before the matrigel would adhere to the surface. Distilled water used in this procedure was sterilised by passing from a syringe through a 0.22µm filter (Nalgene).

A 0.1mgml⁻¹ stock of poly-D-lysine was made using sterile distilled water. This was stored at -20°C.

The surface of each coverslip or slide was aseptically coated with 5.0µgcm⁻² (50µl of 0.1mgml⁻¹ stock per cm²) poly-D-lysine. The 24-well plates/slides were rocked gently to ensure even coating of the surface.

After 5 minutes the excess solution was aspirated from the 24-well plate or chamber slides.

The coverslips or slides were allowed to air dry in the sterile hood for at least 2 hours. Those that were not required immediately were sealed in an airtight container and stored at room temperature for up to one month.

Once the coverslips/slides were dry the matrigel was mixed to homogeneity using a pre-cooled (on ice) pipette. The tube of matrigel itself was kept on ice because it forms a gel rapidly above 4°C.

The matrigel was diluted 1:36 in cold DMEM in a pre-cooled tube.

Enough of the diluted matrigel to cover the growth surface easily was added to each of the coverslips/chamber slides. This was 100µl per well of an 8-well chamber slide. A bent, fire-polished pasteur pipette was used to spread the matrigel over the growth surface.

The matrigel-coated coverslips/slides were incubated in a 37°C incubator for 3 hours.

Any unbound material was aspirated and the coverslips or chambers were rinsed gently with DMEM. Cells were plated on the coated coverslips or chamber slides the same day.

Heat-shock of NT2 cells

Chamber slides containing NT2 stem cells or neurones were sealed by wrapping with plastic film.

The sealed flasks were transferred to an incubator at 42°C for 30 minutes.

Meanwhile, control slides that were not being heat-shocked were fixed (as described below) and stored at 4°C.

Following heat-shock the plastic film was removed from the chamber slides and the cells (except the “0 hours recovery” cells) were returned to the incubator at 37°C, 10% CO₂.

Cells that were given 0 hours' recovery after heat-shock were fixed immediately. The rest of the cells were fixed following 1, 4, 12 or 24 hours' recovery at 37°C.

Immunocytochemistry

NT2 stem cells or neurones were fixed with -20°C methanol (BDH) or acetone (BDH) for 5 minutes, and some were further permeabilised in 0.5% triton X-100. Intracellular antigens were localised by indirect immunocytochemistry using mouse monoclonal and rabbit polyclonal primary antibodies (see Table 10, Appendix). Cells labelled with anti- β -amyloid primary antibody were pre-treated with 80% formic acid for 10 minutes. Visualisation was achieved by fluorescein isothiocyanate (FITC)- or rhodamine (TRITC)-conjugated secondary antibodies, biotinylated secondary antibody followed with FITC- or TRITC-conjugated streptavidin, or by biotinylated secondary antibodies followed by avidin-HRP complex, developed with diaminobenzidine (DAB). Cells were examined by fluorescence or light microscopy respectively. In the case of the fluorescently-labelled secondary antibodies or streptavidin cells were then examined by confocal microscopy.

Fluorescent labelling:

This method of antigen detection was used for both NT2 stem cells and NT2 neurones.

Following fixation cells were re-hydrated in 0.1M phosphate-buffered saline (PBS) for 15 minutes twice.

Cells that were to be labelled with anti- β -amyloid antibody were incubated in 80% formic acid for 15 minutes then washed in PBS for 15 minutes three times.

Endogenous peroxidase activity was quenched by incubating cells in 0.5% hydrogen peroxide (H₂O₂) in methanol for 25 minutes. Cells were then rinsed gently with PBS three times for 10 minutes.

Non-specific binding sites were blocked with 5% normal serum from the species in which the secondary antibody was raised in 3 mg/ml bovine serum albumin (BSA)/PBS. Other blockers that were tested were fish gelatin (2%, 5% in PBS), blotto (dried skimmed milk powder, 1%, 5% in PBS), BSA (1%, 5%, 30% in PBS), and foetal calf serum (FCS, 2%, 5% in PBS). Cells were then rinsed briefly with PBS.

Cells were incubated in primary antibody, diluted in 3% normal serum from the species in which the secondary antibody was raised, in 3 mg/ml BSA/PBS (or another blocker as described in (5) above), for 1 hour at room temperature or overnight at 4°C.

Cells were rinsed with PBS for 10 minutes three times. They were then incubated with secondary antibody conjugated to FITC, TRITC or biotin, diluted in PBS, for 30–45 minutes at room temperature. The cells were rinsed with PBS for 10 minutes three times.

Cells that were labelled with biotinylated secondary antibody were incubated with FITC- or TRITC-conjugated streptavidin for 30 minutes then rinsed with PBS for 10 minutes three times. Cells were mounted with anti-fade and the edges of the coverslips were sealed with nail polish to prevent drying out.

Chromogenic labelling

This method of immunostaining was used for both NT2 stem cells and neurones.

Following fixation cells were re-hydrated in 0.1M phosphate-buffered saline (PBS) for 15 minutes twice. If required cells were microwaved in 0.05M Tris-HCl, pH 7.0, then washed in distilled water for 5 minutes three times.

Cells that were to be labelled with anti- β -amyloid antibody were incubated in 80% formic acid for 15 minutes then washed in PBS for 15 minutes three times.

Endogenous peroxidase activity was quenched by incubating cells in 0.5% H₂O₂ in methanol for 25 minutes. Cells were then washed in 0.1M PBS for 10 minutes three times.

Non-specific binding sites were blocked with normal serum (supplied in a Vectastain Elite ABC kit) from the species in which the secondary antibody was raised, as recommended in the manufacturers' instructions. Cells were washed briefly in PBS.

Cells were incubated with primary antibody diluted in PBS containing 5% normal serum from the species in which the secondary antibody was raised for 1 hour at room temperature or overnight at 4°C.

The cells were washed in PBS for 10 minutes three times. They were then incubated for 30 minutes at room temperature with secondary antibody conjugated to biotin from the Vectastain Elite ABC kit, diluted in PBS according to the manufacturers' instructions. The cells were again washed in PBS for 10 minutes three times.

Cells were incubated with avidin and biotinylated horseradish peroxidase macromolecular complex (ABC) from the Vectastain Elite ABC kit for 30 minutes at room temperature. This complex was made 30 minutes before use, by addition of

Avidin DH and biotinylated horseradish peroxidase H reagents (from the kit) to PBS as described by the manufacturers' instructions.

Cells were washed in PBS for 10 minutes three times then incubated with diaminobenzidine (DAB) peroxidase substrate solution until the desired staining intensity was reached. The cells were washed for 5 minutes in tap water then dehydrated through serial alcohols (70%, 80%, 95%, 100% x 2 ethanol (BDH)) to xylene. Cells were mounted with DePeX.

Localization of intracellular compartments using other markers

The following methods were used to localise nuclei and the endoplasmic reticulum (ER) in NT2 stem cells and neurones.

Nuclei

These were labelled with the dye bis-benzamide. Cells were fixed and steps 1 to 9 of the fluorescent immunolabelling method (described above) were carried out. Bis-benzamide was added to a dilution of 1:25 during the last 10 minutes of the secondary antibody incubation.

Endoplasmic reticulum

Rhodamine-conjugated wheatgerm agglutinin (R-WGA) was used as an alternative marker for the ER. Fluorescence immunocytochemistry was carried out as described above, and R-WGA was added to the wells to a final concentration of 10µg/ml in 0.1M PBS 30 minutes prior to addition of the secondary antibody. The secondary antibody

was added to the R-WGA in PBS for 30 minutes so that the total incubation time of the cells with R-WGA was 1 hour.

Purification and concentration of antibodies using protein

G-agarose

The mouse monoclonal antibodies FC8/A9 and EH4/D8 were purified and concentrated using protein G-agarose beads (GammaBind Plus Sepharose, Pharmacia).

The crude antibody was brought to room temperature and adjusted to pH7 with 0.2M Na_2HPO_4 , pH8.

5ml protein G binding buffer (0.02M sodium phosphate, 0.15M NaCl, pH7.4) was added to a vertical column, from a syringe attached to the top of the column, and run through the outlet valve at the bottom of the column until no air bubbles remained.

1ml slurry of protein G beads in suspension was added to the column. Binding buffer was pumped through the column, using pressure from an air-filled syringe on top of the column, until the beads had been packed down to the 0.5ml mark on the column, with 0.5ml buffer remaining on top of the beads, so that no air bubble was introduced (which would reduce binding and/or elution of the antibodies).

The pH-adjusted antibody was added carefully from a syringe to the top of the column, taking care not to disturb the surface of the beads, and allowed by gravity to run through the column, the antibody binding to the protein G beads. The liquid collected from the bottom of the column was kept until it was ensured that the antibody was collected in a subsequent fraction eluted from the column, as described below.

The column was washed with 5ml binding buffer and the eluate was collected (fraction 1).

The amount of 0.05M Tris-HCl, pH8, needed to neutralise 1ml eluting buffer (0.1M glycine, pH 2.6) was determined. 1ml aliquots of eluting buffer were added to 50µl, 100µl, 150µl, 200µl, 250µl and 300µl Tris-HCl, pH8, and tested with pH paper. It was found that 250µl 0.5M Tris-HCl, pH8, was needed to neutralise each 1ml eluting buffer.

The antibody was eluted from the column by adding 5ml eluting buffer to the top of the column and allowing it to run through by gravity. Five 1ml aliquots of eluate were collected (fractions 2-6) in 1.5ml microcentrifuge tubes. 250µl 0.5M Tris-HCl, pH8, was added to each 1ml aliquot of eluate immediately after collection from the column, to neutralise the eluate and therefore preserve the activity of any antibody contained within each fraction.

The column of protein G beads was cleaned with 1.5ml 10% acetic acid (BDH), the eluate was collected (fraction 7) and 1ml 0.5M Tris-HCl, pH8, was added to neutralise it, in case any antibody was collected in this fraction.

The beads were equilibrated with 20ml binding buffer and the column was sealed and stored at 4°C for re-use.

The optical densities and protein concentrations of the fractions collected were measured at 280nm using a Genequant II spectrophotometer.

ELISA

Enzyme-linked immunosorbent assay (ELISA) was used to confirm that the antibodies concentrated with protein G were still active, and to determine the relative concentrations of the original and concentrated samples. Alkaline phosphatase-conjugated secondary antibody was used, followed by the substrate para-nitrophenyl phosphate. The absorbance of the reaction product, para-nitrophenol, was measured using a plate reader.

'Test' wells of a flat-bottomed 96-well plate were coated with 100µl per well of 5µg/ml antigen conjugated to BSA, in PBS. 100µl per well of 5µg/ml BSA/PBS was added to 'control' wells.

The plate was wrapped in plastic film to prevent evaporation and incubated at room temperature overnight or at 37°C for 1 hour.

The plate was rinsed with distilled water from a wash bottle to remove any unbound material.

All wells were blocked with 100µl 1mg/ml BSA/TBS for 30 minutes. The plate was rinsed with distilled water.

100µl of primary antibody diluted in BSA/TBS was added to each well and incubated for 2 hours at room temperature. The plate was rinsed three times with TBS.

100µl of alkaline phosphatase-conjugated secondary antibody, 1:1000 in BSA/TBS, was added to each well and incubated for 45 minutes at room temperature. The plate was rinsed three times with TBS.

100µl of 10mM para-nitrophenyl phosphate (substrate) in alkaline phosphate (AP) buffer was added to each well. The reaction was stopped by addition of 100µl per well of 1M NaOH (BDH). Absorbance was measured using a plate reader.

Electron Microscopy

Four different methods were tested for collecting, fixing and embedding NT2 stem cells and neurones:

Stem cells:

1. Stem cells were removed from the flasks with cell dissociation solution (Sigma Chemical Co), spun down at 1200 rpm for 5 minutes and fixed as described below. They were then embedded in Unicryl resin.

Neurones:

2. Neurones were scraped from the flask using a flexible plastic rod and the largest individual clusters of neurones were selected and placed in glass vials, fixed as described below and stained with osmium tetroxide. These cells were then embedded in araldite resin in gelatine capsules as described below.
3. Neurones were fixed *in situ* on the glass slides, stained with osmium tetroxide and embedded in araldite resin by placing pre-hardened blocks onto a small amount of unpolymerised resin over the clusters of neuronal cell bodies. When the whole block was polymerised it was snapped off, with the neurones now embedded in it.
4. Neurones were removed from the flasks mechanically (by striking the side of the flask), and spun down in a bench-top microcentrifuge (Gallenkamp) in 1.5ml

microcentrifuge tubes (Scotlab) at 1000 rpm for 5 minutes (which should be slow enough to preserve morphology since NT2 neurones will still grow following centrifugation at this speed). The neurones were then fixed by various methods, as described below. Some of these neurones were stained with osmium tetroxide and embedded in araldite resin and some were embedded in Unicryl resin.

Fixing cells for electron microscopy

Before staining with osmium tetroxide at least three samples of neurones collected by each of the methods described above were fixed for one hour in one of each of the following fixatives:

- 4% paraformaldehyde (BDH) in 0.1M phosphate-buffered saline (PBS)
- 4% paraformaldehyde + 1% glutaraldehyde (BDH) in 0.1M PBS
- 2% paraformaldehyde in 0.1M PBS
- 2% paraformaldehyde + 1% glutaraldehyde in 0.1M PBS
- 2% glutaraldehyde in 0.1M PBS

Cells were then washed briefly with 0.1M PBS.

Before embedding in “Unicryl” resin, neurones which were to be used for immunocytochemical studies (not stained with osmium tetroxide) were fixed for 10 minutes in one of each of the following:

- 4% paraformaldehyde in 0.1M PBS
- 4% paraformaldehyde + 0.05% glutaraldehyde in 0.1M PBS

- 2% paraformaldehyde in 0.1M PBS
- 2% paraformaldehyde + 0.05% glutaraldehyde in 0.1M PBS

Cells were then washed briefly with 0.1M PBS.

Embedding cells in araldite resin

Only NT2 neurones, not stem cells, were embedded in araldite resin. Following collection and fixation of the neurones by the three methods (2, 3 and 4) described above they were processed further either floating in glass vials (method 2), *in situ* on the slides (method 3), or as pellets in the bottoms of 1.5ml microcentrifuge tubes (Scotlab) (method 4). When the cells were in vials or microcentrifuge tubes the reagents were carefully added and removed with pasteur pipettes. When the neurones were still attached to the slides the reagents were pipetted onto the horizontal slides, then poured off following incubation.

1. The PBS used to wash the fixative from the cells was removed.
2. Osmium tetroxide was added and incubated for 1 hour at room temperature in the fume hood.
3. Cells were washed with 0.1M PBS for 5 minutes three times.
4. The cells were dehydrated in serial alcohols: 2 minutes in each of 50%, 75%, 95%, 100%, then 100% dehydrated ethanol (BDH).
5. 1,2-epoxypropane was added and incubated for 30 minutes at room temperature in the fume hood.

6. The 1,2-epoxypropane was removed and replaced with 1:1 epoxypropane:araldite resin containing 1 drop (from a pasteur pipette) of B.D.M.A. accelerator per ml of resin. This was incubated overnight on a mixer in the fume hood.
7. The cells were incubated with araldite resin containing 1 drop of B.D.M.A. accelerator per ml of resin for 8 hours in the fume hood.
8.
 - Clusters of neurones collected by scraping (method 2 above) were transferred to gelatine capsules with 2 drops of araldite resin + accelerator in the bottom, then the capsules were filled to the top with resin + accelerator. These were then placed in an oven at 60°C for 48 hours until the resin had polymerised. (If left in the oven for longer than 48 hours the resin became brittle and sections could not be cut from it.)
 - Neurones that were processed on the slides (method 3 above) were covered with a small drop of unpolymerised araldite resin + accelerator, then pre-hardened blocks of resin were positioned over this and the slides were incubated at 60°C in the oven for 48 hours.

The pre-hardened blocks of resin were prepared by filling empty gelatine capsules with resin + accelerator and incubating in the oven at 60°C for 48 hours, then the ends of the polymerised blocks were sawn off giving a flat surface to place over the cells.

- Neuronal pellets collected by centrifugation were embedded by filling the microcentrifuge tubes with araldite resin + accelerator. These were then incubated in the oven at 60°C for 48 hours until the resin was polymerised.
9. The polymerised resin containing the neurones was removed from the gelatine capsules and the microcentrifuge tubes using a razor blade. The blocks of polymerised resin on the glass cell culture slides were removed by trimming around the edges of the resin on the slides with a razor blade then carefully lifting the block away from the slide with the aid of the razor blade.

Embedding cells in Unicryl resin

Stem cells:

1. Stem cells were removed from the flasks by incubating with cell dissociation solution (Sigma Chemical Co) for 5 minutes at 37°C.
2. They were spun down in 1.5ml microcentrifuge tubes at 1200 rpm for 5 minutes, resuspended in fixative (one of each of the four described above) and agitated gently for 10 minutes to ensure fixation of all of the cells.
3. The cells were spun down again at 1000 rpm for 5 minutes then rinsed gently with 0.1M PBS avoiding disturbing the pellet.
4. The cell pellets were then dehydrated in graded alcohols: 2 minutes in each of 50%, 75%, 90%, 100% and 100% dehydrated ethanol (BDH).
5. 1ml Unicryl resin was added to each of the microcentrifuge tubes and incubated overnight at 4°C.

6. The Unicryl resin was aspirated and replaced with 1ml per tube of fresh resin, and left under an ultra-violet light in the cryostat (Bright Instrument Co. Ltd.) until polymerised (2–3 days). Initially tubes were left in different positions in the cryostat to determine the optimum position (and therefore temperature) for polymerisation of the resin. Once this had been determined the tubes were always left in the same place in the cryostat during polymerisation. The ultra-violet lamp was placed 15cm away from the tubes.
7. The microcentrifuge tubes were cut away from the polymerised blocks of resin with a razor blade.

Neurones:

1. Neurones were removed from the flasks mechanically (by striking the side of the flask)
2. The neurones were spun down in 1.5ml microcentrifuge tubes at 1000 rpm for 5 minutes (which should be slow enough to preserve morphology since NT2 neurones will still grow following centrifugation at this speed).
3. The neurones were resuspended in fixative and agitated gently for 10 minutes, then they were spun down again, rinsed, dehydrated and embedded as described above (steps 3–7) for stem cells.

Coating nickel grids with pyroxylin

A water bath was prepared in a glass dish (surface area approximately 15cm x 15cm) and dust was removed from the surface of the water by dragging fibre-free velin paper across it.

One drop (from a pasteur pipette) of 1.5% pyroxylin in amyl acetate was added to the surface of the water bath.

Once the pyroxylin had spread over the entire surface of the water bath (seen as a multicoloured sheen on the water surface) the nickel grids were placed one at a time, in rows, on the surface. The grids were placed dull surface facing downwards since the sections were to be collected on the dull surface.

A square of bench-coating paper was used to collect the grids from the water bath. The paper was held shiny side facing the grids and rocked swiftly across the grids so that they stuck to the paper.

The grids were dried overnight in a petri dish under a lamp, then removed from the paper when needed.

Cutting and collecting sections for EM

Sections were cut with a Reichert ultra-microtome. Glass knives were made and a “boat” was made on each knife by sticking foil tape loosely around the top of the knife, forming a well. This was sealed with paraffin wax, filled with water, and the sections were allowed to float onto the water when cut. Semi-thin sections were collected from the water bath with a paint brush and placed on glass microscope slides. Ultra-thin sections from araldite resin blocks were collected on formvar-coated copper grids and sections from Unicryl resin blocks were collected on pyroxylin-coated nickel grids.

Staining semi-thin sections with toluidine blue

The section(s) on each slide were covered with toluidine blue and the slides were placed on a hot-plate for approximately 2 minutes, not allowing the toluidine blue to dry.

The toluidine blue was washed off with 70% ethanol (BDH) from a wash bottle. This removed excess stain from the tissue.

The sections were rinsed with distilled water from a wash bottle and observed under a light microscope.

Staining ultra-thin sections with uranyl acetate and lead citrate

A square of parafilm (American National Can) was placed in the bottom of a black petri dish with the surface of the parafilm that was adjacent to the protective paper facing upwards.

For each grid that was to be stained a drop of uranyl acetate was placed on the parafilm with a pasteur pipette.

A grid was placed carefully onto each drop of uranyl acetate with the section facing downwards. The lid was put on the petri dish to exclude light and the sections were incubated for 15–20 minutes.

Each grid was removed with a pair of forceps and rinsed carefully with distilled water from a wash bottle. Excess water was blotted from the grids with filter paper (Whatman).

A drop of lead citrate for each grid was placed on a fresh square of parafilm in the petri dish. Care was taken not to breathe on the lead citrate because carbon dioxide reacts with the lead citrate to form lead oxide crystals. These crystals appear as black deposits under the electron microscope, obscuring the section.

Each grid was placed, section down, onto a drop of lead citrate, the lid was replaced on the petri dish and the sections were incubated with the lead citrate for 2 minutes.

The sections were rinsed with distilled water from a wash bottle and blotted with filter paper to remove excess water, then stored for examination under the electron microscope.

In situ hybridization

AD and control brains (numbered S24–S158) were donated via the Alzheimer's disease Society from Yorkshire to this laboratory directly. Pathological diagnosis was carried out by Professor R. C. A. Pearson in this laboratory. The tissue sections used were 10µm-thick frozen sections that had previously been mounted on gelatin-coated glass microscope slides and pre-treated with 4% paraformaldehyde (BDH), 0.25% acetic anhydride in triethanolamine hydrochloride and dehydrated in alcohols and chloroform (BDH). The oligonucleotide probe was labelled with [³⁵S]. All equipment and solutions used for *in situ* hybridization were autoclaved to destroy any enzymes (nucleases, particularly ribonucleases) with which they may have been contaminated. Gloves were worn at all times to minimise contamination by ribonucleases from the skin.

The sequence of the TGF-β1 antisense oligoprobe (Gibco BRL) was:

5'CGT GGA GCT GAA GCA ATA GTT GGT GTC CAG3'

The sequence of the TGF-β1 sense oligoprobe (Gibco BRL) was:

5'CTG GAC ACC AAC TAT TGC TTC AGC TCC ACG3'

Radiolabelling of oligonucleotide probe

This procedure was carried out using an “oligonucleotide 3’ end labelling system” (NEN/DuPont). The oligoprobe was labelled with $^{35}\text{SdATP}$. 5 μl oligoprobe, 2.5 μl CoCl_2 , 12.5 μl terminal transferase reaction buffer, 7.5 μl pure H_2O (from the kit), 5 μl $^{35}\text{SdATP}$ and 2.5 μl terminal transferase enzyme were added to a reaction vial. This was spun down in a centrifuge at 10 000 rpm for 10 seconds to collect the liquid at the bottom of the vial. The vial containing the reaction mixture was floated in a water bath (Gallenkamp) at 37°C for 1 hour. Following the incubation the reaction was stopped by adding 400 μl reagent A (from the kit) and cooling on ice.

Separation of radiolabelled oligoprobe from unincorporated nucleotides

The radiolabelled probe was separated chromatographically from unincorporated nucleotides using a “NENSORB” nucleic acid purification cartridge (NEN/DuPont) as follows:

The sorbant was settled to the bottom of the purification cartridge by gently tapping it, then the cartridge was clamped vertically.

2ml 100% methanol (HPLC grade; BDH) was added to the purification cartridge to pre-wet the sorbant. This was gently pushed through the column with a syringe until the meniscus reached the top of the sorbant, taking care not to allow the column to dry out.

2ml Reagent A from the oligonucleotide 3’end labelling system (NEP-100; NEN/DuPont) was pushed through the column slowly with the syringe.

The sample containing the labelled probe was added to the cartridge and pushed through gently. The effluent was collected in a microcentrifuge tube (fraction 1). Any unincorporated nucleotides should have been collected in this fraction.

The cartridge was washed gently with 2ml Reagent A and the effluent was collected in microcentrifuge tubes (fractions 2 and 3).

The radiolabelled probe was eluted with 1ml 50% ethanol (BDH). As this was pushed through the column 3 drops of the effluent were collected in tube 4, 14 drops in tube 5, 5 drops in tube 6 and the rest in tube 7.

5 μ l of each fraction was placed in a scintillation tube with 4ml scintillant (Optiphase, Pharmacia LKB) and counted on the scintillation counter (Pharmacia LKB). The highest level of radioactivity corresponds to the fraction containing most of the labelled probe.

The labelled probe was stored at 4°C until used (less than 48 hours).

Care was taken at all times to ensure that the column did not dry out because this would introduce air bubbles that would reduce binding and/or elution of the probe.

***In situ* hybridization procedure**

Calculation of probe labelling

The value obtained from the scintillation counter gives the number of counts in 5 μ l of the fraction containing the labelled probe. From this the volume containing 10⁶ cpm was calculated, and this volume, diluted in hybridization buffer, was added to each section as follows:

Dilution of probe in hybridization buffer

Sufficient hybridization buffer was thawed so that all of the sections could be covered with 100 μ l of buffer. The tube containing the hybridization buffer was placed in a beaker of boiling water for 10 minutes. The buffer was then quenched by placing the tube in an ice-filled container.

The volume of probe required to give a final activity of 10^6 counts per minute (cpm) was added to the hybridization buffer along with 1M dithiothreitol (DTT) to a final concentration of 1% (v/v). This was mixed thoroughly on the "whirlimix".

Calculation of the melt temperature

The melt temperature, T_m , (the temperature at which 50% of the hybrids will spontaneously dissociate) was calculated using the following formula:

$$T_m (\text{°C}) = 16.6\log[M] + 0.41[\text{Pgc}] + 81.5 - \text{Pm} - \text{B/L} - 0.65[\text{Pf}]$$

Where:

M = molar concentration of Na^+ , to a maximum of 0.5 (1 \times SSC contains 0.165M Na^+),

Pgc = percentage of guanine and cytosine in the probe sequence,

Pm = percentage of mismatches between the probe and the target mRNA (usually = 0 for synthetic oligoprobes),

Pf = percentage of formamide in the buffer,

B = 675 for synthetic oligonucleotides of up to 100 bases,

L = probe length in bases.

Hybridization procedure

The incubator was set to the incubation temperature (T_i) for hybridization. This was 15°C lower than the T_m calculated using the formula above.

2 sheets of filter paper (Whatman, no. 1) were placed in the bottom of a bioassay dish (Nunc). This was dampened with 4× standard citrate saline (SSC) to keep the chambers humid and prevent the sections from drying out.

The slides were laid on the filter paper and each section was covered with 100μl hybridization buffer containing 10^6 cpm labelled probe and 1% DTT.

Each section was covered with a square of parafilm (American National Can) to help prevent evaporation.

The lids were placed on the trays (Just Plastics Alternatives) and the sections were incubated overnight at the T_i .

Post-hybridization washing

This removes excess, unhybridized probe from the sections. Care was taken not to allow the slides to dry out until the washing procedure was finished. If the slides are allowed to dry this increases the background staining dramatically, over the slide itself as well as the section. The washing temperature (T_w) used was 15°C lower than the T_m in washing buffer, calculated using the formula described above.

The squares of parafilm were removed from the sections by dipping the slides into a large beaker of 1× SSC at room temperature. Each slide was immediately transferred to a rack in a container filled with 1× SSC so that the slides were not allowed to dry out.

When the parafilm had been removed from all of the slides, the racks of sections were washed in 1× SSC at Tw for 15 minutes. This was repeated 4 times.

The sections were washed in fresh 1× SSC at room temperature for at least 1 hour.

The sections were dipped briefly in purified water (MilliRo 6 Plus, Millipore) to remove excess salt.

The slides were laid on laboratory paper, covered and left to dry overnight.

Autoradiography using film

The sections were exposed to tritium sensitive film (Hyperfilm, Amersham). This film requires long exposure times but has a fine grain emulsion, thus giving good localisation of signal.

Rows of the slides were attached to card with double-sided sticky tape, the sections facing away from the card.

In the darkroom, the card was placed in the x-ray cassette (Genetic Research Instrumentation, Ltd.). The film was laid against the slides with the emulsion-coated surface of the film facing the sections.

The cassette was sealed tightly to exclude any light and stored at room temperature for 3–5 weeks to allow exposure of the sections to the film.

The following solutions were made up for developing the film:

- **Developer:** 400ml Contrast FF (Ilford) in 1600ml purified water
- **Stop bath:** 40ml glacial acetic acid (BDH) in 1960ml purified water (2% v/v)

- **Fixer:** 400ml Hypam Fixer (Ilford) in 1600 ml purified water

In the darkroom, the film was developed by immersing in trays (Just Plastics Alternatives) containing these solutions in the following order:

- a). Developer (5 minutes).
- b). Stop bath (2% acetic acid) (30 seconds).
- c). Fixer (5 minutes).
- d). Tap water (at least 10 minutes). The tap was kept running slowly during this wash.

The film was hung up to air dry.

Autoradiography using dipped sections

Following hybridization of sections the slides were dipped in photographic emulsion (K5 Nuclear emulsion, Ilford). This allows more precise localisation (to single cells when using ^{35}S) of the signal. The radioactivity from the hybridized probe exposes the silver grains in the emulsion. The silver grains can be seen over the site of hybridization following development.

This procedure was carried out following exposure of the sections to tritium sensitive film.

The emulsion was liquefied from its solid form in the dark room. The emulsion was transferred, using plastic forceps, into a glass cylinder in a water bath (Gallenkamp) at 43–45°C until liquefied (about 45 minutes).

The emulsion was diluted with an equal volume of purified water containing a drop of glycerol per 10ml water, at 45°C, and mixed with a glass rod. Care was taken not to introduce air bubbles. The glycerol was added to help to 'plasticize' the emulsion.

The emulsion was left until a blank slide could be dipped into it without bubbles being present in the layer of emulsion coating the slide.

Each of the slides with hybridized sections on them was dipped into the emulsion, then removed slowly and steadily to coat them with a layer of emulsion of even thickness.

The back of each slide was wiped clean and placed flat on an ice-cold metal plate until the emulsion formed into a gel (approximately 15 minutes).

The slides were placed flat on the bench at room temperature to dry (2–3 hours).

Once dry the slides were placed in racks in light-tight boxes containing silica gel (a drying agent) (BDH) and wrapped tightly in black plastic. Decreased humidity minimises fading of the image. The boxes were placed in the refrigerator for 8 weeks to expose the emulsion to the sections.

Before developing, the slides were warmed to room temperature. In the darkroom, the slides were developed by immersing in these solutions in the following order:

- a). Developer (Ilford Phenisol, diluted 1:4 with purified water, 2 minutes).
- b). Stop bath (2% acetic acid, 30 seconds).
- c). Fixer (30% w/v sodium thiosulphate (BDH) in purified water, 5 minutes).
- d). Cold, running tap water (30 minutes).

e). Purified water (briefly).

Sections were counterstained with cresyl violet as follows:

The slides were immersed in 0.1% cresyl violet for 1–2 minutes, then dehydrated in serial alcohols (70%, 80%, 95%, 100% × 2, 2 minutes in each).

The slides were incubated in xylene for at least 15 minutes, then the sections were coverslipped using DPX as mountant.

Quantification of autoradiography

Quantification of the autoradiographic signal from film allows analysis of regional distribution of signal. The signal from dipped sections shows the cellular distribution of the hybridized probe. However, the signal from the dipped sections could not be quantified because there was not sufficient signal present.

Film autoradiography

The film was transilluminated with a light box and the grey density was measured using a video camera and “Freelance” Image Analysis system. The ambient light level was kept constant by carrying out the quantification in a dark room.

“Shade correction” was used to control for differences in background grey level between films. The grey level of a blank area of the film was measured and this was subtracted from every autoradiogram image captured from that film. The mean grey level of 10 circular areas of the same size was calculated for both the grey matter (cortex) and white matter of each section.

The lens diaphragm and magnification of the video camera were kept constant so that all measurements were comparable. The film was clipped down onto the light box so that it did not curl up, altering the grey level measured.

Immunohistochemistry

Blocks of temporal and visual cortex were available from the brains of 16 normal and 14 Alzheimer cases. AD patients were those of Professor Gordon Wilcock in Bristol. Brains were collected with fully informed consent. Patients were at end-stage of dementia. Pathological diagnosis was carried out by Dr. J. W. Neal in Cardiff and paraffin-embedded blocks were provided. The brains had been fixed in 10% formalin and the blocks were stored in 10% formalin prior to embedding in paraffin wax. Further AD brains (numbered S125–S181) were donated via the Alzheimer's disease Society from Yorkshire to this laboratory directly, and pathological diagnosis was carried out in this laboratory by Professor R. C. A. Pearson. These brains had been fixed in 10% formalin and blocks of middle temporal cortex or whole temporal cortex were embedded in paraffin wax as described below.

Embedding blocks of human brain tissue in paraffin wax

Steps 1–5 were carried out in the fume hood.

1. Blocks were taken from 10% formalin and incubated overnight in 70% ethanol (BDH).
2. The blocks were incubated in 80% then 95% ethanol, each for 2 hours.

3. The blocks were incubated in 100% ethanol for 1 hour, then transferred to fresh 100% ethanol for a further hour.
4. The tissue was incubated in chloroform (BDH) overnight.
5. The blocks were transferred to jars of hot (60°C) liquid paraffin wax in an incubator for 3 hours, then this was replaced with fresh paraffin wax for a further 3 hours.
6. The paraffin wax was replaced again, the incubator was sealed and a pump was used to create a vacuum in the incubator for 3 hours. This ensured that the wax penetrated the brain tissue fully.
7. The blocks of brain tissue were embedded in paraffin wax that was then allowed to cool and harden overnight at room temperature.

Cutting and mounting paraffin sections of human brain tissue

10µm sections were cut using a Spencer '820' rotary microtome.

Sections were floated on a water bath (Gallenkamp) at approximately 45°C and collected on tepsa-coated glass microscope slides.

The sections were blotted gently with fibre-free paper to remove excess water then dried overnight in an incubator at 60°C.

Immunohistochemical staining of paraffin-embedded human brain sections

When staining paraffin sections 0.1M tris-buffered saline (TBS) was used instead of 0.1M PBS that was used when staining NT2 cells.

1. Sections were de-waxed in xylene for 20 minutes.
2. Sections were hydrated through serial alcohols (100% x 2, 95%, 80% then 70% ethanol, 2 minutes each) to distilled water (5 minutes).
3. If required sections were microwaved in 0.05M Tris-HCl, pH 7.0, then washed in distilled water for 5 minutes three times.
4. Sections that were to be labelled with anti- β -amyloid antibody were incubated in 80% formic acid for 15 minutes then washed in 0.1M TBS for 15 minutes three times.
5. Endogenous peroxidase activity was quenched by incubating sections in 0.5% H₂O₂ in methanol (BDH) for 25 minutes.
6. Sections were washed in TBS for 10 minutes three times.
7. Non-specific binding sites were blocked with normal serum (supplied in a Vectastain Elite ABC kit) from the species in which the secondary antibody was raised, as recommended in the manufacturers' instructions.
8. Sections were washed briefly in TBS.
9. Sections were incubated with primary antibody diluted in TBS containing 3% triton X-100 and 3mg/ml carrageenan for 1 hour at room temperature or overnight at 4°C.
10. Sections were washed in TBS for 10 minutes three times.
11. Sections were incubated for 30 minutes at room temperature with secondary antibody conjugated to biotin (from the Vectastain Elite ABC kit), diluted in TBS according to the manufacturers' instructions.

12. Sections were washed in TBS for 10 minutes three times.
13. Sections were incubated with avidin and biotinylated horseradish peroxidase macromolecular complex (ABC) from the Vectastain Elite ABC kit for 30 minutes at room temperature. This complex was made 30 minutes before use, by addition of Avidin DH and biotinylated horseradish peroxidase H reagents (from the kit) to TBS as described by the manufacturers' instructions.
14. Sections were washed in TBS for 10 minutes three times.
15. Sections were incubated with diaminobenzidine (DAB) peroxidase substrate solution, enhanced with nickel, until the desired staining intensity was reached.
16. Sections were washed for 5 minutes in tap water.
17. Sections were dehydrated through serial alcohols (70%, 80%, 95%, 100% x 2 ethanol) to xylene.
18. Sections were mounted with DePeX.
19. Photographs of the stained sections were taken using a Leitz 'Dialux 22' microscope.

Steps 1, 2, 4 and 14–17 were carried out in the fume hood.

Immunolabelling of KPI–APP in human brain sections

This immunolabelling procedure included treatment of tissue sections with 2–mercaptoethanol and iodoacetic acid, as follows:

Endogenous peroxidase activity was quenched by incubation in 0.5% H₂O₂ (Sigma Chemical Co.) in methanol.

Sections were microwaved in 0.05M TRIS-HCL (BDH Laboratory Supplies), pH 7.0 for 7 minutes.

Disulphide bonds were reduced with 0.14M 2-mercaptoethanol (Sigma Chemical Co.) in 0.5M TRIS.HCl pH 8 and 1mM EDTA for 3 hours in the dark at room temperature.

Sections were washed for 3 minutes in distilled water and reduced sulphhydryl bonds were alkylated in 250mgml⁻¹ iodoacetic acid (Sigma Chemical Co.) in 0.1M NaOH (BDH), diluted 1 in 10 in 0.5M TRIS.HCl pH 8 and 1mM EDTA, in the dark at room temperature for 20 minutes.

Immunostaining was carried out using a Vectastain Elite ABC kit (Vector Laboratories), as above.

Sections were incubated with anti-KPI antibody, at 1:400 dilution, overnight at 4°C.

Visualisation of the secondary antibody was achieved using diaminobenzidine (DAB), enhanced with nickel (Vector Laboratories).

Quantification of KPI-containing APP in human brain sections

Following immunohistochemical localisation of KPI-containing APP isoforms (KPI-APP) in normal and Alzheimer's disease (AD) paraffin-embedded brain sections, superficial, middle and deep cortical KPI-APP load was quantified using 'Freelance' image analysis. Sections were analysed blind by colour-coding and numbering slides.

During image analysis the ambient light level was kept constant by working in a darkroom and illumination of the slides by the microscope lamp was kept constant. "Shade correction" was used to subtract the background grey level (at the edge of the coverslip, outside the section) from the grey levels measured from the sections. S178 was used as a reference for image analysis by inclusion with each batch of slides that was labelled. S178 therefore controlled for differences in labelling intensity between batches of sections that were immunostained separately. Each reference section was used to determine the threshold for grey level measurement for the corresponding batch of slides. The mean grey level recorded from each section was expressed as a percentage of the mean grey level of the reference section from the same batch. The reference sections were used also to select the minimum object area that would be measured on each section in order that all cells would be measured. In temporal cortex this was $20\mu\text{m}^2$ and in visual cortex the minimum object area was $10\mu\text{m}^2$. The number of objects above the minimum grey level and minimum object area was then measured in each section, and the area and mean grey level of each of these objects were measured. Large blood vessels and plaques were eliminated from the objects selected by the computer for measurement, so that as far as possible the only objects that were measured were cells.

Measurement of amyloid load of temporal cortex of AD brains

Paraffin-embedded sections of middle temporal gyrus were immunolabelled with anti- β -amyloid antibody (Dako), for those brains in which amyloid load had not been measured previously (Radenahmad N., 2000). The amyloid load (percent) for each case was measured over a field that included the entire depth of the temporal cortex, using the Freelance image analysis programme. This measurement thus included all

β -amyloid-immunopositive structures, such as plaques, cerebro-vascular amyloid and diffuse amyloid.

Statistical analysis

All statistical analyses were carried out using SPSS for Windows on a PC. Non-parametric data were analysed using the Mann-Whitney U-Wilcoxon Rank Sum W test. Parametric data were analysed using Student's t-test when Levene's test was not significant. Confounding variables that might affect results were examined using regression analysis.

Materials

Unless otherwise stated, all tissue culture plasticware was obtained from Nunc Inc. and cell culture media were obtained from Gibco BRL. Pipettes and tips were obtained from Gilson. Glass microscope slides were from Chance Propper Ltd. and glass staining jars were from Gallenkamp. Slides were held in plastic staining racks from Just Plastics Ltd. Hotplate/magnetic stirrer and 40°C oven were from Gallenkamp. Unless otherwise indicated, all other reagents were obtained from Sigma Chemicals.

CHAPTER 3: LOCALISATION OF APP AND APLP2

IN NTERA 2 STEM CELLS AND NEURONES

Introduction

NTERa 2 cells as a model system for investigating APP processing

The pluripotent embryonal carcinoma (EC) cell line NTERa 2/D1 (NT2) was cloned from the human teratocarcinoma cell line Tera 2 (Andrews *et al.*, 1984). It is unique in its potential, upon treatment with retinoic acid, to undergo terminal differentiation into a neuronal phenotype (Andrews, 1984). Over 99% pure post-mitotic neuronal cultures can be obtained from this procedure (Pleasure *et al.*, 1992). These neurones resemble closely human central nervous system (CNS) neurones. They contain many neuronal markers, including axonal and dendritic markers, such as highly phosphorylated neurofilament proteins and microtubule-associated protein 2 (MAP 2) respectively, of polarised neurones (Pleasure *et al.*, 1992). NT2 neurones (NT2N) are thus the best available *in vitro* model of human CNS neurones.

Since only the brain is affected by the characteristic pathology of AD it is useful to have a model system in which neuronal versus somatic cells can be studied with respect to APP processing. NT2 stem cells provide a 'control' equivalent non-neuronal model that can be studied in parallel with NT2N cells, to search for any differences between the ways that human CNS neurones and non-neuronal cells process APP and respond to insults that may participate in AD pathogenesis. This cell line was therefore selected to study the subcellular processing of APP in neurones and stem cells, and the effects of

cellular stress, simulated by heat-shock and no feeding, on the subcellular distributions of APP and β -amyloid.

Identification of intracellular compartments in NT2 cells

The aim of this work was to identify the intracellular compartments where APP and β -amyloid are concentrated in NT2 stem cells and neurones. Initially techniques were optimised for identifying the endoplasmic reticulum (ER), Golgi bodies, the trans-Golgi network (TGN), lysosomes and nuclei in both stem cells and neurones. Cells were then double-labelled with antibodies to APP, APLP2 or β -amyloid and markers for intracellular compartments.

Immunolocalisation of APP, APLP2 and β -amyloid in NT2 cells

The presence of APP has been demonstrated in NT2 stem cells and neurones, and β -amyloid has been immunoprecipitated from the cell lysates and conditioned media of NT2 neurones (Wertkin *et al.*, 1993). However, prior to this study the subcellular locations of APP and its derivatives had not been investigated immunocytochemically in NT2 cells.

Indirect immunocytochemistry was used to identify APP, APLP2 and β -amyloid. Non-transfected cells were used to avoid potential alterations of processing pathways arising due to overexpression of APP.

The identification of the amyloid precursor-like proteins, APLP1 and APLP2, which are highly homologous to APP, led to the discovery that antibodies designed previously to recognise APP also recognise APLP2 (Slunt *et al.*, 1994). APLP2 is present in human

brain, as well as many cultured cell lines including NT2, so the intracellular distribution of APLP2 in NT2 cells was characterised immunocytochemically so that it could be compared with the distribution of APP. In addition, an antibody (Alz-90) that recognises only APP and not APLP2, was used to visualise APP in these cells. If APP and APLP2 are processed via different pathways, then previous work that employed antibodies to APP may have resulted in the identification of APLP2 as APP. The locations of these two proteins in NT2 neurones may indicate whether or not they follow similar processing pathways in human brain neurones, as well as shedding light on the identities of cellular compartments in which they are concentrated and thus the route(s) by which they are processed *in vivo*.

Results

Optimisation of cell culture

Stem cells and neurones were plated for immunocytochemistry in chamber slides rather than on coverslips because the chamber slides were easier to handle and allowed more economical use of reagents (in particular neurones and antibodies) because of the small chamber sizes.

When neurones were plated out onto glass coverslips or chamber slides they formed large, floating clusters and did not adhere to the glass. For immunocytochemical detection of antigens a single layer of cells was required on the slides. Therefore the coverslips or chamber slides were coated with poly-D-lysine. The neurones then adhered to the growth surface but remained in clusters, and their processes remained short, terminating in large growth cones, after a week. The coverslips or chamber slides

were therefore coated with poly-D-lysine followed by matrigel. The cells then adhered to the growth medium in an even layer of single cells and small clusters of cells. After 2–3 days the neurones had grown processes and were still evenly spread over the growth surface, but beyond this length of time the neurones gradually migrated towards each other to form clusters. After a week they had elaborated long processes that were in contact with many other cells. These clusters became larger the longer the cultures were kept (up to 4 weeks), so neurones were fixed three days after being plated on matrigel so that individual cells could be seen following immunolabelling.

Optimisation of immunocytochemical labelling

Following fixation of stem cells with -20°C methanol immunostaining of the Golgi apparatus or endoplasmic reticulum was more clearly visible than in cells that were fixed with -20°C acetone, so -20°C methanol was used to fix cells. Some cells that were immunolabelled with anti- β -amyloid were fixed for 5 minutes or 20 minutes in 2% or 4% paraformaldehyde in 0.1M phosphate-buffered saline (PBS), incubated in 80% formic acid for 10 minutes, then permeabilised in 0.3% triton X-100 for 15 minutes before immunostaining.

To block binding of antibodies to non-specific sites 3mg/ml BSA/PBS or 3% normal serum from the species in which the secondary antibody was raised (in PBS) were found to be more effective than blotto or fish gelatin. Both BSA/PBS and normal serum together were more effective than either blocker on its own. 3mg/ml BSA/PBS prevented non-specific binding more effectively than 1mg/ml BSA/PBS. 5mg/ml normal serum or 5% BSA/PBS were no more effective than 3mg/ml or 3% respectively, so the latter were used in all subsequent experiments.

When triton X-100 was used to permeabilise the cells fixed with -20°C methanol there was no difference in the pattern or intensity of labelling in comparison with untreated cells. Many of the cells that were incubated with triton X-100 became detached from the substrate on which they were fixed. This step was therefore omitted from the immunolabelling procedure when cells were fixed in -20°C methanol.

It was found that there was too small an amount of APP in the cells for its distribution to be seen clearly when detected with primary antibody followed with fluorescently labelled secondary antibody. Therefore biotinylated secondary antibodies were used followed with either streptavidin conjugated to a fluorescent molecule (e.g. fluorescein or rhodamine) or ABC (avidin and biotinylated horseradish peroxidase macromolecular complex) followed by DAB (diaminobenzidine). These methods allowed greater amplification of the signal so that the labelled protein could be localised more accurately and the signal was strong enough for photomicroscopy.

All immunolabelling experiments were repeated at least 3 times to ensure that the results were replicable and consistent.

Purification and concentration of antibodies and ELISA

Spectrophotometry of the eluate collected from the protein-G columns used to purify and concentrate the antibodies FC8 and EH4, showed that fraction 2 (following addition of eluting buffer) contained 0.1mg/ml protein in both cases. The activities of both FC8 and EH4 were shown by ELISA to have been retained following purification and concentration with protein G beads. The ELISAs performed also confirmed that the antibodies had been concentrated, FC8 by $\times 2.63$ (Figure 3) and EH4 by $\times 2.67$ (Figure 4).

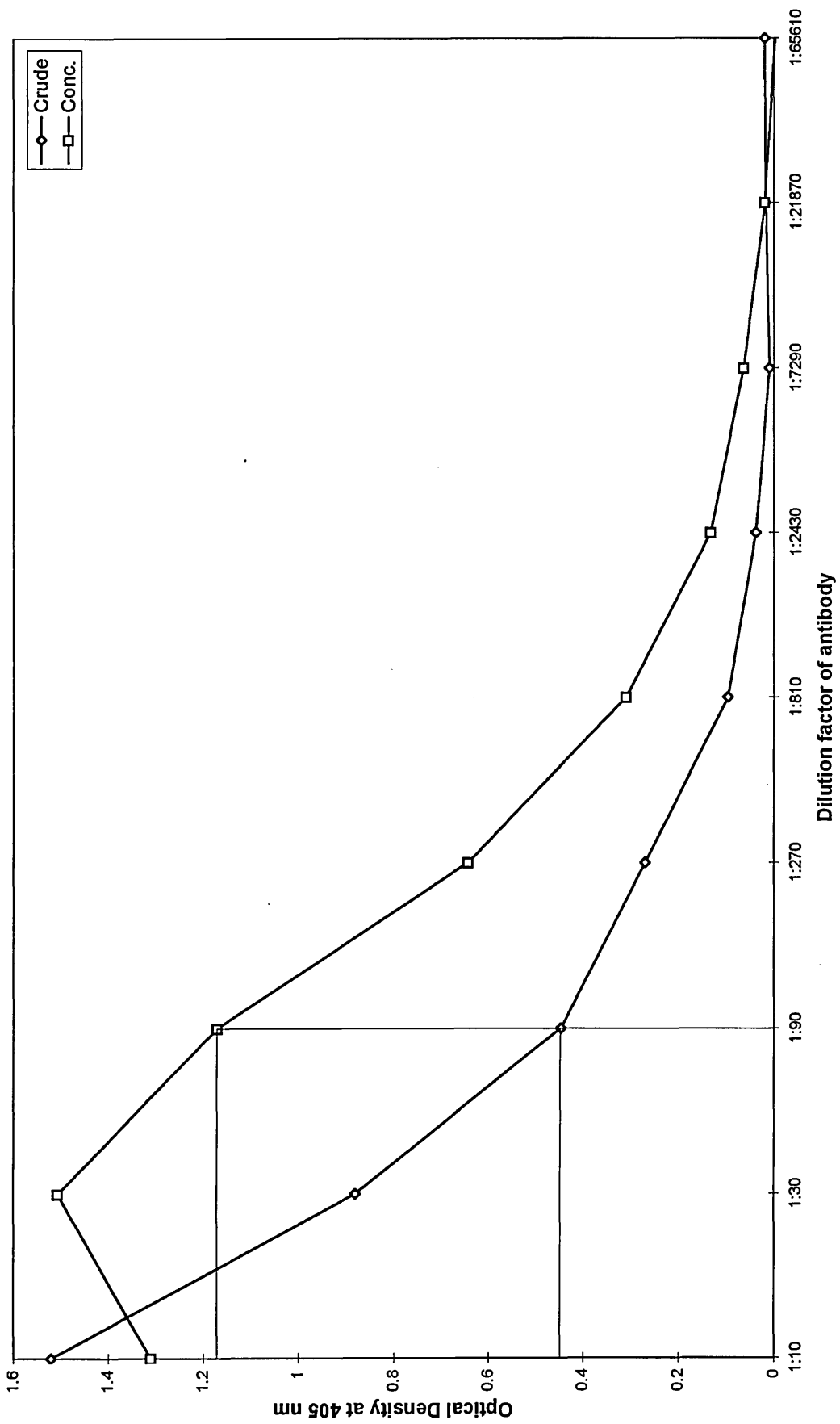


Figure 3
Relative concentrations of crude and concentrated FC8

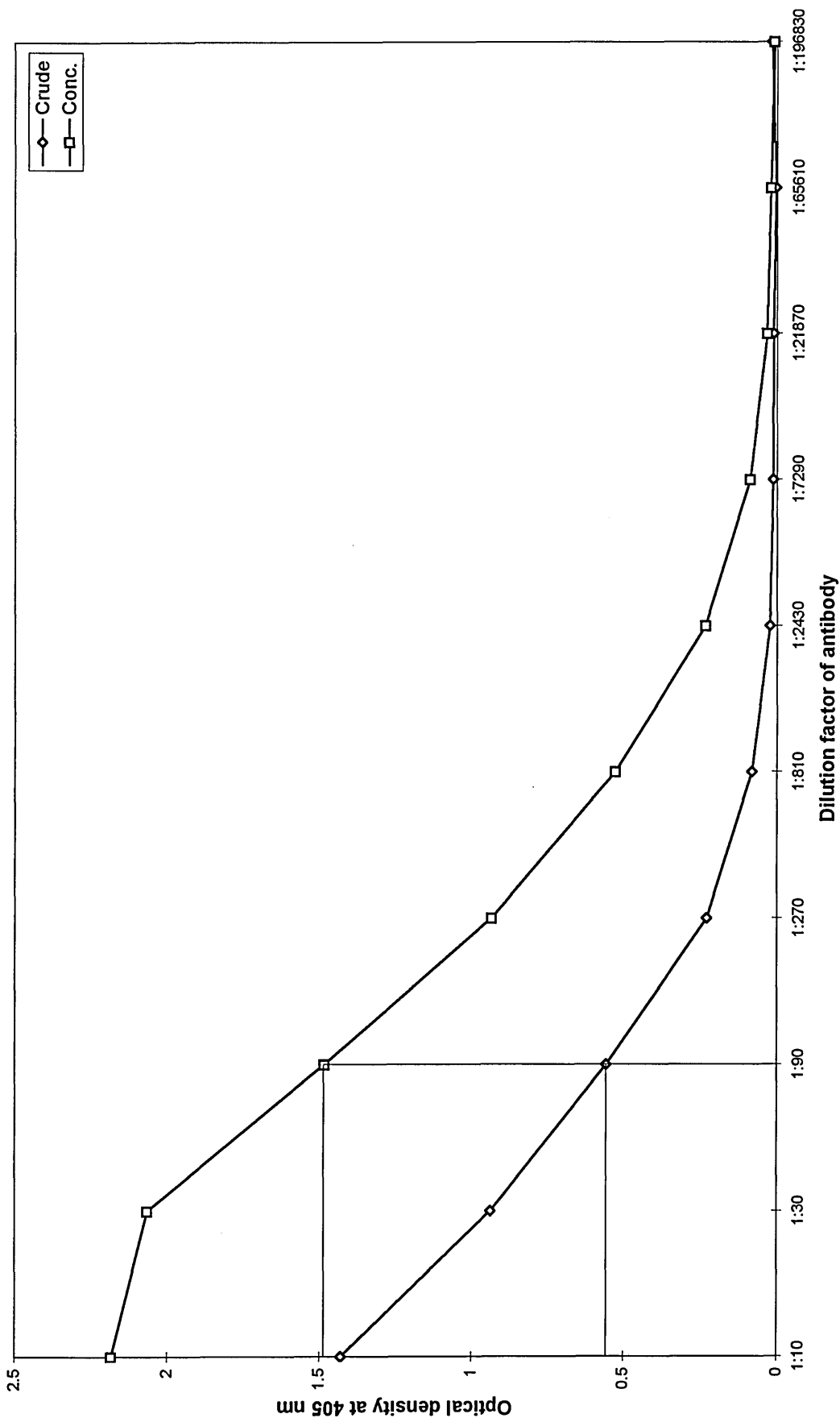


Figure 4
Relative concentrations of crude and concentrated EH4

Immunolocalisation of APP and APLP2 in NTera 2 stem cells

To identify the distribution of specific proteins in stem cells methods were developed by which various subcellular compartments could be identified.

Identification of intracellular compartments

Lysosomes, the Golgi apparatus and endoplasmic reticulum (ER) were visualised using monoclonal and/or polyclonal antibodies. The Golgi apparatus was labelled also with rhodamine-conjugated wheatgerm agglutinin. Nuclei were labelled with bis-benzamide.

Lysosomes

Three antibodies were tested to label lysosomes in stem cells: anti-cathepsin-D, anti-LAMP-1 and anti-LAMP-2 (lysosome associated membrane proteins 1 and 2). Of these anti-LAMP-1 provided the most specific staining (Figure 5). A similar pattern was seen with LAMP-2 immunolabelling (Figure 6), but a slightly larger number of vesicles were immunopositive. With anti-cathepsin-D antibody the cells were intensely immunopositive in the region labelled by the LAMP-1 and LAMP-2 antibodies, but the staining extended beyond the lysosomes. It may have been possible to reduce the staining intensity with this antibody (e.g. by lowering the concentration of primary antibody) to improve its specificity, but the specificity of LAMP-1 was good enough to render this unnecessary. Lysosomes were small and numerous in NT2 stem cells (Figure 5 and Figure 6).

Golgi apparatus

Two antibodies, anti- β -COP and anti-58k, were used to localise the Golgi apparatus. Of these anti-58k (Figure 7 and Figure 8) was found to give slightly more specific labelling, although some labelling was visible beyond the region of the Golgi apparatus with both antibodies. R-WGA presented a similar problem, but had the advantage that it could potentially be used in double-labelling experiments more readily than an antibody because it was less likely to cross-react with antibodies used to label another protein.

When labelled with anti-58k the Golgi apparatus was visible as a cluster of large, intensely stained perinuclear vesicles. Further smaller vesicles that were only faintly stained radiated out through the cytoplasm (Figure 7 and Figure 8).

Endoplasmic reticulum

Two antibodies, anti-PDI (protein disulphide isomerase) and anti-GRP-94, were used to visualise the ER. Of these anti-PDI allowed more specific labelling of the ER, shown in Figure 9.

Nuclei

Nuclei were successfully labelled with the dye bis-benzamide. The stained nuclei appeared blue under the microscope using an ultra-violet filter, which contrasted with the green/red of the FITC/TRITC respectively. However, when the cells were viewed using the blue or green filters (used to view FITC-/TRITC-labelled structures) the staining was so bright that it bled through and the nuclei were still visible.

Immunolabelling of APP and APLP2 in NTera 2 stem cells

The antibodies used to immunolabel APP and APLP2 are described in Table 1, below, and in the appendix (Table 10).

Table 1: Antibodies used for immunodetection of APP and APLP2

Antibody	Antigen raised against	Species raised in	Monoclonal/ Polyclonal
87-4afp	Epitope within C-terminal 20 amino acid residues of full length, membrane-bound, human APP (also recognises APLP2)	Rabbit	Polyclonal
22C11	Epitope within residues 60-100 of the N-terminus of human APP-695	Mouse	Monoclonal
Alz-90	Amino acid residues 511-608 of human APP-695	Mouse	Monoclonal
FC8	Residues 1-19 of β -amyloid (in immunised mice)	Mouse	Monoclonal
EH4	Residues 1-19 of β -amyloid (in immunised mice)	Mouse	Monoclonal
3B11	Residues 596-617 of human APLP2	Mouse	Monoclonal

APLP2 was localised, using the monoclonal antibody 3B11, to large, perinuclear organelles, in the region of the Golgi apparatus (Figure 10 and Figure 11).

Affinity-purified 87-4, a polyclonal antibody that recognises both APP and APLP2, labelled smaller reticular vesicles in NT2 stem cells as well as the darkly stained perinuclear vesicles (Figure 12 and Figure 13) seen with 3B11. The monoclonal antibodies 22C11 and Alz-90 demonstrated that APP extended into many small granularities throughout the cytoplasm (Figure 14 and Figure 15). 22C11 labels both APP and APLP2, but Alz-90 is specific for APP.

Stem cells immunolabelled with FC8, a monoclonal antibody to an epitope within the first 12 amino acids of the β -amyloid sequence of APP, but which does not recognise cleaved β -amyloid, displayed small immunopositive vesicles (Figure 16 and Figure 17). These were similar in appearance and subcellular localisation to those labelled by affinity-purified 87-4. However the larger, more darkly stained perinuclear vesicles seen with 87-4 were not visible. This is consistent with the absence of β -amyloid from APLP2.

Immunostaining with FC8 was very weak so the antibody was concentrated using protein G beads, resulting in a 2.63-fold increase in concentration. Immunolabelling using the concentrated FC8 resulted in slightly darker staining of APP (as seen in Figure 16 and Figure 17) but the contrast between labelled and unlabelled material was not great enough for the antibody to be used for double-immunolabelling.

Immunolocalisation of APP, APLP2 and β -amyloid in NTera 2 neurones

As well as individual identification of subcellular compartments (as performed in stem cells) to aid localisation of APP, APLP2 and β -amyloid, double-labelling experiments were used to localise these proteins more accurately.

Identification of intracellular compartments

As well as the antibodies and markers used in stem cells a further monoclonal antibody was used to label the trans-Golgi network, as described below, to improve the specificity of immunolabelling of this target.

Golgi apparatus

Immunolabelling of the Golgi apparatus with the antibodies (anti- β -COP and anti-58k) used to localise the Golgi apparatus in stem cells was unsuccessful in neurones. Staining extended beyond the cell bodies and into the processes of the neurones. This staining could not be reduced by lowering the concentrations of antibodies used. Rhodamine-conjugated wheatgerm agglutinin labelled the Golgi apparatus in neurones with greater specificity (Figure 18 and Figure 19).

Trans-Golgi network

The monoclonal anti-trans-Golgi network (TGN) antibody labelled the TGN with high specificity. A discrete, perinuclear, reticular structure was intensely immunostained (Figure 20).

Nuclei

The position of the TGN in relation to the nucleus, labelled with bis-benzamide, in an NT2 neurone is illustrated in Figure 21 and Figure 22. More thorough washing (5×5 minutes instead of 3×3 minutes) of the neurones following labelling allowed visualisation of nuclei without the stain bleeding through when cells were viewed through different filters, as occurred with stem cells.

Immunolabelling of APP and APLP2 in Ntera 2 neurones

APLP2 was localised to large, perinuclear vesicles using the antibody 3B11 (Figure 23 and Figure 24) in the region of the TGN. Its distribution was similar in appearance to that seen in NT2 stem cells.

With antibodies 22C11 and Alz-90 APP was visible in structures along the processes of neurones as well as in the perinuclear region (Figure 25 and Figure 26). Alz-90 demonstrated the presence of APP in granular structures in the cytoplasm of neuronal cell bodies (Figure 27 and Figure 28). When labelled with Alz-90, APP was not masked by the presence of APLP2 in the cell body (as it is with 22C11) because Alz-90 recognises only APP and not APLP2.

APP was clearly visible in small granular structures in the growth cones of neurones, whereas APLP2 was not detected in the growth cones with 3B11 (Figure 29–Figure 33).

Co-localisation of APLP2 and APP with the Golgi apparatus in NTera 2 neurones

Neurones were immunolabelled using either 3B11 to detect APLP2 or 22C11 to detect APP (and APLP2) followed with biotinylated secondary antibody, then fluorescein isothiocyanate-conjugated streptavidin. The cells were also incubated with rhodamine-conjugated wheatgerm agglutinin. When examined with a confocal microscope APLP2 was found to be present in the same region as the Golgi apparatus, whereas APP extended beyond the region of the Golgi apparatus and into the neuronal processes. This is shown in Figure 34 and Figure 35.

Immunodetection of β -amyloid in NTera 2 neurones

It has been demonstrated that β -amyloid is present in NTera 2 neurones, but not in NT2 stem cells, by immunoprecipitation and Western blotting (Bowes, 1999). Immunocytochemical labelling was therefore used with the aim of confirming this finding and identifying the subcellular location of this β -amyloid. Stem cells and neurones were immunolabelled with anti- β -amyloid antibody following -20°C

methanol or -20°C acetone fixation for 5 minutes. Half of the cells were treated with 80% formic acid for 10 minutes prior to immunostaining. No β -amyloid was detected in any of these cells. Further batches of neurones were then fixed with 2% or 4% paraformaldehyde in 0.1M PBS for 5 minutes or 20 minutes. Half of these were incubated with 80% formic acid for 10 minutes, and all were permeabilised in 0.3% triton X-100 for 15 minutes and immunostained for β -amyloid. No β -amyloid was immunolabelled in these neurones either. Anti-58k was used as a positive control alongside these experiments and these cells were immunopositive in all cases.

Controls

Immunolabelling with an irrelevant mouse monoclonal antibody, or with pre-immune serum from 87-4, yielded no immunostaining (Figure 36 and Figure 37).

Effects of stress, by heat-shock and no feeding, on β -amyloid, APP and APLP2 in NTERA 2 stem cells and neurones

Effects of heat-shock

Following heat-shock at 42°C and 0% CO_2 for 30 minutes no β -amyloid was detected by immunocytochemistry after recovery times of 0, 1, 4, 12, 24, or 48 hours, nor in control stem cells or neurones that were not subjected to heat-shock. Cells that were in separate wells on the same slides as those stained for β -amyloid were immunolabelled with 3B11 or 22C11 to detect APLP2 or APP respectively. No differences in intensity of immunolabelling of APLP2 or APP were observed under the fluorescence microscope following heat-shock and 0, 1, 4, 12, 24, or 48 hours' recovery, compared to control stem cells or neurones that were not heat-shocked. No alterations in the

distribution patterns of either protein were observed under the microscope following heat-shock and 0, 1, 4, 12, 24, or 48 hours' recovery, compared to control stem cells or neurones that were not heat-shocked.

Effects of no feeding

Neurones were plated on poly-D-lysine- and matrigel-coated chamber slides. After 2 days the medium was replaced with fresh cDMEM to remove any dead cellular material that may have been present due to replating. All experiments were timed from this date. The cells in control chamber slides were fixed after 1 week. Further cells were fixed 2, 3, 4, 5 or 6 weeks after the last date that the medium was replaced. The neurones were immunolabelled with anti- β -amyloid, 22C11 (to label APP) or 3B11 (to label APLP2) followed with biotinylated secondary antibody then streptavidin-conjugated FITC. The cells to be labelled with anti- β -amyloid antibody were treated with 80% formic acid for 10 minutes prior to immunostaining.

When examined under the fluorescence microscope the cells were immunonegative for β -amyloid in all cases. With 22C11 and 3B11 the intensity of immunolabelling and distribution of protein in the stressed cells were indistinguishable from the intensity and distribution of immunopositivity in cells that had not been subjected to stress.

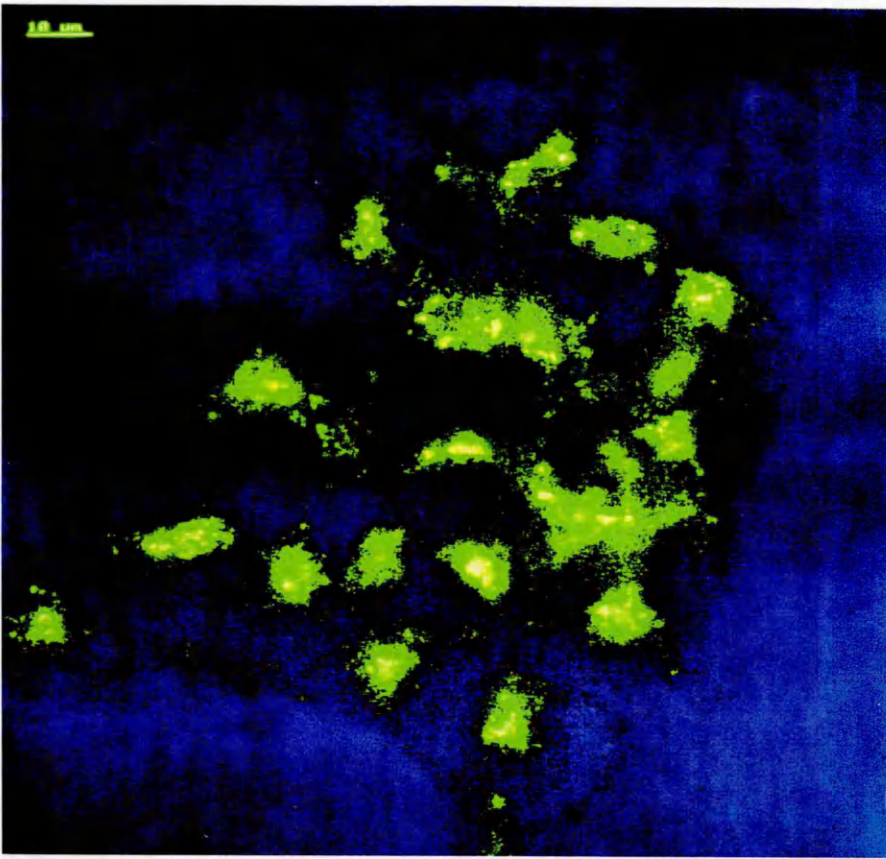


Figure 5

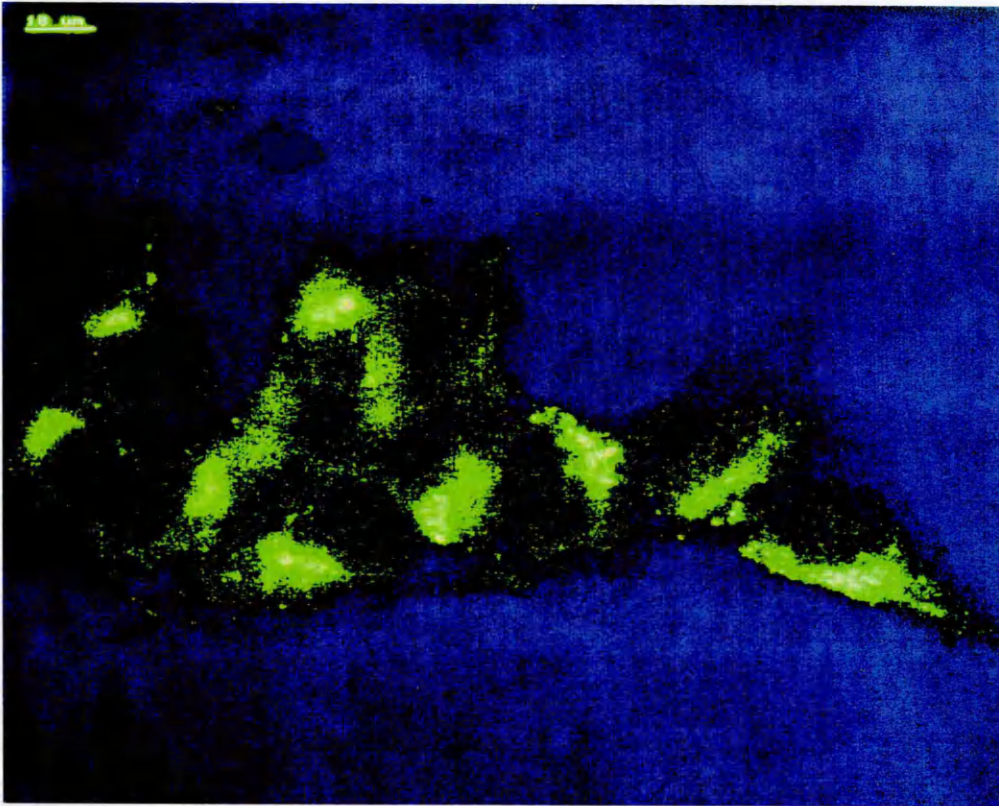


Figure 6

Figure 5 and Figure 6

Shown by indirect immunofluorescence, NT2 stem cells contain numerous, small lysosomes. Cells were fixed in -20°C methanol, then immunolabelled with monoclonal antibodies to lysosome-associated membrane proteins LAMP-1 (Figure 5) and LAMP-2 (Figure 6), followed by FITC-labelled secondary antibody.

Scale bar, top left = $10\mu\text{m}$.

Figure 7 and Figure 8

The Golgi apparatus in NT2 stem cells appears as a cluster of large, perinuclear vesicles, and smaller vesicles radiating out through the cytoplasm. Methanol-fixed cells were stained with anti-58k, a monoclonal antibody that recognises a protein on the cytoplasmic face of the Golgi apparatus, followed by biotinylated secondary antibody and DAB (Figures 7 and 8).

Magnification = $\times 300$

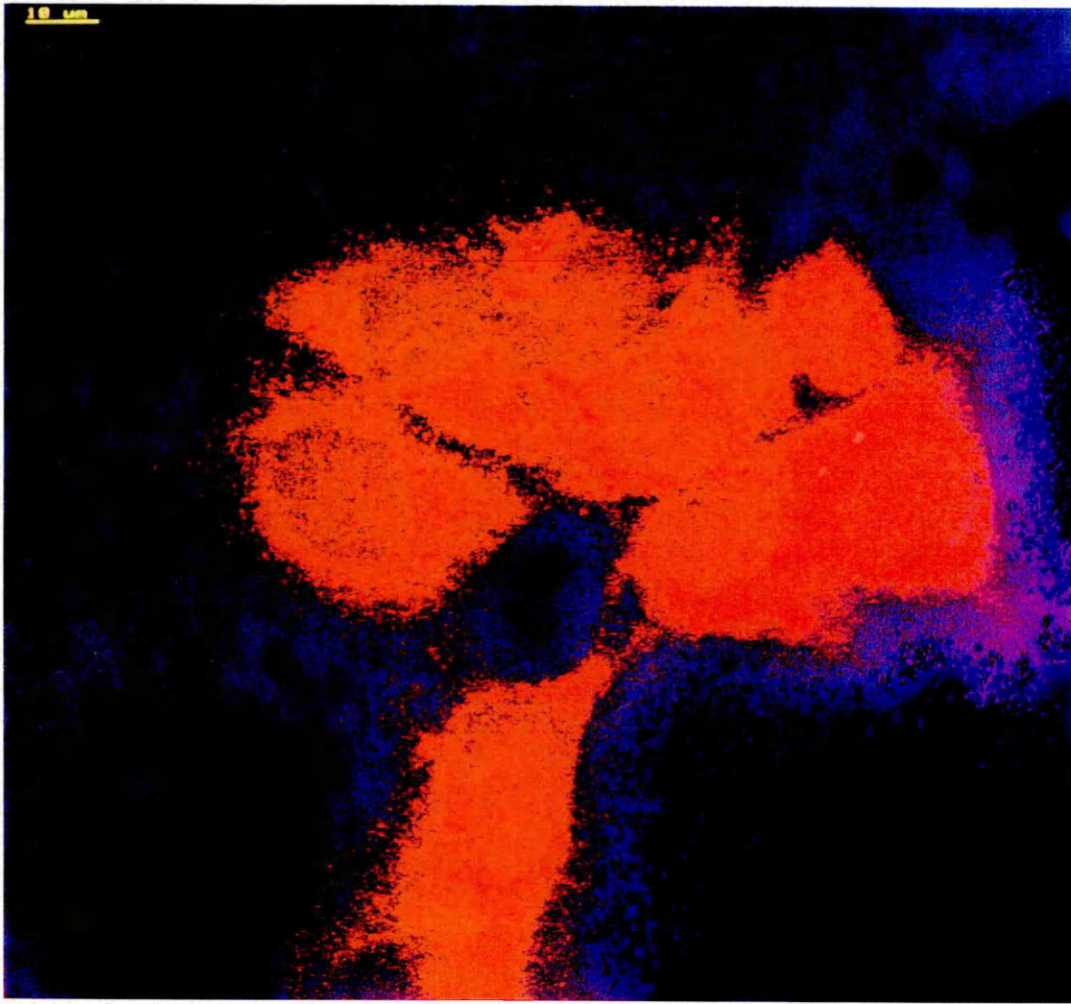


Figure 9

Figure 9

The endoplasmic reticulum in NT2 stem cells is a large, perinuclear structure. NT2 cells were fixed in -20°C methanol, and stained with anti-PDI followed with TRITC-labelled secondary antibody.

Magnification = $\times 200$

Figure 10 and Figure 11

APLP2 is concentrated in large, perinuclear organelles in the region of the Golgi apparatus of NT2 stem cells. Methanol-fixed cells were immunolabelled with 3B11, a monoclonal antibody to APLP2, followed by biotinylated secondary antibody and DAB (Figures 10 and 11).

Magnification = $\times 200$

Figure 12 and Figure 13

Polyclonal antibody 87-4 recognises an epitope in the C-terminus of both APP and APLP2. In methanol-fixed NT2 stem cells, labelled with 87-4 followed by biotinylated secondary antibody and DAB, heavily-stained perinuclear vesicles (as seen with antibody 3B11) are apparent, as well as small, reticular vesicles (Figures 12 and 13).

Magnification = $\times 200$

22C11



Figure 14

Figure 14

In methanol-fixed NT2 stem cells, antibody 22C11 was followed with biotinylated secondary antibody and FITC-conjugated streptavidin. APP and APLP2 were seen extending into numerous small granularities throughout the cytoplasm.

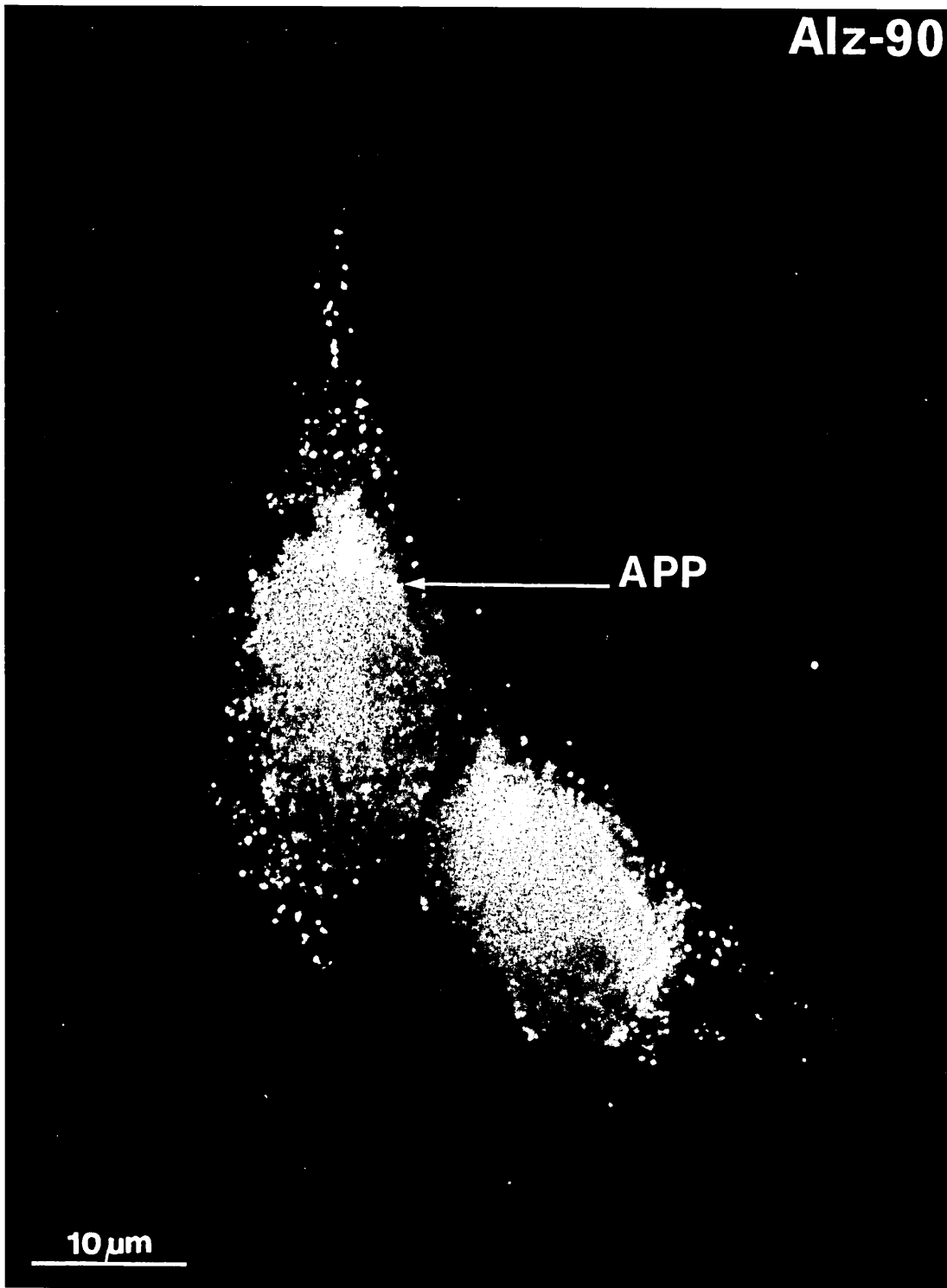


Figure 15

Figure 15

Monoclonal antibody Alz-90, which recognises only APP, and not APLP2, followed by biotinylated secondary antibody and FITC-conjugated streptavidin in methanol-fixed NT2 stem cells. Many small granularities in the cytoplasm were stained, but with less frequency than when cells were labelled with 22C11.

Figure 16 and Figure 17

Small, reticular vesicles were stained in the cytoplasm of NT2 stem cells immunolabelled with monoclonal antibody FC8, which is directed to an epitope within the first 12 amino acids of the β -amyloid sequence of APP. Methanol-fixed cells were stained with FC8 followed by biotinylated secondary antibody and DAB (Figures 16 and 17). The large, perinuclear vesicles stained by 87-4 are not immunopositive, but the smaller vesicles are, consistent with the absence of β -amyloid from APLP2.

Magnification = $\times 200$

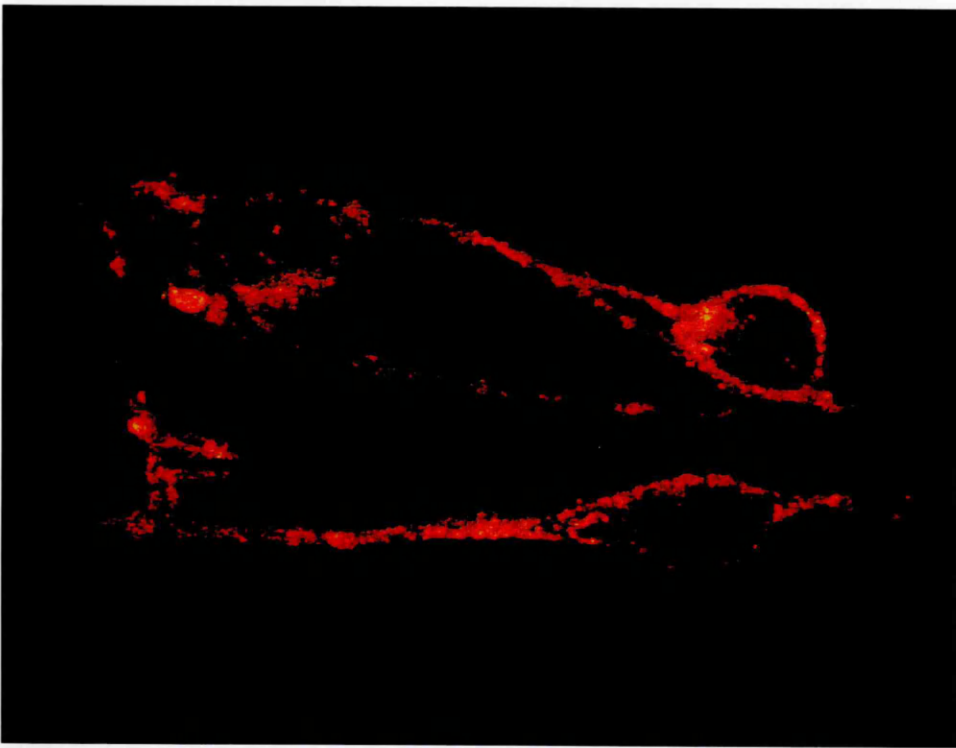


Figure 18

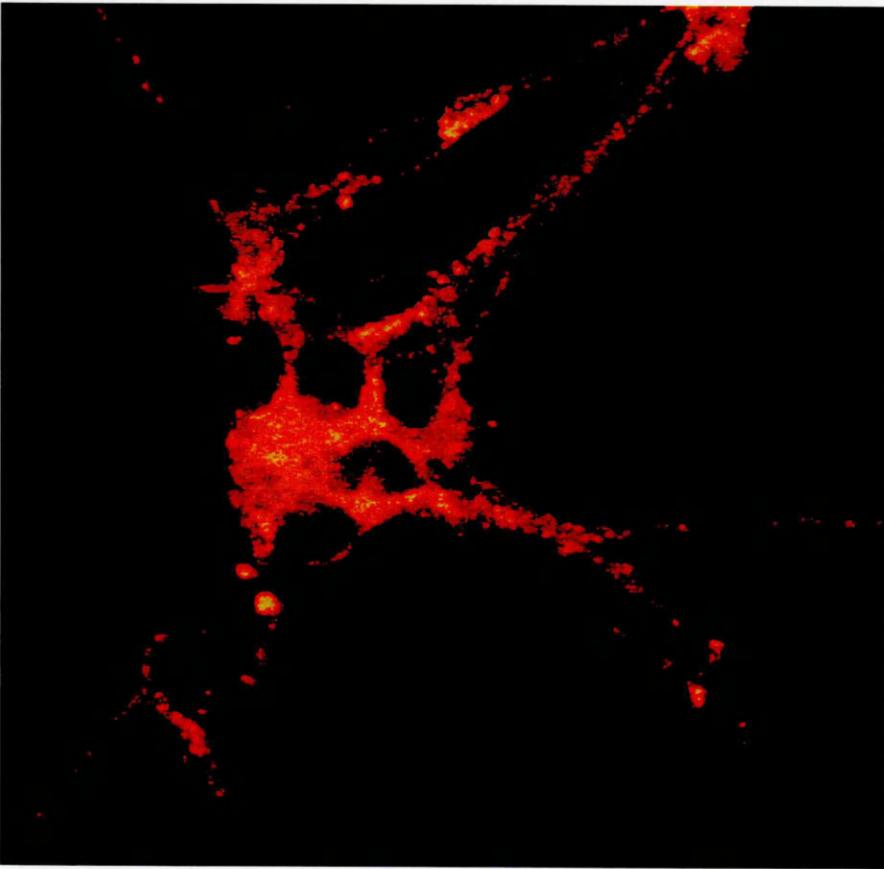


Figure 19

Figure 18 and Figure 19

Rhodamine-conjugated wheatgerm agglutinin labelled the perinuclear Golgi apparatus in NT2N neurones, as well as further vesicles that extend into the processes (Figures 18 and 19). Cells were fixed in -20°C methanol. Images were obtained by confocal microscopy.

Magnification, Figure 18 = $\times 200$, Figure 19 = $\times 75$

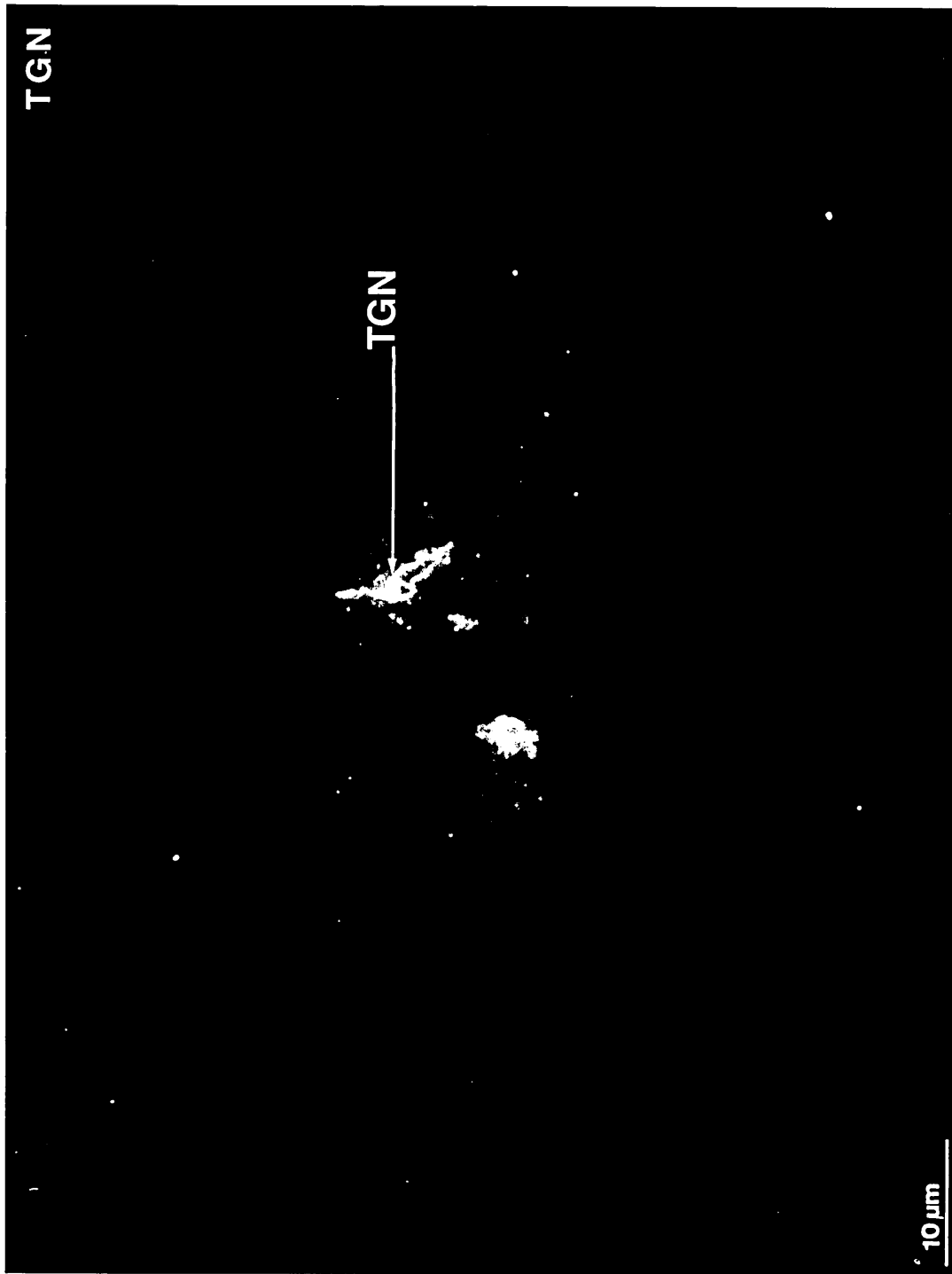


Figure 20

Figure 20

The trans-Golgi network (TGN) in NT2N neurones is a discrete, perinuclear, reticular structure. Methanol-fixed NT2N neurones were stained with monoclonal anti-TGN antibody, followed by biotinylated secondary antibody and FITC-conjugated streptavidin.

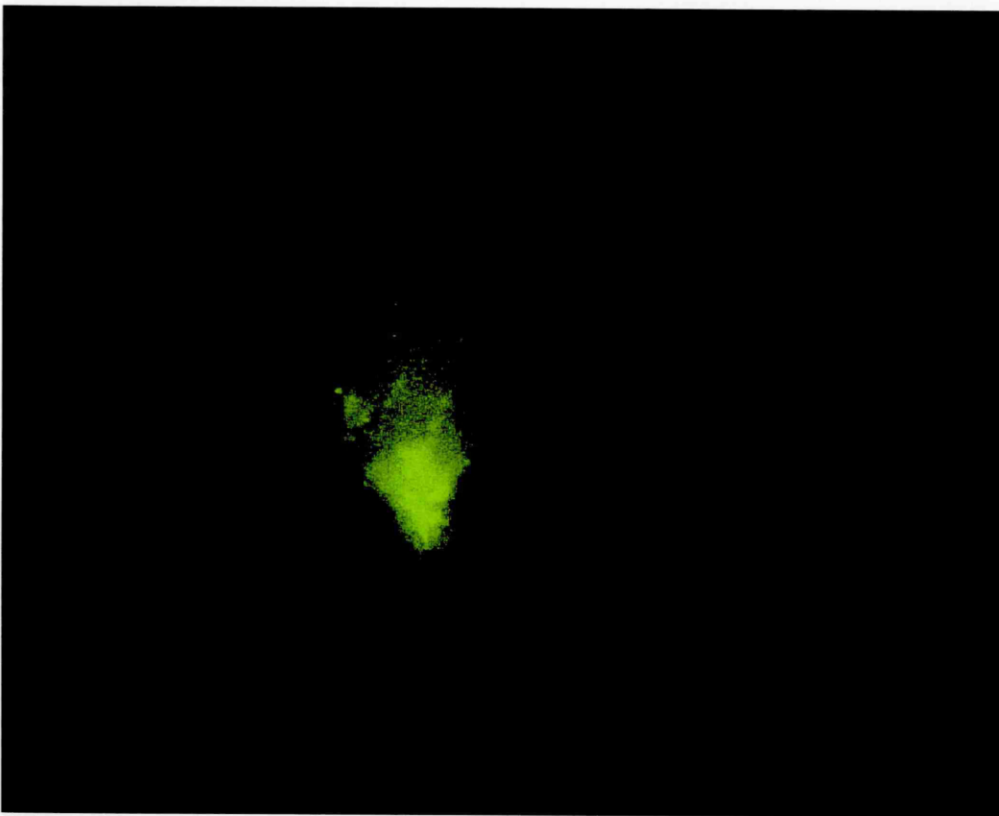


Figure 21

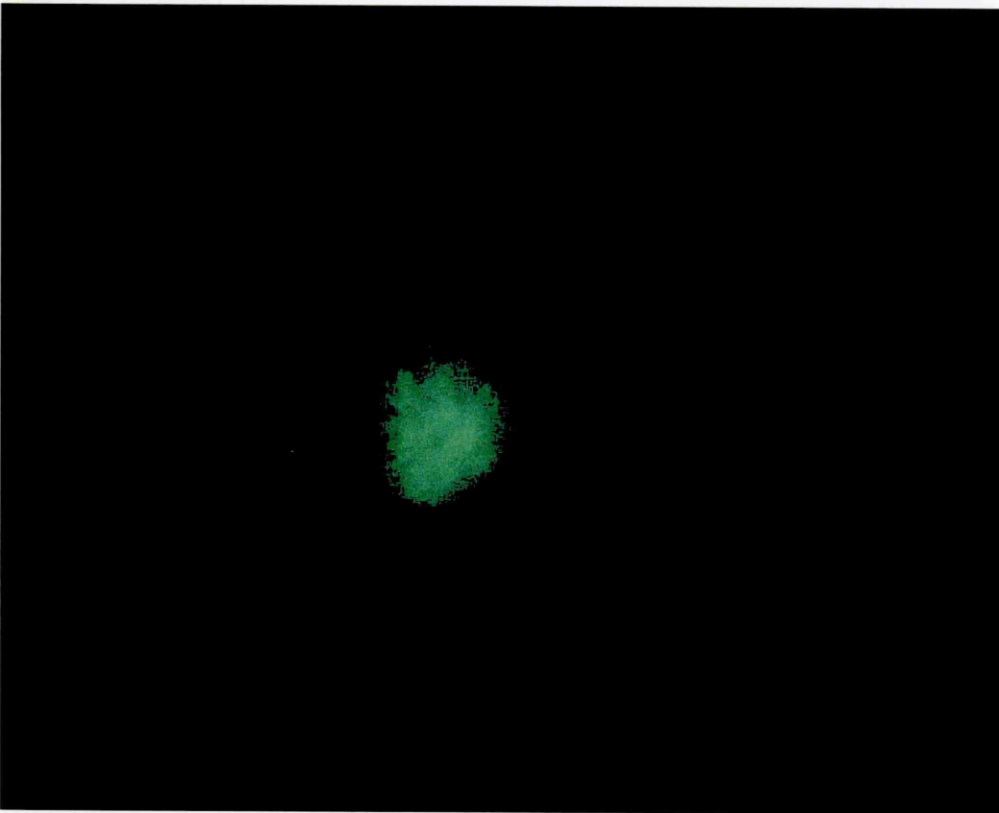


Figure 22

Figure 21 and Figure 22

The TGN in an NT2N neurone (Figure 21), stained as in Figure 20, showing its position adjacent to the nucleus of the same cell (Figure 22), stained with the dye bis-benzamide.

Magnification = $\times 200$

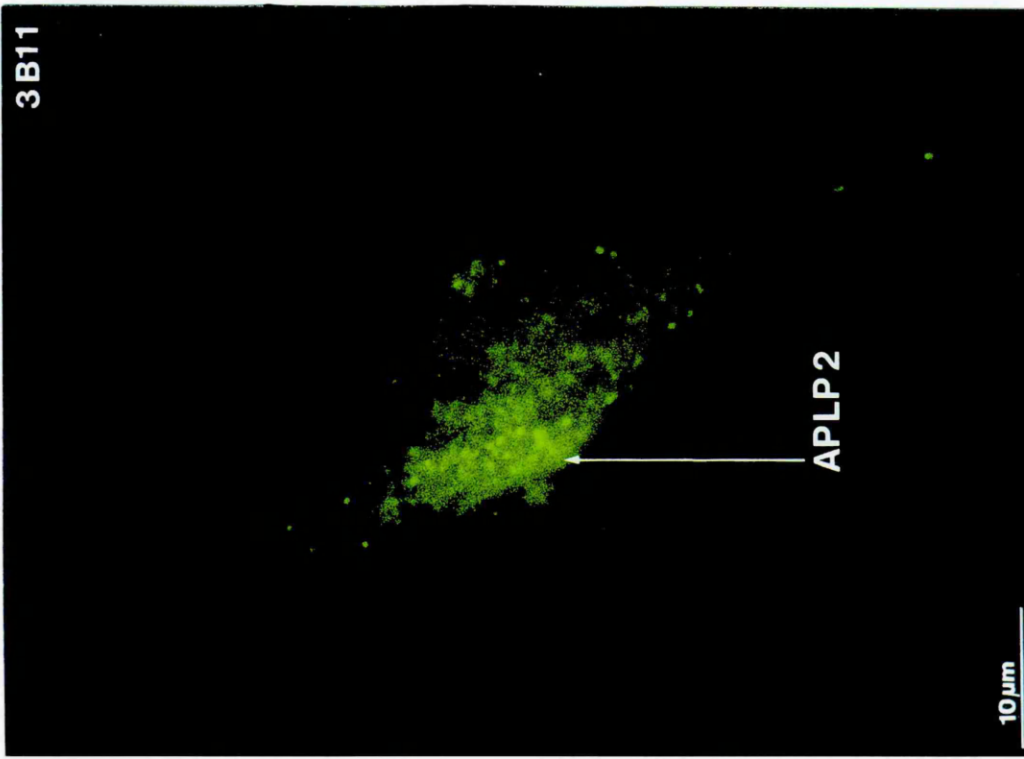


Figure 23

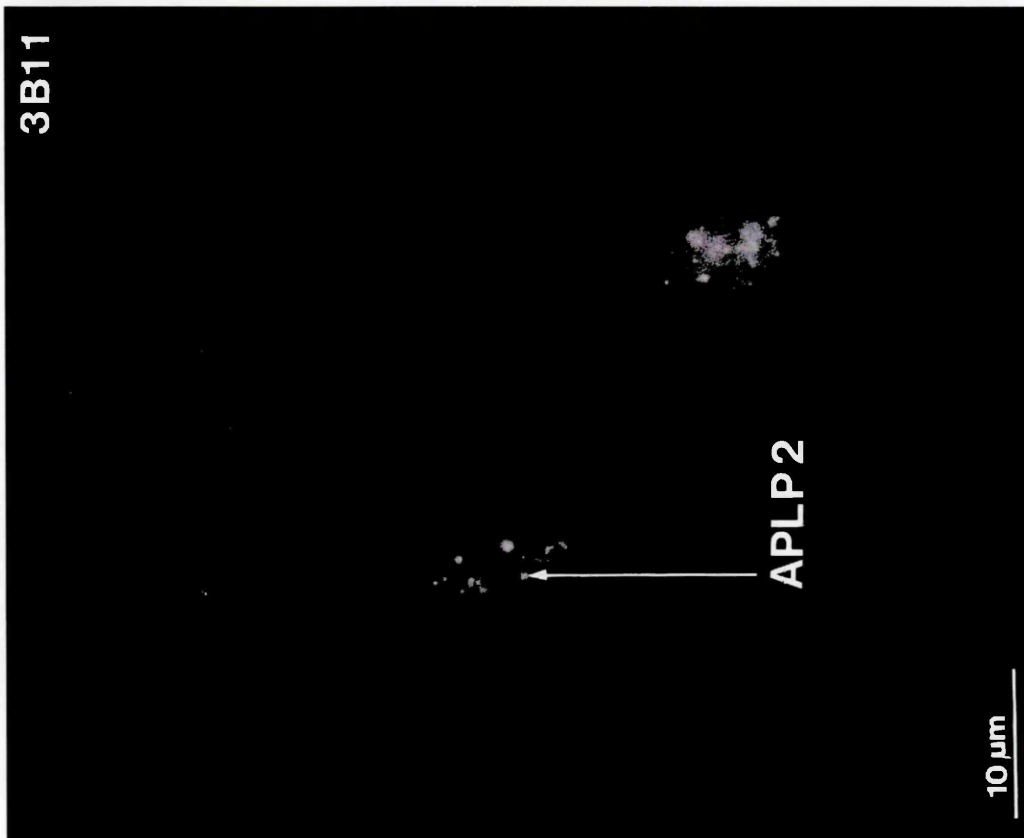


Figure 24

Figure 23 and Figure 24

APLP2 was restricted to large, perinuclear vesicles in the region of the TGN in NT2N neurones, similar to its distribution in stem cells. Methanol-fixed cells were stained with monoclonal antibody 3B11, followed with biotinylated secondary antibody and FITC-conjugated streptavidin (Figures 23 and 24).

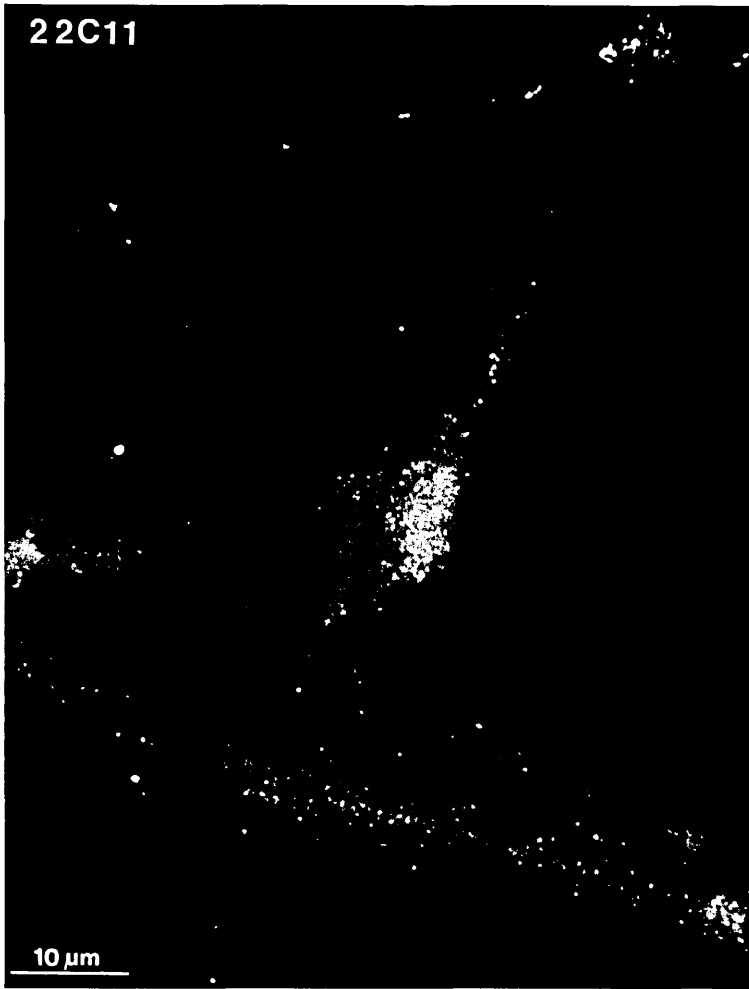


Figure 25

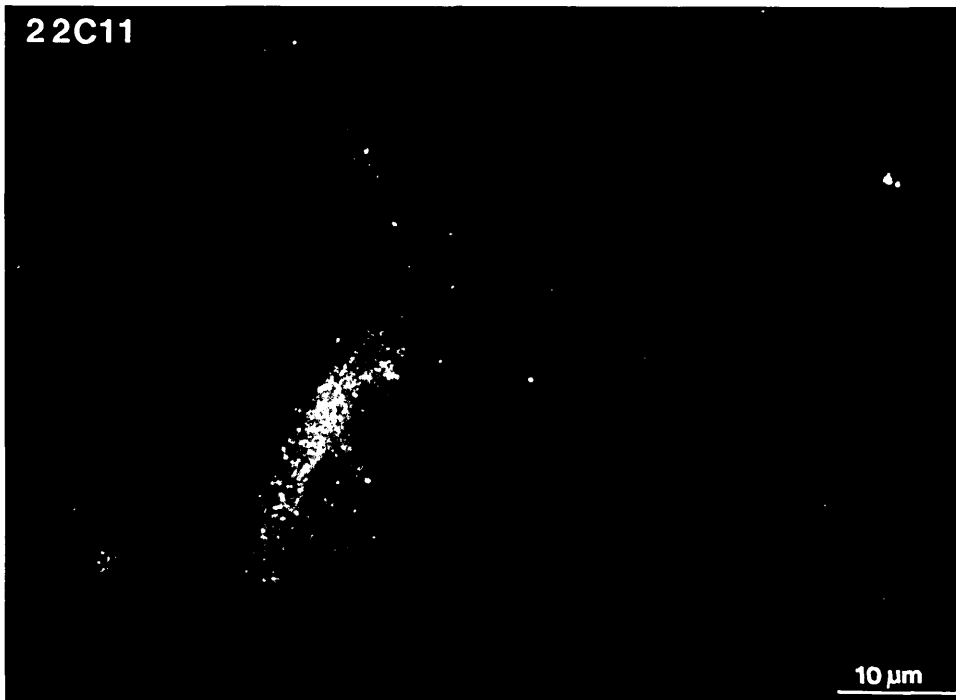


Figure 26

Figure 25

APP was present in the cytoplasm of NT2N neurones beyond the region of the Golgi apparatus. Here, immunolabelled structures are visible along the processes of neurones as well as in the perinuclear area. Methanol-fixed neurones were stained with monoclonal antibody 22C11, followed with biotinylated secondary antibody and FITC-conjugated streptavidin.

Figure 26

An NT2N neurone, immunolabelled with antibody 22C11 as in Figure 25, again showing the presence of perinuclear APP and APLP2.

Alz-90

APP

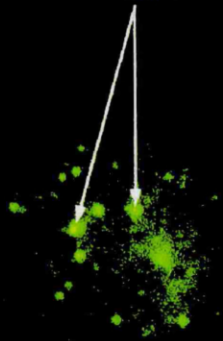


10 μ m

Figure 27

Alz-90

APP



10 μ m

Figure 28

Figure 27 and Figure 28

Monoclonal antibody Alz-90, which recognises APP but not APLP2, demonstrated the presence of APP in granular structures in the cytoplasm of neuronal cell bodies, when not masked by labelling of APLP2. Methanol-fixed neurones were stained with Alz-90 followed by biotinylated secondary antibody and FITC-conjugated streptavidin (Figures 27 and 28).

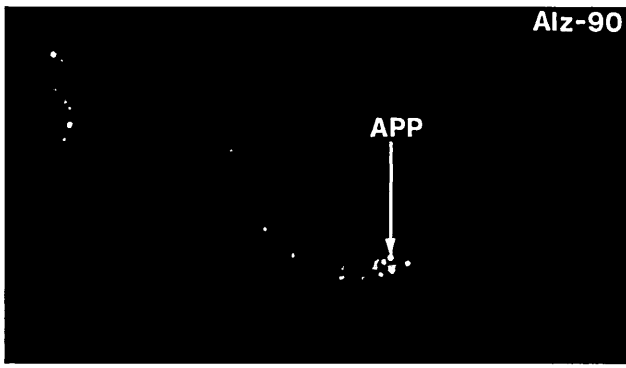


Figure 29

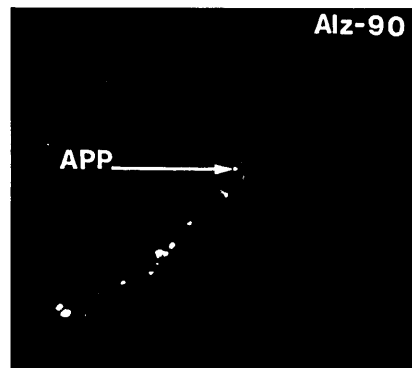


Figure 32



Figure 30

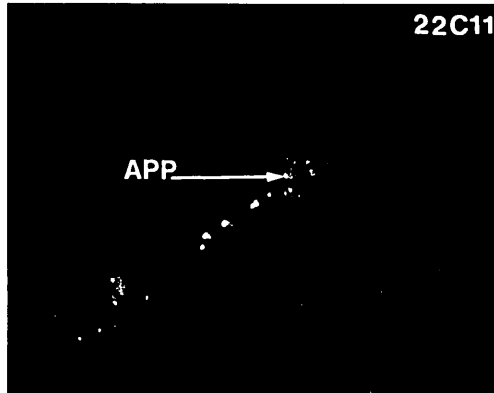


Figure 33

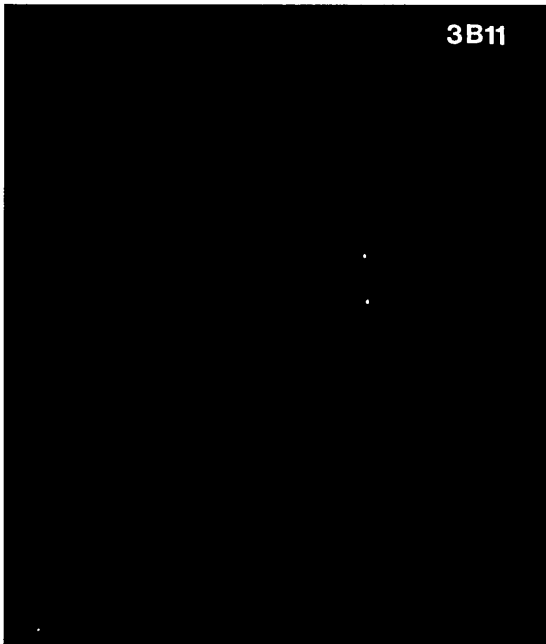


Figure 31



Figure 29 to Figure 33

APP was present in the growth cones of NT2N neurones, as shown with antibodies Alz-90 (Figure 29 and Figure 32), and 22C11 (Figure 30 and Figure 33), but APLP2 was not seen in the growth cones of neurones labelled with 3B11 (Figure 31). Methanol fixed cells were labelled with antibodies Alz-90 (Figure 29 and Figure 32), 22C11 (Figure 30 and Figure 33), or 3B11 (Figure 31), followed with biotinylated secondary antibody and FITC-conjugated streptavidin.

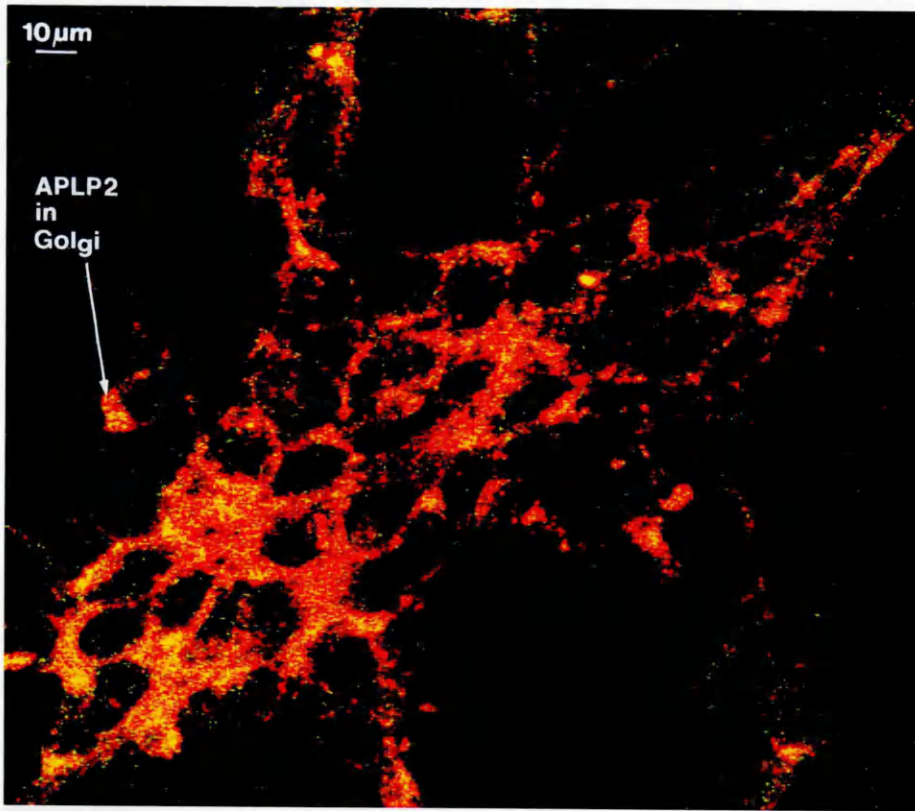


Figure 34

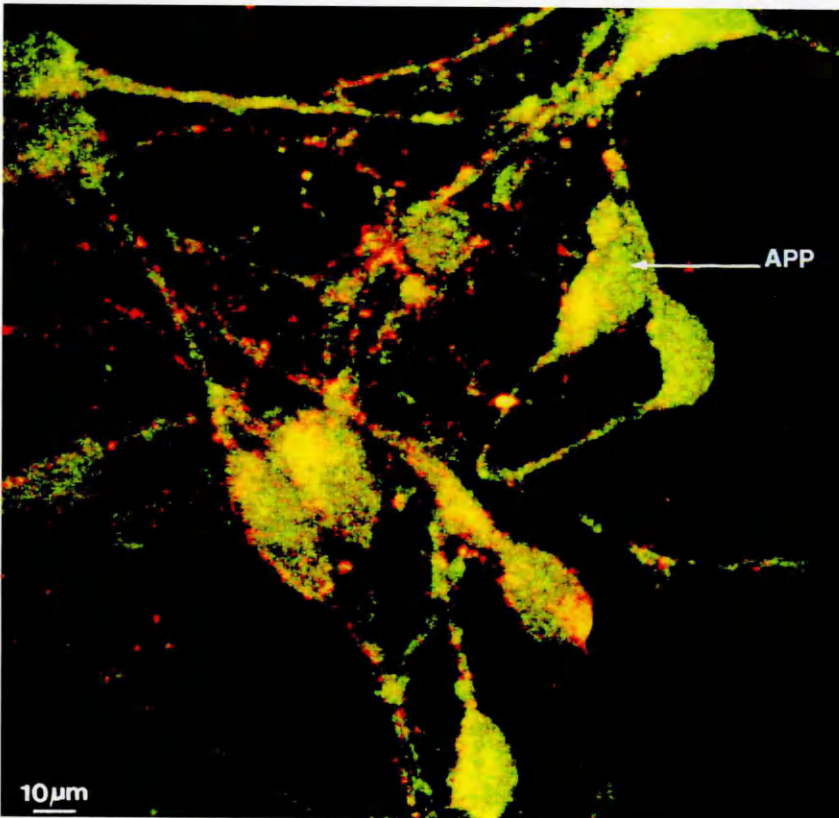


Figure 35

Figure 34 and Figure 35

Red = wheatgerm agglutinin (Golgi apparatus); Green = 3B11; Yellow = overlap.

Red = wheatgerm agglutinin (Golgi apparatus); Green = 22C11; Yellow = overlap.

Double-labelling of the Golgi apparatus and APLP2 (3B11) in NT2N neurones (Figure 34) confirmed that APLP2 was concentrated in the Golgi apparatus. Double-labelling of the Golgi apparatus and APP (and APLP2) with 22C11 (Figure 35) confirmed that APP extended into the cytoplasm of neurones beyond the region of the Golgi apparatus (green staining). Methanol-fixed neurones were immunolabelled with 3B11 or 22C11, followed with biotinylated secondary antibody and FITC-conjugated streptavidin, and incubated with rhodamine-conjugated wheatgerm agglutinin. Images were obtained by confocal microscopy.

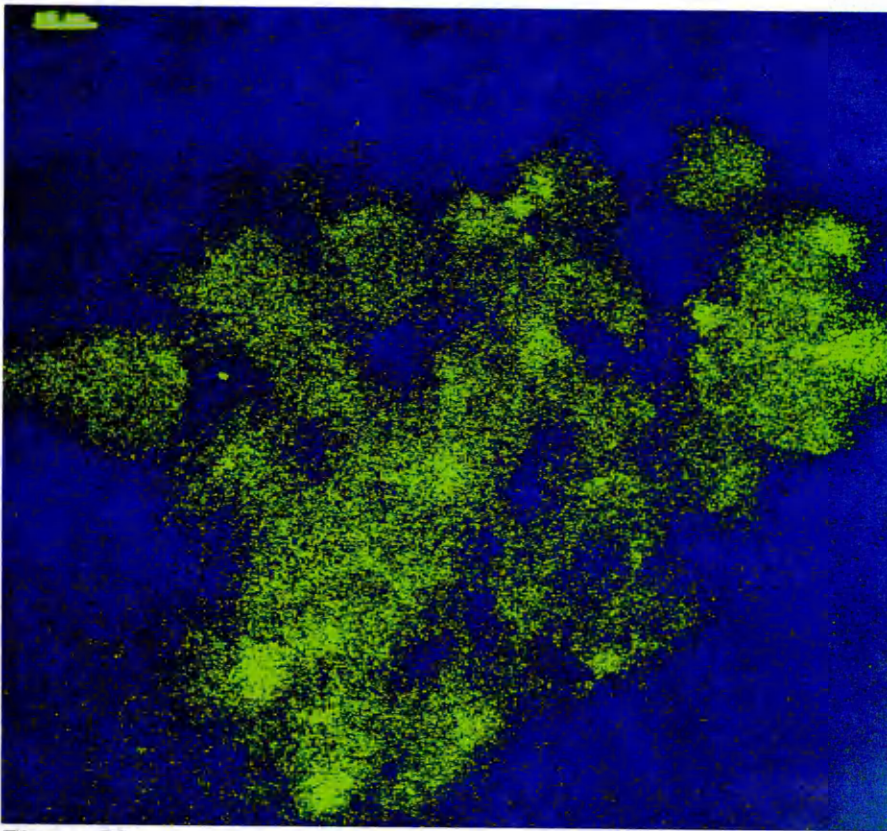


Figure 36

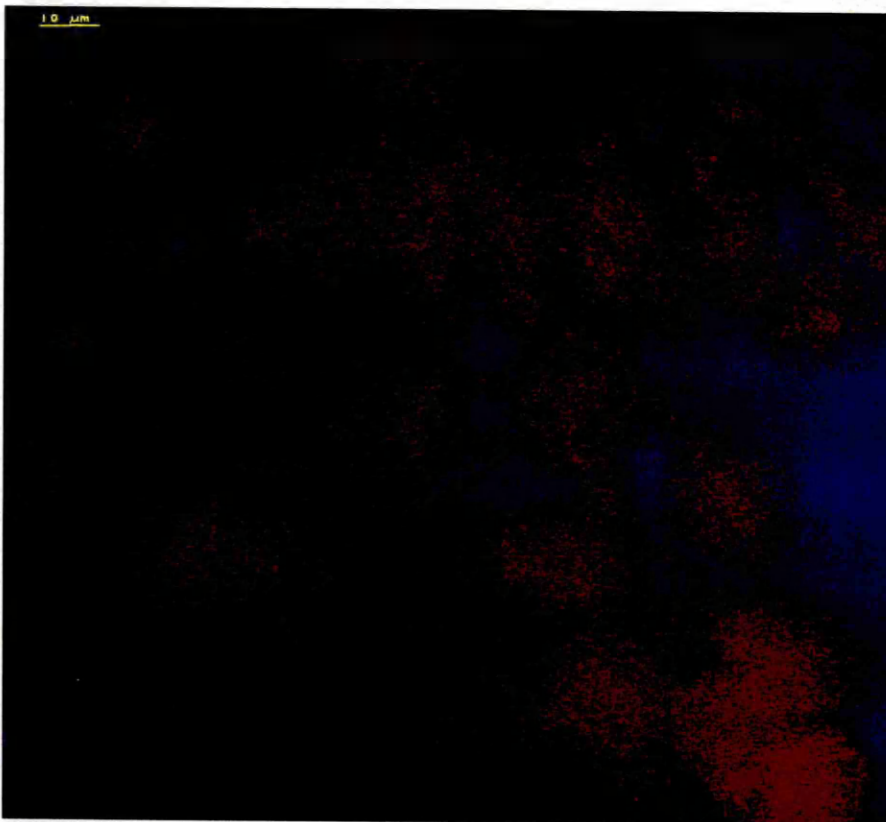


Figure 37

Figure 36 and Figure 37

Controls: No specific labelling was seen when methanol-fixed NT2 stem cells were stained with an irrelevant mouse monoclonal antibody (Figure 36) or pre-immune serum from 87-4 (Figure 37) followed by biotinylated secondary antibody and FITC-conjugated streptavidin. Both photographs are overexposed to demonstrate the presence of cells.

Discussion

In summary, there were similarities in the distributions of both APP and APLP2, in stem cells compared with neurones. In both stem cells and neurones, APLP2 was included within the region containing APP, but APP extended beyond the location of APLP2. No β -amyloid was detected in stem cells or neurones. No production of β -amyloid or alterations in cellular APP or APLP2 content or distribution were noted in stem cells or neurones upon heat-shock or no feeding.

Subcellular localisation of APP and APLP2

APP was present in small, intracellular compartments throughout much of the cytoplasm of NT2 stem cells, whereas APLP2 was found in larger, perinuclear organelles, in the region of the Golgi apparatus (Campbell *et al.*, 1996). In NT2N neurones, APLP2 was detected in similar large, perinuclear organelles, identified by double-labelling as Golgi vesicles. In neurones APP extended into smaller vesicles beyond the Golgi apparatus, and was detected in small, granular structures in processes and growth cones (Campbell *et al.*, 1997).

A previous study of APP in untransfected NT2 cells, using metabolically-labelled APP, indicated that the half-life of APP holoprotein turnover is approximately 1 hour in stem cells and 3 hours in neurones (Wertkin *et al.*, 1993). In neurones most of the APP was degraded before becoming O-glycosylated, inferring that proteolysis occurred without the full-length protein being routed to the plasma membrane. β -amyloid was detected in the cell lysate, as well as in media, from neurones but not from stem cells. This β -amyloid therefore may have been generated directly from immature APP without its

reaching the plasma membrane, or from the smaller amount of mature APP following its re-internalisation from the plasma membrane to the endosomal-lysosomal system. In the present study APP was not seen at the plasma membrane when cells were viewed by either conventional or confocal microscopy, although it is possible that the protein is delivered here and cleaved rapidly so that it remains below the level of abundance necessary for detection by immunocytochemistry.

In the hamster primary visual pathway metabolically-labelled APP was shown, by Western blot analysis, to be transported rapidly to the growing tips of axons (Moya *et al.*, 1994), analagous to the localisation of APP to the growth cones of NT2N neurones in this study. In hamster retinal ganglion cells fast axonal transport of both APP and APLP2 to the presynaptic terminal has been demonstrated (Lyckman *et al.*, 1998). Here there was rapid turnover of APP and APLP2, independently of visual activity.

In polarised rat hippocampal neurones, transfected with tagged human APP695, APP was delivered first to the axonal surface, then routed by transcytosis to the dendritic surface (Simons *et al.*, 1995). In contrast, in polarised epithelial cells (in which axonally-routed proteins are usually delivered to the apical membrane, and dendritically-routed proteins to the basolateral membrane) APP is delivered, directly, basolaterally, suggesting that neurone-specific sorting and processing mechanisms may exist.

In COS-1 cells, transiently transfected with human APP770 or mouse APLP2 cDNA, both APP and APLP2 were present in cellular structures labelled by lentil lectin that binds to oligosaccharides specific to the Golgi compartment (Slunt *et al.*, 1994).

The variability in APP and APLP2 distributions found in these different cell types may result from a high degree of heterogeneity of processing of APP and APLP2 in neuronal versus non-neuronal cells, and in different subtypes of neurones. This, in turn, may reflect the confinement of AD pathology to areas containing specific neuronal subtypes in AD brains.

Discrimination between APP and APLP2

The identification of the amyloid precursor-like protein 2, APLP2, (Slunt *et al.*, 1994) added confusion to the interpretation of previous, and some subsequent, studies of APP by immunological methods. APLP2 is a 751 amino acid polypeptide with high homology (including regions with up to 72% identity) to APP-751. Slunt *et al.* reported that APLP2 and APP have almost identical expression patterns in mouse brain, as determined by *in situ* hybridisation histochemistry. Four widely used anti-APP antibodies, Ab 369, 22C11, LN27.7 and LN21.9, were demonstrated to cross-react with APLP2. Furthermore, immature forms of APP-770 and APLP2, and secreted forms of APP-695 and APLP2, co-migrated in SDS-polyacrylamide gel electrophoresis.

This study demonstrated overlap in the intracellular locations where APP and APLP2 are concentrated in NT2 stem cells and neurones. The similarity of NT2N neurones to human CNS neurones raises the possibility that this may also be the case in the human brain, which also expresses APLP2, thus highlighting the need to differentiate between these two highly related polypeptides when performing immunological studies of APP in human brain.

The similarity between APP and APLP2 may in fact prove useful to the study of APP processing mechanisms, because APLP2 does not contain the β -amyloid region. Subtle

differences in the cellular processing of these two proteins may aid identification of amyloidogenic proteolytic processing routes that are followed by APP but not APLP2, thus suggesting points at which therapeutic intervention may be applied to reduce production of the β -amyloid peptide.

Routes of amyloidogenic and non-amyloidogenic processing of

APP

The absence of β -amyloid immunostaining in NT2N cells may have been due to low levels of β -amyloid in the cells, below the level necessary for immunodetection. The β -amyloid may have been washed out of cells fixed with -20°C methanol. Alternatively, the antigenic site may have been inaccessible to the primary antibody because the β -amyloid was in an inappropriate conformation or bound to a chaperone molecule. It is unlikely that no β -amyloid was present in these cells since it had been detected previously, by immunoprecipitation and Western blotting, in cells derived from the same original stock of passage 30 stem cells (Bowes, 1999). β -amyloid was also reported to be present in cell lysate (as well as media) from untransfected NT2N neurones by immunoprecipitation (Wertkin *et al.*, 1993). However, it was unclear whether this β -amyloid was produced directly from intracellular, immature APP or if it was generated in the endosomal-lysosomal system following re-internalisation of mature APP from the plasma membrane.

Subsequently to the present investigation, in NT2N neurones overexpressing APP-695, both β -amyloid (40) and β -amyloid (42) were identified by enzyme-linked immunosorbent assay (ELISA) in cell lysates and media (Cook *et al.*, 1997). Following retention of APP in the endoplasmic reticulum/intermediate compartment

(ER/IC) β -amyloid secretion was abolished, intracellular β -amyloid (40) production was eliminated, but intracellular β -amyloid (42) synthesis was unchanged. A similar pattern was seen in uninfected cells, except that in these cells there was a gradual accumulation of intracellular β -amyloid (42) rather than a steady-state, higher abundance of the peptide, probably because overexpression of APP-695 saturated the cells' capacity for β -amyloid (42) generation or accumulation. Both β -secretase and γ -secretase cleavage of APP thus appeared occur in the ER/IC, but only to produce the 42 amino acid β -amyloid peptide. This suggested that β -amyloid (40) generation occurs in a more distal compartment where either the γ -secretase enzyme acts at a different point in APP or another γ -secretase enzyme cleaves APP at an alternative site. Further evidence for β -secretase cleavage of APP occurring in the ER/IC of neurones was provided by a pulse-chase study of NT2N cells, demonstrating production of β -secretase-cleaved N-terminal APP fragment (APP β) following retention of endogenous APP in the ER/IC (Chyung *et al.*, 1997).

In other cell types a variable, but often similar, picture of β -amyloid production is seen. In an electron microscopical examination of primary rat hippocampal neurones β -amyloid (42) was immunolocalised in the ER, and β -amyloid (40) in the TGN, a few budding, coated vesicles and some multilamellar late endosomes. In contrast, in COS-7 cells, used as a model of non-neuronal cells, no β -amyloid was detected intracellularly but both β -amyloid (40) and (42) were present at the cell surface (Hartmann *et al.*, 1997). In N2a neuroblastoma cells, doubly transfected with human APP-695 and human PS1, and primary rat cerebral cortical neurones, β -amyloid (1-40), (x-40), (1-42) and (x-42) were all produced in the TGN and packaged into post-TGN secretory vesicles. β -amyloid (x-42) was generated also in the ER and retained there in a

detergent-insoluble state (Greenfield *et al.*, 1999). Of the β -amyloid in the TGN, some (including both β -amyloid (40) and (42)) was detergent-soluble and some was not. In rat brain β -amyloid has been found in a detergent-insoluble, glycolipid-enriched membrane domain (DIG), along with endoproteolytic fragments of APP and PS1 (Lee *et al.*, 1998). These DIGs, membranous 'rafts' that may participate in protein trafficking, often of proteins involved in signalling, have a high lipid content, including cholesterol and GM1. β -amyloid has affinity for these lipids, which have been reported to promote intra-membranous peptide aggregation and amyloid β -sheet formation, suggesting that this may be a site of intracellular initiation of β -amyloid aggregation (Lee *et al.*, 1998).

In human AD brain, intracellular β -amyloid is present in cells with DNA damage (LaFerla *et al.*, 1997). This β -amyloid immunoreactivity was found in the same cytoplasmic granules as apolipoprotein E (apo E) and correlated with accumulation of apoE and gp330 (a cell surface receptor that binds apo E). Extracellular β -amyloid deposition was evident only upon neuronal cell death, initially as halos of β -amyloid immunoreactivity around individual neurones, then as β -amyloid plaques containing numerous neuronal cell ghosts. By comparison with analysis of nuclear DNA fragmentation, it appeared that neuronal cell death occurred before extracellular deposition of β -amyloid.

These events have been suggested to be preceded by synaptic abnormalities and/or loss that are accompanied by increased APP and abnormally phosphorylated tau in the cell bodies of the affected neurones, and accumulation of APP in astrocytes and microglia (Martin *et al.*, 1994; Masliah *et al.*, 1994). More recently, neuronal mRNAs were found to predominate in senile plaques, supporting the suggestion that senile plaques form at

sites where neurones degenerate in AD (Ginsberg *et al.*, 1999). Bahr *et al.*, (1998) found that exposure of rat hippocampal slices to exogenous β -amyloid (42) resulted in accumulation of β -amyloid in the somata of CA1 pyramidal neurones. This was followed by build-up of amyloidogenic C-terminal fragments (CTFs) in the somata, apical and basal dendrites of these neurones, and in bands of punctate structures resembling synapses in the molecular layer of the dentate gyrus and the stratum lacunosum-moleculare of CA3. The synaptophysin concentration was found by immunoblot analysis to be reduced by 50% following β -amyloid (42) treatment. β -amyloid (40), in contrast, accumulated throughout the hippocampal slice without selectivity of area. Thus a self-perpetuating cycle may occur in AD, whereby any factor that precipitates an increase in concentration of intracellular β -amyloid (42), such as increased APP expression or a shift towards amyloidogenic APP proteolysis, results in further increase of APP expression and/or a further increase in amyloidogenic processing. This may result in synaptic abnormality and loss, followed by retrograde neuronal death then extracellular deposition of β -amyloid and formation of amyloid plaques.

The effects of stress on APP processing

Cellular stress and the inflammatory response have been implicated in the pathogenesis of AD. The cellular stress response involves a rapid, transient change in the pattern of gene expression, including induction of the heat-shock proteins and suppression of synthesis of most other proteins (Dewji *et al.*, 1995). The APP gene contains a heat-shock element (Salbaum *et al.*, 1988) that has been shown to increase APP transcription, in NT2 stem cells and in HeLa cells, upon activation by heat-shock (Dewji *et al.*, 1995). In the lesions of AD brains heat-shock proteins including ubiquitin

and HSP70 are present (Pappolla *et al.*, 1995), as well as abnormally phosphorylated tau (Grundke–Iqbal *et al.*, 1986), which is also elevated in the brains of heat–shocked rats (Papazosomenos and Yuan, 1991).

Previous studies of the effects of heat–shock on cultured cells have reported elevation of APP expression. There was a 5– to 8–fold rise in APP mRNA levels, with a peak at 4 hours post–heat–shock, in human umbilical vein endothelial cells (HUVECs) exposed to a temperature of 42°C for 30 minutes (Ciallella *et al.*, 1994). This was followed by increased APP protein in media peaking at 1 hour post–heat–shock, and APP immunoreactivity with a peak at 12 hours post–heat–shock. Immunopositive APP was in a perinuclear Golgi–like region and discrete, granular cytoplasmic structures, much like the pattern of APP immunoreactivity found in NT2 stem cells in the present study.

In both C6 glioma cells and N2a neuroblastoma cells, heat–shock at 44°C for 30 minutes increased frequency of detection of APP, with a Golgi–like distribution, from fewer than 10% of unstressed cells to over 90% of stressed cells following 4–6 hours of recovery (Pappolla *et al.*, 1995).

NT2 stem cells and HeLa cells, transiently transfected with a fragment of the human APP promoter including the heat–shock element, heat–shocked at 43°C for 1–3 hours, followed by 24 hours' recovery, displayed induction of APP gene expression (Dewji *et al.*, 1995).

In the present study, following cellular stress by heat–shock or deprivation from nutrients no β –amyloid was detected in cells, and the distributions and staining intensities of APP and APLP2 were unchanged upon investigation by immunocytochemistry. The bulk of evidence from similar studies indicates that APP

expression is likely to be upregulated in NT2 cells following stress. In particular, the report by Dewji *et al.* (1995), that there is increased transcription of APP in NT2 stem cells following heat-shock, suggested that APP protein might be upregulated in the present study also (although the cells used by Dewji *et al.* were transfected with a fragment of the APP promoter). More recently, in NT2N neurones oxidative stress has been shown, by immunoprecipitation and Western blotting, to increase intracellular β -amyloid production while APP expression was unaltered (Paola *et al.*, 2000).

It may be that there were small changes in APP and/or β -amyloid production, following heat-shock, which were too subtle to be detected immunocytochemically. Furthermore, there may have been alterations in APP mRNA splicing that could not be seen with the anti-APP antibody used, 22C11, which labels all APP isoforms. The anti-KPI antibody described in a later chapter, which was developed after termination of this study, may be of use in further immunocytochemical study of APP in NT2 cells following heat-shock. In a human foetal astrocytic cell line heat-shock has been shown to increase KPI-containing APP mRNA but not APP-695 or APLP2 mRNA (Shepherd *et al.*, 2000). As discussed below (chapter 6), there appears to be a shift in splicing of APP mRNA in AD in favour of KPI-containing isoforms. It would be interesting to see if this change is induced in NT2N neurones under conditions of stress.

β -amyloid did not appear to be accumulated intracellularly in either unstressed or stressed NT2 stem cells or neurones. β -amyloid may have not been detected in the cells because it was washed out of those that were fixed with -20°C methanol. It may have been in an inappropriate conformation or bound to a chaperone molecule, rendering the antigenic site inaccessible to the primary antibody. Although β -amyloid had been detected by Western blotting in cells derived from the same original stock of stem cells

(Bowes, 1999), it may be that subsequent passaging of the cells had resulted in subcloning of a phenotype that no longer accumulated intracellular β -amyloid.

This work was terminated due to difficulties in producing a consistent supply of large enough quantities of NT2N neurones, because of the long time period required for cellular differentiation, with regular feeding resulting in a high infection rate. Furthermore, the lack of immunocytochemical detection of intracellular β -amyloid presented a hindrance to studying amyloidogenic pathways of APP processing in these cells by immunocytochemistry.

CHAPTER 4: DEVELOPMENT OF A PROTOCOL

FOR ELECTRON MICROSCOPICAL

EXAMINATION OF NTERA 2 CELLS

Introduction

Prior to this study NTERA 2 cells had not been examined successfully by electron microscopy (EM) before. The purpose of this work was to define methods by which NT2 cells can be prepared for EM and immuno-EM and to investigate the distribution of Alzheimer-related peptides and proteins in NT2 cells by immuno-EM.

Cultures of mature primary rat hippocampal neurones have previously been examined by EM and immuno-EM by processing and embedding *in situ* on glass coverslips prior to cutting ultra-thin sections and staining with uranyl acetate and lead citrate (Hartmann *et al.*, 1997). Therefore this method was used, along with collection of cells by scraping or by centrifugation followed by processing and embedding, to determine protocols for EM and immuno-EM of NT2 stem cells and neurones.

Methods

Initially cells were stained with osmium tetroxide so that the quality of their morphological preservation could be examined, and embedded in araldite resin, an epoxy resin. Other cells were embedded in Unicryl resin, an acrylic resin suitable for immuno-EM, then semi-thin sections were stained with toluidine blue and examined under the light microscope. Ultra-thin sections were stained with uranyl acetate and

lead citrate for examination under the electron microscope. Unicryl resin is preferable to an epoxy resin for immuno-EM because it allows water to penetrate the tissue, so it does not have to be removed from the sections before immunostaining. In addition, Unicryl resin can be polymerised at very low temperatures by ultra-violet light. This helps to prevent loss of antigenicity caused by polymerisation of araldite resin at 60°C.

Results

Stem cells collected by centrifugation

Stem cells that were collected by centrifugation, embedded in Unicryl resin and stained with uranyl acetate and lead citrate, were found, upon examination of toluidine-blue-stained semi-thin sections, to contain cellular material. However, examination of ultra-thin sections of cells fixed with 2% paraformaldehyde and 0.05% glutaraldehyde under the electron microscope showed that the cells had poorly preserved morphology. This is illustrated in Figure 38, Figure 39, Figure 40 and Figure 41, which show the disruption of the plasma membrane and absence of cytoarchitecture within the cells. In some cases fragments of organelles are visible, and possibly whole nuclei, but cells fixed and embedded in this manner were not sufficiently intact to be used for immuno-EM.

Neurones collected by centrifugation

When neurones were harvested by centrifugation a much larger cell pellet was obtained than when neurones were collected by scraping or processed *in situ*. The cell pellets did not disintegrate during processing. Some of these cells were stained with osmium

tetroxide and embedded in araldite resin, while another batch was embedded in unicryl resin without staining with osmium tetroxide.

Semithin sections of the neurones collected by centrifugation and embedded in araldite resin were stained with toluidine blue, but it was difficult to tell from these sections whether or not there were any neurones present: if there were any neurones present their morphology had not been preserved. Therefore no ultra-thin sections were cut from these blocks.

Neurones collected by scraping

The least successful method of collecting neurones was by scraping from the flask because the clusters of neurones were so small that most of them were lost during the subsequent washes, fixation and staining. The only material that was successfully stained with osmium tetroxide and embedded in araldite resin was found, on examination of semi-thin sections, not to contain neurones. This material may have been matrigel.

Neurones processed *in situ*

Those neurones that were processed *in situ* on the glass slides were successfully retained in the resin blocks, but the clusters of cell bodies were so small that only about 50–70 ultra-thin sections could be cut from each block. Two ultra-thin sections were successfully cut and collected from these block fixed with 2% paraformaldehyde. These were stained with uranyl acetate and lead citrate and examined under the electron microscope, but it was not clear whether or not the material contained in these sections was neuronal tissue. The sections were too thick for any cells that may have been

present to be seen clearly, and the resin blocks may have been left in the oven for too long, thus becoming too brittle to cut evenly, because the sections had a 'wrinkled' appearance. If the material present in the sections was neuronal tissue it was too severely disrupted for its morphology to be seen. It is possible that these sections contained only matrigel.

Comparison of methods

Too few sections were collected, stained and examined for a comparison to be made between the quality of tissue preservation by different fixatives.

With each of the techniques that were tested for embedding cells there either was very poor preservation of cell morphology or the scant populations of cells were lost during the procedure. The lack of any obvious solutions to these problems meant that the length of time that would be required to solve them was beyond the available time, so this work was discontinued.

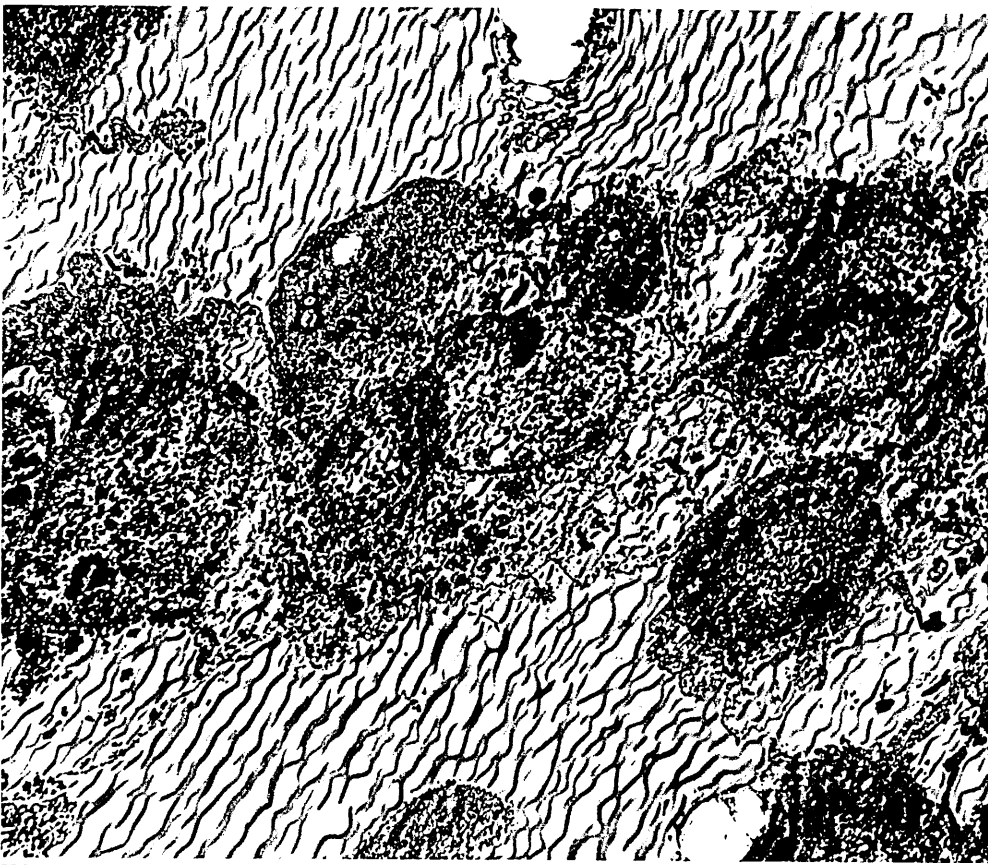


Figure 38

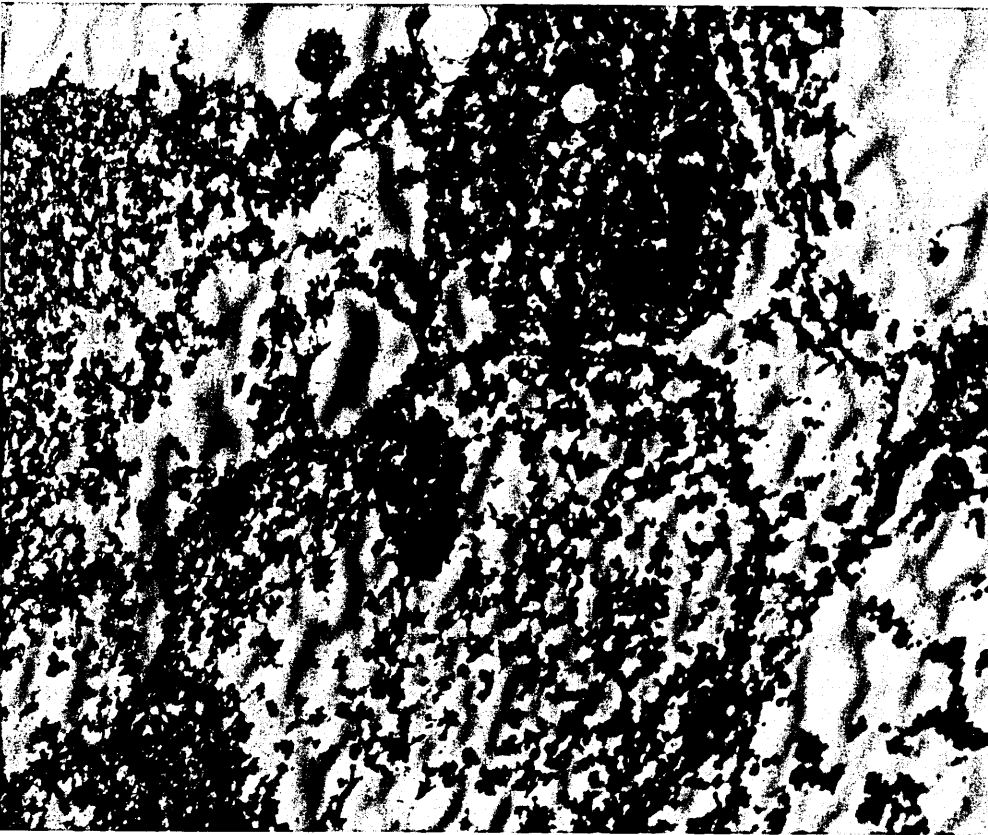


Figure 39

Figure 38

Electron micrograph of a semithin section of NT2 stem cells collected by centrifugation, fixed in 2% paraformaldehyde and 0.5% glutaraldehyde, embedded in Unicryl resin and stained with uranyl acetate and lead citrate. Fragments of cell membrane, organelles and possibly nucleus are visible. The cytoarchitecture is severely disrupted and the resin appears creased.

Magnification = $\times 2\ 600$

Figure 39

Higher power electron micrograph of the NT2 stem cells seen in Figure 38. Possible nuclear material is seen here.

Magnification = $\times 7\ 900$

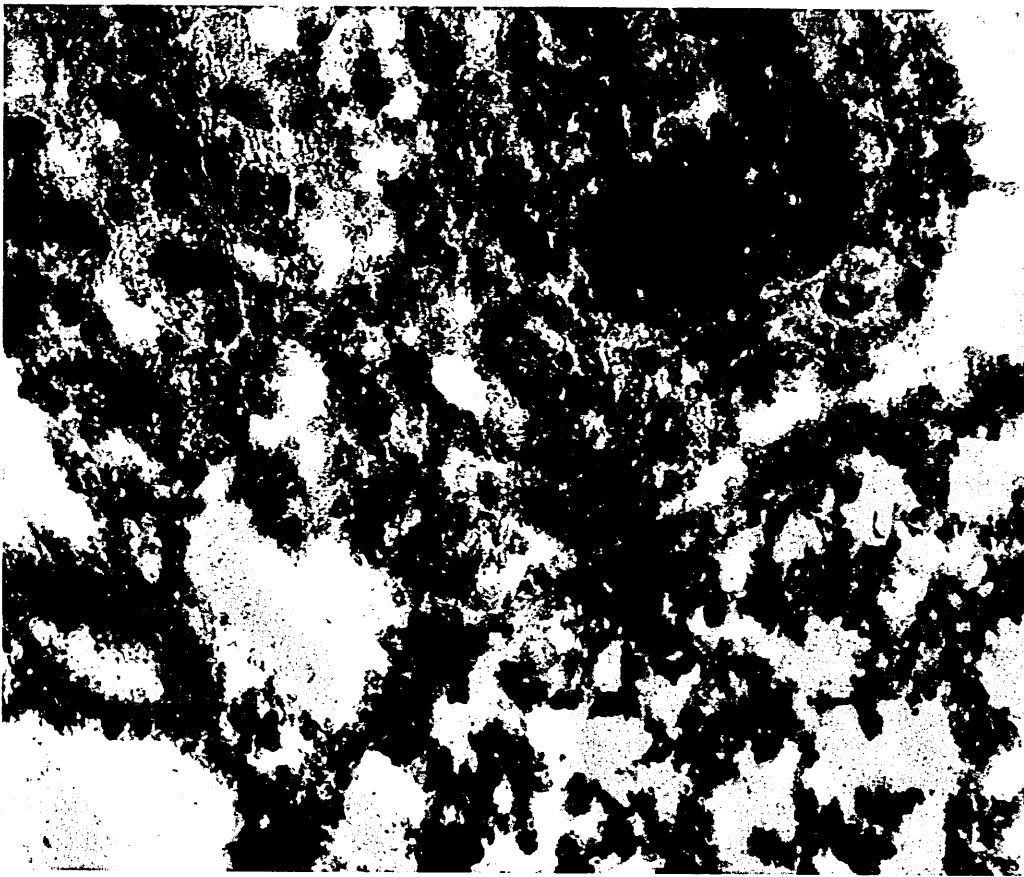


Figure 40

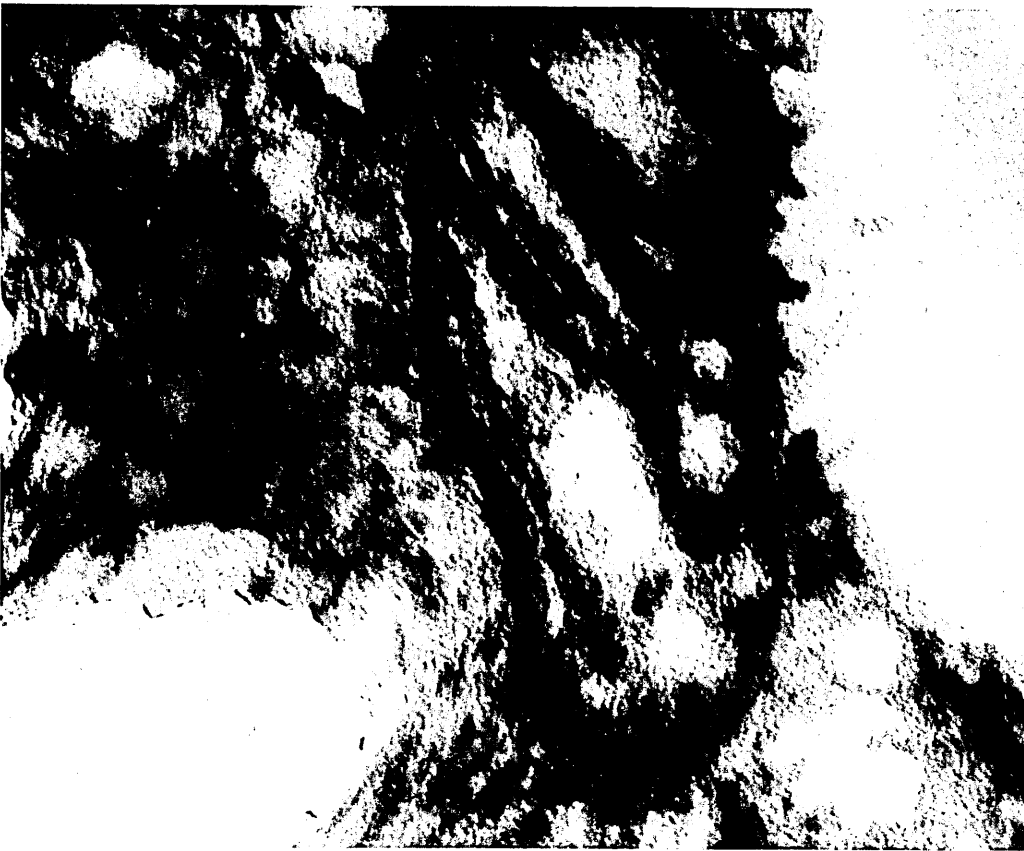


Figure 41

Figure 40

Higher power electron micrograph of the area of NT2 stem cell material shown in Figure 40, showing a possible nucleus.

Magnification = $\times 21\ 000$

Figure 41

High power electron micrograph of an organelle, possibly a mitochondrion, within the area of NT2 stem cells shown in Figure 38.

Magnification = $\times 64\ 000$

Discussion

Collection of NT2 stem cells or neurones by centrifugation appeared to disrupt their morphology too much for successful EM examination. Neurones that were scraped from the cell culture vessels were barely visible to the naked eye and therefore too easily lost during the lengthy osmication and embedding procedure. Although no neurones were identified in sections cut from those that were processed *in situ*, this seemed the most promising of the techniques attempted. If cellular material was retained in the resin blocks on removal of the glass slides, these neurones would be expected to be relatively intact in comparison to those that were processed following removal from the culture surface and thus subjected to greater mechanical stress. Indeed traces of the neuronal processes and their clusters of cell bodies were visible with a magnifying glass on the surfaces of the blocks exposed on removal of the slides.

Since completion of this work the results of two studies have been published in which NT2 cells were successfully examined by EM. The first of these studies described co-cultures of NT2 neurones with primary rat astrocytes as well as pure NT2N cultures on poly-D-lysine and matrigel (Hartley *et al.*, 1999). In the co-cultures the neurones spread out over the astrocyte cell layer rather than forming the clusters seen when NT2 neurones are grown on matrigel. These cells were fixed *in situ* with 2% glutaraldehyde in phosphate-buffered saline (PBS) overnight at 4°C, osmicated and stained with uranyl acetate, then embedded in partially pre-hardened blocks of EPON resin. This method resulted in preservation of morphology sufficient to identify synapses and intracellular structures. In the pure neuronal cultures few synapses were present and these contained small clusters of vesicles without synaptic densities. In the co-cultures many synaptic

densities were seen, with associated small, clear vesicles, and large, dense-cored or clear vesicles.

In the second of these studies NT2 neurones grown on poly-D-lysine- and matrigel-coated coverslips were examined by EM and immuno-EM for neurotransmission type (Guillemain *et al.*, 2000). Neurones were fixed in 4% paraformaldehyde and 0.5% glutaraldehyde in 0.1M PBS for 1 hour at room temperature. One set of cultures was immunolabelled and all cultures were then osmicated and embedded in araldite resin *in situ*. Punches 1.5mm in diameter were made through the cultures and these were mounted on araldite blocks. After ultra-thin sections were cut, non-immunolabelled sections were stained with uranyl acetate and lead citrate. This paper describes in detail the ultrastructure of the NT2 neurones examined by EM. Cell bodies with a large, regular nucleus and clear cytoplasm, and a smaller number of cell bodies with an irregular nucleus and dense cytoplasm were described. Golgi saccules, smooth and rough endoplasmic reticulum, mitochondria and polymorphic autophagic-like vacuoles were identified in both of these cell types. Axon-like and dendrite-like processes were described. Few classical synaptic contacts were present in the clusters of cell bodies, but a number of typical synaptic contacts were observed between axon-like and axon-like or between axon-like and dendrite-like processes, with symmetrical membrane densifications and numerous synaptic-like vesicles. The immuno-EM successfully labelled neurotransmitters in the cytoplasm of cell bodies and dendrites of NT2 neurones.

The similarity of the techniques used in the two studies described above to the method used in this study for *in situ* embedding of NT2 neurones suggests that neurones may have been successfully embedded in the blocks that were processed *in situ*. The sections

that were cut may have been too thick for the cells to be seen under the electron microscope, or the cells may have been discarded in sections that were not collected. Alternatively, the optimum concentrations of paraformaldehyde and glutaraldehyde may not have been used so that cells were poorly preserved. The ultra-thin sections of *in situ* neurones that were examined by EM were from the block that was fixed with 2% paraformaldehyde, whereas Hartley *et al.* (1999) used 2% glutaraldehyde and Guillemain *et al.* (2000) used 4% paraformaldehyde plus 0.5% glutaraldehyde.

This *in situ* method of processing NT2 cells for EM or immuno-EM, optimised according to the methods described by Hartley *et al.* (1999) and Guillemain *et al.* (2000) should be of use in future studies of EM localisation of proteins and peptides implicated in the pathogenesis of AD.

CHAPTER 5: KPI-CONTAINING APP IN THE

HUMAN BRAIN

Uncovering of a KPI domain epitope of Alzheimer's amyloid precursor protein for immunohistochemistry in human brain

Introduction

The amyloid precursor protein is expressed by most cells of the human body. Differential splicing of the primary RNA transcript of APP generates eight protein products of differing length, APP-695 being the most abundant in brain, followed by APP-751 and APP-770. The latter two of these contain a Kunitz protease inhibitory (KPI)-encoded region (Ponte *et al.*, 1988; Tanzi *et al.* 1988; Kitaguchi *et al.*, 1988). Much research to date has focussed on APP-695 because, unlike KPI-containing isoforms (KPI-APP), its distribution is restricted to the brain. However, evidence suggests that the ratio of KPI-APP/APP-695 isoform mRNA is elevated in the brain with age and in AD (Johnson *et al.*, 1990; Wightson-Benn *et al.*, 1995). More recently it has been demonstrated that the KPI-APP protein level in the soluble subcellular fraction of AD brains is significantly higher than in normal brains (Moir *et al.*, 1998). Furthermore, the increase in APP-751/APP-695 mRNA ratio in hippocampal pyramidal neurones shows a strong, linear, positive correlation with senile plaque density in the hippocampus and entorhinal cortex (Johnson *et al.*, 1990).

The present study investigates the pre-treatments needed to allow for the use of a novel polyclonal antibody that is specific for KPI-APP. Methods are described that uncover the epitope to allow detection of the antigen by immunoprecipitation and immunohistochemistry.

Methods

Antibody production, immunoprecipitations, SDS-PAGE and Western blotting were carried out by D. Parkinson (Campbell *et al.*, 1999).

Antibody production

Polyclonal antibodies (Ab993) to the KPI domain of APP were generated in a rabbit by D. Parkinson (Sheffield Hallam University), by immunisation with a synthetic peptide. The peptide sequence and its alignment to the KPI domains of APP and amyloid precursor-like protein 2 (APLP 2) are shown in Figure 42.

Immunohistochemical staining of human brain sections

Immunostaining was performed on 10µm-thick sections of formalin-fixed, paraffin-embedded whole temporal cortex of 3 neurologically normal human brains (Table 2).

Table 2: Brains used for immunohistochemical staining.

Case no.	Age	Sex	P.M. Delay/hours	Cause of death
S156	93	Female	25	Ischaemic heart disease
S172	84	Male	48	Emphysema
S131	82	Male	58	Carcinoma of the lung

Endogenous peroxidase activity was quenched by incubation in 0.5% H₂O₂ (Sigma Chemical Co) in methanol. Immunostaining was then carried out using a Vectastain Elite ABC kit (Vector Laboratories), as indicated in the kit. The sections were incubated with anti-KPI antibody, at 1:400 dilution, overnight at 4°C. Visualisation of the secondary antibody was achieved using diaminobenzidine (DAB), enhanced with nickel (Vector Laboratories).

Prior to immunostaining, pre-treatment A was performed on three sections, three sections were given pre-treatment B, three were given pre-treatment C and three were given pre-treatment D. This was repeated for each of the three brains. The pre-treatments were as follows:

A: Microwaved in 0.05M Tris-HCl (BDH Laboratory Supplies), pH 7.0 for 7 minutes.

B: Reduction with 0.14M 2-mercaptoethanol (Sigma Chemical Co) in 0.5M Tris-HCl (pH 8) and 1mM EDTA for 3 hours in the dark at room temperature. These sections were then washed for 3 minutes in distilled water and reduced sulphhydryl bonds were alkylated in 250mg/ml iodoacetic acid (Sigma Chemical Co) in 0.1M NaOH, diluted

1:10 in 0.5M Tris-HCl (pH 8) and 1mM EDTA, in the dark at room temperature for 20 minutes.

C: Pre-treatment A followed by B.

D: Incubation with 80% formic acid (BDH Laboratory Supplies) for 20 minutes.

Alongside each of the above pre-treatments, three sections were given no pre-treatment prior to immunostaining, and the primary antibody was omitted from one section. The control section from which the primary antibody was omitted was given the pre-treatment that was being investigated in the positive sections.

Controls included pre-absorption of the primary antibody with the antigen, and substitution of the primary antibody with non-immune serum. Twelve sections were treated with pre-absorbed antibody and twelve with non-immune serum, and groups of three of these were given pre-treatments A, B, C or none. Pre-immune serum from the immunised rabbit was not available, therefore non-immune serum from another rabbit was used. Positive control sections from the same brain, labelled with anti-KPI primary antibody, 1:400, were stained alongside these sections.

Results

Western blots

This work was carried out by D. Parkinson (Sheffield Hallam University). Cell culture medium conditioned by retinoic acid-treated NT2 cells was used to characterise the KPI-specific antibody used in this study since these human cells produce both KPI-containing APP and APP-695 (Pleasure and Lee, 1993; Wertkin *et al.*, 1993). Two

monoclonal antibodies, 6E10 and DE2, that recognise epitopes within residues 1–16 of the β -amyloid peptide sequence, were used on immunoblots to identify all forms of secreted, α -secretase-cleaved APP. The preparation and characterisation of 6E10 has been described previously (Ghiso *et al.*, 1992). DE2 was raised against β -amyloid 1–16 by D. Parkinson (Sheffield Hallam University). Both 6E10 and DE2 recognised bands of 115kDa and 105kDa (Figure 43, A). These results demonstrate that DE2 has similar properties to 6E10, and it was used for subsequent immunoprecipitations. Rabbit antiserum Ab993 stained only the 115kDa band (Figure 43, B).

While Ab993 stains KPI-containing APP on immunoblots without pre-treatment other than the standard solubilising in detergent containing a reducing agent, it does not immunoprecipitate any APP when used with untreated medium (Figure 43, B). After NT2 medium was treated with 2-mercaptoethanol to reduce disulphide bonds, followed by iodoacetamide to alkylate the cysteine residues and prevent reformation of the disulphide bonds, DE2 still immunoprecipitated the 115kDa band (Figure 43, B). These results indicate that binding of Ab993 to the KPI domain requires reduction of disulphide bonds to reveal its epitope.

Immunohistochemistry

The results of immunostaining of sections from the brain of an 84-year-old male who died of emphysema are shown in Figure 44. Sections that were not pre-treated displayed weak immunostaining of cell bodies in the grey matter of the temporal cortex (D). These were predominantly pyramidal cells in layers three and five, though not all pyramidal cells were immunopositive. In addition there was visible granular immunostaining of the neuropil and positive staining of probable astrocyte cell bodies.

Pre-treatment of sections with 2-mercaptoethanol and iodoacetate enhanced this staining (C), and sections that were microwaved were slightly more strongly immunolabelled (B). However, sections given both of the above pre-treatments exhibited the greatest level of immunoreactivity (A). In these sections extension of immunostaining into the dendrites of pyramidal cells was apparent, consonant with the positive staining of the surrounding neuropil.

Other cell types that were stained may have been neuronal or glial, but were not easily identifiable due to their lack of distinctive morphology. Formic acid pre-treatment of sections did not confer any enhancement of immunostaining.

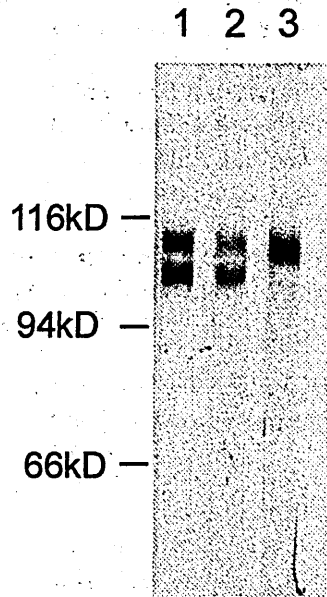
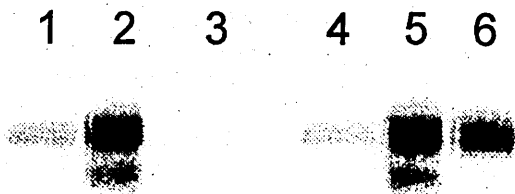
Control sections incubated with primary antibody pre-absorbed with peptide antigen were immunonegative (E) were immunonegative, whether pre-treated as described above or not pre-treated. No immunostaining was seen on omission of the primary antibody (F). In both these treatments the sections were so pale that photomicroscopy required significant underexposure relative to that used when photographing the immunopositive sections. Photomicrographs of the sections in E and F taken at the same settings as figures A and D were blank (data not shown).

Similar results were obtained with two other cases: a 93-year-old female, cause of death was ischaemic heart disease; and an 82-year-old male, cause of death was carcinoma of the lung (data not shown).

	287		345
APP	VVREVCSEQAETGPCRAMISRWYFDVTEGKCAPFFYGGCGGNRNNFDTEEYCMVCGSA		
antigen	CSEQAETGPCRAMISRWF		
APLP2	VKAVCSQEAMTGPCRAVMPRWYFDLSKGKCVRFIYGGCGGNRNNFESEDYCMVCKAMI		
	306		364

Figure 42

Amino acid sequences of Kunitz protease inhibitor domain of APPs. The sequences for the Kunitz protease inhibitor domain are shown from the SWISSPROT entries for APP (Accession Number P05067) and APLP2/APPH (Accession Number Q06481). Identical amino acid residues between the peptide antigen used, by D. Parkinson (Sheffield Hallam University), for raising the KPI antiserum are shown as vertical bars.

A**B****Figure 43**

Characterisation of APP antibodies by Western blotting (work performed by D. Parkinson, Sheffield Hallam University). The samples were separated on 6.5% polyacrylamide gels, transferred to nitrocellulose and then subjected to Western blotting. (A) Separate lanes of Ntera 2 medium were immunoblotted with 6E10 (lane 1), DE2 (lane 2) or Ab993 (lane 3). The mobility of molecular weight markers is shown to the left of lane 1. (B) Ntera 2 medium was immunoprecipitated with either DE2 (lanes 2 and 5) or Ab993 (lanes 3 and 6). Samples for lanes 1–3 were untreated while lanes 4–6 were reduced and alkylated prior to immunoprecipitation. Lanes 1 and 4 contain a sample of medium. All lanes were immunoblotted with DE2.

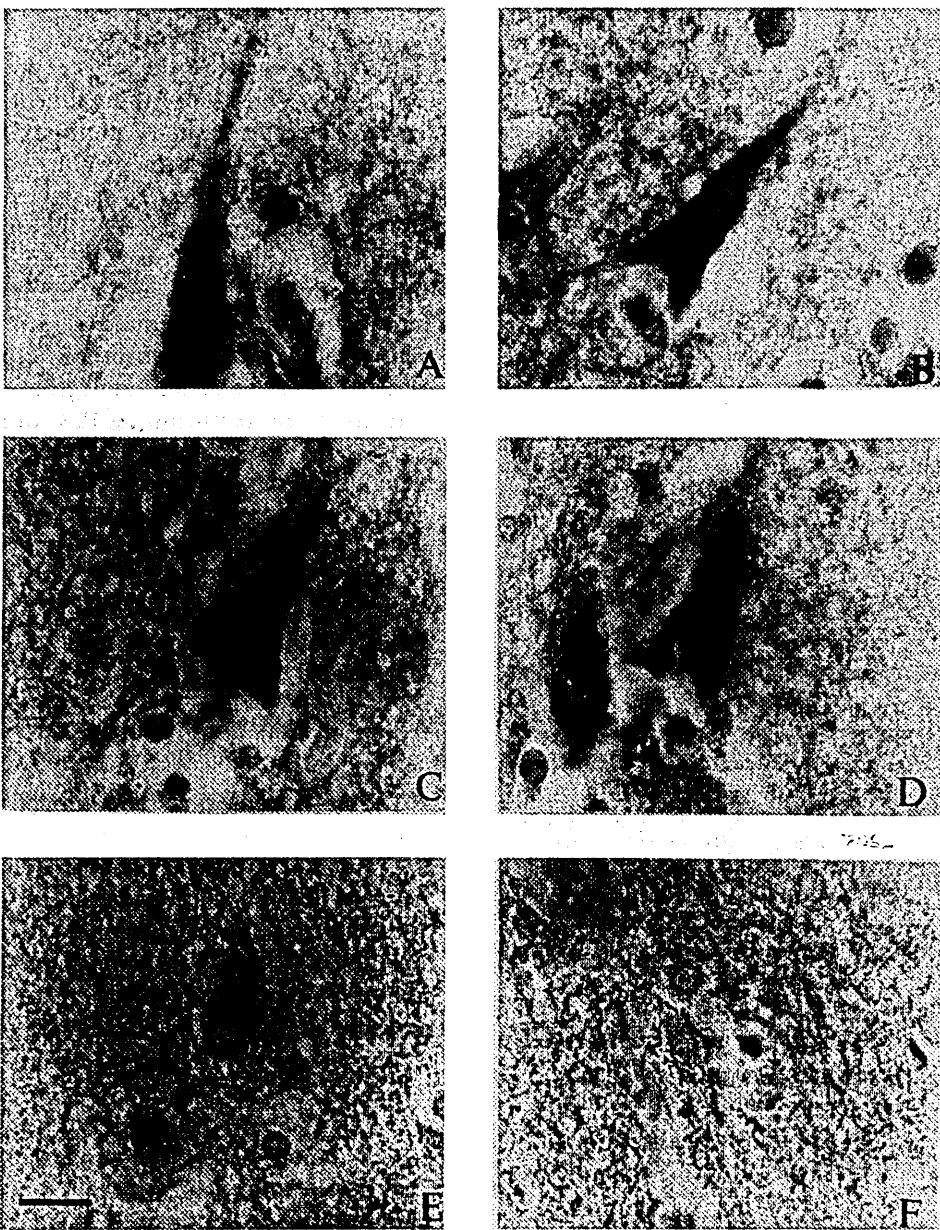


Figure 44

Immunohistochemical staining of KPI-containing APP in human brain. Photomicrographs of upper layer II pyramidal neurones in the middle temporal gyrus of case S172. (a) Pre-treated with 2-mercaptoethanol and microwaving. (b) Pre-treated with microwaving. (c) Pre-treated with 2-mercaptoethanol. (d) No pre-treatment. (e) Sections pre-treated with 2-mercaptoethanol and microwaving and antibody pre-absorbed with peptide. (f) Pre-treated with 2-mercaptoethanol and microwaving and primary antibody omitted.

Discussion

A polyclonal antibody to the KPI domain of APP was generated in a rabbit. Immunoblots obtained with this antibody suggest high specificity (Figure 43).

The KPI antibody does not immunoprecipitate native APP (Figure 43). Examination of the SWISSPROT entry for APP (Accession Number P05067) reveals potential disulphide bonds between residue pairs 291–341, 300–324 and 316–337, which are within the KPI domain (residues 287–345, all APP–770 numbering). These disulphide bonds may obscure the epitope recognised by Ab993. This idea is supported by the results from immunoprecipitation of APP (Figure 43) and therefore formed the rationale for pre-treatment of brain sections for immunohistochemical localisation of APP.

This antibody is suitable for immunodetection of KPI-containing APP isoforms in paraffin-embedded human brain, following uncovering of the KPI domain epitope by pre-treatments evaluated in this study. Microwaving the sections enhanced immunostaining more than 2-mercaptoethanol. However, these effects were additive, therefore it is likely that the two pre-treatments uncover the epitope by different mechanisms.

It has been suggested that heat-mediated antigen retrieval for immunohistochemistry may uncover antigenic sites by providing the energy to rupture hydroxyl bonds between formalin and protein, and by chelation of calcium from the sections by the salt solution (Morgan *et al.*, 1994). Removal of calcium from the sections would break the fixative bonds permanently, thus revealing antigens. The pH of the buffer also appears to influence the efficacy of antigen retrieval by this method (Shi *et al.*, 1993).

This study compared the effects of heat-mediated antigen retrieval with reduction using 2-mercaptoethanol or no pre-treatment.

The results of this investigation show that both heating and disulphide bond reduction increase staining by the anti-KPI antibody when applied to paraffin-embedded human brain. Microwaving the sections enhanced immunostaining more than 2-mercaptoethanol did. However, these effects were additive and, therefore, it is likely that the two pre-treatments uncover the epitope by different mechanisms.

The methods described here most probably act by reduction of disulphide bonds that normally mask the antigenic site, followed by alkylation to prevent the bonds from re-forming. This technique, therefore, may be useful for uncovering other antigens that are potentially hidden by disulphide bonds and cannot be exposed by other methods of antigen retrieval.

The absence of immunolabelling by an antibody that was pre-absorbed with the antigen demonstrates the specificity of Ab993 for the KPI domain epitope of APP. Lack of staining by non-immune serum indicates that all immunostaining seen with Ab993 was due to labelling of the antigen by specific antibodies.

APP is a member of a multigene family, including APLP1 and APLP2, and alternatively spliced variants of these other genes that include KPI domains have been reported (Slunt *et al.*, 1994; Sandbrink *et al.*, 1994). As shown in Figure 42, the peptide immunogen used to raise the KPI antibody has 68% identity with the corresponding sequence in the KPI domain of human APLP2, though non-identical residues separate the peptide into three short domains that may reduce the likelihood of cross-reactivity with APLP2. Preliminary results indicate that the antibody has negligible

cross-reactivity with APLP2 from brain so the results reported here most likely correspond to KPI-APP.

At present the cellular distribution of KPI-APP protein in human brain has not been described. This study suggests that KPI-APP is localised in pyramidal neurones as well as astrocytes. Staining of neuronal processes and of the neuropil suggests transport of the protein throughout the cell. As discussed above, mRNA data suggest that KPI-APP protein levels may be elevated in AD brains, since the ratio of KPI-APP/APP-695 is elevated in AD in comparison with normal brains. This antibody provides a tool with which the answers to these questions can be investigated.

This study demonstrates the importance of examining the structure of proteins that cannot readily be recognised by antibodies raised against distinct peptide regions. Epitopes that are potentially masked by the formation of disulphide bonds can be revealed using both heat-mediated antigen retrieval and reduction with 2-mercaptoethanol. Treatment with 2-mercaptoethanol allows detection of KPI-containing APP by Western blotting, following immunoprecipitation, and can be used to enhance the results of immunolabelling following microwaving.

Unlike other antibodies that are presently available for the study of APP, this antibody specifically recognises KPI-containing isoforms. When used with the pre-treatments described here, it will be of use in further studies of the amount and distribution of KPI-APP protein in AD brains, complementing the research that has been done on APP mRNA in AD.

CHAPTER 6: KPI-CONTAINING AMYLOID

PRECURSOR PROTEIN IN THE BRAIN IN

NORMAL HUMANS AND IN ALZHEIMER'S

DISEASE

Introduction

Much recent research has highlighted the role played in Alzheimer's disease (AD) of APP isoforms that harbour the Kunitz-type serine protease inhibitory (KPI) domain. Alternative splicing of exons 7 and 8 of APP RNA gives rise to APP isoforms that do or do not contain the KPI sequence. APP-770 contains both exons 7 (the KPI domain) and 8 (the OX-2 domain), APP-751 contains exon 7 but not 8, and APP-695 contains neither exon (Ponte *et al.*, 1988; Tanzi *et al.* 1988; Kitaguchi *et al.*, 1988). Other minor APP-related isoforms that have been detected in human brain, amyloid precursor-related protein-365 (APRP-365) and APRP-563, also include the KPI domain (Neve *et al.*, 1990; Jacobsen *et al.*, 1991).

APP-695 mRNA is expressed preferentially in brain, principally in the neurones of association neocortex. KPI-containing APP (KPI-APP) mRNA is present in most tissues, including brain, and its distribution in the brain is more homogeneous than that of APP-695. Both KPI-APP and non-KPI-APP mRNAs are found in the hippocampal pyramidal neurones of Ammon's horn, the expression of the former being higher in these neurones in normal adults (Neve *et al.*, 1988). In contrast, pyramidal cells of other cortical regions tend to express more non-KPI-APP than KPI-APP mRNA.

It has been demonstrated *in vitro* that expression of KPI-APP versus non-KPI-APP results in a shift in APP cleavage, generating a higher proportion of β -secretase-cleaved β -amyloid (1-40)/(1-42) and a correspondingly lower proportion of α -secretase-cleaved products that do not contain the whole β -amyloid sequence (Ho *et al.*, 1996). The transgenic mice produced by Games *et al.* (1995) expressed human APP (hAPP) that included introns 6-8, allowing alternative splicing of exons 7 and 8 and expression of hAPP-695, -751 and -770. The particularly high expression level of KPI-containing hAPP isoforms relative to APP-695, along with the high expression level of hAPP, inclusion of the V717F familial AD mutation, and the use of a PDGF- β promoter, may have contributed to the extensive AD-like pathology exhibited in these animals.

There are many conflicting reports on the levels of expression of KPI-APP versus non-KPI-APP mRNA isoforms in the human brain with increasing age and in AD. The levels of expression of KPI-APP mRNA isoforms have been demonstrated to be increased (Tanaka *et al.*, 1989; Rockenstein *et al.*, 1995), decreased (Johnson *et al.*, 1988; Robinson *et al.*, 1994), or unchanged (Johnson *et al.*, 1989; Ohyagi *et al.*, 1992) in AD compared with normal age-matched control individuals. However, the prevailing evidence suggests that, whether APP mRNA levels are elevated or reduced in AD, the ratio of KPI-APP/non-KPI-APP mRNA is increased in AD in comparison with normal aged controls or non-AD dementias (Tanaka *et al.*, 1989; Johnson *et al.*, 1990; Wightton-Benn *et al.*, 1995; Johnston *et al.*, 1996).

Although there have been many attempts to quantify levels of KPI-APP and non-KPI-APP mRNA isoforms in human brain, the corresponding protein levels and distribution have not been characterised. Moir *et al.* (1998) used whole hemispheres to

quantify the overall levels of KPI-APP and non-KPI-APP protein in the membrane fraction and the soluble fraction of AD versus normal and neurological control brains. This study revealed an increase in KPI-APP in the soluble subcellular fraction in AD, lending support to the majority of the RNA studies.

Here a polyclonal antibody specific for the KPI domain epitope of APP was used to characterise, by indirect immunohistochemistry, the cellular distribution of KPI-APP protein in the temporal and visual cortices of normal human brains and in the temporal cortex of AD brains. The SWISSPROT entry for APP (Accession Number: P05067) shows that it contains a cysteine residue on either side of the KPI domain epitope to which the antibody was raised. It is likely that a disulphide bond forms between these cysteine residues, preventing antibodies from gaining access to the KPI domain. 2-mercaptoethanol is a reducing agent that breaks disulphide bonds, thus allowing the antibodies to bind to the KPI domain. Therefore tissue sections were pre-treated with 2-mercaptoethanol before incubation with the primary antibody. The reduced disulphide bonds could potentially re-form so, following incubation with 2-mercaptoethanol, the reduced bonds were alkylated with sodium iodoacetic acid. This method is described in detail elsewhere (Campbell *et al.*, 1999) and in the preceding chapter.

A wide age range of normal brains was used to determine the effects of ageing on KPI-APP protein expression. Serial sections of whole temporal cortex from an AD case, with extensive KPI deposits, were immunostained with antibodies to paired helical filaments (PHF), amyloid precursor-like protein 2 (APLP2), β -amyloid and KPI-APP to investigate the relationships between these proteins. Amyloid load has been shown to correlate well with degree of dementia (Cummings and Cotman, 1995). Therefore the

amyloid load of each of the brains was quantified and compared with the amount of KPI-APP protein detected.

Methods

Immunolabelling of KPI-APP in AD and normal brains

Brain sections from 16 normal cases and 14 AD cases (see Table 3) were immunolabelled with anti-KPI antibody, allowing analysis of the distribution and intensity of KPI-containing APP immunopositivity in normal and AD brains. Brains were fixed in 10% formalin. Blocks of middle temporal and visual cortex were taken from each of the normal brains, and middle or whole temporal cortex was taken from each of the AD brains. 10µm-thick sections were cut from the paraffin-embedded tissue blocks and mounted on TESPA-coated slides. These were immunolabelled with anti-KPI antibody as described in the 'methods' chapter. Microwave antigen retrieval has been described previously to improve immunolabelling of APP in formalin-fixed, paraffin-embedded human brain sections (Sherriff *et al.*, 1994). In this study, sections were boiled twice in citrate buffer (pH 6). Quality of immunostaining following this method of microwave antigen retrieval was compared with that described in the methods chapter above (0.05M Tris-HCl, pH 7, for 3, 7 or 10 minutes). Microwaving in 0.05M Tris-HCl, pH 7, for 7 minutes resulted in the best enhancement of immunostaining intensity, without sections detaching from the slides, so this method was selected.

Controls included pre-absorption of the primary antibody with the antigen, and substitution of the primary antibody with non-immune serum. Pre-immune serum from

the immunised rabbit was not available, so non-immune serum from another rabbit was used. Positive control sections from the same brain, labelled with anti-KPI primary antibody, 1:400, were stained alongside these sections.

Initially, middle temporal cortex from S178, an AD case that was known to contain a large amount of β -amyloid, was immunolabelled. These sections were strongly immunopositive for KPI-containing APP. This case was therefore used as a positive control, and one section of S178 was included with each batch of sections immunolabelled with anti-KPI antibody. Another section of S178 was labelled, as a control omitting the primary antibody, with each batch of sections. Three sections from each tissue block were immunostained with anti-KPI.

Image analysis of KPI immunostaining

All of these sections were then examined using the image analysis programme "Freelance". Sections were analysed blind by colour-coding and numbering slides. Two areas of superficial cortex and the adjacent two areas of middle cortex and deep cortex were analysed in each section, giving a total of six measurements of each of superficial, middle and deep cortex from each tissue block. These corresponded approximately to laminae I-II, III-IV and V-VI respectively. In sections of temporal cortex the middle temporal gyrus was selected for analysis, and in visual cortex the primary visual cortex was selected.

Immunolabelling of serial sections to localise KPI-APP in AD

temporal cortex

13 serial sections of an AD case were immunolabelled with anti- β -amyloid (Dako), anti-KPI, anti-PHF (ICN Biomedicals) and 3B11 (anti-APLP2 (M.-T. Webster and P. Francis)), in the following order:

β A, KPI, 3B11, KPI, PHF, KPI, β A, KPI, PHF, KPI, 3B11, KPI, β A

Sections of whole temporal cortex were used, from a case with a large number of extracellular KPI-positive deposits present in the temporal cortex.

Sections that were immunolabelled with anti- β -amyloid were pre-treated with 80% formic acid (BDH Laboratory Supplies) for 20 minutes prior to incubation with the primary antibody. Those that were labelled with anti-KPI were pre-treated with 2-mercaptoethanol and iodoacetate as described above.

Measurement of amyloid load of temporal cortex of AD brains

Paraffin-embedded sections of middle temporal gyrus were immunolabelled with anti- β -amyloid antibody (Dako), for those brains in which amyloid load had not been measured previously (Radenahmad N., 2000). The amyloid load (percent) for each case was measured over a field that included the entire depth of the temporal cortex, using the Freelance image analysis programme. This measurement thus included all β -amyloid-immunopositive structures, such as plaques, cerebro-vascular amyloid and diffuse amyloid.

Table 3: Summary of control and AD cases used for KPI immunohistochemistry.
P.M.D. = post-mortem delay; S.D. = standard deviation; N = number of cases.

Diagnosis	Variable	Mean	S.D.	Min.	Max.	N
Control	Age/ years	70.94*	11.72	40	93	16
	P.M.D./ hours	32.75	12.31	24	58	16
	pH	6.44	0.49	5.58	7.21	13
AD	Age/ years	79.50*	8.49	60	94	14
	P.M.D./ hours	36.54	20.46	3	70	14
	PH	6.02	0.03	6.00	6.04	2

* Significant difference, $p < 0.05$.

Table 4 & Table 5: Summary of results of image analysis of KPI immunohistochemistry for control brains, n = 16, (Table 4), and AD brains, n = 14, (Table 5). S.D. = standard deviation; Nos. = numbers of cells; Cor. Nos. = corrected numbers of cells; Dia. = diameter of cells (μm); Area = area of cells (μm^2); Sup. = superficial laminae; Mid. = middle laminae; De. = deep laminae; Tot. = total of all laminae.

Table 4: Controls.

Variable	Mean	SD	Minimum	Maximum
Nos. Sup.	0.40	0.63	0.00	2.17
Nos. Mid.	0.52	0.79	0.00	2.33
Nos. De.	0.61	0.83	0.00	2.67
Nos. Tot.	1.53	1.70	0.00	4.83
Cor. Nos. Sup.	0.11**	0.18	0.00	0.60
Cor. Nos. Mid.	0.14**	0.20	0.00	0.58
Cor. Nos. De.	0.13*	0.18	0.00	0.67
Cor. Nos. Tot.	0.42*	0.46	0.00	1.33
Dia. Sup./μm	13.08	16.78	0.00	47.56
Dia. Mid./μm	16.24	20.08	0.00	70.66
Dia. De./μm	25.53	22.31	0.00	66.63
Dia. Tot./μm	18.28	16.00	0.00	56.03
Area Sup./μm^2	20.54	26.37	0.00	74.70
Area Mid./μm^2	25.51	31.55	0.00	111.00
Area De./μm^2	40.10	35.05	0.00	104.67
Area Tot./μm^2	28.72*	25.14	0.00	88.02

*Significant difference, $p < 0.05$; **significant difference, $p < 0.01$.

Table 5: AD.

Variable	Mean	SD	Minimum	Maximum
Nos. Sup.	2.65	3.63	0.00	14.17
Nos. Mid.	3.19	3.61	0.00	13.50
Nos. De.	2.82	3.02	0.00	10.50
Nos. Tot.	8.67	9.96	0.00	38.17
Cor. Nos. Sup.	0.73**	0.93	0.00	3.58
Cor. Nos. Mid.	0.75**	0.91	0.00	3.19
Cor. Nos. De.	0.55*	0.60	0.00	1.95
Cor. Nos. Tot.	1.98*	2.28	0.00	8.44
Dia. Sup./μm	25.73	10.25	0.00	44.87
Dia. Mid./μm	31.78	18.25	0.00	64.30
Dia. De./μm	39.56	20.32	0.00	76.11
Dia. Tot./μm	32.36	12.91	0.00	52.96
Area Sup./μm^2	40.42	16.10	0.00	70.47
Area Mid./μm^2	49.92	28.67	0.00	101.00
Area De./μm^2	62.15	31.92	0.00	119.55
Area Tot./μm^2	50.83*	20.28	0.00	83.19

*Significant difference, $p < 0.05$; **significant difference, $p < 0.01$.

Results

The AD cases were significantly older than the normal control cases (AD 79.5 ± 8.5 years, normal 71 ± 11.7 years, t-test: $t = -2.31$, $p = 0.029$). There was no significant difference in post-mortem delay between the AD and normal groups.

Results of image analysis of KPI immunohistochemistry

The results of image analysis are summarized in Table 4 and Table 5. There was no significant difference in cell size between the normal and AD cases when superficial, middle or deep laminae were examined separately. However, on analysis of all laminae together, the overall area of KPI-immunopositive cells was greater in AD cases than normals ($U = 33.0$, $p = 0.0257$, Mann-Whitney U – Wilcoxon Rank Sum W Test). This is shown in Figure 45. Counts of cell numbers were therefore corrected to account for this size difference, using the Abercrombie correction (Abercrombie, 1946).

Using corrected cell numbers, there were more KPI-positive cells labelled in AD cases than in normals in the superficial ($U = 39.5$, $p = 0.0021$), middle ($U = 44.0$, $p = 0.0040$) and deep ($U = 52.0$, $p = 0.0121$) laminae, and in total ($U = 51.5$, $p = 0.0116$) (Mann-Whitney U – Wilcoxon Rank Sum W Test). This is illustrated in Figure 46.

Post-mortem delay (pmd) was the major determinant of cell numbers in control brains, in AD brains, and in all cases (Figure 47), by multiple regression analysis of cell numbers with the variables age, pmd (and pH in control cases; pH values were available for only two AD cases), pmd making a 76% contribution to the correlation ($\beta = 0.76$, $T = 3.875$, $p = 0.0038$).

On multiple regression analysis of corrected total cell numbers in all cases, with the variables diagnosis, age and pmd, the major determinant of total cell numbers, and of cell numbers in the superficial, middle and deep laminae, was diagnosis, followed by pmd. On analysis of total cell numbers, diagnosis made a 51% contribution to the correlation (beta = 0.51, T = 2.80, p = 0.0097), and pmd made a 37% contribution (beta = -0.37, T = -2.21, p = 0.036).

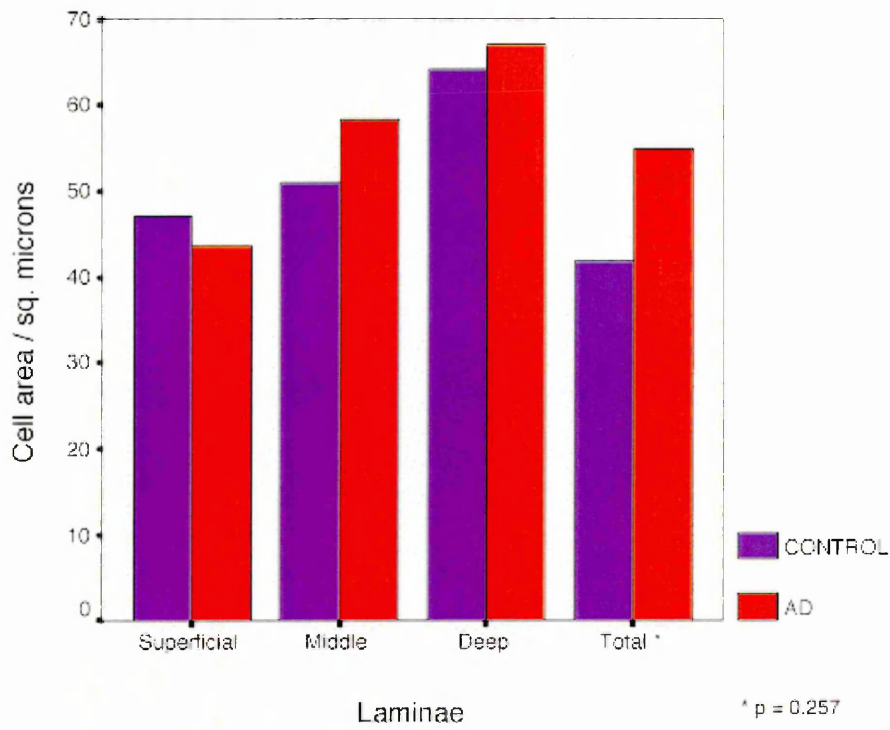


Figure 45
KPI-positive cell size in middle temporal gyrus

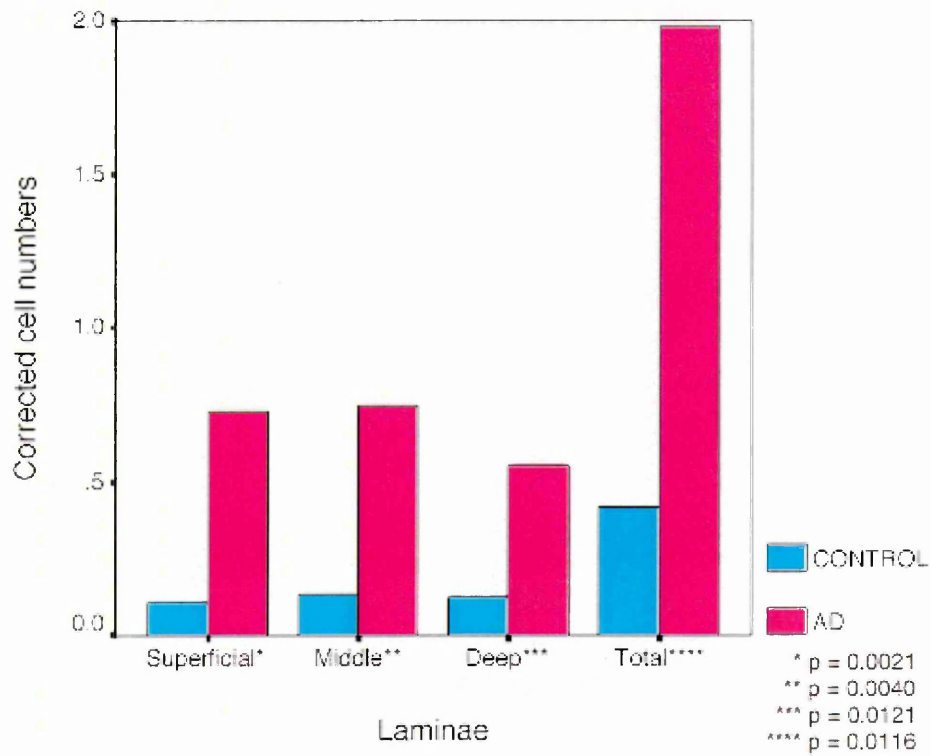


Figure 46
KPI-positive corrected cell numbers in the middle temporal gyrus

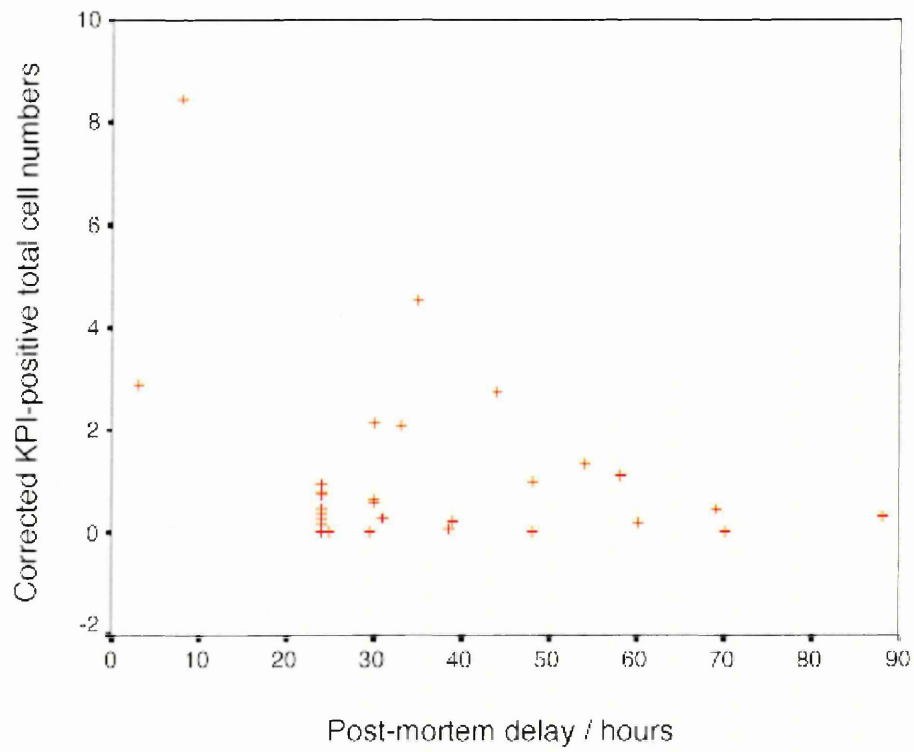


Figure 47

Scatterplot showing variation of corrected KPI-positive cell numbers with post-mortem delay in all laminae in all cases

Distribution of KPI-containing APP in human brain by immunohistochemistry

In AD brains KPI-containing neurones were more common than tangles (labelled with anti-PHF). Layer V pyramidal neurones in the temporal lobe were often strongly KPI-immunopositive (Figure 48 and Figure 50), and this is where numerous tangles were found (Figure 49, Figure 51 and Figure 52). Many smaller, non-pyramidal cells in cortical layers II to VI were KPI-positive (Figure 53). The neuropil was stained with anti-KPI (Figure 54), suggesting that KPI may be present in many neuronal processes and/or glia.

Anti-KPI (Figure 54) labels plaques with the approximate frequency and intensity of anti-PHF (Figure 55), and with less frequency and intensity than β -amyloid (Figure 56). The implication is that KPI is in the neuritic elements of plaques since burnt out and diffuse plaques do not always have KPI staining (Figure 57, Figure 59, and Figure 61 *c.f.* Figure 58, Figure 60 and Figure 62). An example of a plaque in which the neuritic element appears immunostained with anti-KPI is shown in Figure 63 and Figure 64.

All blood vessels with cerebro-vascular amyloid (CVA) (labelled with anti- β -amyloid) and some without CVA were immunostained for KPI (Figure 65 *c.f.* Figure 66, Figure 54 *c.f.* Figure 56, and Figure 63 *c.f.* Figure 64).

Sections immunolabelled with 3B11 showed no staining of APLP2 (Figure 67). Immunolabelling with antibody that had been pre-absorbed with the antigen, or with non-immune rabbit serum, yielded no immunostaining (Figure 68 and Figure 69).

Amyloid load of brains

β -amyloid loads in the temporal cortices of the AD cases, along with ages and pmd of these cases, are summarised in Table 6 below.

Table 6: Summary of β -amyloid loads in temporal cortices of AD cases. P.M.D. = post-mortem delay; S.D. = standard deviation; N = number of cases.

Variable	Mean	S.D.	Min.	Max.	N
Age/ years	79.50	8.49	60.00	94.00	14
P.M.D./ hours	36.54	20.46	3.00	70.00	13
Amyloid load/%	5.14	4.65	0.07	14.27	14

On multiple regression analysis of corrected KPI-positive cell numbers in the AD cases, with the variables age, pmd and β -amyloid load in the temporal cortex, the major determinant of KPI-positive total cell numbers was pmd, which made a 77% contribution to the correlation (beta = -0.770 , T = -2.586 , p = 0.029). Neither β -amyloid load nor age were significant determinants of KPI-positive cell numbers.

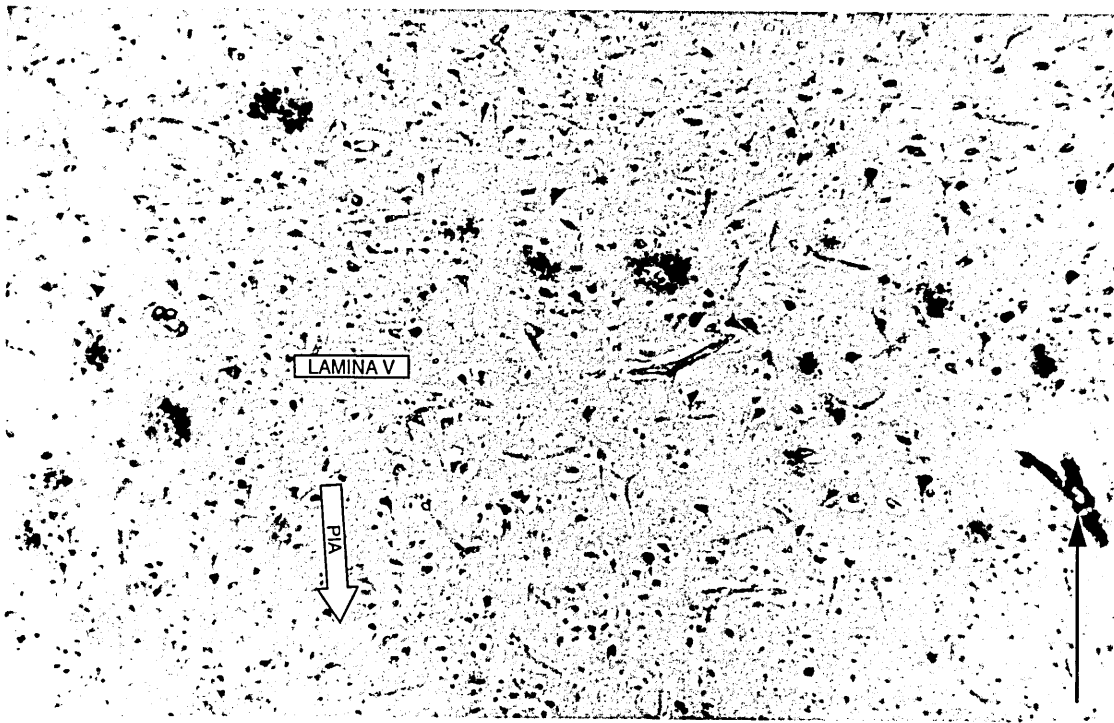


Figure 48

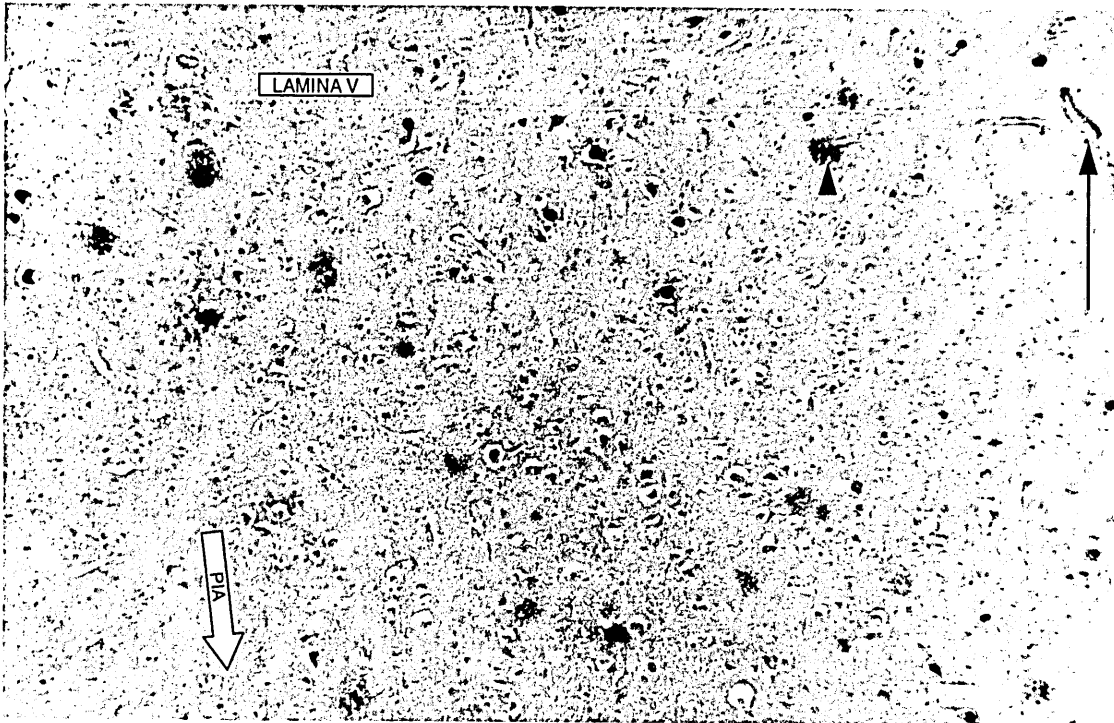


Figure 49

Figure 48

KPI immunolabelling in cortex at the superior temporal sulcus of an AD case, showing many heavily stained lamina V pyramidal neurones, as well as staining of plaques, blood vessels and the neuropil. 10 μ m-thick sections of formalin-fixed, paraffin-embedded tissue were microwaved and treated with 2-mercaptoethanol and iodoacetic acid, then labelled with anti-KPI antibody followed with biotinylated secondary antibody, ABC and DAB.

Arrow indicates the same blood vessel as in Figure 49 and Figure 50.

Magnification = $\times 20$

Figure 49

Serial section to Figure 48, showing that tangle-bearing neurones belong to a similar population to the KPI-positive cells. Section was labelled with anti-PHF followed with biotinylated secondary antibody, ABC and DAB.

Arrow indicates the same blood vessel as in Figure 48 and Figure 50. Arrowhead indicates the same plaque as in Figure 51.

Magnification = $\times 20$

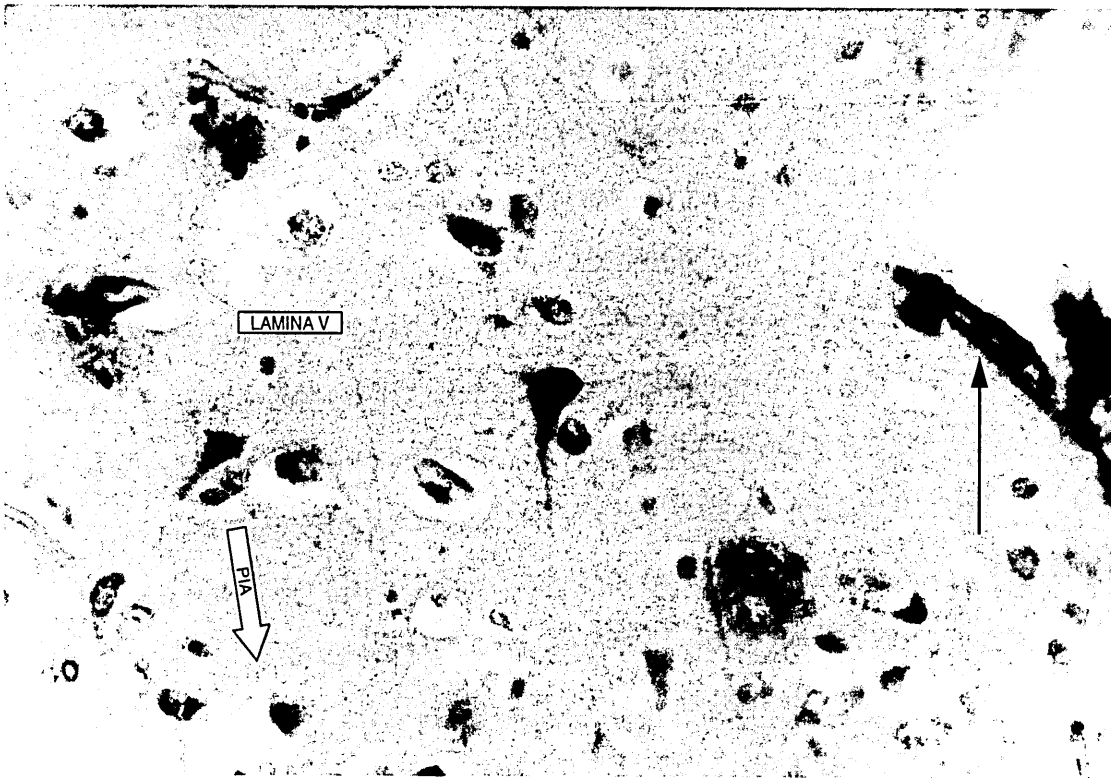


Figure 50

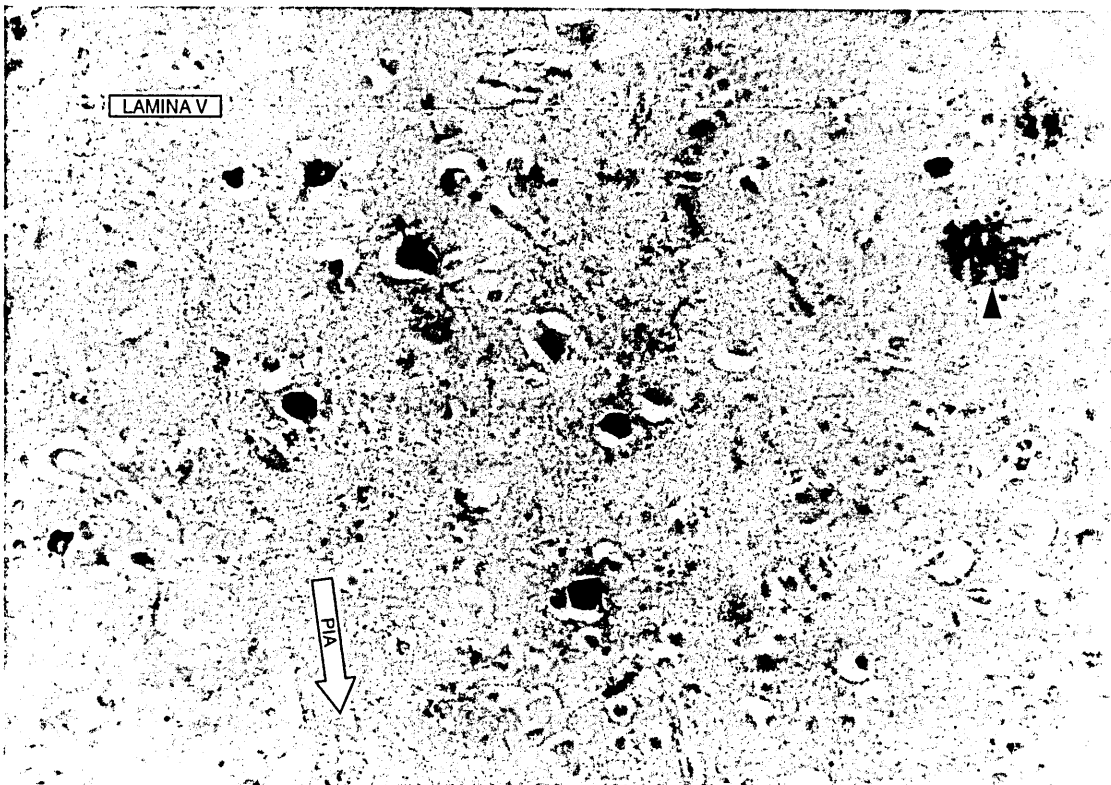


Figure 51

Figure 50

Higher power magnification of the section seen in Figure 48, showing a heavily immunostained, KPI-positive lamina V pyramidal neurone (centre).

Arrow indicates the same blood vessel as in Figure 48 and Figure 49.

Magnification = $\times 80$

Figure 51

Higher power magnification of the section seen in Figure 49, showing the PHF-positive, tangle-bearing cells in lamina V.

Arrowhead indicates the same plaque as in Figure 49.

Magnification = $\times 80$

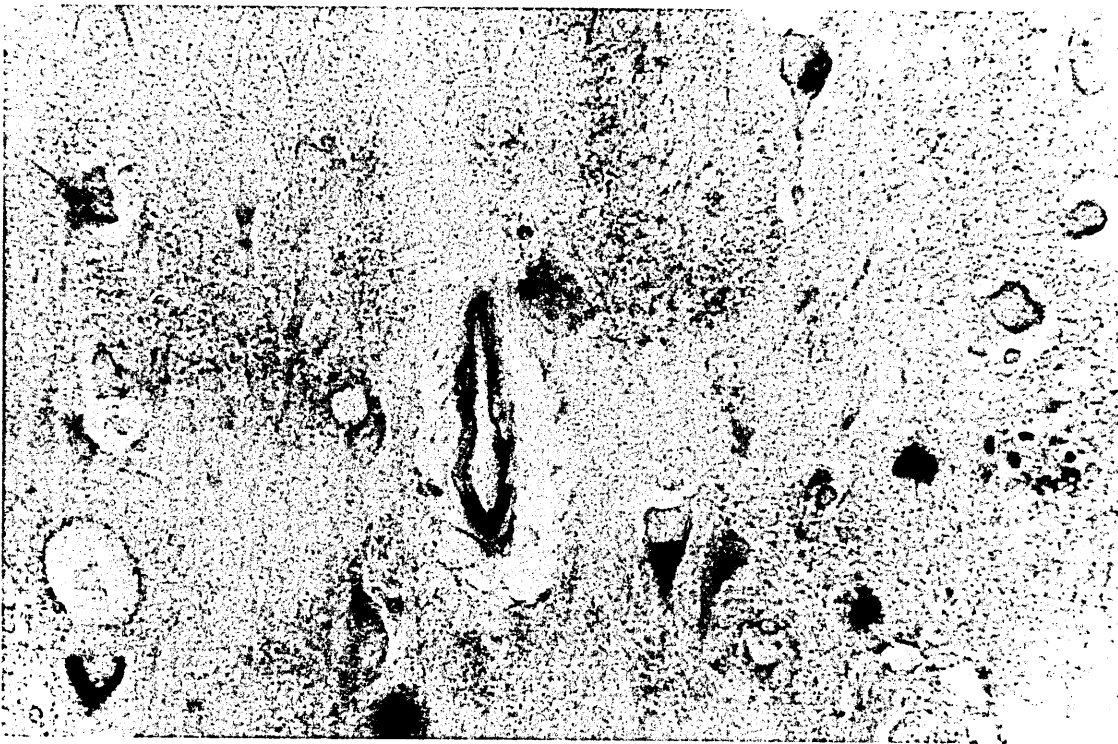


Figure 52

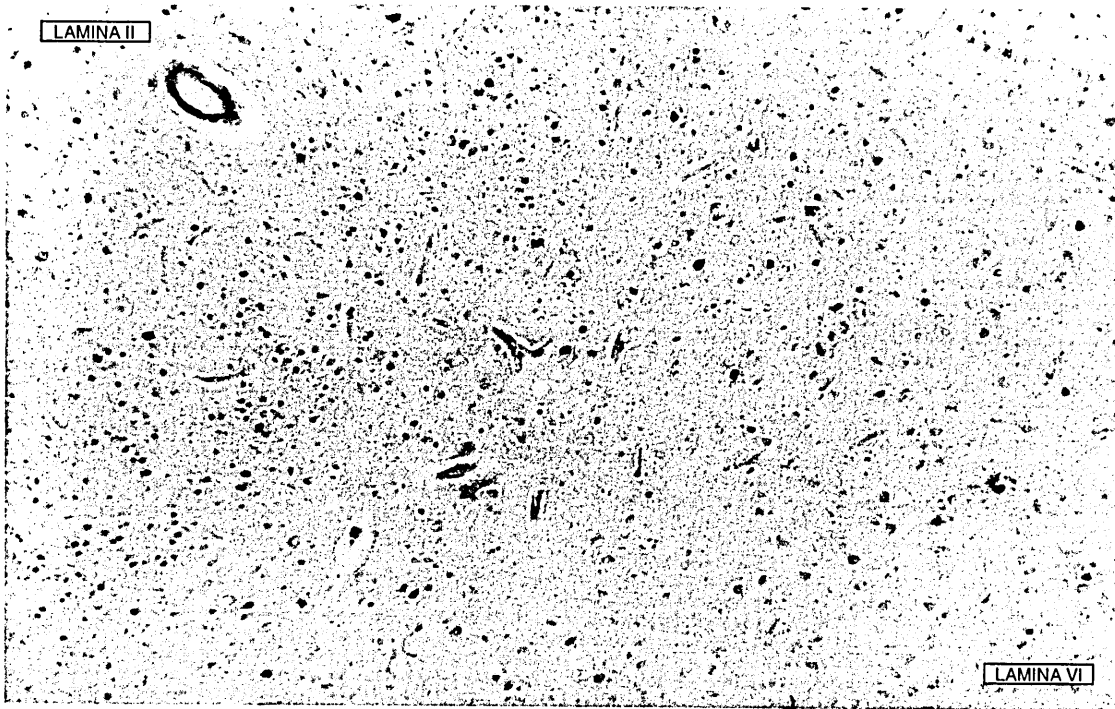


Figure 53

Figure 52

Typical examples of the many tangle-bearing pyramidal neurones in the hippocampal cortex of the same AD brain as in Figure 48–Figure 51. Section was stained with anti-PHF antibody followed by biotinylated secondary antibody, ABC and DAB.

Magnification = $\times 80$

Figure 53

KPI staining in middle temporal cortex of an AD case, showing many immunopositive smaller, non-pyramidal, cells in laminae II (top left of photomicrograph) to VI (bottom right). Section was microwaved and treated with 2-mercaptoethanol and iodoacetic acid, then labelled with anti-KPI antibody followed with biotinylated secondary antibody, ABC and DAB.

Magnification = $\times 15$

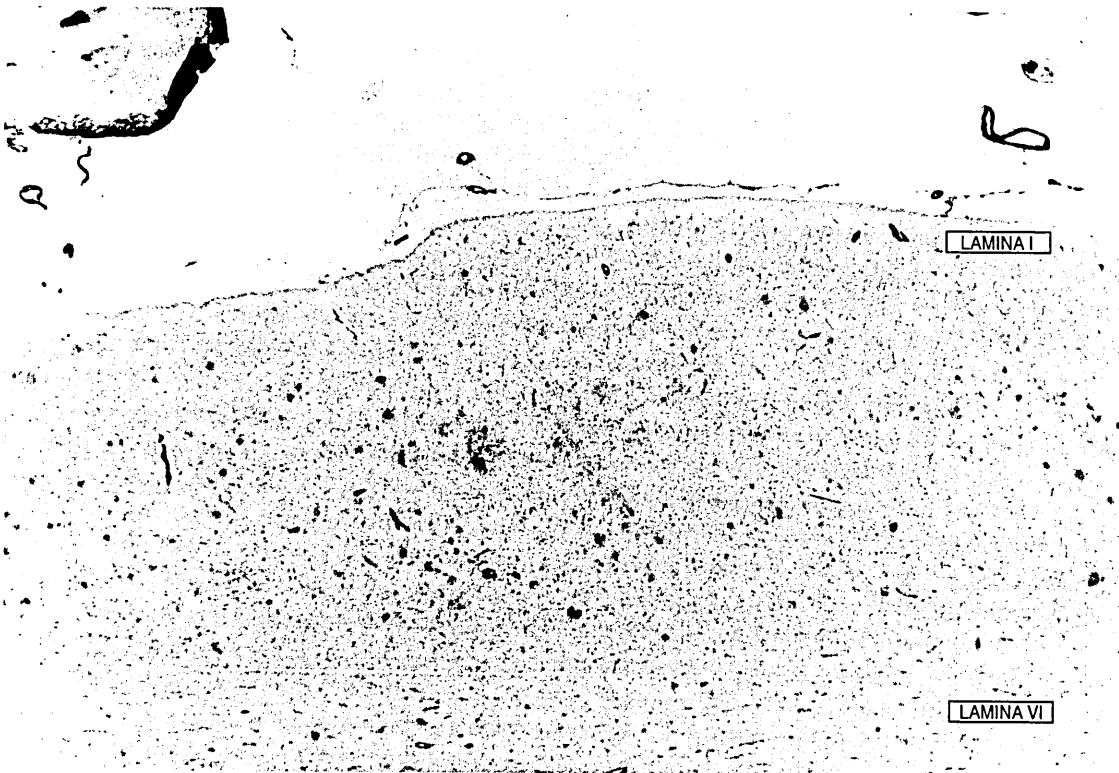


Figure 54

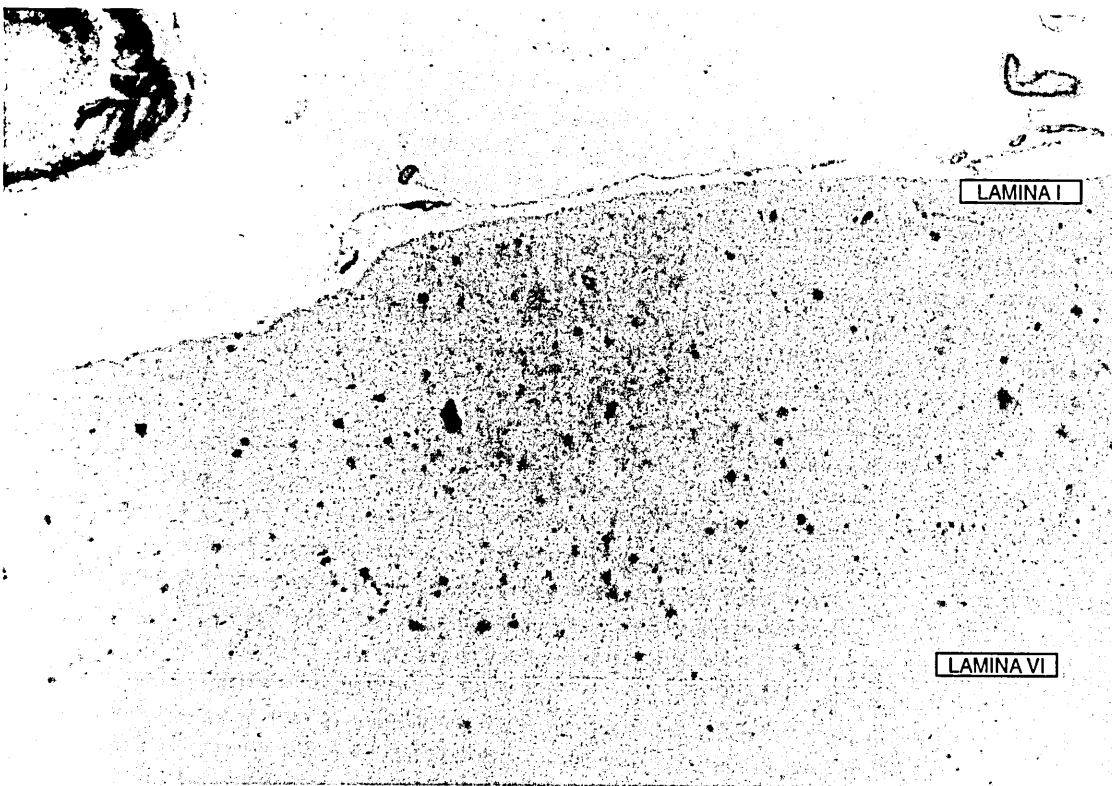


Figure 55

Figure 54

Low power KPI staining of the whole depth of the cortex at the superior temporal sulcus from the case shown in Figure 48–Figure 52. The neuropil is stained, as well as plaques in similar numbers and intensity to those labelled with anti–PHF antibody (Figure 55). Several immunopositive blood vessels can be seen. Section was microwaved and treated with 2–mercaptoethanol and iodoacetic acid, then labelled with anti–KPI antibody followed with biotinylated secondary antibody, ABC and DAB.

Magnification = $\times 8$

Figure 55

Serial section to that shown in Figure 54 above. PHF–positive plaques are present in similar numbers and labelled with similar intensity to those stained with anti–KPI antibody (Figure 54). Section was labelled with anti–PHF, followed with biotinylated secondary antibody, ABC and DAB.

Magnification = $\times 8$

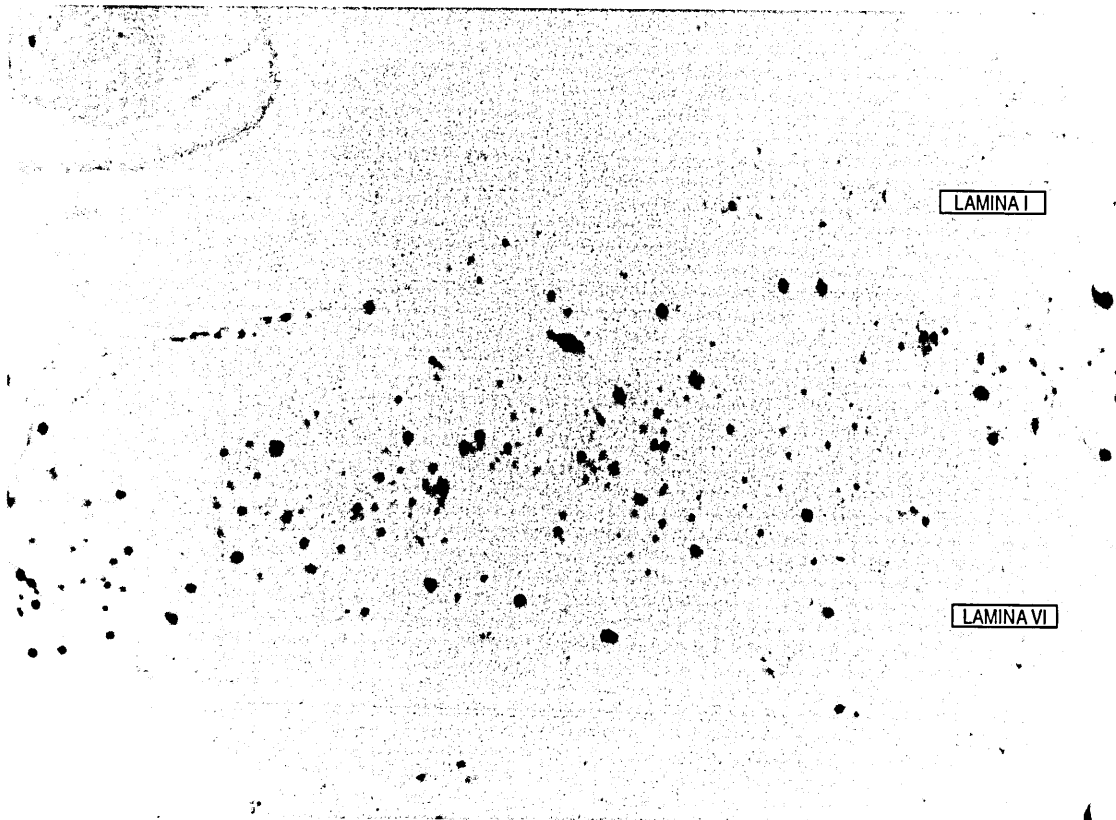


Figure 56

Figure 56

Serial section to those in Figure 54–Figure 55. β -amyloid-positive plaques are more numerous than KPI- or PHF-positive plaques. Blood vessels that are KPI-positive (Figure 54) are not β -amyloid-positive. Section was microwaved in 80% formic acid prior to immunostaining with anti- β -amyloid antibody, followed by biotinylated secondary antibody, ABC and DAB.

Magnification = $\times 8$

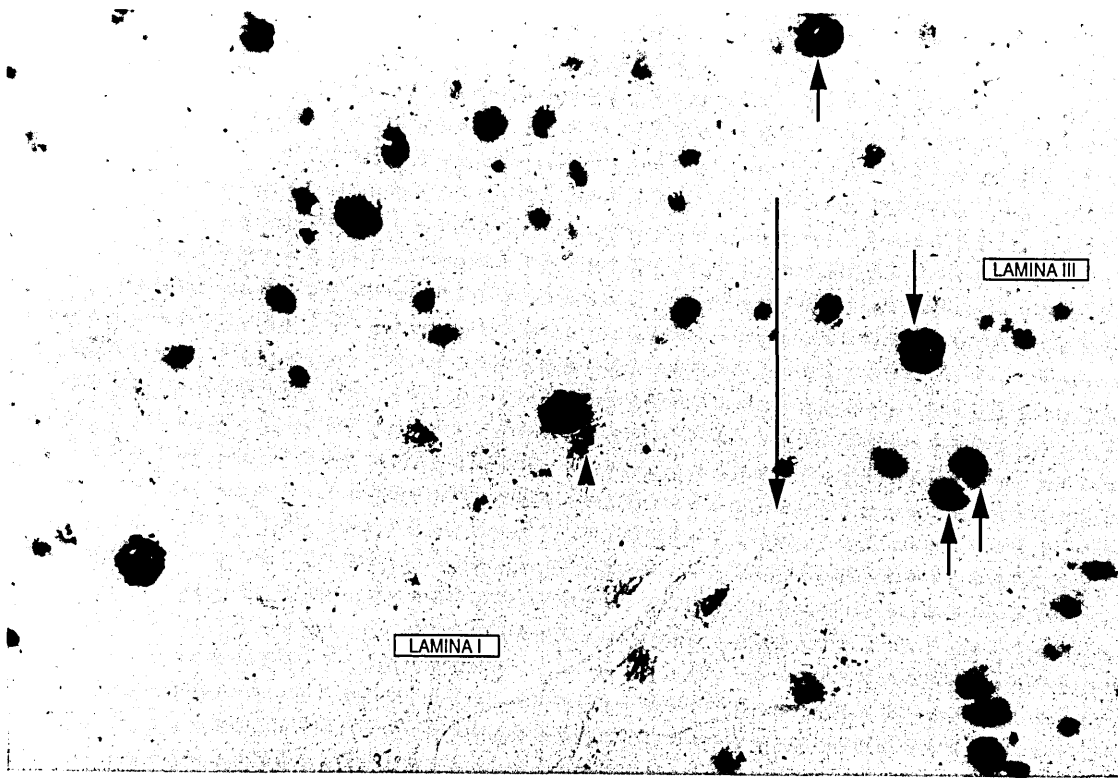


Figure 57

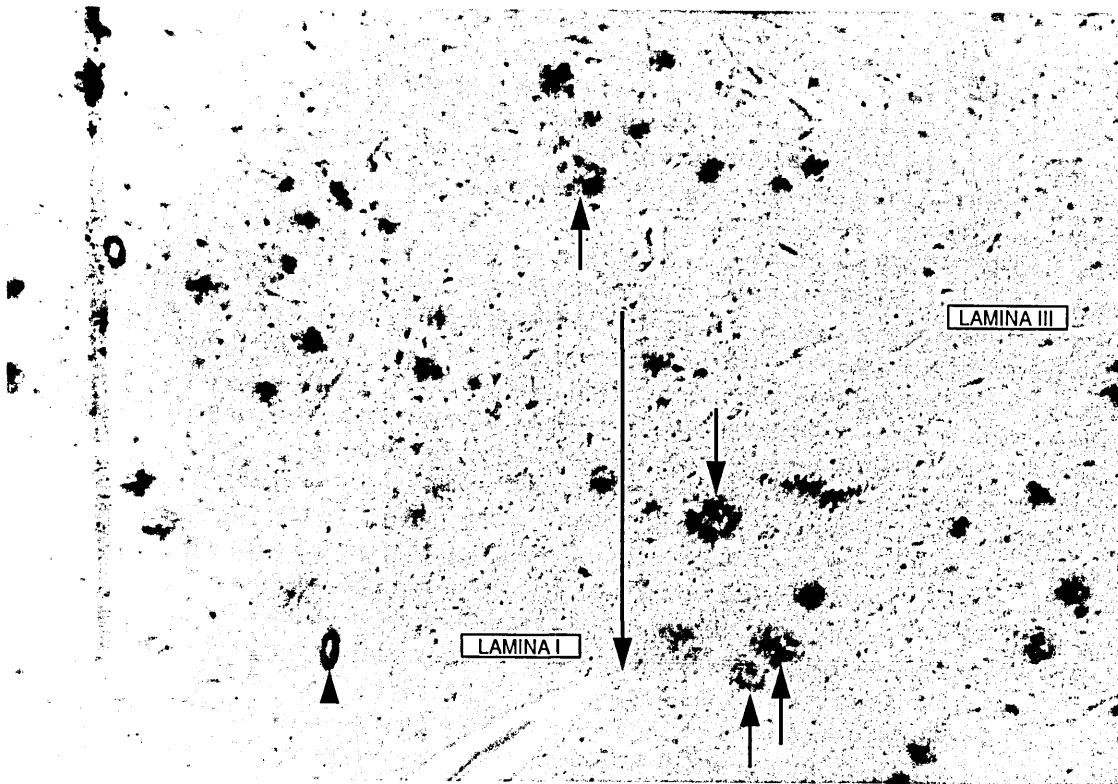


Figure 58

Figure 57 and Figure 58

Serial sections of cortex around the collateral sulcus of the AD case shown in Figure 48–Figure 52, immunolabelled with anti- β -amyloid antibody (Figure 57) and anti-KPI antibody (Figure 58). The fundus of the sulcus (long arrow) and the same blood vessel (arrowhead) are indicated. The blood vessel indicated is both β -amyloid-positive and KPI-positive. Examples of neuritic β -amyloid plaques, in which the neuritic element appears to be KPI-positive, are indicated (short arrows). The upper section was treated with 80% formic acid before immunostaining with anti- β -amyloid followed with biotinylated secondary antibody, ABC and DAB. The lower section was microwaved and treated with 2-mercaptoethanol and iodoacetic acid, then labelled with anti-KPI antibody followed with biotinylated secondary antibody, ABC and DAB.

Magnification = $\times 20$ (top and bottom)

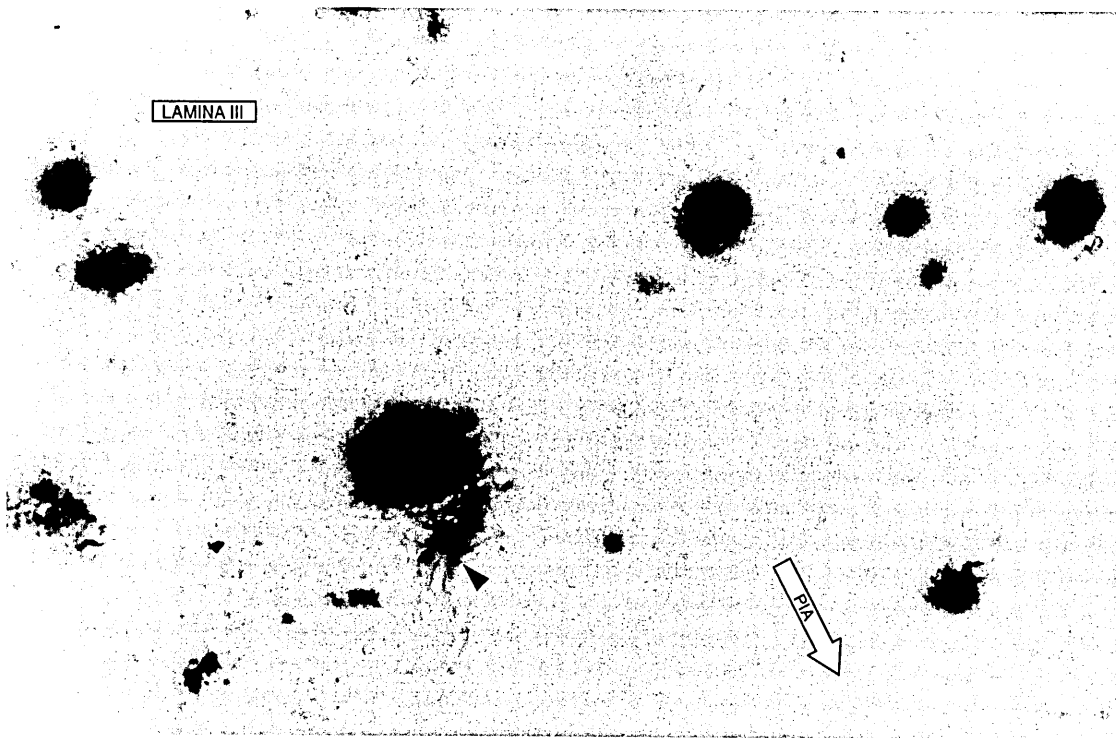


Figure 59

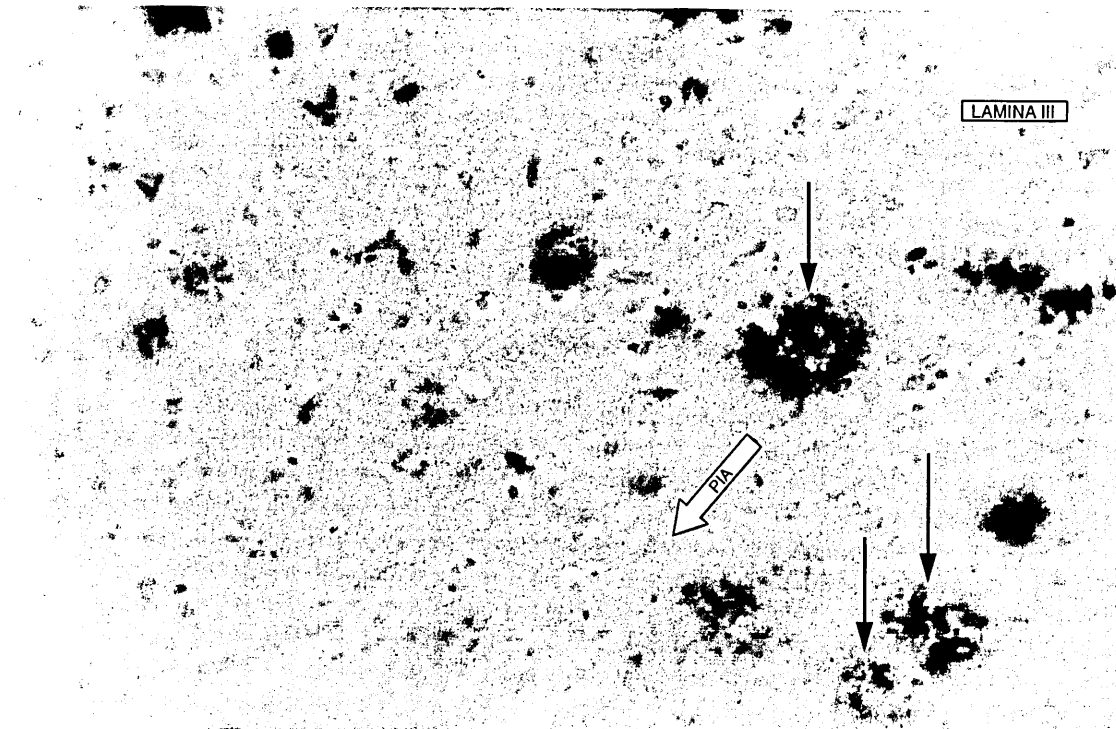


Figure 60

Figure 59

Higher power magnification of β -amyloid-positive plaques seen in Figure 57. The same blood vessel is indicated (arrowhead).

Magnification = $\times 80$

Figure 60

Higher power magnification of KPI-containing mature plaques seen in Figure 58 (arrows). The KPI-positive material appears as a “halo” surrounding the plaque core, implying a neuritic pattern of KPI distribution.

Magnification = $\times 80$

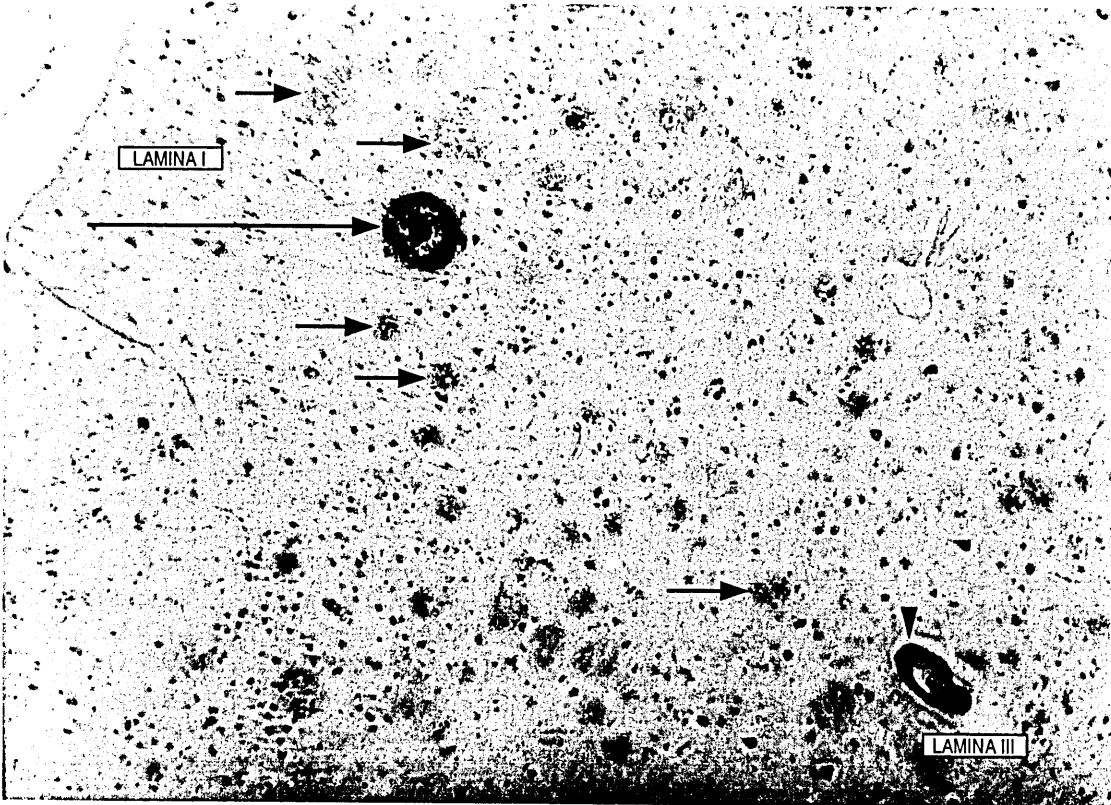


Figure 61

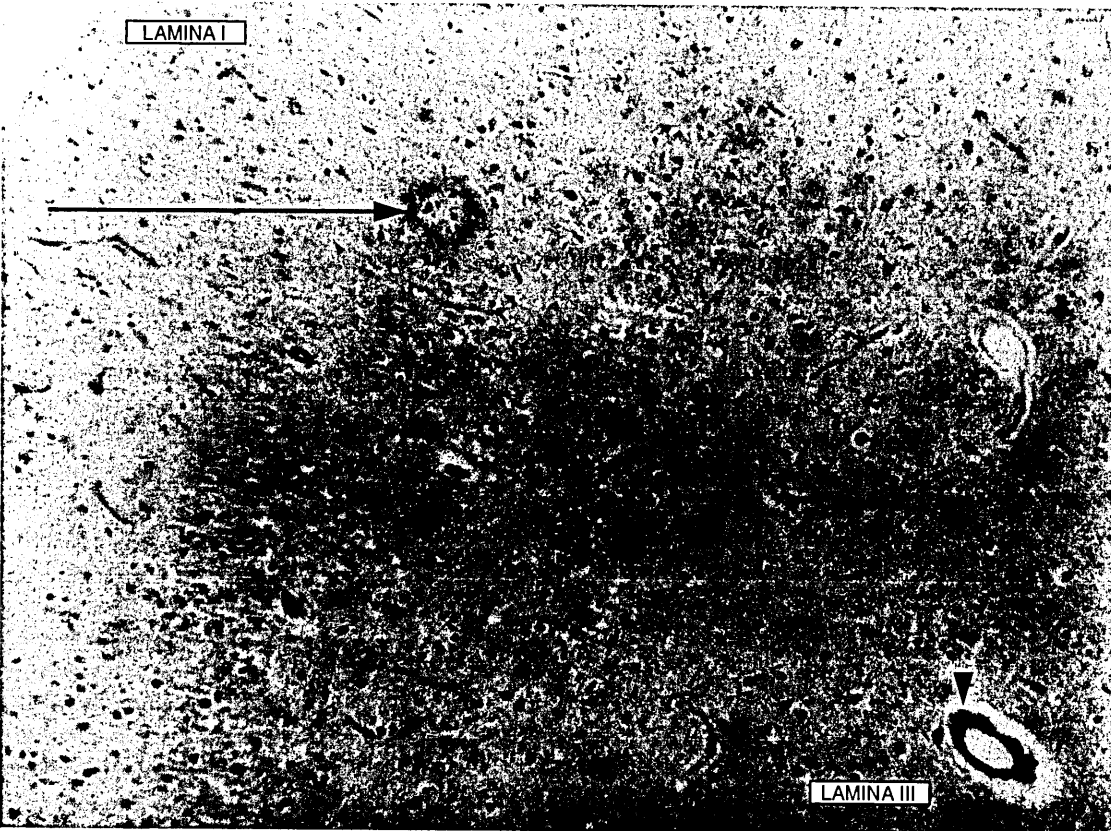


Figure 62

Figure 61 and Figure 62

Serial sections of the AD case shown in Figure 53. Many diffuse β -amyloid plaques are seen (short arrows, Figure 61), which are not immunolabelled with anti-KPI antibody (Figure 62). The same neuritic plaque, in which the neuritic element is KPI-positive, is indicated (long arrow), and the same blood vessel, which is both β -amyloid- and KPI-positive, is shown (arrowhead).

The upper section was treated with 80% formic acid before immunostaining with anti- β -amyloid followed with biotinylated secondary antibody, ABC and DAB. The lower section was microwaved and treated with 2-mercaptoethanol and iodoacetic acid, then labelled with anti-KPI antibody followed with biotinylated secondary antibody, ABC and DAB.

Magnification = $\times 20$

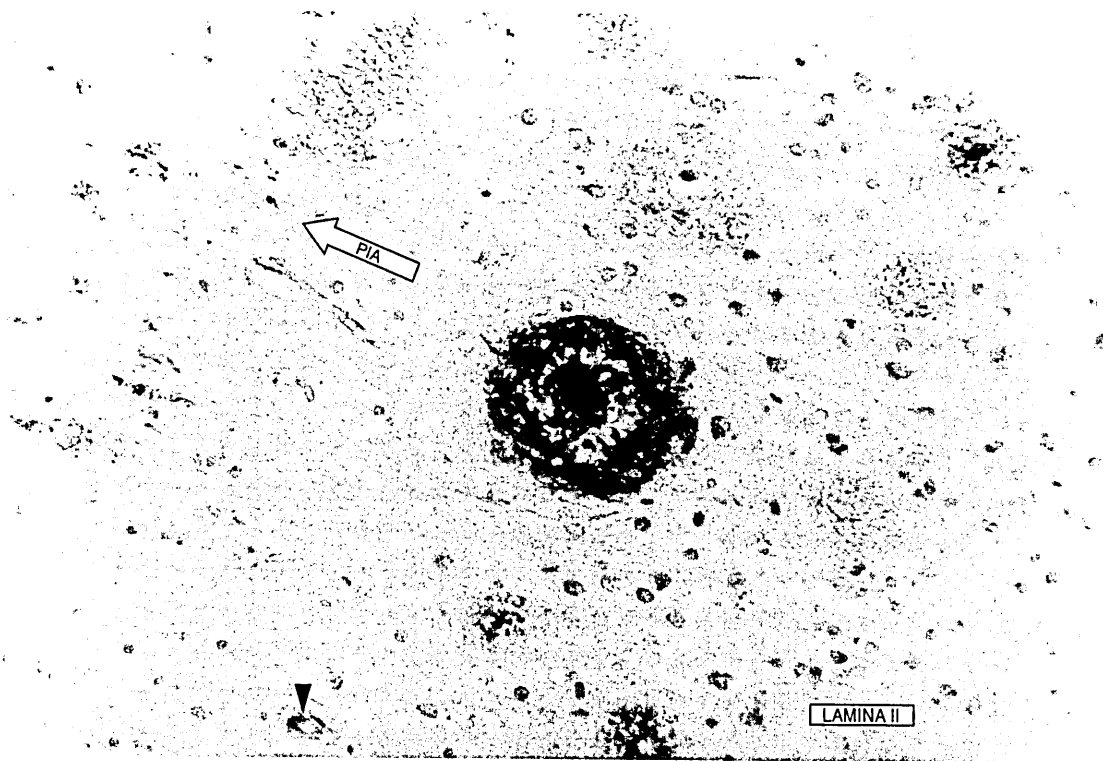


Figure 63

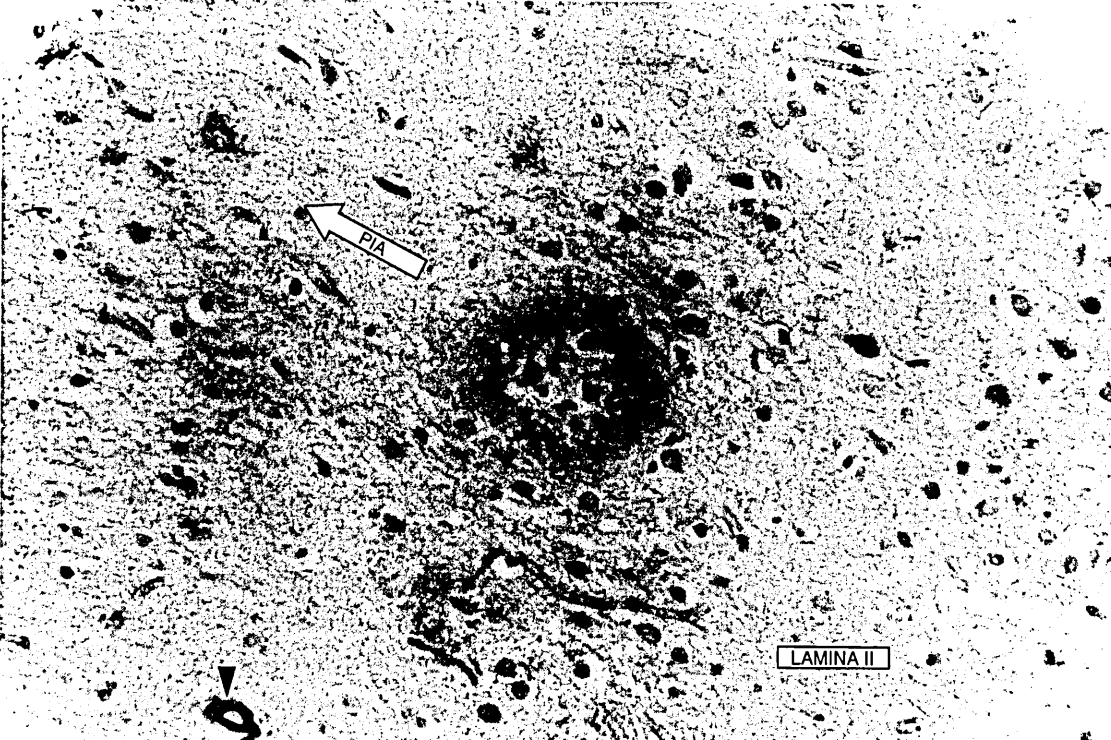


Figure 64

Figure 63 and Figure 64

Higher power photomicrographs of the neuritic plaque indicated in Figure 61 and Figure 62. Immunolabelled with anti- β -amyloid its heavily stained β -amyloid core is apparent, surrounded by a β -amyloid-positive neuritic element (Figure 63). In an adjacent serial section, immunostained with anti-KPI antibody, the core of this plaque is not stained, but the neuritic element is (Figure 64). Surrounding diffuse plaques, labelled by anti- β -amyloid (Figure 63), are KPI-negative (Figure 64).

At the bottom left (arrowhead) is a blood vessel that is β -amyloid-negative but KPI-positive.

The upper section was treated with 80% formic acid before immunostaining with anti- β -amyloid followed with biotinylated secondary antibody, ABC and DAB. The lower section was microwaved and treated with 2-mercaptoethanol and iodoacetic acid, then labelled with anti-KPI antibody followed with biotinylated secondary antibody, ABC and DAB.

Magnification = $\times 80$

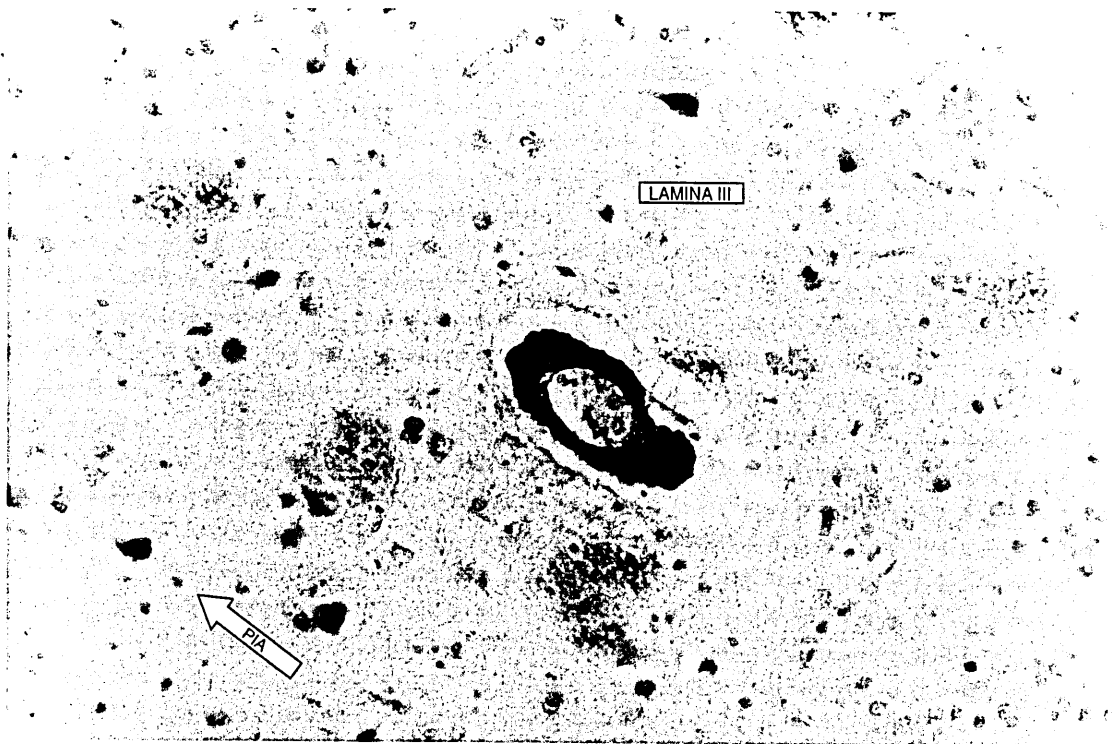


Figure 65

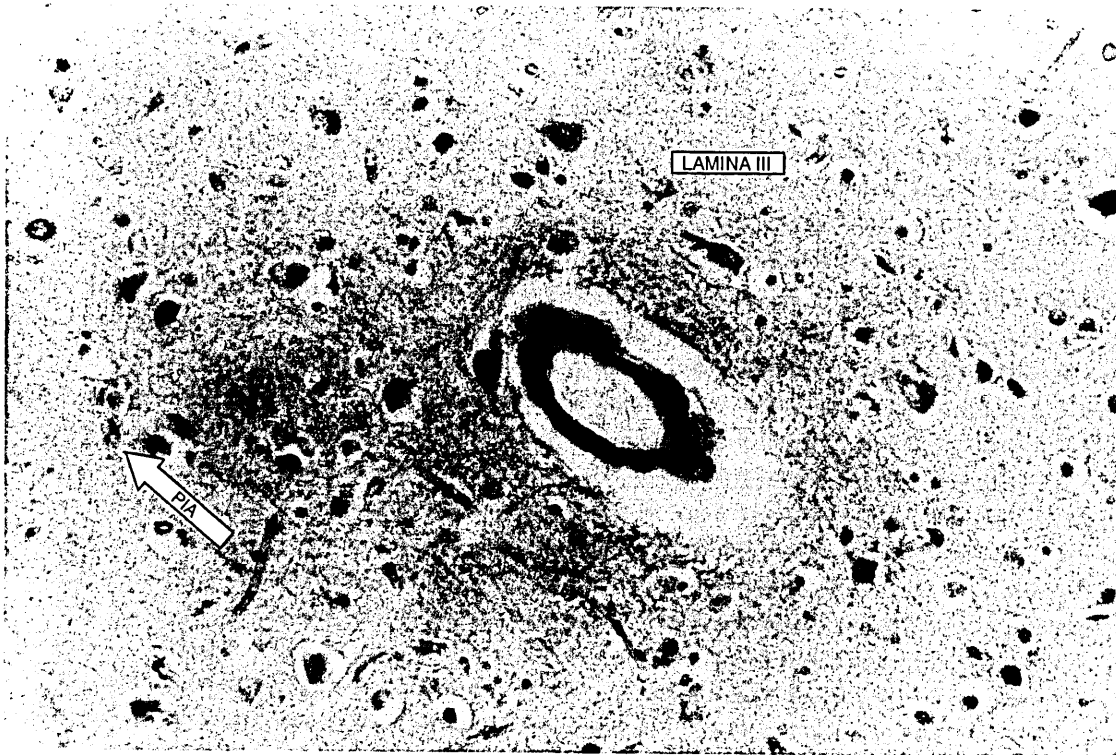


Figure 66

Figure 65 and Figure 66

Higher power photomicrographs of the blood vessel indicated in Figure 61 and Figure 62. This large vessel is labelled by both anti- β -amyloid (Figure 65) and anti-KPI (Figure 66) antibodies.

The upper section was treated with 80% formic acid before immunostaining with anti- β -amyloid followed with biotinylated secondary antibody, ABC and DAB. The lower section was microwaved and treated with 2-mercaptoethanol and iodoacetic acid, then labelled with anti-KPI antibody followed with biotinylated secondary antibody, ABC and DAB.

Magnification = $\times 80$

LAMINA VI

LAMINA I

Figure 67

LAMINA V

PIA

Figure 68

Figure 67

No APLP2 was immunolabelled with antibody 3B11 in AD cases. The section seen here was taken at the collateral sulcus of the AD case that is shown in Figure 48–Figure 52. Some tissue sections were microwaved prior to immunostaining and others were not. Sections were then labelled with antibody 3B11 followed with biotinylated secondary antibody, ABC and DAB. The section shown here was not microwaved. There was no difference in immunostaining in sections that were microwaved.

Magnification = $\times 8$

Figure 68

No immunostaining was seen in sections of AD brains that were microwaved, treated with 2–mercaptoethanol and iodoacetic acid, then labelled with anti–KPI antibody that had been pre–absorbed with the antigen, followed by biotinylated secondary antibody, ABC and DAB.

Magnification = $\times 90$

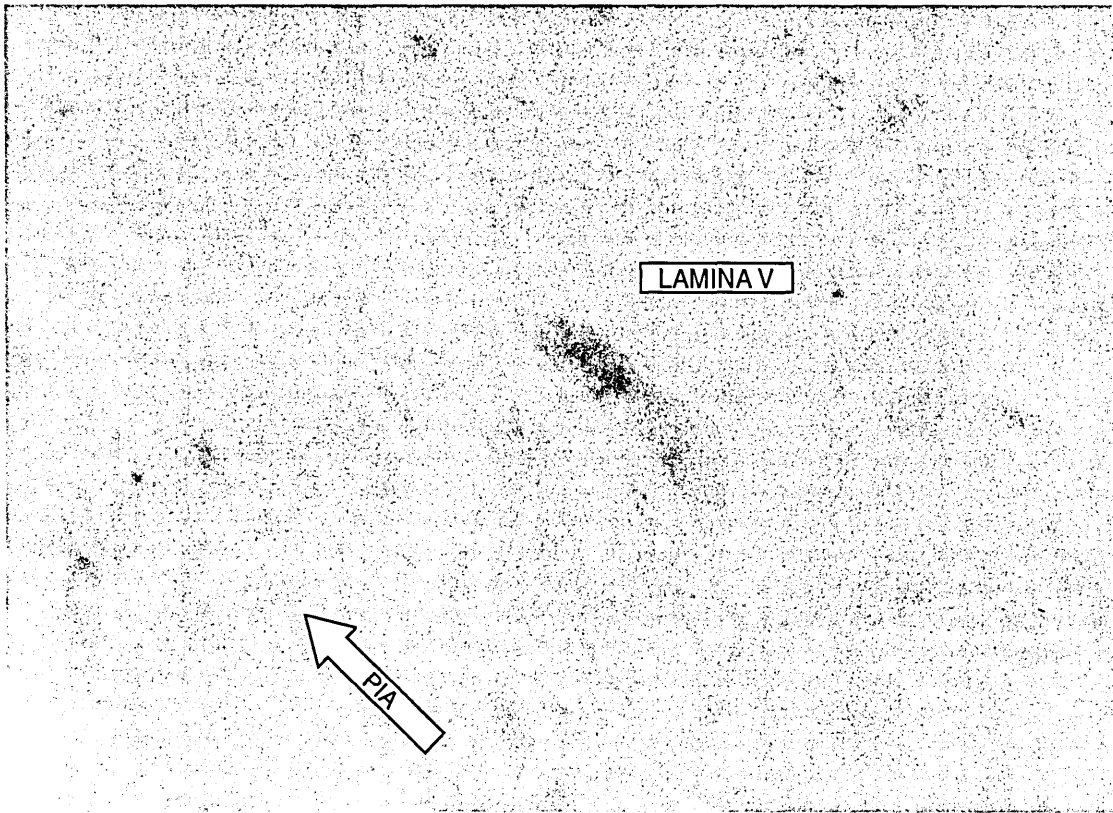


Figure 69

Figure 69

No immunostaining was seen in sections of AD brains that were microwaved, treated with 2-mercaptoethanol and iodoacetic acid, then labelled with non-immune serum from the same rabbit in which the anti-KPI antibody was raised, followed by biotinylated secondary antibody, ABC and DAB.

Magnification = $\times 90$

Discussion

An increased incidence of KPI cell staining was found in AD compared with control cases by counting cells using image analysis. Thus the increased KPI-/non-KPI-APP ratio indicated by mRNA studies (Tanaka *et al.*, 1989; Johnson *et al.*, 1990; Wighton-Benn *et al.*, 1995; Johnston *et al.*, 1996) appears to be accompanied by up-regulation of KPI-APP protein in cells of the temporal and visual cortices in AD compared with normal aged controls. In control subjects (as well as in AD) KPI protein expression was found to be unchanged with age. In one previous study mRNA data has shown an increased proportion of KPI-/non-KPI-APP with age, though absolute levels of mRNA isoforms were not reported (Tanaka *et al.*, 1993). Only 6 control brains were analysed by Tanaka *et al.*, and of these only one was neurologically normal, two had Parkinson's disease and three had cerebral infarction, whereas the present study consisted of 16 neurologically normal control subjects. A further study of APP mRNA including 41 neurologically normal controls (Robinson *et al.*, 1994) revealed only a small, non-significant increase in KPI/APP-695 ratio, and an overall decrease in KPI-APP mRNA level with age.

Pmd had a secondary influence on KPI-positive cell numbers. A comprehensive study of the effects of pmd and pre-mortem variables on APP mRNA in human frontal cortex (Harrison *et al.*, 1994) did not find any correlation between pmd and APP mRNA levels. However, a reduction in APP mRNA was found with decreased glutamate decarboxylase (GAD) activity (vulnerable to poor agonal state), with terminal pyrexia (non-significant), and with increasing duration of terminal coma (non-significant). Pre-mortem factors that affect APP mRNA levels might be expected to similarly affect

the corresponding protein levels. Although these data were not available for the brains used in this study, brain pH, which is reduced with poor agonal state, was known for the controls. No correlation was found between pH and KPI protein levels in control cases, but it is possible that other pre-mortem variables exerted an influence, and that KPI protein levels in the AD cases may have been influenced by pre-mortem course.

KPI staining in AD was closely related to the pathology. Cells that were KPI-immunopositive were the same population that are susceptible to tangles. Previous studies have identified KPI-APP mRNA in hippocampal granule and pyramidal neurones in normal and AD brains (Spillantini *et al.*, 1989), neurones of the association neocortex in normal adult brains (Neve *et al.*, 1988), and white matter oligodendrocytes in normal and AD brains (Harrison *et al.*, 1994). Neve *et al.*, (1988) examined cellular distribution of KPI-APP mRNA by *in situ* hybridization in frontal association cortex, inferior temporal association cortex, striate (primary visual) cortex and motor cortex. Highest expression levels were found in the frontal and temporal association areas, with homogeneously strong hybridization in layers II – VI. Motor cortex displayed moderate expression, which was strongest in layers III and V. In striate cortex weak hybridization predominated in layers III and V/VI. The pattern of KPI protein distribution observed in this study closely matches these descriptions of mRNA expression patterns, and roughly follows the distribution of pyramidal cells.

KPI staining was also present in the neuropil, possibly in neuronal processes and/or glia. Fast anterograde axonal transport of APP has been described (Moya *et al.*, 1994), and APP has been localised at presynaptic terminals (Lyckman *et al.*, 1998). In visual and temporal neocortex APP-695 and APP-751 mRNAs have been reported to be principally neuronal, and APP-770 mRNA mainly glial (Wightton-Benn *et al.*, 1995). It

therefore seems likely that KPI protein is indeed present in both neuronal processes and glia. Many, if not all, plaques were immunolabelled for KPI and the KPI tended to be in the neuritic element of plaques. The presence of KPI in the neuropil and in the neuritic element of plaques suggests that an up-regulation of KPI in neuronal processes may be a precursor to plaque formation.

Cerebro-vascular amyloid (CVA) appeared to be accompanied by an increase in KPI, but many KPI-positive vessels did not have β -amyloid deposits. The presence of strong KPI immunoreactivity in a population of blood vessels that includes but exceeds those with CVA implies that KPI accumulation may precede and induce CVA deposition. Fibrillar β -amyloid has been shown to bind to a site within amino acid residues 18–119 of the N-terminus of KPI-APP, and it was suggested that CVA may thus induce accumulation of KPI-APP at sites of cerebral amyloid angiopathy (Wagner *et al.*, 2000). However, the present study, together with the findings of Wagner *et al.* (2000), indicates that upregulation of KPI-APP precedes and may augment cerebro-vascular accumulation of fibrillar β -amyloid.

Neuronal loss is a prominent feature of AD (Perry, 1991). In rat brain, KPI-containing APP-751 mRNA is elevated following neurotoxic damage or persistent focal ischaemia (Solà *et al.*, 1993; Abe *et al.*, 1991). The observed increased incidence of KPI-positive cell staining in AD brains may reflect this up-regulation of KPI-APP mRNA in rat brain as a response to neuronal injury. Transgenic mice expressing high levels of hAPP-751 and -770 (bearing the V717F familial AD mutation) displayed extensive AD-like pathology, implying that overexpression of KPI-containing APP isoforms may have contributed to development of this pathology (Games *et al.*, 1995).

Gliosis and activation of glial cells in AD (Perry, 1991) are further factors that may alter the proportions of different APP isoforms in the brain. Cultured glial cells normally express a higher proportion of KPI-APP than non-KPI-APP mRNA (Gray and Patel, 1993a). Activation of glial cells may augment their production of KPI-APP, as demonstrated *in vitro* (Gray and Patel, 1993a and b; Sudoh *et al.*, 1996; Shepherd *et al.*, 2000) and in neuronal injury in rat brains (Iverfeldt *et al.*, 1993).

Johnson *et al.* (1990) found a strong linear relationship between the increased APP-751/-695 mRNA ratio in pyramidal cells and senile plaque density in AD hippocampus and entorhinal cortex. Although no relationship was found between KPI-positive cell numbers and β -amyloid load in the present study, it might be of interest to compare β -amyloid load with KPI load, in view of the apparent extracellular KPI deposits that were identified.

The increase in numbers of KPI-containing cells and presence of KPI in the neuropil and blood vessels in AD brains that were uncovered in this study has implications for the mechanism by which β -amyloid deposits develop in the CNS in AD. If KPI-APP has a different conformation to non-KPI-APP this may render it less susceptible to α -secretase cleavage, or alter its cellular trafficking thus reducing its exposure to α -secretase. The KPI domain might inhibit α -secretase, shifting APP processing from α -secretase to β -secretase cleavage, resulting in generation of more amyloidogenic fragments. Increased β -amyloid secretion was reported in cultured cells expressing hAPP-751 in comparison with those expressing hAPP-695 (Ho *et al.*, 1996), further supporting a role for the APP-751 isoform in amyloidogenesis. Alternatively, normal β -amyloid clearance could be impaired if KPI inhibits the enzyme(s) responsible for β -amyloid degradation. Breakdown of secreted APP has been found to be inhibited by

KPI in cultures of chick neurones, thus altering the normal balance of sAPP in the extracellular environment (Caswell *et al.*, 1999).

It should be noted that APRP-563 mRNA has been found to be increased in AD brains (Neve *et al.*, 1990). This amyloid precursor-related isoform contains the KPI domain, and hence could potentially be labelled by the antibody employed in this study. It does not contain the β -amyloid sequence but the presence of the KPI domain could still affect processing of other, β -amyloid-containing, APP isoforms as described above.

This study describes an increased incidence of KPI-immunopositivity in temporal and visual cortices in AD. A close relationship is outlined between the KPI domain and the pathology of AD, with the implication that KPI accumulation is a precursor to β -amyloid deposition in plaques and as CVA.

CHAPTER 7: TRANSFORMING GROWTH

FACTOR- β 1 *IN SITU* IN THE HUMAN BRAIN

Introduction

Transforming growth factor- β 1 (TGF- β 1) is a member of a family of peptide cytokines first named for their ability to stimulate transformation of fibroblasts. TGF- β 1-3 are widely expressed in human tissues and, of these, TGF- β 1 has been studied most extensively. TGF- β 1 is involved with cell proliferation and differentiation, the inflammatory response, immune regulation, and regulates the extracellular matrix (ECM) by promoting synthesis of matrix protein and stimulating protease inhibitors that prevent matrix degradation (Ebadi et al, 1997; Zhao and Schwartz, 1998). TGF- β affects gene transcription via Smads (homologues of *mad*, a signal transduction gene product in *Drosophila*), signal transducer proteins that carry the signal from cell surface TGF- β receptors to the nucleus (Heldin *et al.*, 1997). In normal mammalian brains it is usually expressed by astrocytes, microglia, oligodendrocytes, microvessel endothelial cells and, to a lesser extent, neurones (Macvilay and Fabry, 1997; Mattson *et al.*, 1997).

Immunohistochemical studies have demonstrated the presence of TGF- β 1 in normal human brains. Here it has been found in capillaries of the hippocampus and entorhinal cortex, but not in cell bodies or plaques (Van der Wal *et al.*, 1993). Another study, of frontal cortex from just one normal human brain, found TGF- β 1 immunoreactivity and mRNA (by *in situ* hybridization) in astrocytes, microglia and oligodendrocytes, but not neurones (Da Cunha *et al.*, 1993). Greater immunoreactivity for TGF- β 1 has been demonstrated in AD brains in comparison with normal controls. In AD it has been

immunolabelled in diffuse plaques, neurofibrillary tangles, blood vessels and, occasionally, in glial cells (Van der Wal *et al.*, 1993) and in the neuritic element of senile plaques (Peress and Perillo, 1995).

Recently, bigenic mice were developed that overexpress human APP (hAPP) and porcine TGF- β 1 (Wyss-Coray *et al.*, 1997). Singly transgenic mice overexpressing porcine TGF- β 1 in astrocytes display perivascular astrocytosis, up-regulation and accumulation of extracellular matrix components laminin and fibronectin in the brain, and develop hydrocephalus (Wyss-Coray *et al.*, 1995). Heterozygous, low-expressor mice, that do not develop this pathology, were used to create the bigenic mice. PDGF-hAPP mice, overexpressing mutant hAPP (V717F), particularly the KPI-containing isoforms, develop AD-like amyloid deposits (Games *et al.*, 1995; Rockenstein *et al.*, 1995). However, in the hAPP/TGF- β 1 bigenic mice there was accelerated deposition of β -amyloid in comparison to the singly transgenic hAPP mice. Subsequently, TGF- β 1 singly transgenic mice were found to develop age- and TGF- β 1-dose-dependent amyloid deposits around cortical capillaries at around 6 months of age (Wyss-Coray *et al.*, 2000). This amyloid deposition was preceded by up-regulation of the basement membrane proteins perlecan and fibronectin and thickening of cortical capillary basement membranes. It was then followed by microvascular degenerative changes similar to those found in AD brains. These findings highlight a potential role for TGF- β 1 in initiating or promoting the development of β -amyloid deposits in AD. Furthermore, a possible association was made recently between a TGF- β 1 genetic polymorphism and AD (Luedeking *et al.*, 2000).

Although TGF- β 1 protein distribution in normal versus AD human brain has been investigated immunohistochemically, its mRNA expression has not been characterised,

other than in frontal cortex from the single normal human brain in which TGF- β 1 mRNA was localised, by *in situ* hybridization histochemistry (ISHH), by Da Cunha *et al.* (1993). This study therefore set out to quantify TGF- β 1 mRNA expression by ISHH in human frontal, temporal, hippocampal and visual cortex and underlying white matter, in AD and control cases. These four areas were chosen for the characteristic early development of AD pathology in frontal, temporal and hippocampal cortex and later involvement of visual cortex, and their varying amounts of β -amyloid deposition and APP expression throughout the progression of the disease. Hybridized, radiolabelled sections were first exposed to film in order to quantify the overall level of expression of TGF- β 1 mRNA in grey matter and white matter of each of the brain areas. Sections dipped in emulsion were then developed and counterstained with cresyl violet for analysis under a light microscope to identify cell types containing TGF- β 1 mRNA.

In situ hybridization histochemistry

This technique is used to detect a specific nucleotide sequence in tissue sections. When added to the tissue sections, under appropriate conditions, the probe will hybridize (form base pairs) with the target sequence, but not with other, non-complementary, nucleic acid sequences in the tissue. A synthetic oligoriboprobe (Gibco BRL) was selected to detect TGF- β 1 mRNA in human brain sections. The probe was radiolabelled with ^{35}S and the hybrids (paired probe and target strands) were detected by autoradiography, the resulting signal being proportional to the amount of target mRNA present in the tissue.

The sequence of the TGF- β 1 antisense oligoprobe was:

5'CGT GGA GCT GAA GCA ATA GTT GGT GTC CAG3'

The sequence of the TGF- β 1 sense oligoprobe was:

5'CTG GAC ACC AAC TAT TGC TTC AGC TCC ACG3'

Results of *in situ* hybridization histochemistry

Separation of radiolabelled oligoprobe from unincorporated nucleotides

Fraction 5 from each sample passed through a purification cartridge was found to contain the majority of the radiolabelled probe. Fraction 5 from all of the samples of labelled sense or antisense probe were mixed, and the scintillation counter was used to obtain the number of counts per 5 μ l of the combined sense fractions and the combined antisense fractions.

The combined sense probe contained 1205950 counts per 5 μ l. Thus 4.14 μ l contained 10⁶ counts, so 4.14 μ l labelled probe was added per 100 μ l hybridization buffer (volume added to each section).

The combined antisense probe contained 2138750 counts per 5 μ l. Thus 2.33 μ l contained 10⁶ counts, so 2.33 μ l labelled probe was added per 100 μ l hybridization buffer.

Calculation of incubation and washing temperatures for *in situ* hybridization

$$T_m (\text{°C}) = 16.6\log[M] + 0.41[\text{Pgc}] + 81.5 - P_m - B/L - 0.65[\text{Pf}]$$

Melt temperature and incubation temperature for incubation buffer

$$T_m = 16.6\log[0.5] + 0.41[53.33] + 81.5 - 0 - 675/30 - 0.65[50]$$

$$T_m = 43.37^\circ\text{C}$$

$$\text{Therefore } T_i = 43.37 - 15 = 28.37^\circ\text{C}$$

Melt temperature and wash temperature for washing buffer

$$T_m = 16.6\log[0.165] + 0.41[53.33] + 81.5 - 0 - 675/30 - 0.65[0]$$

$$T_m = 99.34^\circ\text{C}$$

$$\text{Therefore } T_w = 99.34 - 15 = 84.34^\circ\text{C}$$

Quantification of autoradiography using film

The first batch of sections that was hybridized was left against film for 3 weeks. When developed, the film was underexposed and was too pale to be quantified. Therefore the following film was exposed to the second batch of sections for 5 weeks. This film was dark enough for the results to be quantified. The first batch of sections was hippocampus and visual cortex, and the second batch was frontal cortex and temporal cortex. The results below therefore include only frontal and temporal cortex. The ages and post-mortem delays of control and AD cases are shown in Table 7.

The mean grey levels of film exposed to some sections could not be quantified because these sections had dried out during the ISHH procedure, resulting in an abnormally high signal, or sections were damaged occasionally. There were therefore different numbers of cases in the frontal (AD: $n = 13$; control: $n = 4$) and temporal (AD: $n = 9$; control: $n = 8$) groups. These groups were tested independently for differences in mean post-mortem delay (pmd) or age (Table 8). (Age was known for all cases, but pmd was not available for three cases.) Using Student's t -test there was no significant difference

in pmd between controls and AD cases in either frontal or temporal groups. On analysis of frontal cases using Student's t-test there was no significant difference in age between controls and AD. Levene's test for equality of variances gave a significant result ($F = 6.592$, $p = 0.021$) for the temporal group when age was analysed. Therefore the Mann-Whitney-U-Wilcoxon-Rank-Sum-W test was used. This showed that the AD cases in the temporal group were significantly older than the controls ($U = 13.5$, $p = 0.030$). However, regression analysis showed that mean grey levels in temporal cortex were not dependent on age ($T = 1.571$, $p = 0.147$).

There was a small, statistically significant increase in amount of TGF- β 1 mRNA in temporal cortex ($t = 2.43$, $p = 0.028$) and temporal white matter ($t = 2.30$, $p = 0.037$) in AD cases versus controls (see Table 9) using Student's t-test. There was no significant difference in amount of TGF- β 1 mRNA in frontal cortex or white matter in AD cases in comparison with controls using Student's t-test.

Table 7 and Table 8: Summary of ages and post-mortem delays of control and AD cases used for TGF- β 1 ISHH. P.M.D. = post-mortem delay; S.D. = standard deviation; N = number of cases.

Table 7: All cases.

Variable	Diagnosis	Mean	S.D.	Min.	Max.	N
Age/ years	Control	70.55	16.28	40	93	11
	AD	83.00	7.70	67	98	15
P.M.D./ hours	Control	36.28	11.86	20.50	58.00	10
	AD	42.54	14.51	19.00	69.00	13

Table 8: Frontal versus temporal.

Variable	Area	Diagnosis	Mean	S.D.	N
Age/years	Frontal	Control	74.00	5.89	4
		AD	82.54	7.95	13
	Temporal	Control	69.00	18.83	8
		AD	87.00*	5.83	9
P.M.D./ hours	Frontal	Control	39.00	12.73	4
		AD	41.00	14.82	11
	Temporal	Control	34.25	11.04	7
		AD	45.29	11.93	7

* p<0.05

Table 9: Mean grey levels of film exposed to control and AD sections. FGM = frontal grey matter; FWM = frontal white matter; TGM = temporal grey matter; TWM = temporal white matter; mean = mean of mean grey levels; S.D. = standard deviation; N = number of cases.

Area	Diagnosis	Mean	S.D.	N
FGM	Control	211.52	23.14	4
	AD	227.71	16.05	13
FWM	Control	183.67	38.76	4
	AD	184.86	33.38	13
TGM	Control	197.86	33.97	8
	AD	229.57*	18.44	9
TWM	Control	165.88	29.42	8
	AD	198.07*	28.36	9

* p<0.05

Results of autoradiography using dipped sections

Very few silver grains were visible on the dipped sections following counterstaining even though they had been exposed for a long time (8 weeks) after being dipped in emulsion. The silver grains that were present were not clustered over cells, as would be seen if cells had been labelled specifically, but were randomly distributed over the sections, so quantification was not possible.

Discussion

A modest, significant increase in TGF- β 1 mRNA was detected in AD temporal cortex and white matter in comparison with controls. Although the temporal AD cases were older than temporal controls, the mean grey levels of these cases were not affected by age, as shown by regression analysis, so the observed increase in TGF- β 1 mRNA was not caused by the difference in mean age between the two groups.

The film that was exposed to the hippocampal and visual sections for 3 weeks was underexposed. This was probably due to low sensitivity of the probe because, after 5 weeks of exposure to the frontal and temporal sections, the second batch of film was exposed sufficiently for quantification. Since sections were not dipped in emulsion until after exposure to film, the initially weak radioactive signal may have decayed to such an extent that the emulsion was not exposed to a sufficiently strong signal for the mRNA to be detected by this method. Unfortunately, this meant that cell types containing elevated TGF- β 1 mRNA in AD could not be identified and compared with the cell types that were found to contain high levels of KPI-APP protein.

These results are in agreement with immunohistochemical studies that have demonstrated increased levels of TGF- β 1 protein in AD brains. TGF- β 1 was found in comparable amounts and distributions in cortical capillaries of control and AD brains (Van der Wal *et al.*, 1993) but was not found in plaques or cell bodies in normal aged brains (Van der Wal *et al.*, 1993; Peress and Perillo, 1995). Van der Wal *et al.* (1993) described TGF- β 1 immunoreactivity in β -amyloid-immunopositive plaques and thioflavin-labelled (β -amyloid-positive) plaques and tangles in the dentate gyrus and entorhinal cortex of AD brains. TGF- β 1-positive plaques were located mostly in the molecular layer of the dentate gyrus. Bielschowsky silver stain, which does not label early plaques, co-localised only rarely with TGF- β 1 on serial sections, suggesting that TGF- β 1 predominates in diffuse rather than neuritic plaques.

Using a different primary antibody, TGF- β 1 was identified in the neuritic element of senile plaques, by comparison with non-serial tau- versus β -amyloid-immunolabelled sections (Peress and Perillo, 1995). Although neither study found notable cellular TGF- β 1 staining in AD brains Van der Wal *et al.* detected faint immunopositivity in glial cells that co-stained with anti-glial fibrillary acidic protein (GFAP) or anti-leukocyte common antigen (LCA), identified as astrocytes and microglia respectively, in the hippocampus and entorhinal cortex. In the normal frontal cortex studied by Da Cunha *et al.* (1993), TGF- β 1 mRNA was found in astrocytes, microglia and oligodendrocytes, but no TGF- β 1 immunoreactivity was found, suggesting that, although mRNA may be synthesised constitutively it might only be translated under pathological conditions. In brains from patients with acquired immunodeficiency syndrome (AIDS), the amount of TGF- β 1 immunoreactive protein correlated positively with interleukin-1, which is elevated also in AD brains (Da Cunha *et al.*, 1993).

Elevated levels of TGF- β have been found in pre- and post-mortem serum and post-mortem CSF of AD patients in comparison with controls, the levels of serum TGF- β correlating with disease severity (Chao *et al.*, 1994a and b), lending additional support to the involvement of TGF- β in AD.

Animal and *in vitro* studies provide further insight into the regulation and role of TGF- β 1 in the brain. TGF- β 1 has been suggested to participate in the response to neuronal injury. TGF- β 1 mRNA is upregulated in rat brain following hypoxia-ischaemia (Klempt *et al.*, 1992), cerebral lesions (Logan *et al.*, 1992), hippocampal deafferentation or kainic acid-induced neurodegeneration (Morgan *et al.*, 1993). The latter two studies found mRNA increases in astrocytes, macrophages and endothelial cells (Logan *et al.*, 1992), and astrocytes, reactive microglia and macrophage-like cells (Morgan *et al.*, 1993). TGF- β 1 mRNA has been reported to be elevated also in cases of cerebral infarction in humans, in lesion-associated astrocytes and macrophages (Peress and Perillo, 1995) and neurones (Ata *et al.*, 1997). TGF- β 1 may offer neuroprotection, or aid glial scar formation accompanied by promotion of ECM deposition, similar to its role in peripheral scar formation (Logan *et al.*, 1992). As implied by its induction in deafferented areas of the brain, it may play a role in the reactive synaptogenesis that follows deafferentation, analogous to the abortive neuronal sprouting seen in AD. Indeed, TGF- β can induce production of nerve growth factor and neurotrophin-3 (Flanders *et al.*, 1998).

Several *in vitro* studies have shown TGF- β 1 to be neuroprotective against β -amyloid-induced neurodegeneration in primary rat hippocampal neurones and in human NTera 2 neurones (Prehn *et al.*, 1996; Ren and Flanders, 1996; Ren *et al.*, 1997) and against cytotoxic hypoxia and excitotoxic insult in primary chick neurones (Prehn

et al., 1993). It has been speculated that the mechanism of this neuroprotection may be related to the influence of TGF- β 1 on expression of the Bcl-2 and Bcl-x_L oncoproteins. These are involved with protection against neuronal cell death, particularly via programmed cell death or apoptosis. Both were upregulated following treatment of neurones with TGF- β 1, whereas expression of Bax, which counteracts the neuroprotective effects of Bcl-2, was unaffected (Prehn *et al.*, 1996). There is increased Bcl-2 protein expression in neurones adjacent to those that have died in AD brains (Glenner, 1988). It is therefore possible that this is mediated via TGF- β 1. Evidence from these *in vitro* studies suggests that TGF- β 1 may also exert neuroprotective effects via prevention of β -amyloid-induced loss of mitochondrial potential and function (Prehn *et al.*, 1996; Ren *et al.*, 1997). AD brains show signs that mitochondrial function is impaired (Gibson *et al.*, 1999) so it may be speculated that TGF- β 1 is upregulated in attempt to restore mitochondrial function.

Many more suggestions have been made as to the role of TGF- β 1 in AD. In NTERa 2 neurones it increases levels of presenilin 1 (PS1) mRNA (Ren *et al.*, 1999). PS1 was recently demonstrated to be responsible for γ -secretase cleavage of APP, thus potentially increasing β -amyloid production (Wolfe *et al.*, 1999; Kimberley *et al.*, 2000). Treatment of mouse hippocampal slice cultures with TGF- β 1 increased cellular accumulation and plaque-like deposition of β -amyloid (Harris-White *et al.*, 1998). TGF- β was shown to be required for β -amyloid-induced increase in cytosolic calcium in olfactory neuroblasts, a potential mechanism of neurotoxicity (Wolozin *et al.*, 1995; Cotter *et al.*, 1999). TGF- β 1 elevates APP mRNA in rat astrocytes (Gray and Patel, 1993a and b) and human astrocytes (Amara *et al.*, 1999), and increases both APP mRNA and protein in mouse microglia (Mönning *et al.*, 1994), thus potentially

augmenting β -amyloid production. Gray and Patel (1993a and b) demonstrated greater elevation of KPI-containing isoforms of APP than APP-695, and it is likely, as discussed elsewhere in this work, that KPI-APP levels are increased in AD. This elevation of APP by TGF- β 1 may be elicited by induction of APP mRNA stabilisation by TGF- β 1 such that steady-state levels of APP mRNA are increased (Amara *et al.*, 1999). Infusion of TGF- β 1 into the lateral ventricle of rats elevates expression of tubulin- α 1, glial fibrillary acidic protein (GFAP) and clusterin mRNAs, cytoskeletal proteins that are also increased in AD (Laping *et al.*, 1994). β -amyloid itself may in turn regulate the actions of TGF- β in the brain. It was demonstrated *in vitro* that β -amyloid monomer acts as a TGF- β antagonist, and β -amyloid aggregates can have TGF- β partial agonist or antagonist activity depending on the TGF- β function measured, thus potentially inhibiting the neuroprotective property of TGF- β and/or augmenting activation of glial cells (Huang *et al.*, 1998).

A drawback of *in vitro* studies of TGF- β is that the actions of such cytokines tend to be influenced by the context in which they are studied. For example, TGF- β treatment of microglial cells grown on fibronectin (which is upregulated in TGF- β 1 transgenic mice that exhibit amyloid deposition (Wyss-Coray *et al.*, 2000)) or laminin resulted in up-regulation of APP mRNA, whereas in microglia grown on collagen or uncoated plastic culture dishes APP mRNA expression was decreased (Mönning *et al.*, 1994). Thus the *in vivo* conditions under which TGF- β is expressed can be expected to modulate its actions. Elevation of TGF- β 1 in AD may increase the production of ECM proteins and alter levels of other cytokines that in turn modify the role of TGF- β 1 in AD in comparison to the normal human brain. This complexity must be borne in mind when attempting to extrapolate *in vitro* findings to the human brain, or indeed when

analysing results from animal models, where the environment in which TGF- β is expressed differs from that of the human brain.

This work adds strength to the evidence in favour of up-regulation of TGF- β 1 mRNA in AD. It was discontinued due to the weakness of signal given by the oligoprobe and the lack of availability of an alternative TGF- β 1 probe. However, the results obtained here indicate that further studies of TGF- β 1 mRNA expression in AD, using larger sample sizes and a more effective TGF- β 1 probe, might successfully confirm its suggested up-regulation in AD brains and clarify the cellular origin(s) of this finding.

CHAPTER 8: DISCUSSION

In NT2 stem cells and neurones, APLP2 and APP were detected immunocytochemically in the region of the Golgi apparatus. Whereas APLP2 was concentrated principally in this perinuclear region, APP extended into compartments throughout most of the cytoplasm of stem cells, and into small, granular structures along the processes and in growth cones of neurones. The overlap in distributions of the β -amyloid-containing APP and non- β -amyloid-containing APLP2 in NT2 cells emphasises the need to use antibodies that distinguish between the two when investigating amyloidogenesis in human brain. Differences in intracellular locations of APP and APLP2 that were identified in NT2N neurones may aid description of amyloidogenic pathways, if β -amyloid is generated in a subcellular compartment where APP but not APLP2 is concentrated in human CNS-type neurones. Ultimately, comparison of the structures of APP and APLP2 and their intracellular routing may also help identification of the structural features of APP that signal its sorting and routing for amyloidogenic processing. Thus targets may be set for therapeutic intervention to redirect APP towards non-amyloidogenic routes.

The presence of APP in neuronal processes and growth cones is analogous to its fast axonal transport to the tips of growing axons, and to mature presynaptic terminals, of neurones from the hamster primary visual pathway (Moya *et al.*, 1994; Lyckman *et al.*, 1998). At presynaptic terminals APP may be involved in neurite outgrowth via interaction with components of the extracellular matrix such as laminin or HSPGs (Kibbey *et al.*, 1993; Small *et al.*, 1994). It may function, itself, as a cell adhesion molecule (Pangalos *et al.*, 1995), or a cell surface receptor (Shimokawa *et al.*, 1993). It

has also been postulated to participate in recycling of substances such as histones, proteases and matrix proteins into cells, particularly where there is a high membrane turnover as in endocytosis, phagocytosis and exocytosis (Potempska *et al.*, 1993; Beer *et al.*, 1995). If APP is involved in maintenance and repair of mature neuronal synapses in human brain, its aberrant processing could be detrimental to synapses in AD brain and result in their degeneration, particularly in areas of high synaptic plasticity such as the memory pathways of the hippocampus. Indeed, synaptic abnormalities or loss, accompanied by increased APP and abnormally phosphorylated tau, have been suggested to precede neuronal intracellular accumulation of β -amyloid (Martin *et al.*, 1994; Masliah *et al.*, 1994). This, in turn, has been postulated to precede neuronal cell death and then extracellular β -amyloid deposition (LaFerla *et al.*, 1997). The presence of APP in NT2N processes and growth cones means that these neurones are potentially a useful model in which axonal transport of APP and its function at growth cones and possibly synapses of human CNS-type neurones may be studied. Presenilin 1 (PS1), which is responsible for γ -secretase APP cleavage, has been immunolocalised in NT2 and NT2N cell bodies and dendrites (Cook *et al.*, 1996; Parkinson, 1998), so it would be of interest to compare, by double immunocytochemical labelling, APP distribution with PS1 distribution in NT2 neurones.

β -amyloid could not be detected in NT2 cells by immunocytochemistry, and no β -amyloid production, or alteration of APP or APLP2 distributions or staining intensities, were seen following cellular stress. It is possible that too little β -amyloid was present in NT2 cells in the present study for its detection by immunocytochemistry. Intracellular β -amyloid in untransfected NT2 neurones has been demonstrated previously by immunoprecipitation (Wertkin *et al.*, 1993) and subsequently to this

study, by ELISA (Cook *et al.*, 1997), β -amyloid (42) being generated in the endoplasmic reticulum (ER)/intermediate compartment (IC), and β -amyloid (40) distally to the ER/IC. Pulse-chase labelling of endogenous APP also demonstrated β -cleavage of APP following its retention in the ER/IC of NT2N cells (Chyung *et al.*, 1997). These findings are similar to those in primary rat hippocampal neurones where β -amyloid (42) was present only in ER, and β -amyloid (40) was found in TGN, secretory vesicles and late endosomes (Hartmann *et al.*, 1997). This pattern was closely followed in N2a neuroblastoma cells, doubly transfected with hAPP-695 and PS1, and primary rat cerebral cortical neurones, where β -amyloid (42) was produced in ER as well as in TGN, whereas β -amyloid (40) was generated only in the TGN (Greenfield *et al.*, 1999).

Apart from the present study, the effects of heat-shock on APP processing in NT2 cells has only been performed using transfected stem cells, overexpressing APP (Dewji *et al.*, 1995), in which there was increased APP transcription following heat-shock. The effects of oxidative stress on APP processing in untransfected NT2N cells resulted in increases in both intracellular and extracellular β -amyloid production while APP levels remained unchanged, (seen by immunoprecipitation and Western blotting), possibly via increased β I and β II protein kinase C (PKC) activity (Paola *et al.*, 2000).

Immunocytochemical detection of intracellular β -amyloid, produced from endogenous APP, may require greater signal amplification following antibody binding than was possible with the techniques used in this study. Alternatively, the peptide may have been washed out of methanol-fixed cells and/or inaccessible in those fixed with paraformaldehyde and glutaraldehyde. Different methods of antigen retrieval may be of use in detecting intracellular β -amyloid in these cells, such as treatment of cells with

protease (e.g. trypsin), which may break bonds between the target and the fixative (Polak and Van Noorden, 1997).

Processing of NT2 cells *in situ*, on the slides on which they were grown in culture, was the most promising of the methods that were evaluated for examination of cells by electron microscopy (EM). As discussed above, in chapter 4, two subsequent studies have employed very similar methods to the one described here, and described the ultrastructure of NT2 neurones co-cultured with astrocytes (Hartley *et al.*, 1999) and characterised the neurotransmission type of NT2 neurones by immuno-EM (Guillemain *et al.*, 2000). Adaptation of the method described in the present study for collecting resin-embedded cells directly from the culture surface, for example by growing cells on coverslips as described by Guillemain *et al.* (2000), should allow successful collection of NT2 cells for future EM and immuno-EM studies. Thus, localisation of APP and possibly β -amyloid in these cells by immuno-EM, as originally proposed in this study, appear possible.

A potential mechanism by which β -amyloid production may be increased in AD, is through altered expression of APP isoforms. It was demonstrated *in vitro* that expression of APP-751 in comparison with non-KPI-APP resulted in increased secretion of β -amyloid (42) and decreased α -secretase cleavage products (Ho *et al.*, 1996). Astrocytes, which were the major producers of β -amyloid in primary cultures from foetal human cerebral cortex (Busciglio *et al.*, 1993), contain a higher proportion of KPI-APP than APP-695 (Gray and Patel, 1993a). In areas of human brains with AD pathology, an increased KPI-/non-KPI-APP mRNA ratio has been found (Tanaka *et al.*, 1989; Johnson *et al.*, 1990; Wighton-Benn *et al.*, 1995; Johnston *et al.*, 1996), specifically in AD pyramidal neurones (Neve *et al.*, 1988), raising the possibility that

β -amyloid production by these cells may be elevated. Therefore, KPI-APP protein in human brain was investigated immunohistochemically, to assess its distribution in normal human brains in comparison with AD brains.

Paraffin-embedded human brain sections were immunolabelled using a novel polyclonal antibody to the KPI domain of APP, generated in a rabbit. A protocol was established for uncovering the KPI domain epitope, by reduction and alkylation of disulphide bonds prior to immunostaining. Microwaving the sections (which is thought to uncover antigens by breaking hydroxyl bonds between the protein and formalin fixative and chelation of calcium from sections (Shi *et al.*, 1993; Morgan *et al.*, 1994)) enhanced this immunostaining in an additive manner, implying that these pre-treatments uncover the epitope by different mechanisms. The method described for uncovering the KPI domain is of potential use for detection of epitopes of other proteins that may be masked similarly by disulphide bonds. In normal human brains KPI-APP was localised, with this antibody, to pyramidal neurones, probably astrocytes, and the neuropil, suggesting transport of KPI-APP along cell processes.

Comparison of neurologically normal, aged, control brains with AD cases revealed a significantly increased incidence of KPI cellular staining, in terms of cell counts. This supports the increased ratio of KPI-/non-KPI-APP mRNA found previously in AD brains compared with normal aged controls (Tanaka *et al.*, 1989; Johnson *et al.*, 1990; Wighton-Benn *et al.*, 1995; Johnston *et al.*, 1996). KPI protein expression was unaffected by age, in both control and AD cases. KPI staining in AD was related closely to the pathology, and was present in the neuropil, possibly in the processes of neurones and/or glia. In addition, many plaques were immunolabelled, and KPI was present in the neuritic element of plaques, suggesting that KPI-APP up-regulation in neurites may

precede β -amyloid plaque formation. Double-immunolabelling studies in this laboratory have since shown that KPI-APP and β -amyloid are probably not entirely or precisely co-localised (Bielby *et al.*, 2000). Presence of KPI in the neuropil may reflect the APP immunolabelled in processes of NT2N neurones, described above, in axons and presynaptic terminals in the hamster primary visual pathway (Moya *et al.*, 1994; Lyckman *et al.*, 1998), and in axons and dendrites of rat hippocampal neurones (Simons *et al.*, 1995). NT2N neurones may therefore provide a model in which KPI-APP processing can be studied using this anti-KPI antibody, in comparison with non-KPI-APP, to investigate whether or not presence of the KPI domain alters subcellular neuronal processing of APP.

Cellular staining was strongest in layer V pyramidal neurones, and many layer III pyramidal cells and small, non-pyramidal cells in layers II to VI were KPI-positive. Previous descriptions of KPI-APP mRNA distribution have reported it to be expressed in similar cell types. It was present in hippocampal pyramidal and granule cells in normal and AD brains (Spillantini *et al.*, 1989), and layers II-VI of frontal and temporal association neocortex, layers III and V of the motor cortex and layers III and V/VI of the striate cortex in normal adult brains (Neve *et al.*, 1988). KPI-positive blood vessels included and exceeded the population that were β -amyloid-positive, implying that KPI accumulation may be a precursor to cerebro-vascular amyloid deposition. The KPI domain inhibits certain serine proteases, including blood coagulation factors, the effect on factor XIa being potentiated by binding of fibrillar β -amyloid to the N-terminal region of APP (Wagner *et al.*, 2000). Thus accumulation of KPI-APP in cerebral blood vessels in AD may create a microenvironment that is predisposed towards haemorrhaging, particularly once cerebral amyloid angiopathy develops.

The increase in KPI-APP protein demonstrated in AD brains may occur as part of a response to neuronal injury, as suggested by animal models of neurotoxic damage or ischaemia (Solà *et al.*, 1993; Abe *et al.*, 1991). Activated glial cells (such as the astrocytes, microglia and macrophages associated with senile plaques), as well as the neurones immunolabelled in this study by anti-KPI, may produce elevated levels of KPI-APP (Shepherd *et al.*, 2000).

TGF- β 1 mRNA was found to be increased significantly in AD temporal cortex and white matter, in agreement with immunohistochemical studies that have found up-regulation of TGF- β 1 protein in AD brains compared with normal controls (Van der Wal *et al.*, 1993; Peress and Perillo, 1995). TGF- β 1 mRNA also is up-regulated in reactive astrocytes, microglia, macrophages and endothelial cells in response to neuronal injury in rat brains (Klempt *et al.*, 1992; Logan *et al.*, 1992; Morgan *et al.*, 1993). In humans, in cases of cerebral infarction, it has been reported to be elevated in lesion-associated astrocytes, macrophages and neurones (Peress and Perillo, 1995; Ata *et al.*, 1997).

The increase of KPI-APP in astrocytes by TGF- β 1 (Gray and Patel, 1993a and b), together with the acceleration of development of AD pathology when TGF- β 1 is expressed in conjunction with hAPP (V717F) in bigenic mice (Wyss-Coray *et al.*, 1997), support a potential causal role of overexpressed TGF- β 1 in up-regulating KPI-APP in AD. Thus, it can be speculated, the altered ratio of APP isoforms may result in APP being metabolised in such a way that β -amyloid is over-produced (Ho *et al.*, 1996), or the KPI domain inhibits its degradation, and amyloid deposition ensues. Low-level overexpression of TGF- β 1 in recently developed singly transgenic mice resulted in increased vascular basement membrane proteins, perlecan and fibronectin,

and thickened cortical capillary basement membranes, as is seen in AD (Wyss–Coray *et al.*, 2000). These changes were followed by age– and dose–dependent amyloid deposition around cortical capillaries, and microvascular degeneration, similar to the cerebro–vascular amyloid and microvascular abnormalities of AD (Miyakawa *et al.*, 1974; Selkoe, 1994b). It may be speculated that upregulated TGF– β 1, in the presence of human APP, might induce similar increased production of extracellular matrix components and amyloid deposition in the vicinity of TGF– β 1–containing neurones and glia, and that KPI may enhance this process. It would be interesting to assess whether overexpression of TGF– β 1 alters the ratio of KPI–/non–KPI–APP in regions of basement membrane protein and amyloid deposition in these transgenic mice. Similarly, it would be useful to investigate the effects of TGF– β 1 on APP isoforms in human CNS–type neurones, such as NT2N cells, to see if there is upregulation of KPI–APP, as found in astrocytes (Gray and Patel, 1993a and b).

In NT2 neurones, TGF– β 1 has already been shown to increase levels of presenilin 1 (PS1) mRNA (Ren *et al.*, 1999). PS1 is likely to be responsible for intra–membranous γ –secretase cleavage of APP (similarly to PS1–mediated intra–membranous Notch–1 cleavage), thus potentially increasing β –amyloid production (De Strooper *et al.*, 1999; Wolfe *et al.*, 1999; Kimberley *et al.*, 2000). Exposure of mouse hippocampal slice cultures to TGF– β 1 increased cellular accumulation and plaque–like deposition of β –amyloid (Harris–White *et al.*, 1998). It would therefore be of interest also to investigate whether TGF– β 1 increases β –amyloid production in NT2 neurones. These cells may then provide a model in which to isolate any neuronal mechanisms by which TGF– β 1 may potentially influence β –amyloid deposition in AD brains.

Importantly, this work has illustrated some of the ever-widening variety of molecules and their pathways that are implicated in development of AD pathology. The number of potential therapeutic targets that are thus being identified may reflect the apparently heterogeneous population of subtypes of AD pathogenesis, which might therefore each respond better to therapeutic intervention targeted to different regulators of APP processing, and perhaps specific cell types. At the same time, adverse effects on similarly regulated proteins (such as Notch-1 in comparison with γ -secretase cleavage of APP) must be avoided. It may be necessary to target only a specific pool of APP, so as to preserve its normal functions, and the functions of the APLPs. This work has contributed to characterisation of a human CNS-type neuronal cell culture system in which APP and APLP2 can be immunolocalised to overlapping intracellular compartments. The effects of potential therapeutic agents can thus be investigated in these cells, to give a picture of their putative effects on human CNS neurones versus somatic cell types. NT2 cells are also of potential use in further investigations of KPI-APP, which was demonstrated here to have increased cellular incidence in AD and to be closely related to AD pathology.

In the hAPP V717F transgenic mice generated by Games *et al.* (1995), intraperitoneally injected anti- β -amyloid antibodies crossed the blood-brain barrier, decorated the amyloid plaques in the brains of the mice, and induced clearance of these plaques (Bard *et al.*, 2000). The antibodies appeared to act by triggering microglia to clear the plaques via Fc receptor-mediated phagocytosis and degradation of peptide. This potential AD therapy is now the subject of intensive research, with the hope that it may be possible to reverse the accumulation of AD pathological features and symptoms in humans by this means. However, development of a therapeutic intervention that acts at an earlier point

in the cascade of events that results in amyloid deposition may be a more effective treatment. For example, inhibition of the β - or γ - secretase enzymes, to lower β -amyloid production and thus potentially inhibit formation of toxic aggregates, can be postulated to prevent development of associated pathological features of the disease such as dystrophic neurites, neurofibrillary tangles, astrocytosis and cell death. Thus, intervention aimed at a more primitive stage of the disease process might prevent neuronal loss and cognitive decline more effectively than might removal of β -amyloid aggregates once these have already perhaps caused secondary damage and begun symptomatic development.

Further to this work, NT2 cells will provide a model cell type in which the effects of agents implicated in the pathogenesis of AD can be studied, in relation to APP processing, subcellular localisation and transport, and β -amyloid generation, in the context of human CNS-type neurones versus non-neuronal cell types. In particular, regulation of the secretase enzymes that have been identified recently could be usefully studied in these cells. With reference to this work, it would be of interest to clarify whether or not TGF- β 1 augments γ -secretase APP processing by PS1, following the description of PS1 mRNA upregulation by TGF- β 1 in NT2 neurones. Similarly, it would be useful to investigate whether TGF- β 1 elevates KPI-APP more than non-KPI-APP in NT2 neurones, as it appears to in astrocytes (Gray and Patel, 1993a and b), and whether or not this is linked to increased amyloidogenesis, and/or how it relates to PS1 regulation by TGF- β 1. The efficacies of potentially therapeutic β - and γ -secretase inhibitors could be tested in these cells, as a model of the effects they may have in CNS neurones in AD. For example, immunoprecipitation and Western blotting could be used to quantify the relative proportions of amyloidogenic and

non-amyloidogenic APP fragments generated following application of β - and γ -secretase inhibitors.

This work has characterised the distributions of APP and APLP2 in NT2 stem cells and neurones, emphasising the partial overlap in sites of intracellular concentration of APP and APLP2, and thus the need for use of antibodies that distinguish between these two molecules in studies of APP and amyloidogenesis. Any effects of cellular stress, by heat-shock or no feeding, on APP and APLP2 distributions and β -amyloid production were not detectable by indirect immunocytochemistry. More recent investigations by other researchers have delineated methods by which NT2 cells can be studied by EM (Hartley *et al.*, 1999; Guillemain *et al.*, 2000), suggesting that optimisation of the similar methods that were tested here might enable immuno-EM characterisation of APP and β -amyloid in these cells. A protocol was established for immunolabelling of KPI-APP in brain tissue, and increased cellular incidence of KPI-APP in AD compared to neurologically normal controls and association of this isoform with AD pathology were identified. TGF- β 1 mRNA was demonstrated, by *in situ* hybridization histochemistry, to be elevated significantly in AD brains compared with controls, supporting previous immunohistochemical evidence for upregulation of TGF- β 1 protein in AD brains.

APPENDIX

Tris-phosphate-buffered saline (TBS), 0.1M, pH7.4 – 7.8

25g Tris-HCl (BDH)

6g Na₂HPO₄ (BDH)

1.25g NaH₂PO₄.2H₂O (BDH)

35g NaCl (BDH)

5L Distilled H₂O

Concentrated HCl added to adjust to pH7.4 – 7.8

Phosphate-buffered saline (PBS), 0.1M, pH7.4

Solution A

27.6g NaH₂PO₄.H₂O (BDH) in 1L distilled H₂O

or

32.0g NaH₂PO₄.2H₂O (BDH) in 1L distilled H₂O

Solution B

28.4g Na₂HPO₄ anhydrous (BDH) in 1L distilled H₂O

or

36.0g Na₂HPO₄.2H₂O (BDH) in 1L distilled H₂O

Mixed 1 part solution A : 4 parts solution B.

Diluted 1 : 2 with distilled H₂O to give 0.1M PBS.

Concentrated HCl added to adjust to pH7.4

Alkaline Phosphatase (AP) buffer, pH9.5

100mM TRIS.HCl (BDH)

100mM NaCl (BDH)

5mM MgCl₂ (BDH)

Anti-fade

20mg p-phenylenediamine

2ml 1× PBS

18ml glycerol

Stored at -20°C.

20× Standard saline citrate (SSC)

175.3g NaCl (BDH)

88.2g Na Citrate (BDH)

800ml Autoclaved diethylpyrocarbonate (DEPC) treated water

Adjusted to pH7.0 with concentrated HCl or 10N NaOH (BDH).

Autoclaved DEPC treated water added to make up to 1 litre.

Hybridization buffer

10ml 20× SSC

1ml 50× Denhardt's solution

0.5ml 0.1M EDTA

1ml Denatured herring sperm DNA

5mg yeast tRNA

5mg Poly A

25ml deionized formamide

5g dextran sulphate

Made up to 50ml with 20mM phosphate buffer.

Table 10: primary antibodies

Antibody	Antigen/Compartment labelled	Species raised in	Mab/Pab	Source
87-4afp	APP and APLP2	Rabbit	Pab	Dr. D. Parkinson
22C11	N-terminal epitope on human APP	Mouse	Mab	Boehringer Mannheim
Alz-90	APP	Mouse	Mab	Boehringer Mannheim
FC8	N-terminus of APP	Mouse	Mab	Dr. D. Parkinson
EH4	N-terminus of APP	Mouse	Mab	Dr. D. Parkinson
HE1	Non-biological	Mouse	Mab	Dr. D. Parkinson
3B11	APLP2	Mouse	Mab	Dr. M-T. Webster, Dr. P. Francis
Anti-58K	58kD peripheral Golgi membrane protein	Mouse	Mab	Sigma
Anti-β-COP	Golgi β -COP (coatamer protein)	Mouse	Mab	Sigma
Anti-TGN	Trans-Golgi network	Sheep	Mab	Dr. V. Poonambalam
Anti-PDI	Endoplasmic reticulum	Rabbit	Pab	Dr. T. Wileman
Anti-GRP-94	Endoplasmic reticulum	Rabbit	Pab	Dr. T. Wileman
Anti-LAMP-1	Lysosome-associated membrane protein-1	Mouse	Mab	DSHB
Anti-LAMP-2	Lysosome-associated membrane protein-2	Mouse	Mab	DSHB

Antibody	Antigen/Compartment labelled	Species raised in	Mab/Pab	Source
Anti-cathepsin-D	Lysosomal protein Cathepsin-D	Rabbit	Pab	Dr. T. Wileman
Anti-PHF	Human paired helical filaments	Rabbit	Pab	ICN Biomedicals
Anti-β-amyloid	Residues 8-17 of human β -amyloid	Mouse	Mab	Dako

Mab = monoclonal antibody; Pab = polyclonal antibody; Dr. D. Parkinson: Sheffield Hallam University; Dr. T. Wileman: Institute of Animal Health, Pirbright.

ACKNOWLEDGEMENTS

The author would like to express thanks to Dr. David Parkinson at Sheffield Hallam University, and Professor R. Carl A. Pearson at the University of Sheffield, for their invaluable supervision and support during this work.

Many thanks to Professor Gordon Wilcock in Bristol for brains donated for this research, and to Dr. J. W. Neal in Cardiff who carried out pathological diagnosis on brains used in this work. Thanks to Professor P. W. Andrews at the University of Sheffield, who provided the original stock of Ntera 2 stem cells for this study.

The author would like to thank Maurice Sanders, for providing expert technical support, as well as Mick Turton, Peter Loxley and Dr. M. Cambray–Deakin for help with photomicroscopy, and Dr. G. Cope for advice regarding electron microscopy.

Thanks to all other members of the laboratories in which this work was carried out, for the advice and support they provided: Paul Heath, Simone Bowes, Wendy Wighton–Benn, Simon Wright, Paul Orange, Claire Shepherd, Keren Bielby, Nisa Radenahmad and Sharon Pycock.

Thanks also to Giles Campbell for advice on preparation and printing of this final manuscript.

This work was funded by the Wellcome Trust.

REFERENCES

- Abe K., Tanzi R. E., and Kogure K. (1991) Selective induction of Kunitz-type protease inhibitor domain-containing amyloid precursor protein mRNA after persistent focal ischemia in rat cerebral cortex. *Neurosci. Lett.* **125**, 172–174.
- Abercrombie M. (1946) Estimation of nuclear population from microtome sections. *Anatom. Rec.* **94**, 239–247.
- Ackerman S. L., Knowles B. B., and Andrews P. W. (1994) Gene regulation during neuronal and non-neuronal differentiation of NTera2 human teratocarcinoma-derived stem cells. *Mol. Brain Res.* **25**, 157–162.
- Alloul K., Sauriol L., Kennedy W., Laurier C., Tessier G., Novosel S., and Contandriopoulos A. (1998) Alzheimer's disease: a review of the disease, its epidemiology and economic impact. *Arch. Gerontol. Geriatr.* **27**, 189–221.
- Amara F. M., Junaid A., Clough R. R., and Liang B. (1999) TGF- β_1 , regulation of Alzheimer amyloid precursor protein mRNA expression in a normal human astrocyte cell line: mRNA stabilization. *Mol. Brain Res.* **71**, 42–49.
- Andrews P. W. (1984) Retinoic acid induces neuronal differentiation of a cloned human embryonal carcinoma cell line *in vitro*. *Develop. Biol.* **103**, 285–293.
- Andrews P. W., Damjanov I., Simon D., Banting G. S., Carlin C., Dracopoli N. C., and Føgh J. (1984) Pluripotent embryonal carcinoma clones derived from the human teratocarcinoma cell line Tera-2. *Lab. Invest.* **50**, 147–162.
- Armstrong R. A., Winsper S. J., and Blair J. A. (1995) Hypothesis: is Alzheimer's disease a metal-induced immune disorder? *Neurodegeneration* **4**, 107–111.
- Asami-Odaka A., Ishibashi Y., Kikuchi T., Kitada C., and Suzuki N. (1995) Long amyloid β -protein secreted from wild-type human neuroblastoma IMR-32 cells. *Biochemistry* **34**, 10272–10278.
- Ashall F., and Goate A. M. (1994) Role of the β -amyloid precursor protein in Alzheimer's disease. *Trends Biochem. Sci.* **19**, 42–46.
- Ata A. K., Funa K., and Olsson Y. (1997) Expression of various TGF- β isoforms and type I receptor in necrotizing human brain lesions. *Acta Neuropathol.* **93**, 326–333.
- Bahr B. A., Hoffman K. B., Yang A. J., Hess U. S., Glabe C. G., and Lynch G. (1998) Amyloid β protein is internalized selectively by hippocampal field CA1 and causes neurons to accumulate amyloidogenic carboxyterminal fragments of the amyloid precursor protein. *J. Comp. Neurol.* **397**, 139–147.
- Bard F., Cannon C., Barbour R., Burke R.-L., Games D., Grajeda H., Guido T., Hu K., Huang J., Johnson-Wood K., Khan K., Kholodenko D., Lee M., Lieberburg I., Motter

- R., Nguyen M., Soriano F., Vasquez N., Weiss K., Welch B., Seubert P., Schenk D., and Yednock T. (2000) Peripherally administered antibodies against amyloid β -peptide enter the central nervous system and reduce pathology in a mouse model of Alzheimer disease. *Nat. Med.* **6**, 916–919.
- Barger S. W., Fiscus R. R., Ruth P., Hofmann F., and Mattson M. P. (1995) Role of cyclic GMP in the regulation of neuronal calcium and survival by secreted forms of β -amyloid precursor. *J. Neurochem.* **64**, 2087–2096.
- Barinaga M. (1995) Missing Alzheimer's gene found. *Science* **269**, 917–918.
- Barrow C. J., and Zagorski M. G. (1991) Solution structures of β peptide and its constituent fragments: relation to amyloid deposition. *Science* **253**, 179–182.
- Beal M. F. (2000) Energetics in the pathogenesis of neurodegenerative diseases. *Trends Neurosci.* **23**, 298–304.
- Beer J., Masters C. L., and Beyreuther K. (1995) Cells from peripheral tissues that exhibit high APP expression are characterized by their high membrane fusion activity. *Neurodegen.* **4**, 51–59.
- Benzi G., and Moretti A. (1995) Are reactive oxygen species involved in Alzheimer's disease? *Neurobiol. Aging* **16**, 661–674.
- Bertram L., Blacker D., Mullin K., Keeney D., Jones J., Basu S., Yhu S., McInnis M. G., Go R. C., Vekrellis K., Selkoe D. J., Saunders A. J., and Tanzi R. E. (2000) Evidence for genetic linkage of Alzheimer's disease to chromosome 10q. *Science* **290**, 2302–2303.
- Bielby K. E., Campbell E., Parkinson D., Neal J. W., Sanders M. W., and Pearson R. C. A. (2000) Accumulation of KPI-containing APP in Alzheimer's disease. *Eur. J. Neurosci.* **12**, suppl. **12**, 103.07.
- Borg J-P., Ooi J., Levy E., and Margolis B. (1996) The phosphotyrosine interaction domains of X11 and FE65 bind to distinct sites on the YENPTY motif of amyloid precursor protein. *Mol. and Cell. Biol.* **16**, 6229–6241.
- Bowes S. M. (1999) Processing of Alzheimer's amyloid precursor protein in cultured cells. *PhD thesis, Sheffield Hallam Univ.*
- Boyles J. K., Pitas R. E., Wilson E., Mahley R. W., and Taylor J. M. (1985) Apolipoprotein E associated with astrocytic glia of the central nervous system and with nonmyelinating glia of the peripheral nervous system. *J. Clin. Invest.* **76**, 1501–1513.
- Braak H., and Braak E. (1991) Neuropathological staging of Alzheimer-related changes. *Acta Neuropathol.* **82**, 239–259.
- Brenneman D. E., and Gozes I. (1996) A femtomolar-acting neuroprotective peptide. *J. Clin. Invest.* **97**, 2299–2307.

- Brion J. P., Couck A. M., and Conreur J. L. (1995) Calcineurin (phosphatase 2B) is present in neurons containing neurofibrillary tangles and in a subset of senile plaques in Alzheimer's disease. *Neurodegeneration* **4**, 13–21.
- Busciglio J., Gabuzda D. H., Matsudaira P., and Yankner B. A. (1993) Generation of β -amyloid in the secretory pathway in neuronal and nonneuronal cells. *Proc. Natl. Acad. Sci. U. S. A.* **90**, 2092–2096.
- Bush A. I., Pettingell W. H., Multhaup G., Paradis M. D., Vonsattel J.-P., and Gusella J. F. (1994) Rapid induction of Alzheimer A β -amyloid formation by zinc. *Science* **265**, 1464–1467.
- Buxbaum J. D., Liu K.-N., Luo Y., Slack J. L., Stocking K. L., Peschon J. J., Johnson R. S., Castner B. J., Cerretti D. P., and Black R. A. (1998) Evidence that tumour necrosis factor α converting enzyme is involved in regulated α -secretase cleavage of the Alzheimer amyloid protein precursor. *J. Biol. Chem.* **273**, 27765–27767.
- Calingasan N. Y., Gandy S. E., Baker H., Sheu K.-F. R., Smith J. D., Lamb B. T., Gearhart J. D., Buxbaum J. D., Harper C., Selkoe D. J., Price D. L., Sisodia S. S., and Gibson G. E. (1996) Novel neuritic clusters with accumulations of amyloid precursor protein and amyloid precursor-like protein 2 immunoreactivity in brain regions damaged by thiamine deficiency. *Am. J. Pathol.* **149**, 1063–1071.
- Campbell E., Bowes S. M., Pearson R. C. A., Francis P. T., Parkinson D. (1997) Differential intracellular localization of APP and APLP2 in NTera2 neurons. *Soc. Neurosci. Abstr.* **321.17**.
- Campbell E., Bowes S. M., Pearson R. C. A., Parkinson D., Francis P., and Webster M.-T. (1996) APP and APLP2 are found in different intracellular compartments in NTera2 cells. *Soc. Neurosci. Abstr.* **22**, 189.
- Campbell E., Pearson R. C. A., and Parkinson D. (1999) Methods to uncover an antibody epitope in the KPI domain of Alzheimer's amyloid precursor protein for immunohistochemistry in human brain. *J. Neurosci. Meth.* **93**, 133–138.
- Caporaso G. L., Takei K., Gandy S. E., Matteoli M., Mundigl O., Greenard P., and De Camilli P. (1994) Morphologic and biochemical analysis of the intracellular trafficking of the Alzheimer β A4 amyloid precursor protein. *J. Neurosci.* **14**, 3122–3138.
- Caswell M. D., Mok S. S., Henry A. A., Cappai R., Klug G., Beyreuther K., Masters C. L., and Small D. H. (1999) The amyloid β -protein precursor of Alzheimer's disease is degraded extracellularly by a Kunitz protease inhibitor domain-sensitive trypsin-like serine protease in cultures of chick sympathetic neurons. *Eur. J. Biochem.* **266**, 509–516.
- Chao C. C., Ala T. A., Hu S., Crossley K. B., Sherman R. E., Peterson P. K., and Frey W. H. (1994a) Serum cytokine levels in patients with Alzheimer's disease. *Clin. Diagnos. Lab. Immunol.* **1**, 433–436.

Chao C. C., Hu S., Frey W. H., Ala T. A., Tourtellotte W. W., and Peterson P. K. (1994b) Transforming growth factor β in Alzheimer's disease. *Clin. Diagnos. Lab. Immunol.* **1**, 109–110.

Chevallier N., Vizzavona J., Marambaud P., Baur C. P., Spillantini M., Fulcrand P., Martinez J., Goedert M., Vincent J.-P., and Checler F. (1997) Cathepsin D displays in vitro β -secretase-like specificity. *Brain Research* **750**, 11–19.

Chyung A. S. C., Greenberg B. D., Cook D. G., Doms R. W., and Lee V. M.-Y. (1997) Novel β -secretase cleavage of β -amyloid precursor protein in the endoplasmic reticulum/intermediate compartment of NT2N cells. *J. Cell Biol.* **138**, 671–680.

Ciallella J. R., Rangnekar V. V., and McGillis J. P. (1994) Heat shock alters Alzheimer's β -amyloid precursor protein expression in human endothelial cells. *J. Neurosci. Res.* **37**, 769–776.

Citron M., Westaway D., Xia W. M., Carlson G., Diehl T., Levesque G., Johnson-Wood K., Lee M., Seubert P., Davis A., Kholodenko D., Motter R., Sherrington R., Perry B., Yao H., Strome R., Lieberburg I., Rommens J., Kim S., Schenk D., Fraser P., Hyslop P. S., Selkoe D. J. (1997) Mutant presenilins of Alzheimer's disease increase production of 42-residue amyloid beta-protein in both transfected cells and transgenic mice. *Nature Med.* **3**, 67–72.

Clarris H. J., Key B., Beyreuther K., Masters C. L., and Small D. H. (1995) Expression of the amyloid protein precursor of Alzheimer's disease in the developing rat olfactory system. *Dev. Brain Res.* **88**, 87–95.

Cook D. G., Forman M. S., Sung J. C., Leight S., Kolson D. L., Iwatsubo T., Lee V. M.-Y., and Doms R. W. (1997) Alzheimer's A β (1–42) is generated in the endoplasmic reticulum/intermediate compartment of NT2N cells. *Nature Medicine* **3**, 1021–1023.

Cook D. G., Sung J. C., Golde T. E., Felsenstein K. M., Wojczyk B. S., Tanzi R. E., Trojanowski J. Q., Lee V. M.-Y., and Doms R. W. (1996) Expression and analysis of presenilin 1 in a human neuronal system: localization in cell bodies and dendrites. *Proc. Natl. Acad. Sci. U. S. A.* **93**, 9223–9228.

Coria F., Moreno A., Rubio I., Garcia M. A., Morato E., and Mayor Jr. F. (1993) The cellular pathology associated with Alzheimer β -amyloid deposits in non-demented aged individuals. *Neuropathol. Appl. Neurobiol.* **19**, 261–268.

Corder E. H., Saunders A. M., Strittmatter W. J., Schmechel D. E., Gaskell P. C., Small G. W., Roses A. D., Haines J. L., and Pericak-Vance M. A. (1993) Gene dose of apolipoprotein E type 4 allele and the risk of Alzheimer's disease in late onset families. *Science* **261**, 921–923.

Corsellis J. A. N. Ageing and the dementias. In: Blackwood W., and Corsellis J. A. N., eds, (1976) *Greenfield's Neuropathology*, 3rd edit. Edward Arnold (Publishers) Ltd., 25 Hill Street, London.

Cotter R. L., Burke W. J., Thomas V. S., Potter J. F., Zheng J., and Gendelman H. E. (1999) Insights into the neurodegenerative process of Alzheimer's disease: a role for

mononuclear phagocyte-associated inflammation and neurotoxicity. *J. Leukoc. Biol.* **65**, 416–427.

Coulson E. J., Barrett G. L., Storey E., Bartlett P. F., Beyreuther K., and Masters C. L. (1997) Down-regulation of the amyloid protein precursor of Alzheimer's disease by antisense oligonucleotides reduces neuronal adhesion to specific substrata. *Brain Res.* **770**, 72–80.

Couratier P., Sindou P., Tabaraud F., Diop A. G., Spencer P. S., and Hugon J. (1995) Modulation of tau neuronal expression induced by NMDA, non-NMDA and metabotropic glutamate receptor agonists. *Neurodegeneration* **4**, 33–41.

Crain B. J., Hu W., Sze C.-I., Slunt H. H., Koo E. H., Price D. L., Thinakaran G., and Sisodia S. S. (1996) Expression and distribution of amyloid precursor protein-like protein-2 in Alzheimer's disease and in normal brain. *Am. J. Pathol.* **149**, 1087–1095.

Cummings B. J., and Cotman C. W. (1995) Image analysis of β -amyloid load in Alzheimer's disease and relation to dementia severity. *Lancet* **346**, 1524–1528.

Cunningham D. D. (1993) Protease nexin-2/amyloid β -protein precursor: a cerebral anticoagulant? *J. Clin. Invest.* **92**, 2090.

Da Cunha A., Jefferson J. A., Jackson R. W., and Vitkovi L., (1993) Glial cell-specific mechanisms of TGF- β 1 induction by IL-1 in cerebral cortex. *J. Neuroimmunol.* **42**, 71–86.

Davis R. E., Miller S., Herrnstadt C., Ghosh S. S., Fahy E., Shinobu L. A., Galasko D., Thal L. J., Beal M. F., Howell N., and Parker W. D. Jr. (1997) Mutations in mitochondrial cytochrome *c* oxidase genes segregate with late-onset Alzheimer disease. *Proc. Natl. Acad. Sci. U. S. A.* **94**, 4526–4531.

De la Torre J. C. (1997) Cerebromicrovascular pathology in Alzheimer's disease compared to normal aging. *Gerontol.* **43**, 26–43.

De la Torre J. C., and Mussivand T. (1993) Can disturbed brain microcirculation cause Alzheimer's disease? *Neurol. Res.* **15**, 146–153.

De Serres M., Sherman D., Chestnut W., Merrill B. M., Viveros O. H., and Diliberto E. J. Jr. (1993) Proteolysis at the secretase and amyloidogenic cleavage sites of the β -amyloid precursor protein by acetylcholinesterase and butyrylcholinesterase using model peptide substrates. *Cell. Mol. Neurobiol.* **13**, 279–287.

De Strooper B., Annaert W., Cupers P., Saftig P., Craessaerts K., Mumm J. S., Schroeter E. H., Schrijvers V., Wolfe M. S., Ray W. J., Goate A., and Kopan R. (1999) A presenilin-1-dependent γ -secretase-like protease mediates release of Notch intracellular domain. *Nature* **398**, 518–521.

De Strooper B., Umans L., Van Leuven F., and Van Den Berghe H. (1993) Study of the synthesis and secretion of normal and artificial mutants of murine amyloid precursor protein (APP) occurs in a late compartment of the default secretion pathway. *J. Cell Biol.* **121**, 295–304.

- Dewji N. N., Do C., and Bayney R. M. (1995) Transcriptional activation of Alzheimer's β -amyloid precursor protein gene by stress. *Mol. Brain Res.* **33**, 245–253.
- Dewji N. N., and Singer S. J. (1996) Genetic clues to Alzheimer's disease. *Nature* **271**, 159–160.
- Dovey H. F., Suomensaari-Chrysler S., Lieberburg I., Sinha S., and Keim P. S. (1993) Cells with a familial Alzheimer's disease mutation produce authentic β -peptide. *Neuroreport* **4**, 1039–1042.
- Dresse A., Marechal D., Scuvee-Moreau J., and Seutin V. (1994) Towards a pharmacological approach of Alzheimer's disease based on the molecular biology of the amyloid precursor protein (APP). *Life Sci.* **55**, 2179–2187.
- Duff K., and Hardy J. (1995) Mouse model made. *Nature* **373**, 476–477.
- Dugan J. M., deWit C., McConlogue L., and Maltese W. A. (1995) The Ras-related GTP-binding protein, Rab1B, regulates early steps in exocytic transport and processing of β -amyloid precursor protein. *J. Biol. Chem.* **270**, 10982–10989.
- Dyrks T., Dyrks E., Mönning U., Urmoneit B., Turner J., and Beyreuther K. (1993) Generation of β A4 from the amyloid protein precursor and fragments thereof. *FEBS Lett.* **335**, 89–93.
- Dyrks T., Mönning U., Beyreuther K., and Turner J. (1994) Amyloid precursor protein secretion and β A4 amyloid generation are not mutually exclusive. *FEBS Lett.* **349**, 210–214.
- Ebadi M., Bashir R. M., Heidrick M. L., Hamada F. M., El Refaey H., Hamed A., Helal G., Baxi M. D., Cerutis D. R., and Lassi N. K. (1997) Neurotrophins and their receptors in nerve injury and repair. *Neurochem. Int.* **30**, 347–374.
- Eber O. (1996) Endocrinology and Alzheimer's disease. *Neuropsych.* **10**, 128–133.
- El-Agnaf O. M. A., Irvine G. B., Guthrie D. J. S., and Walsh D. (1996) Properties of some peptides related to amyloid β -peptide. *Biochem. Soc. Trans.* **24**, 59S.
- Ertekin-Taner N., Graff-Rudford N., Younkin L. H., Eckman C., Baker M., Adamson J., Ronald J., Blangero J., Hutton M., and Younkin S. G. (2000) Linkage of plasma Abeta42 to a quantitative locus on chromosome 10 in late-onset Alzheimer's disease pedigrees. *Science* **290**, 2303–4.
- Esiri M. M., Hyman B. T., Beyreuther K., and Masters C. L. Ageing and dementia. In: Graham D. I., And Lantos P. L., eds, (1997) *Greenfield's Neuropathology*, 6th edit., Vol. 2. Arnold, 338 Euston Road, London.
- Esler W. P., Kimberly W. T., Ostaszewski B. L., Diehl T. S., Moore C. L., Tsai J. Y., Rahmati T., Xia W., Selkoe D. J., and Wolfe M. S. (2000) Transition-state analogue inhibitors of gamma-secretase bind directly to presenilin-1. *Nat. Cell Biol.* **2**, 428–434.

Estus S., Golde T. E., Kunishita T., Blades D., Lowery D., Eisen M., Usiak M., Qu X., Tabira T., Greenberg B. D., and Younkin S. G. (1992) Potentially amyloidogenic, carboxyl-terminal derivatives of the amyloid protein precursor. *Science* **255**, 726–728.

Farzan M., Schnitzler C. E., Vasilieva N., Leung D., and Choe H. (2000) BACE2, a beta-secretase homolog, cleaves at the beta site and within the amyloid-beta region of the amyloid-beta precursor protein. *Proc. Natl. Acad. Sci. U. S. A.* **97**, 9712–9717.

Ferreira A., Caceres A., and Kosik K. S. (1993) Intraneuronal compartments of the amyloid precursor protein. *J. Neurosci.* **13**, 3112–3123.

Fillit H., and Leveugle B. (1995) Disorders of the extracellular matrix and the pathogenesis of senile dementia of the Alzheimer's type. *Lab. Invest.* **72**, 249–253.

Fiore F., Zambrano N., Minopoli G., Donini V., Duilio A., and Russo T. (1995) The regions of the Fe65 protein homologous to the phosphotyrosine interaction/phosphotyrosine binding domain of Shc bind the intracellular domain of the Alzheimer's amyloid precursor protein. *J. Biol. Chem.* **270**, 30853–30856.

Flanders K. C., Ren R. F., and Lippa C. F. (1998) Transforming growth factor- β s in neurodegenerative disease. *Prog. Neurobiol.* **54**, 71–85.

Flood F. M., Cowburn R. F., and Johnston J. A. (1997) Presenilin-1, amyloid precursor protein and amyloid precursor-like protein 2 mRNA levels in human superior frontal cortex during aging. *Neurosci. Lett.* **235**, 17–20.

Fowler C. J., Cowburn R. F., and Joseph J. A. (1997) Alzheimer's, ageing and amyloid: an absurd allegory? *Gerontology* **43**, 132–142.

Frautschy S. A., Yang F., Calderón L., and Cole G. M. (1996) Rodent models of Alzheimer's disease: rat A β infusion approaches to amyloid deposits. *Neurobiol. Aging* **17**, 311–321.

Frisoni G. B., Calabresi L., Geroldi C., Bianchetti A., D'Acquarica A. L., Govoni S., Sirtori C. R., Trabucchi M., and Franceschini G. (1994) Apolipoprotein E ϵ 4 allele in Alzheimer's disease and vascular dementia. *Dementia* **5**, 240–242.

Fukushima D., Konishi M., Maruyama K., Miyamoto T., Ishiura S., and Suzuki K. (1993) Activation of the secretory pathway leads to a decrease in the intracellular amyloidogenic fragments generated from the amyloid protein precursor. *Biochem. Biophys. Res. Commun.* **194**, 202–207.

Gabuzda D., Busciglio J., Chen L. B., Matsudaira P., and Yankner B. A. (1994) Inhibition of energy metabolism alters the processing of amyloid precursor protein and induces a potentially amyloidogenic derivative. *J. Biol. Chem.* **269**, 13623–13628.

Games D., Adams D., Alessandrini R., Barbour R., Berthelette P., Blackwell C., Carr T., Clemens J., Donaldson T., Gillespie F., Guido T., Hagopian S., Johnson-Wood K., Khan K., Lee M., Leibowitz P., Lieberburg I., Little S., Masliah E., McConlogue L., Montoya-Zavala M., Mucke L., Paganini L., Penniman E., Power M., Schenk D., Seubert P., Snyder B., Soriano F., Tan H., Vitale J., Wadsworth S., Wolozin B., and

Zhao J. (1995) Alzheimer-type neuropathology in transgenic mice overexpressing V717F β -amyloid precursor protein. *Nature* **373**, 523–527.

Ghisso J., Matsubara E., Koudinov A., Choi-Miura N. H., Tomita M., Wisniewski T., and Frangione B. (1993) The cerebrospinal-fluid soluble form of Alzheimer's amyloid beta is complexed to SP-40,40 (apolipoprotein J), an inhibitor of the complement membrane-attack complex. *Biochem. J.* **293**, 27–30.

Ghisso J., Wisniewski T., Vidal R., Rostagno A., and Frangione B. (1992) Epitope map of two polyclonal antibodies that recognize amyloid lesions in patients with Alzheimer's disease. *Biochem. J.* **282**, 517–522.

Gibson G. E., Park L. C. H., Zhang H., Sorbi S., and Calingasan N. Y. (1999) Oxidative stress and a key metabolic enzyme in Alzheimer brains, cultured cells, and an animal model of chronic oxidative deficits. *Ann. N. Y. Acad. Sci.* **893**, 79–94.

Ginsberg S. D., Crino P. B., Hemby S. E., Weingarten J. A., Lee V. M.-Y., Eberwine J. H., and Trojanowski J. Q. (1999) Predominance of neuronal mRNAs in individual Alzheimer's disease senile plaques. *Ann. Neurol.* **45**, 174–181.

Glenner G. G. (1988) Alzheimer's disease: its proteins and genes. *Cell* **52**, 307–308.

Golde T. E., Estus S., Younkin L. H., Selkoe D. J., and Younkin S. G. (1992) Processing of the amyloid protein precursor to potentially amyloidogenic derivatives. *Science* **255**, 728–730.

Goodbourn S. (1995) Notch takes a short cut. *Nature* **377**, 288–289.

Gray C. W., and Patel A. J. (1993a) Induction of β -amyloid precursor protein isoform mRNAs by bFGF in astrocytes. *Neuroreport* **4**, 811–814.

Gray C. W., and Patel A. J. (1993b) Regulation of β -amyloid precursor protein isoform mRNAs by transforming growth factor- β 1 and interleukin- 1β in astrocytes. *Mol. Brain Res.* **19**, 251–256.

Greenfield J. P., Tsai J., Gouras G. K., Hai B., Thinakaran G., Checler F., Sisodia S. S., Greengard P., and Xu H. (1999) Endoplasmic reticulum and trans-Golgi network generate distinct populations of Alzheimer β -amyloid peptides. *Proc. Natl. Acad. Sci. U. S. A.* **96**, 742–747.

Grundke-Iqbal I., Iqbal K., Tung Y.-C., Quinlan M., Wisniewski H. M., and Binder L. I. (1986) Abnormal phosphorylation of the microtubule-associated protein tau in Alzheimer cytoskeletal pathology. *Proc. Natl. Acad. Sci. U. S. A.* **83**, 4913–4917.

Guénette S. Y., Chen J., Jondro P. D., and Tanzi R. E. (1996) Association of a novel human FE65-like protein with the cytoplasmic domain of the β -amyloid precursor protein. *Proc. Natl. Acad. Sci. U. S. A.* **93**, 10832–10837.

Guillemain I., Alonso G., Patey G., Privat A., and Chaudieu I. (2000) Human NT2 neurons express a large variety of neurotransmission phenotypes in vitro. *J. Comp. Neurol.* **422**, 380–395.

- Gupta–Bansal R., Frederickson R. C. A., and Brunden K. R. (1995) Proteoglycan–mediated inhibition of A β proteolysis. *J. Biol. Chem.* **270**, 18666–18671.
- Haass C., Koo E. H., Mellon A., Hung A. Y., and Selkoe D. J. (1992a) Targeting of cell–surface β –amyloid precursor protein to lysosomes: alternative processing into amyloid–bearing fragments. *Nature* **357**, 500–503.
- Haass C., Koo E. H., Teplow D. B., and Selkoe D. J. (1994) Polarized secretion of β –amyloid precursor protein and amyloid β –peptide in MDCK cells. *Proc. Natl. Acad. Sci. U. S. A.* **91**, 1564–1568.
- Haass C., Schlossmacher M. G., Hung A. Y., Vigo–Pelfrey C., Mellon A., Ostaszewski B. L., Lieberburg I., Koo E. H., Schenk D., Teplow D. B., and Selkoe D. J. (1992b) Amyloid β –peptide is produced by cultured cells during normal metabolism. *Nature* **359**, 322–325.
- Haass C., and Selkoe D. J. (1993) Cellular processing of β –amyloid precursor protein and the genesis of amyloid β –peptide. *Cell* **75**, 1039–1042.
- Hanzel D. K., Trojanowski J. Q., Johnston R. F., and Loring J. F. (1999) High–throughput quantitative histological analysis of Alzheimer’s disease pathology using a confocal digital microscanner. *Nature Biotech.* **17**, 53–57.
- Harrison P. J. (1995) On the neuropathology of Schizophrenia and its dementia: neurodevelopmental, neurodegenerative, or both? *Neurodegeneration* **4**, 1–12.
- Harrison P. J., Barton A. J. L., Procter A. W., Bowen D. M., and Pearson R. C. A. (1994) The effects of Alzheimer’s disease, other dementias, and premortem course on β –amyloid precursor protein messenger RNA in frontal cortex. *J. Neurochem.* **62**, 635–644.
- Harris–White M. E., Chu T., Balverde Z., Sigel J. J., Flanders K. C., and Frautschy S. A. (1998) Effects of transforming growth factor– β (isoforms 1–3) on amyloid deposition, inflammation, and cell targeting in organotypic hippocampal slice cultures. *J. Neurosci.* **18**, 10366–10374.
- Hartley R. S., Margulis M., Fishman P. S., Lee V. M.–Y., and Tang C.–M. (1999) Functional synapses are formed between human NTERA2 (NT2N, hNT) neurons grown on astrocytes. *J. Comp. Neurol.* **407**, 1–10.
- Hartmann T., Bieger S. C., Brühl B., Tienari P. J., Nobuo I., Allsop D., Roberts G. W., Masters C. L., Dotti C. G., Unsicker K., and Beyreuther K. (1997) Distinct sites of intracellular production for Alzheimer’s disease A β 40/42 amyloid peptides. *Nature Medicine* **3**, 1016–1020.
- Hawkins P. N., Rossor M. N., Gallimore J. R., Miller B., Moore E. G., and Pepys M. B. (1994) Concentration of serum amyloid P component in the CSF as a possible marker of cerebral amyloid deposits in Alzheimer’s disease. *Biochem. Biophys. Res. Commun.* **201**, 722–726.

- Heldin C.-H., Miyazono K., and ten Dijke P. (1997) TGF- β signalling from cell membrane to nucleus through SMAD proteins. *Nature* **390**, 465–471.
- Henneberg N., and Hoyer S. (1995) Desensitization of the neuronal insulin receptor: a new approach in the etiopathogenesis of late-onset sporadic dementia of the Alzheimer type (SDAT)? *Arch. Gerontol. Geriatr.* **21**, 63–74.
- Herreman A., Serneels L., Annaert W., Collen D., Schoonjans L., and De Strooper B. (2000) Total inactivation of γ -secretase activity in presenilin-deficient embryonic stem cells. *Nature Cell Biol.* **2**, 461–462.
- Hidalgo J., Muñiz M., and Velasco A. (1995) Trimeric G proteins regulate the cytosol-induced redistribution of Golgi enzymes into the endoplasmic reticulum. *J. Cell Sci.* **108**, 1805–1815.
- Ho L., Fukuchi K., and Younkin S. G. (1996) The alternatively spliced Kunitz protease inhibitor domain alters amyloid β protein precursor processing and amyloid β protein production in cultured cells. *J. Biol. Chem.* **271**, 30929–30934.
- Howlett D. R., Jennings K. H., Lee D. C., Clark M. S. G., Brown F., Wetzel R., Wood S. J., Camilleri P., and Roberts G. W. (1995) Aggregation state and neurotoxic properties of Alzheimer beta-amyloid peptide. *Neurodegen.* **4**, 23–32.
- Hoyer S. (1993) Intermediary metabolism disturbance in AD/SDAT and its relation to molecular events. *Prog. Neuro-Psychopharmacol. & Biol. Psychiat.* **17**, 199–228.
- Huang S. S., Huang F. W., Xu J., Chen S., Hsu C. Y., and Huang J. S. (1998) Amyloid β -peptide possesses a transforming growth factor- β activity. *J. Biol. Chem.* **273**, 27640–27644.
- Hussain I., Powell D., Howlett D. R., Tew D. G., Meek T. D., Chapman C., Gloger I. S., Murphy K. E., Southan C. D., Ryan D. M., Smith T. S., Simmons D. L., Walsh F. S., Dingwall C., and Christie G. (1999) Identification of a novel aspartic protease (Asp 2) as β -secretase. *Molec. Cell. Neurosci.* **14**, 419–427.
- Hyman B. T., Marzloff K., and Arriagada P. V. (1993) The lack of accumulation of senile plaques or amyloid burden in Alzheimer's disease suggests a dynamic balance between amyloid deposition and resolution. *J. Neuropathol. Exp. Neurol.* **52**, 594–600.
- Ikeda K., Akiyama H., Haga C., and Haga S. (1992) Evidence that neurofibrillary tangles undergo glial modification. *Acta Neuropathol.* **85**, 101–104.
- Inoue S., Kuroiwa M., and Kisilevsky R. (1999) Basement membranes, microfibrils and β -amyloid fibrillogenesis in Alzheimer's disease: high resolution ultrastructural findings. *Brain Res. Rev.* **29**, 218–231.
- Iverfeldt K., Walaas S. I., and Greengard P. (1993) Altered processing of Alzheimer amyloid precursor protein in response to neuronal degeneration. *Proc. Natl. Acad. Sci. U. S. A.* **90**, 4146–4150.

- Iwatsubo T., Odaka A., Suzuki N., Mizusawa H., Nukina N., and Ihara Y. (1994) Visualization of A β 42(43) and A β 40 in senile plaques with end-specific A β monoclonals: evidence that an initially deposited species is A β 42(43). *Neuron* **13**, 45–53.
- Izumi R., Yamada T., Yoshikai S., Sasaki H., Hattori M., and Sakaki Y. (1992) Positive and negative regulatory elements for the expression of the Alzheimer's disease amyloid precursor-encoding gene in mouse. *Gene* **112**, 189–195.
- Jacobsen J. S., Blume A. J., and Vitek M. P. (1991) Quantitative measurement of alternatively spliced amyloid precursor protein mRNA expression in Alzheimer's disease and normal brain by S₁ nuclease protection analysis. *Neurobiol. Aging* **12**, 585–592.
- Jarret J. T., Berger E. P., and Lansbury, Jr. P. T. (1993) The carboxy terminus of the β -amyloid protein is critical for the seeding of amyloid formation: implications for the pathogenesis of Alzheimer's disease. *Biochem.* **32**, 4693–4697.
- Jarriault S., Brou C., Logeat F., Schroeter E. H., Kopan R., and Israel A. (1995) Signalling downstream of activated mammalian Notch. *Nature* **377**, 355–358.
- Johnson S. A., McNeill T., Cordell B., and Finch C. E. (1990) Relation of neuronal APP-751/APP-695 mRNA ratio and neuritic plaque density in Alzheimer's disease. *Science* **248**, 854–857.
- Johnson S. A., Pasinetti G. M., May P. C., Ponte P. A., Cordell B., and Finch C. E. (1988) Selective reduction of mRNA for the β -amyloid precursor protein that lacks a kunitz-type protease inhibitor motif in cortex from Alzheimer brains. *Exp. Neurol.* **102**, 264–268.
- Johnson S. A., Rogers J., and Finch C. E. (1989) APP-695 transcript prevalence is selectively reduced during Alzheimer's disease in cortex and hippocampus but not in cerebellum. *Neurobiol. Aging* **10**, 267–272.
- Johnston J. A., Norgren S., Ravid R., Wasco W., Winblad B., Lannfelt L., and Cowburn R. F. (1996) Quantification of APP and APLP2 mRNA in APOE genotyped Alzheimer's disease brains. *Mol. Brain Res.* **43**, 85–95.
- Johnston J., O'Neill C., Lannfelt L., Winblad B., and Cowburn R. F. (1994) The significance of the Swedish APP 670/671 mutation for the development of Alzheimer's disease amyloidosis. *Neurochem. Int.* **25**, 73–80.
- Jolly-Tornetta C., Gao Z.-Y., Lee V. M.-Y., and Wolf B. A. (1998) Regulation of amyloid precursor protein secretion by glutamate receptors in human Ntera 2 neurons (NT2N). *J. Biol. Chem.* **273**, 14015–14021.
- Kalaria R. N., Bhatti S. U., Palatinsky E. A., Pennington D. H., Shelton E. R., Chan H. W., Perry G., and Lust W. D. (1993) Accumulation of the β -amyloid precursor protein at sites of ischemic injury in rat brain. *Neuroreport* **4**, 211–214.

- Kametani F., Tanaka K., Ishii T., Ikeda S.-I., Kennedy H. E., and Allsop D. (1993) Secretary form of Alzheimer amyloid precursor protein 695 in human brain lacks β /A4 amyloid immunoreactivity. *Biochem. Biophys. Res. Commun.* **191**, 392–398.
- Kelly J. W. (1996) Alternative conformations of amyloidogenic proteins govern their behavior. *Curr. Op. Struc. Biol.* **6**, 11–17.
- Khan S. M., Cassarino D. S., Abramova N. N., Keeney P. M., Borland M. K., Trimmer P. A., Krebs C. T., Bennett J. C., Parks J. K., Swerdlow R. H., Parker W. D. Jr., and Bennett J. P. Jr. (2000) Alzheimer's disease cybrids replicate β -amyloid abnormalities through cell death pathways. *Ann. Neurol.* **48**, 148–155.
- Kibbey M. C., Jucker M., Weeks B. S., Neve R. L., Van Nostrand W. E., and Kleinman H. K. (1993) β -Amyloid precursor protein binds to the neurite-promoting IKVAV site of laminin. *Proc. Natl. Acad. Sci. U. S. A.* **90**, 10150–10153.
- Kimberly W. T., Xia W. M., Rahmati T., and Selkoe D. J. (2000) The transmembrane aspartates in presenilin 1 and 2 are obligatory for gamma-secretase activity and amyloid beta-protein generation. *J. Biol. Chem.* **275**, 3173–3178.
- Kitaguchi N., Takahashi Y., Tokushima Y., Shiojiri S., and Ito H. (1988) Novel precursor of Alzheimer's disease amyloid protein shows protease inhibitory activity. *Nature* **331**, 530–532.
- Klempt N. D., Sirimanne E., Gunn A. J., Klempt M., Singh K., Williams C., and Gluckman P. D. (1992) Hypoxia-ischemia induces transforming growth factor β_1 mRNA in the infant rat brain. *Mol. Brain Res.* **13**, 93–101.
- Knauer M. F., Orlando R. A., and Glabe C. G. (1996) Cell surface APP751 forms complexes with protease nexin 2 ligands and is internalized via the low density lipoprotein receptor-related protein (LRP). *Brain Res.* **740**, 6–14.
- König G., Mönning U., Czech C., Prior R., Banati R., Schreiter-Gasser U., Bauer J., Masters C. L., and Beyreuther K. (1992) Identification and differential expression of a novel alternative splice isoform of the β A4 amyloid precursor protein (APP) mRNA in leukocytes and brain microglial cells. *J. Biol. Chem.* **267**, 10804–10809.
- König G., Salbaum J. M., Wiestler O., Lang W., Schmitt H. P., Masters C. L., and Beyreuther K. (1991) Alternative splicing of the β A4 amyloid gene of Alzheimer's disease in cortex of control and Alzheimer's disease patients. *Mol. Brain Res.* **9**, 259–262.
- Koo E. H., Sisodia S. S., Cork L. C., Unterbeck A., Bayney R. M., and Price D. L. (1990) Differential expression of amyloid precursor protein mRNAs in cases of Alzheimer's disease and in aged nonhuman primates. *Neuron* **2**, 97–104.
- Koo E. H., and Squazzo S. L. (1994) Evidence that production and release of amyloid β -protein involves the endocytic pathway. *J. Biol. Chem.* **269**, 17386–17389.
- Kosik K. S. (1992) Alzheimer's disease: a cell biological perspective. *Science* **256**, 780–783.

- Kuentzel S. L., Ali S. M., Altman R. A., Greenberg B. D., and Raub T. J. (1993) The Alzheimer β -amyloid protein precursor/protease nexin-II is cleaved by secretase in a *trans*-Golgi secretory compartment in human neuroglioma cells. *Biochem. J.* **295**, 367-378.
- Ladinsky M. S., Kremer J. R., Furcinitti P. S., McIntosh J. R., and Howell K. E. (1994) HVEM tomography of the *trans*-Golgi network: structural insights and identification of a lace-like vesicle coat. *J. Cell Biol.* **127**, 29-38.
- Ladror U. S., Wang G. T., Klein W. L., Holzman T. F., and Krafft G. A. (1994) Potential β PP-processing proteinase activities from Alzheimer's and control brain tissues. *J. Prot. Chem.* **13**, 357-366.
- La Ferla F. M., Troncoso J. C., Strickland D. K., Kawas C. H., and Jay G. (1997) Neuronal cell death in Alzheimer's disease correlates with apoE uptake and intracellular A β stabilization. *J. Clin. Invest.* **100**, 310-320.
- Lammich S., Kojro E., Postina R., Gilbert S., Pfeiffer R., Jasionowski M., Haass C., and Fahrenholz F. (1999) Constitutive and regulated α -secretase cleavage of Alzheimer's amyloid precursor protein by a disintegrin metalloprotease. *Proc. Natl. Acad. Sci. U. S. A.* **96**, 3922-3927.
- Lansbury P. T. Jr. (1999) Evolution of amyloid: what normal protein folding may tell us about fibrillogenesis and disease. *Proc. Natl. Acad. Sci. U. S. A.* **96**, 3342-3344.
- Laping N. J., Morgan T. E., Nichols N. R., Rozovsky I., Young-Chan C. S., Zarow C., and Finch C. E. (1994) Transforming growth factor- β 1 induces neuronal and astrocyte genes: tubulin α 1, glial fibrillary acidic protein and clusterin. *Neuroscience* **58**, 563-572.
- Lee S.-J., Liyanage U., Bickel P. E., Xia W., Lansbury P. T. Jr., and Kosik K. S. (1998) A detergent-insoluble membrane compartment contains A β *in vivo*. *Nature Med.* **4**, 730-734.
- Levitan D., and Greenwald I. (1995) Facilitation of *lin-12*-mediated signalling by *sel-12*, a *Caenorhabditis elegans* S182 Alzheimer's disease gene. *Nature* **377**, 351-354.
- Levy E., Carman M. D., Fernandez-Madrid I. J., Power M. D., Lieberburg I., Van Duinen S. G., Bots G. T. A. M., Luyendijk W., and Frangione B. (1990) Mutation of the Alzheimer's disease amyloid gene in hereditary cerebral hemorrhage, Dutch type. *Science* **248**, 1124-1126.
- Levy-Lahad E., Wijsman E. M., Nemens E., Anderson L., Goddard K. A. B., Weber J. L., Bird T. D., and Schellenberg G. D. (1995a) A familial Alzheimer's disease locus on chromosome 1. *Science* **269**, 970-973.
- Levy-Lahad E., Wasco W., Poorkaj P., Romano D. M., Oshima J., Pettingell W. H., Yu C., Jondro P. D., Schmidt S. D., Wang K., Crowley A. C., Fu Y-H., Guenette S. Y., Galas D., Nemens E., Wijsman E. M., Bird T. D., Schellenberg G. D., and Tanzi R. (1995b) Candidate gene for the chromosome 1 familial Alzheimer's disease locus. *Science* **269**, 973-977.

Li Y.-M., Xu M., Lai M.-T., Huang Q., Castro J. L., DiMuzio-Mower J., Harrison T., Lellis C., Nadin A., Neduvelil J. G., Register R. B., Sardana M. K., Shearman M. S., Smith A. L., Shi X.-P., Yin K.-C., Shafer J. A., and Gardell S. J. (2000) Photoactivated γ -secretase inhibitors directed to the active site covalently label presenilin 1. *Nature* **405**, 689–694.

Lin X., Koelsch G., Wu S., Downs D., Dashti A., and Tang J. (2000) Human aspartic protease memapsin 2 cleaves the β -secretase site of β -amyloid precursor protein. *Proc. Natl. Acad. Sci. U. S. A.* **97**, 1456–1460.

Lippa C. F., Hamos J. E., Smith T. W., Pulaski-Salo D., and Drachman D. A. (1993) Vascular amyloid deposition in Alzheimer's disease neither necessary nor sufficient for the local formation of plaques and tangles. *Arch. Neurol.* **50**, 1088–1092.

Logan A., Frautschy S. A., Gonzalez A.-M., Sporn M. B., and Baird A. (1992) Enhanced expression of transforming growth factor β 1 in the rat brain after a localized cerebral injury. *Brain Res.* **587**, 216–225.

Lyckman A. W., Confalon A. M., Thinakaran G., Sisodia S. S., and Moya K. L. (1998) Post-translational processing and turnover kinetics of presynaptically targeted amyloid precursor superfamily proteins in the central nervous system. *J. Biol. Chem.* **273**, 11100–11106.

Macvilay S., and Fabry Z. (1997) TGF β cytokine production by murine brain microvessel endothelial cells. *Neural Notes* **3**, 21–23.

Mantyh P. W., Ghilardi J. R., Rogers S., DeMaster E., Allen C. J., Stimson E. R., and Maggio J. E. (1993) Aluminium, iron, and zinc ions promote aggregation of physiological concentrations of β -amyloid peptide. *J. Neurochem.* **61**, 1171–1174.

Martin B. L., Schrader-Fischer G., Busciglio J., Duke M., Paganetti P., and Yankner B. A. (1995) Intracellular accumulation of β -amyloid in cells expressing the Swedish mutant amyloid precursor protein. *J. Biol. Chem.* **270**, 26727–26730.

Martin J. B. (1999) Molecular basis of the neurodegenerative disorders. *New Eng. J. Med.* **340**, 1970–1980.

Martin L. J., Pardo C. A., Cork L. C., and Price D. L. (1994) Synaptic pathology and glial responses to neuronal injury precede the formation of senile plaques and amyloid deposits in the aging cerebral cortex. *Am. J. Pathol.* **145**, 1358–1381.

Martinez O., Schmidt A., Salaméro J., Hoflack B., Roa M., and Goud B. (1994) The small GTP-binding protein rab6 functions in intra-Golgi transport. *J. Cell. Biol.* **127**, 1575–1588.

Martins R. N., Muir J., Brooks W. S., Creasey H., Montgomery P., Sellers P., and Broe G. A. (1993) Plasma amyloid precursor protein is decreased in Alzheimer's disease. *Neuroreport* **4**, 757–759.

- Maruyama K., Kawamura Y., Asada H., Ishiura S., and Obata K. (1994) Cleavage at the N-terminal site of Alzheimer amyloid β /A4 protein is essential for its secretion. *Biochem. Biophys. Res. Commun.* **202**, 1517–1523.
- Masliah E., Mallory M., Hansen L., DeTeresa R., Alford M., and Terry R. (1994) Synaptic and neuritic alterations during the progression of Alzheimer's disease. *Neurosci. Lett.* **174**, 67–72.
- Masters C. L., Multhaup G., Simms G., Pottgiesser J., Martins R. N., and Beyreuther K. (1985) Neuronal origin of a cerebral amyloid: neurofibrillary tangles of Alzheimer's disease contain the same protein as the amyloid of plaque cores and blood vessels. *EMBO J.* **4**, 2757–2763.
- Mattson M. P., Barger S. W., Furukawa K., Bruce A. J., Wyss-Coray T., Mark R. J., and Mucke L. (1997) Cellular signaling roles of TGF β , TNF α and β APP in brain injury responses and Alzheimer's disease. *Brain Res. Rev.* **23**, 47–61.
- Mattson M. P., Cheng B., Culwell A. R., Esch F. S., Lieberburg I., and Rydel R. E. (1993) Evidence for excitoprotective and intraneuronal calcium-regulating roles for secreted forms of the β -amyloid precursor protein. *Neuron* **10**, 243–254.
- McLoughlin D. M., and Miller C. J. (1996) The intracellular cytoplasmic domain of the Alzheimer's disease amyloid precursor protein interacts with phosphotyrosine-binding domain proteins in the yeast two-hybrid system. *FEBS Letters* **397**, 197–200.
- Meier-Ruge W., Bertoni-Freddari C., and Iwangoff P. (1994) Changes in brain glucose metabolism as a key to the pathogenesis of Alzheimer's disease. *Gerontol.* **40**, 246–252.
- Mills J., and Reiner P. B. (1999) Regulation of amyloid precursor protein cleavage. *J. Neurochem.* **72**, 443–460.
- Miyakawa T., Shimoji A., Kuramoto R., and Higuchi Y. (1982) The relationship between senile plaques and cerebral blood vessels in Alzheimer's disease and senile dementia. *Virchows Arch.* **40**, 121–129.
- Miyakawa T., Sumiyoshi S., Murayama E., and Deshimaru M. (1974) Ultrastructure of capillary plaque-like degeneration in senile dementia. *Acta Neuropathol.* **29**, 229–236.
- Miyazaki K., Hasegawa M., Funahashi K., and Umeda M. (1993) A metalloproteinase inhibitor domain in Alzheimer amyloid protein precursor. *Nature* **362**, 839–841.
- Moir R. D., Lynch T., Bush A. I., Whyte S., Henry A., Portbury S., Multhaup G., Small D. H., Tanzi R. E., Beyreuther K., and Masters C. L. (1998) Relative increase in Alzheimer's disease of soluble forms of cerebral A β -amyloid protein precursor containing the Kunitz protease inhibitory domain. *J. Biol. Chem.* **273**, 5013–5019.
- Mönning U., Sandbrink R., Banati R. B., Masters C. L., and Beyreuther K. (1994) Transforming growth factor β mediates increase of mature transmembrane amyloid precursor protein in microglial cells. *FEBS Letters* **342**, 267–272.

- Morgan J. M., Navabi H., Schmid K. W., and Jasani B. (1994) Possible role of tissue-bound calcium ions in citrate-mediated high-temperature antigen retrieval. *J. Pathol.* **174**, 301–307.
- Morgan T. E., Nichols N. R., Pasinetti G. M., and Finch C. E. (1993) TGF- β 1 mRNA increases in macrophage/microglial cells of the hippocampus in response to deafferentation and kainic acid-induced neurodegeneration. *Exp. Neurol.* **120**, 291–301.
- Morin P. J., Abraham C. R., Amaratunga A., Johnson R. J., Huber G., Sandell J. H., and Fine R. E. (1993) Amyloid precursor protein is synthesised by retinal ganglion cells, rapidly transported to the optic nerve plasma membrane and nerve terminals, and metabolized. *J. Neurochem.* **61**, 464–473.
- Moya K. L., Benowitz L. I., Schneider G. E., and Allinquant B. (1994) The amyloid precursor protein is developmentally regulated and correlated with synaptogenesis. *Dev. Biol.* **161**, 597–603.
- Mucke L., Masliah E., Yu G.-Q., Mallory M., Rockenstein E. M., Tatsuno G., Hu K., Kholodenko D., Johnson-Wood K., and McConlogue L. (2000) High-level neuronal expression of A β _{1–42} in wild-type human amyloid protein precursor transgenic mice: synaptotoxicity without plaque formation. *J. Neurosci.* **20**, 4050–4058.
- Mufson E. J. (1997) NGF, p75^{NTR} and TrkA in Alzheimer's disease. *Neural Notes* **3**, 16–19.
- Müller U., Gajic V., Steinback J., Aguzzi A., Herms J., Tremml P., Sisodia S., Wolfer D. P., and Lipp H.-P. (1998) Single and combined gene deficiencies of APP/APLP-family members. *Eur. J. Neurosci.* **10**, suppl. **10**, 32.05.
- Multhaup G., Bush A. I., Pollwein P., and Masters C. L. (1994) Interaction between the zinc(II) and the heparin binding site of the Alzheimer's disease β A4 amyloid precursor protein (APP). *FEBS Lett.* **355**, 151–154.
- Murphy G. M. Jr., Forno L. S., Higgins L., Scardina J. M., Eng L. F., and Cordell B. (1994) Development of a monoclonal antibody specific for the COOH-terminal of β -amyloid 1–42 and its immunohistochemical reactivity in Alzheimer's disease and related disorders. *Am. J. Pathol.* **144**, 1082–1088.
- Myers A., Holmans P., Marshall H., Kwon J., Meyer D., Ramic D., Shears S., Booth J., DeVrieze F. W., Crook R., Hamshire M., Abraham R., Tunstall N., Rice R., Carty S., Lillystone S., Kehoe P., Rudrasingham V., Jones L., Lovestone S., Perez-Tur J., Williams J., Owen M. J., Hardy J., and Goate A. M. (2000) *Science* **290**, 2304–5.
- Näslund J., Haroutunian V., Mohs R., Davis K. L., Davies P., Greengard P., and Buxbaum J. D. (2000) Correlation between elevated levels of amyloid β -peptide in the brain and cognitive decline. *J. A. M. A.* **283**, 1571–1577.
- Neill D., Hughes D., Edwardson J. A., Rima B. K., and Allsop D. (1994) Human IMR-32 neuroblastoma cells as a model cell line in Alzheimer's disease research. *J. Neurosci. Res.* **39**, 482–493.

- Neve R. L., Finch E. A., and Dawes L. R. (1988) Expression of the Alzheimer amyloid precursor gene transcripts in the human brain. *Neuron* **1**, 669–677.
- Neve R. L., Rogers J., and Higgins G. A. (1990) The Alzheimer amyloid precursor-related transcript lacking the β /A4 sequence is specifically increased in Alzheimer's disease brain. *Neuron* **5**, 329–338.
- Nilsson T., Pypaert M., Hoe M. H., Slusarewicz P., Berger E. G., and Warren G. (1993) Overlapping distribution of two glycosyltransferases in the Golgi apparatus of HeLa cells. *J. Cell Biol.* **120**, 5–13.
- Nishimoto I., Okamoto T., Matsuura Y., Takahashi S., Okamoto T., Murayama Y., and Ogata E. (1993) Alzheimer amyloid protein precursor complexes with brain GTP-binding protein G_o . *Nature* **362**, 75–79.
- Nitsch R. M., Blusztajn J. K., Pittas A. G., Slack B. E., Growdon J. H., and Wurtman R. J. (1992) Evidence for a membrane defect in Alzheimer disease brain. *Proc. Natl. Acad. Sci. U. S. A.* **89**, 1671–1675.
- Nolan C. C., and Brown A. W. (1989) Reversible neuronal damage in hippocampal pyramidal cells with triethyllead: the role of astrocytes. *Neuropathol. Appl. Neurobiol.* **15**, 441–457.
- Norstedt C., Caporaso G. L., Thyberg J., Gandy S. E., and Greengard P. (1993) Identification of the Alzheimer β /A4 amyloid precursor protein in clathrin-coated vesicles purified from PC12 cells. *J. Biol. Chem.* **268**, 608–612.
- Ohyagi Y., Takahashi K., Satoh Y., Makifuchi T., and Tabira T. (1992) Cerebral cortical amyloid protein precursor mRNA expression is similar in Alzheimer's disease and other neurodegenerative diseases. *J. Neurol. Sci.* **111**, 33–38.
- Owen M., Liddell M., and McGuffin P. (1994) Alzheimer's disease. An association with apolipoprotein E4 may help unlock the puzzle. *BMJ* **308**, 672–673.
- Palmert M. R., Golde T. E., Cohen M. L., Kovacs D. M., Tanzi R. E., Gusella J. F., Usiak M. F., Younkin L. H., and Younkin S. G. (1988) Amyloid protein precursor messenger RNAs: differential expression in Alzheimer's disease. *Science* **241**, 1080–1084.
- Pangalos M. N., Efthimiopoulos S., Shioi J., Mytilineou C., and Robakis N. K. (1995) The chondroitin sulfate attachment site of appican is formed by splicing out of exon 15 of the amyloid precursor gene. *Soc. Neurosci. Abstracts* **21**, 85.5.
- Paola D., Domenicotti C., Nitti M., Vitali A., Borghi R., Cottalasso D., Zaccheo D., Odetti P., Strocchi P., Marinari U. M., Tabaton M., and Pronzato M. A. (2000) Oxidative stress induces increase in intracellular amyloid β -protein production and selective activation of β I and β II PKCs in NT2 cells. *Biochem. Biophys. Res. Commun.* **268**, 642–646.

- Papasozomenos S. C., and Yuan S. (1991) Altered phosphorylation of tau protein in heat-shock rats and patients with Alzheimer's disease. *Proc. Natl. Acad. Sci. U. S. A.* **88**, 4543–4547.
- Papastoitsis G., Siman R., Scott R., and Abraham C. R. (1994) Identification of a metalloprotease from Alzheimer's disease brain able to degrade the β -amyloid precursor protein and generate amyloidogenic fragments. *Biochemistry* **33**, 192–199.
- Pappolla M. A., Sambamurti K., Efthimiopoulos S., Refolo L., Omar R. A., and Robakis N. K. (1995) Heat-shock induces abnormalities in the cellular distribution of amyloid precursor protein (APP) and APP fusion proteins. *Neurosci. Lett.* **192**, 105–108.
- Parkinson D. (1998) Localization of presenilin 1 in NTera2 cells. *Eur. J. Neurosci.* **10**, suppl. **10**, 32.07.
- Paterlini M., Valerio A., Baruzzi F., Memo M., and Spano P. (1998) Opposing regulation of tau protein levels by ionotropic and metabotropic glutamate receptors in human NT2 neurons. *Neurosci. Lett.* **243**, 77–80.
- Pearson R. C. A., and Powell T. P. S. (1989) The neuroanatomy of Alzheimer's disease. *Rev. Neurosci.* **2**, 101–122.
- Peress N. S., and Perillo E. (1995) Differential expression of TGF- β 1, 2 and 3 isotypes in Alzheimer's disease: a comparative immunohistochemical study with cerebral infarction, aged human and mouse control brains. *J. Neuropathol. Exp. Neurol.* **54**, 802–811.
- Perry G. Alzheimer's Disease. In: Smith B., and Adelman G., eds, (1991) *Neuroscience Year: supplement 2 to the Encyclopedia of Neuroscience*. Birkhäuser Boston, Cambridge, MA.
- Perry G. (1993) Neuritic plaques in Alzheimer's disease originate from neurofibrillary tangles. *Med. Hypoth.* **40**, 257–258.
- Perry G., Cras P., Siedlak S. L., Tabaton M., and Kawai M. (1992) β protein immunoreactivity is found in the majority of neurofibrillary tangles of Alzheimer's disease. *Am. J. Pathol.* **140**, 283–290.
- Phillips A. O., Steadman R., Topley N., and Williams D. J. (1995) Elevated D-glucose concentrations modulate TGF- β 1 synthesis by human cultured renal proximal tubular cells. *Am. J. Pathol.* **147**, 362–374.
- Pike C. J., Walencewicz A. J., Glabe C. G., and Cotman C. W. (1991) In vitro aging of β -amyloid protein causes peptide aggregation and neurotoxicity. *Brain Res.* **563**, 311–314.
- Pileri S. A., Roncador G., Ceccarelli C., Piccioli M., Briskomatis A., Sabattini E., Ascani S., Santini D., Piccaluga P. P., Leone O., Damiani S., Ercolessi C., Sandri F., Pieri F., Leoncini L., and Falini B. (1997) Antigen retrieval techniques in immunohistochemistry: comparison of different methods. *J. Pathol.* **183**, 116–123.

Pitas R. E., Boyles J. K., Lee S. H., Foss D., and Mahley R. W. (1987) Astrocytes synthesize apolipoprotein E and metabolize apolipoprotein E-containing lipoproteins. *Biochem. Biophys. Acta* **917**, 148–161.

Pleasure S. J., and Lee V. M.-Y. (1993) Ntera-2 cells – a human cell-line which displays characteristics expected of a human committed neuronal progenitor-cell. *J. Neurosci. Res.* **35**, 585–602.

Pleasure S. J., Page C., and Lee V. M.-Y. (1992) Pure, postmitotic, polarized human neurons derived from Ntera 2 cells provide a system for expressing exogenous proteins in terminally differentiated neurons. *J. Neurosci.* **12**, 1802–1815.

Poirier J. (1994) Apolipoprotein E in animal models of CNS injury and in Alzheimer's disease. *TINS* **17**, 525–530.

Poirier J., Davignon J., Bouthillier D., Kogan S., Bertrand P., and Gauthier S. (1993) Apolipoprotein E polymorphism and Alzheimer's disease. *Lancet* **342**, 697–699.

Polak J. M., and Van Noorden S. (1997) *Introduction to immunocytochemistry*, 2nd edit. BIOS Scientific Publishers Limited, 9 Newtec Place, Oxford.

Ponte P., Gonzalez-De Whitt P., Schilling J., Miller J., Hsu D., Greenberg B., Davis K., Wallace W., Lieberburg I., Fuller F., and Cordell B. (1988) A new A4 amyloid mRNA contains a domain homologous to serine proteinase inhibitors. *Nature* **331**, 525–527.

Potempska A., Ramakrishna N., Wisniewski H. M., and Miller D. L. (1993) Interaction between the β -amyloid peptide precursor and histones. *Arch. Biochem. Biophys.* **304**, 448–453.

Prehn J. H. M., Bindokas V. P., Jordán J., Galindo M. F., Ghadge G. D., Roos R. P., Boise L. H., Thompson C. B., Krajewski S., Reed J. C., and Miller R. J. (1996) Protective effect of transforming growth factor- β 1 on β -amyloid neurotoxicity in rat hippocampal neurons. *Mol. Pharmacol.* **49**, 319–328.

Prehn J. H. M., Peruche B., Unsicker K., and Krieglstein J. (1993) Isoform-specific effects of transforming growth factors- β on degeneration of primary neuronal cultures induced by cytotoxic hypoxia or glutamate. *J. Neurochem.* **60**, 1665–1672.

Price D. L., Borchelt D. R., and Sisodia S. S. (1993) Alzheimer disease and the prion disorders amyloid β -protein and prion protein amyloidodes. *Proc. Natl. Acad. Sci. U. S. A.* **90**, 6381–6384.

Price J. L. (1993) The relationship between tangle and plaque formation during healthy aging and mild dementia. *Neurobiol. Aging* **14**, 661–663.

Rabouille C., Hui N., Hunte F., Kieckbusch R., Berger E. G., Warren G., and Nilsson T. (1995) Mapping the distribution of Golgi enzymes involved in the construction of complex oligosaccharides. *J. Cell Sci.* **108**, 1617–1627.

Radenahmad N. (2000) An immunohistochemical study in the neocortex of Alzheimer's disease. *PhD thesis, Univ. of Sheffield.*

- Ramakrishna N., Smedman M., and Gillam B. (1996) Suppression of Alzheimer amyloid precursor protein (APP) expression by exogenous APP mRNA. *Arch. Biochem. Biophys.* **326**, 243–251.
- Ren R. F., and Flanders K. C. (1996) Transforming growth factors- β protect primary rat hippocampal neuronal cultures from degeneration induced by β -amyloid peptide. *Brain Res.* **732**, 16–24.
- Ren R. F., Hawver D. B., Kim R. S., and Flanders K. C. (1997) Transforming growth factor- β protects human hNT cells from degeneration induced by β -amyloid peptide: involvement of the TGF- β type II receptor. *Mol. Brain Res.* **48**, 315–322.
- Ren R. F., Lah J. J., Diehlmann A., Kim E. S., Hawver D. B., Levey A. I., Beyreuther K., and Flanders K. C. (1999) Differential effects of transforming growth factor- β s and glial cell line-derived neurotrophic factor on gene expression of presenilin-1 in human post-mitotic neurons and astrocytes. *Neuroscience* **93**, 1041–1049.
- Roberts G. W., Nash M., Ince P. G., Royston M. C., and Gentleman S. M. (1993) On the origin of Alzheimer's disease: a hypothesis. *Neuroreport* **4**, 7–9.
- Robinson C. A., Clark A. W., Parhad I. M., Fung T. S., and Bou S. S. (1994) Gene expression in Alzheimer neocortex as a function of age and pathologic severity. *Neurobiol. Aging* **15**, 681–690.
- Rockenstein E. M., McConlogue L., Tan H., Power M., Masliah E., and Mucke L. (1995) Levels and alternative splicing of amyloid β protein precursor (APP) transcripts in brains of APP transgenic mice and humans with Alzheimer's disease. *J. Biol. Chem.* **270**, 28257–28267.
- Rogaev E. I., Sherrington R., Rogaeva E. A., Levesque G., Ikeda M., Liang Y., Chi H., Lin C., Holman K., Tsuda T., Mar L., Sorbi S., Nacmias B., Piacentini S., Amaducci L., Chumakov I., Cohen D., Lannfelt L., Fraser P. E., Rommens J. M., and St. George-Hyslop P. H. (1995) Familial Alzheimer's disease in kindreds with missense mutations in a gene on chromosome 1 related to the Alzheimer's disease type 3 gene. *Nature* **376**, 775–778.
- Rosenberg R. N. (2000) The molecular and genetic basis of AD: the end of the beginning. *Neurology* **54**, 2045–2054.
- Rosenblum W. I. (1999) The presence, origin, and significance of A β peptide in the cell bodies of neurons. *J. Neuropathol. Exp. Neurol.* **58**, 575–581.
- Rossor M. (1993) Alzheimer's disease. *BMJ* **307**, 779–782.
- Rothman J. E., and Wieland F. T. (1996) Protein sorting by transport vesicles. *Science* **272**, 227–234.
- Rutka J. T., Apodaca G., Stern R., and Rosenblum M. (1988) The extracellular matrix of the central and peripheral nervous systems: structure and function. *J. Neurosurg.* **69**, 155–170.

Sahasrabudhe S. R., Brown A. M., Hulmes J. D., Jacobsen J. S., Vitek M. P., Blume A. J., and Sonnenberg J. L. (1993) Enzymatic generation of the amino terminus of the β -amyloid peptide. *J. Biol. Chem.* **268**, 16699–16705.

Salbaum M., Weidemann A., Lemaire G., Masters C. L., and Beyreuther K. (1988) The promoter of Alzheimer's disease amyloid A4 precursor gene. *Eur. Mol. Biol. Org. J.* **7**, 2807–2813.

Salehi A., Heyn S., Gonatas N. K., and Swaab D. F. (1995) Decreased protein synthetic activity of the hypothalamic tuberomammillary nucleus in Alzheimer's disease as suggested by smaller Golgi apparatus. *Neurosci. Lett.* **193**, 29–32.

Sambamurti K., Sevlever D., Koothan T., Refolo L. M., Pinnix I., Gandhi S., Onstead L., Younkin L., Prada C. M., Yager D., Ohyagi Y., Eckman C. B., Rosenberry T. L., and Younkin S. G. (1999) Glycosylphosphatidylinositol-anchored proteins play an important role in the biogenesis of the Alzheimer's amyloid β -protein. *J. Biol. Chem.* **274**, 26810–26814.

Sanan D. A., Weisgraber K. H., Russel S. J., Mahley R. W., Huang D., Saunders A., Schmechel D., Wisniewski T., Frangione B., Roses A. D., and Strittmatter W. J. (1994) Apolipoprotein E associates with β -amyloid peptide of Alzheimer's disease to form novel monofibrils. *J. Clin. Invest.* **94**, 860–869.

Sandbrink R., Masters C. L., and Beyreuther K. (1994) Similar alternative splicing of a non-homologous domain in β A4-amyloid protein precursor-like protein. *J. Biol. Chem.* **269**, 14227–14234.

Sandbrink R., Mönning U., Masters C. L., and Beyreuther K. (1997) Expression of the APP gene family in brain cells, brain development and aging. *Gerontology* **43**, 119–131.

Sanderson K. L., Butler L., and Ingram V. M. (1997) Aggregates of a beta-amyloid peptide are required to induce calcium currents in neuron-like human teratocarcinoma cells: relation to Alzheimer's disease. *Brain Res.* **744**, 7–14.

Santiard-Baron D., Gosset P., Nicole A., Sinet P.-M., Christen Y., and Ceballos-Picot I. (1999) Identification of β -amyloid-responsive genes by RNA differential display: early induction of a DNA damage-inducible gene, *gadd-45*. *Exp. Neurol.* **158**, 206–213.

Saunders A. M., Schmechel K., Breitner J. C. S., Benson M. D., Brown W. T., Goldfarb L., Goldgaber D., Manwaring M. G., Szymanski M. H., McCown N., Dole K. C., Schmechel D. E., Strittmatter W. J., Pericak-Vance M. A., and Roses A. D. (1993a) Apolipoprotein E ϵ 4 allele distributions in late-onset Alzheimer's disease and in other amyloid-forming diseases. *Lancet* **342**, 710–711.

Saunders A. M., Strittmatter W. J., Schmechel D., St. George-Hyslop P. H., Pericak-Vance M. A., Joo S. H., Rosi B. L., Gusella J. F., Crapper-MacLachlan D. R., Alberts M. J., Hulette C., Crain B., Goldgaber D., and Roses A. D. (1993b) Association of apolipoprotein E allele ϵ 4 with late-onset familial and sporadic Alzheimer's disease. *Neurology* **43**, 1467–1472.

- Saura J., Luque J. M., Cesura A. M., Da Prada M., Chan–Palay V., Huber G., Löffler J., and Richards J. G. (1994) Increased monoamine oxidase B activity in plaque-associated astrocytes of Alzheimer brains revealed by quantitative enzyme radioautography. *Neuroscience* **62**, 15–30.
- Schmechel D. E., Saunders A. M., Strittmatter W. J., Crain B. J., Hulette C. M., Joo S. H., Pericak–Vance M. A., Goldgaber D., and Roses A. D. (1993) Increased amyloid β -peptide deposition in cerebral cortex as a consequence of apolipoprotein E genotype in late-onset Alzheimer disease. *Proc. Natl. Acad. Sci. U. S. A.* **90**, 9649–9653.
- Schnabel J. (1993) New Alzheimer's therapy suggested. *Science* **260**, 1719–1720.
- Schubert D., Schroeder R., LaCorbiere M., Saithoh T., and Cole G. (1988) Amyloid β protein precursor is possibly a heparan sulphate proteoglycan core protein. *Science* **241**, 223–226.
- Scott J. (1993) Apolipoprotein E and Alzheimer's disease. *The Lancet* **342**, 696.
- Scott S. A., Johnson S. A., Zarow C., and Perlmutter L. S. (1993) Inability to detect β -amyloid protein precursor mRNA in Alzheimer plaque-associated microglia. *Exp. Neurol.* **121**, 113–118.
- Seelig H. P., Schranz P., Schröter H., Wiemann C., Griffiths G., and Renz M. (1994) Molecular genetic analyses of a 376-kilodalton Golgi complex membrane protein (giantin). *Mol. Cell. Biol.* **14**, 2564–2576.
- Selkoe D. J. (1994a) Amyloid β -protein precursor: new clues to the genesis of Alzheimer's disease. *Curr. Op. Neurobiol.* **4**, 708–716.
- Selkoe D. J. (1994b) Normal and abnormal biology of the β -amyloid precursor protein. *Annu. Rev. Neurosci.* **17**, 489–517.
- Selkoe D. J. (1995) Missense on the membrane. *Nature* **375**, 734–735.
- Selkoe D. J. (1999) Translating cell biology into therapeutic advances in Alzheimer's disease. *Nature* **399** supp **24**, A23–A31.
- Seubert P., Oltersdorf T., Lee M. G., Barbour R., Blomquist C., Davis D. L., Bryant K., Fritz L. C., Galasko D., Thal L. J., Lieberburg I., and Schenk D. B. (1993) Secretion of β -amyloid precursor protein cleaved at the amino terminus of the β -amyloid peptide. *Nature* **361**, 260–263.
- Shastry B. S., and Giblin F. J. (1999) Genes and susceptible loci of Alzheimer's disease. *Brain Res. Bull.* **48**, 121–127.
- Shea T. B. (1994) Amyloid precursor protein as a glial-derived growth factor. *TINS* **17**, 338–339.
- Shepherd C. E., Bowes S., Parkinson D., Cambray–Deakin M., and Pearson R. C. A. (2000) Expression of amyloid precursor protein in human astrocytes *in vitro*: isoform-specific increases following heat shock. *Neuroscience* **99**, 317–325.

Sherriff F. E., Bridges L. R., and Jackson P. (1994) Microwave antigen retrieval of β -amyloid precursor protein immunoreactivity. *Neuroreport* **5**, 1085–1088.

Sherrington R., Rogaev E. I., Liang Y., Rogaeva E. A., Levesque G., Ikeda M., Chi H., Lin C., Li G., Holman K., Tsuda T., Mar L., Foncin J-F., Bruni A. C., Montesi M. P., Sorbi S., Rainero I., Pinessi L., Nee L., Chumakov I., Pollen D., Brookes A., Sanseau P., Polinsky R. J., Wasco W., Da Silva H. A. R., Haines J. L., Pericak-Vance M. A., Tanzi R. E., Roses A. D., Fraser P. E., Rommens J. M., and St. George-Hyslop P. H. (1995) Cloning of a gene bearing missense mutations in early-onset familial Alzheimer's disease. *Nature* **375**, 754–760.

Shi S-R., Imam A., Young L., Cote R. J., and Taylor C. R. (1993) Antigen retrieval immunohistochemistry under the influence of pH using monoclonal antibodies. *J. Histochem. Cytochem.* **43**, 193–201.

Shimokawa M., Yanagisawa K., Nishiye H., and Miyatake T. (1993) Identification of amyloid precursor protein in synaptic plasma membrane. *Biochem. Biophys. Res. Commun.* **196**, 240–244.

Shindler K. S., and Roth K. A. (1996) Double immunofluorescent staining using two unconjugated primary antisera raised in the same species. *J. Histochem. Cytochem.* **44**, 1331–1335.

Shoji M., Golde T. E., Ghiso J., Cheung T. T., Estus S., Shaffer L. M., Cai X-D., McKay D. M., Tintner R., Frangione B., and Younkin S. G. (1992) Production of the Alzheimer amyloid β protein by normal proteolytic processing. *Science* **258**, 126–129.

Siman R., Mistretta S., Durkin J. T., Savage M. J., Loh T., Trusko S., and Scott R. W. (1993) Processing of the β -amyloid precursor. Multiple proteases generate and degrade potentially amyloidogenic fragments. *J. Biol. Chem.* **268**, 16602–16609.

Simons M., Ikonen E., Tienari P. J., Cid-Arregui A., Mönning U., Beyreuther K., and Dotti C. G. (1995) Intracellular routing of human amyloid protein precursor: axonal delivery followed by transport to the dendrites. *J. Neurosci. Res.* **41**, 121–128.

Simpson P. (1995) The Notch connection. *Nature* **375**, 736–737.

Sinha S., Anderson J. P., Barbour R., Basi G. S., Caccavello R., Davis D., Doan M., Dovey H. F., Frigon N., Hong J., Jacobson-Croak K., Jewett N., Keim P., Knops J., Lieberburg I., Power M., Tan H., Tatsuno G., Tung J., Schenk D., Seubert P., Suomensari S. M., Wang S., Walker D., Zhao J., McConlogue L., and John V. (1999) Purification and cloning of amyloid precursor protein β -secretase from human brain. *Nature* **402**, 537–540.

Sinha S., and Lieberburg I. (1999) Cellular mechanisms of β -amyloid production and secretion. *Proc. Natl. Acad. Sci. U. S. A.* **96**, 11049–11053.

Sisodia S. S. (1992) β -amyloid precursor protein cleavage by a membrane-bound protease. *Proc. Natl. Acad. Sci. U. S. A.* **89**, 6075–6079.

- Sisodia S. S., Koo E. H., Hoffman P. N., Perry G., and Price D. L. (1993) Identification and transport of full-length amyloid precursor proteins in rat peripheral nervous system. *J. Neurosci.* **13**, 3136–3142.
- Slunt H. H., Thinakaran G., Von Koch C., Lo A. C. Y., Tanzi R. E., Sisodia S. (1994) Expression of a ubiquitous, cross-reactive homologue of the mouse β -amyloid precursor protein (APP). *J. Biol. Chem.* **269**, 2637–2644.
- Small D. H., Nurcombe V., Reed G., Clarris H., Moir R., Beyreuther K., and Masters C. L. (1994) A heparin-binding domain in the amyloid protein precursor of Alzheimer's disease is involved in the regulation of neurite outgrowth. *J. Neurosci.* **14**, 2117–2127.
- Snow A. D., Lara S., Nochlin D., and Wight T. N. (1989) Cationic dyes reveal proteoglycans structurally integrated within the characteristic lesions of Alzheimer's disease. *Acta Neuropathol.* **78**, 113–123.
- Snow A. D., Mar H., Nochlin D., Kimata K., Kato M., Suzuki S., Hassell J., and Wight T. N. (1988) The presence of heparan sulfate proteoglycans in the neuritic plaques and congophilic angiopathy in Alzheimer's disease. *Am. J. Pathol.* **133**, 456–463.
- Snow A. D., Mar H., Nochlin D., Sekiguchi R. T., Kimata K., Koike Y., and Wight T. N. (1990) Early accumulation of heparan sulfate in neurons and in the beta-amyloid protein-containing lesions of Alzheimer's disease and Down's syndrome. *Am. J. Pathol.* **137**, 1253–1270.
- Snow A. D., Sekiguchi R. T., Nochlin D., Kalaria R. N., and Kimata K. (1994) Heparan sulfate proteoglycan in diffuse plaques of hippocampus but not of cerebellum in Alzheimer's disease brain. *Am. J. Pathol.* **144**, 337–347.
- Solà C., García-Ladona F. J., Mengod G., Probst A., Frey P., and Palacios J. M. (1993) Increased levels of the Kunitz protease inhibitor-containing β APP mRNAs in rat brain following neurotoxic damage. *Mol. Brain Res.* **17**, 41–52.
- Solans A., Estivill X., and De La Luna S. (2000) A new aspartyl protease on 21q22.3, BACE2, is highly similar to Alzheimer's amyloid precursor protein beta-secretase. *Cytogenet. Cell Genet.* **89**, 177–184.
- Spillantini M. G., Hunt S. P., Ulrich J., and Goedert M. (1989) Expression and cellular localization of amyloid β -protein precursor transcripts in normal human brain and in Alzheimer's disease. *Mol. Brain Res.* **6**, 143–150.
- Stamler J. S. (1996) A radical vascular connection. *Nature* **380**, 108–111.
- Steiner H., Capell A., and Haass C. (1999) Proteolytic processing and degradation of Alzheimer's disease relevant proteins. *Biochem. Soc. Transact.* **27**, 234–242.
- Storey E., Beyreuther K., and Masters C. L. (1996) Alzheimer's disease amyloid precursor protein on the surface of cortical neurons in primary culture co-localizes with adhesion patch components. *Brain Res.* **735**, 217–231.

Strittmatter W. J., Saunders A. M., Schmechel D., Pericak-Vance M., Enghild J., Salvesen G. S., and Roses A. D. (1993) Apolipoprotein E: high-avidity binding to β -amyloid and increased frequency of type 4 allele in late-onset familial Alzheimer disease. *Proc. Natl. Acad. Sci. U. S. A.* **90**, 1977–1981.

Struhl G., and Greenwald I. (1999) Presenilin is required for activity and nuclear access of Notch in *Drosophila*. *Nature* **398**, 522–525.

Sudoh S., Kawakami H., and Nakamura S. (1996) Serum deprivation alters the expression and the splicing at exons 7, 8 and 15 of the β -amyloid precursor protein in the C6 glioma cell line. *Mol. Brain Res.* **39**, 12–22.

Suzuki N., Cheung T. T., Cai X.-D., Odaka A., Otvos L., Eckman C., Golde T. E., and Younkin S. G. (1994a) An increased percentage of long amyloid β protein secreted by familial amyloid β protein precursor (β APP₇₁₇) mutants. *Science* **264**, 1336–1340.

Suzuki N., Iwatsubo T., Odaka A., Ishibashi Y., Kitaka C., and Ihara Y. (1994b) High tissue content of soluble β 1–40 is linked to cerebral amyloid angiopathy. *Am. J. Pathol.* **145**, 452–460.

Swerdlow R. H., Parks J. K., Cassarino D. S., Maguire D. J., Maguire R. S., Bennet J. P. Jr., Davis R. E., and Parker W. D. Jr. (1997) Cybrids in Alzheimer's disease: a cellular model of the disease? *Neurology* **49**, 918–925.

Tabaton M., Nunzi M. G., Xue R., Usiak M., Autilio-Gambetti L., and Gambetti P. (1994) Soluble amyloid β -protein is a marker of Alzheimer amyloid in brain but not in cerebrospinal fluid. *Biochem. Biophys. Res. Commun.* **200**, 1598–1603.

Takemura M., Nakamura S., Akiguchi I., Ueno M., Oka N., Ishikawa S., Shimada A., Kimura J., and Takeda T. (1993) β /A4 proteinlike immunoreactive granular structures in the brain of senescence-accelerated mouse. *Am. J. Pathol.* **142**, 1887–1897.

Tanaka M., Gong J. S., Zhang J., Yoneda M., and Yagi K. (1998) Mitochondrial genotype associated with longevity. *Lancet* **351**, 185–186.

Tanaka S., Nakamura S., Kimura J., and Ueda K. (1993) Age-related change in the proportion of amyloid precursor protein mRNAs in the grey matter of cerebral cortex. *Neurosci. Lett.* **163**, 19–21.

Tanaka S., Nakamura S., Ueda K., Kameyama M., Shiojiri S., Takahashi Y., Kitaguchi N., and Ito H. (1988) Three types of amyloid protein precursor mRNA in human brain: their differential expression in Alzheimer's disease. *Biochem. Biophys. Res. Commun.* **157**, 472–479.

Tanaka S., Shiojiri S., Takahashi Y., Kitaguchi N., Ito H., Kameyama M., Kimura J., Nakamura S., and Ueda K. (1989) Tissue-specific expression of three types of β -protein precursor mRNA: enhancement of protease inhibitor-harboring types in Alzheimer's disease brain. *Biochem. Biophys. Res. Commun.* **165**, 1406–1414.

Tanzi R. E., McClatchey A. I., Lamperti E. D., Villa-Komaroff L., Gusella J. F., and Neve R. L. (1988) Protease inhibitor domain encoded by an amyloid protein precursor mRNA associated with Alzheimer's disease. *Nature* **331**, 528–530.

Tate-Ostroff B., Majocha R. E., and Marotta C. A. (1989) Identification of cellular and extracellular sites of amyloid precursor protein extracytoplasmic domain in normal and Alzheimer disease brains. *Proc. Natl. Acad. Sci. U. S. A.* **86**, 745–749.

Thomas T., Thomas G., McLendon C., Sutton T., and Mullan M. (1996) β -amyloid-mediated vasoactivity and vascular endothelial damage. *Nature* **380**, 168–171.

Tokuhiro S., Tomita T., Iwata H., Kosaka T., Saido T. C., Maruyama K., and Iwatsubo T. (1998) The presenilin 1 mutation (M146V) linked to familial Alzheimer's disease attenuates the neuronal differentiation of NTERA 2 cells. *Biochem. Biophys. Res. Commun.* **244**, 751–755.

Tombaugh G. C., and Sapolsky R. M. (1992) Corticosterone accelerates hypoxia- and cyanide-induced ATP loss in cultured hippocampal astrocytes. *Brain Res.* **588**, 154–156.

Turner R. S., Suzuki N., Chyung A. S. C., Younkin S. G., and Lee V. M.-Y. (1996) Amyloids β_{40} and β_{42} are generated intracellularly in cultured human neurons and their secretion increases with maturation. *J. Biol. Chem.* **271**, 8966–8970.

Ueki A., Kawano M., Namba Y., Kawakami M., and Ikeda K. (1993) A high frequency of apolipoprotein E4 isoprotein in Japanese patients with late-onset nonfamilial Alzheimer's disease. *Neurosci. Lett.* **163**, 166–168.

Uetsuki T., Takemoto K., Nishimura I., Okamoto M., Niinobe M., Momoi T., Miura M., and Yoshikawa K. (1999) Activation of neuronal caspase-3 by intracellular accumulation of wild-type Alzheimer amyloid precursor protein. *J. Neurosci.* **19**, 6955–6964.

Usami M., Yamao-Harigaya W., and Maruyama K. (1993) The triplet of lysine residues (Lys⁷²⁴-Lys⁷²⁵-Lys⁷²⁶) of Alzheimer's amyloid precursor protein plays an important role in membrane anchorage and processing. *J. Neurochem.* **61**, 239–246.

Van der Wal E. A., Gomez-Pinilla F., and Cotman C. W. (1993) Transforming growth factor- β 1 is in plaques in Alzheimer and Down pathologies. *Neuroreport* **4**, 69–72.

Van Duinen S. G., Maat-Schieman M. L. C., Bruijn J. A., Haan J., and Roos R. A. C. (1995) Cortical tissue of patients with hereditary cerebral hemorrhage with amyloidosis (Dutch) contains various extracellular matrix deposits. *Lab. Invest.* **73**, 183–189.

Vassar R., Bennett B. D., Babu-Khan S., Kahn S., Mendiaz E. A., Denis P., Teplow D. B., Ross S., Amarante P., Loeloff R., Luo Y., Fisher S., Fuller J., Edenson S., Lile J., Jarosinski M. A., Biere A. L., Curran E., Burgess T., Louis J.-C., Collins F., Treanor J., Rogers G., and Citron M. (1999) β -secretase cleavage of Alzheimer's amyloid precursor protein by the transmembrane aspartic protease BACE. *Science* **286**, 735–741.

Vassiliadis S., and Athanassakis I. (1996) Adsorptive or by pit formation endocytosis of immunoglobulins without loss of function as potential biotherapeutic application. *Cancer Biother. Radiopharm.* **11**, 259–266.

Verbeek M. M., Otte-Höller I., Van den Born J., Van den Heuvel L. P. W. J., David G., Wesseling P., and De Waal R. M. W. (1999) Agrin is a major heparan sulfate proteoglycan accumulating in Alzheimer's disease brain. *Am. J. Pathol.* **155**, 2115–2125.

Vigo-Pelfrey C., Lee D., Keim P., Lieberburg I., and Schenk D. B. (1993) Characterization of β -amyloid peptide from human cerebrospinal fluid. *J. Neurochem.* **61**, 1965–1968.

Vito P., Lacaná E., and D'Adamio L. (1996) Interfering with apoptosis: Ca^{2+} -binding protein *ALG-2* and Alzheimer's disease gene *ALG-3*. *Science* **271**, 521–525.

Wagner M. R., Keane D. M., Melchor J. P., Auspaker K. R., and Van Nostrand W. E. (2000) Fibrillar amyloid β -protein binds protease nexin-2/amyloid β -protein precursor: stimulation of its inhibition of coagulation factor XIa. *Biochemistry* **39**, 7420–7427.

Wagner S. L., Peskind E. R., Nochlin D., Provow S., Farrow J. S., Pandian M. R., Cleveland M., Ito R. K., and Farlow M. R. (1994) Decreased levels of soluble amyloid β -protein precursor are associated with Alzheimer's disease in concordant and discordant monozygous twin pairs. *Ann. Neurol.* **36**, 215–220.

Webster M-T., Groome N., Francis P. T., Pearce B. R., Sherriff F. E., Thinakaran G., Felsenstein K. M., Wasco W., Tanzi R. E., and Bowen D. M. (1995) A novel protein, amyloid precursor-like protein 2, is present in human brain, cerebrospinal fluid and conditioned media. *Biochem. J.* **310**, 95–99.

Weidemann A., König G., Bunke D., Fischer P., Salbaum J. M., Masters C. L., and Beyreuther K. (1989) Identification, biogenesis and localization of precursors of Alzheimer's disease A4 amyloid protein. *Cell* **57**, 115–126.

Wertkin A. M., Turner R. S., Pleasure S. J., Golde T. E., Younkin S. G., Trojanowski J. Q., and Lee V. M.-Y. (1993) Human neurons derived from a teratocarcinoma cell line express solely the 695-amino acid amyloid precursor protein and produce intracellular β -amyloid or A4 peptides. *Proc. Natl. Acad. Sci. U. S. A.* **90**, 9513–9517.

Wetzel D. M., Bohn M. C., Kazee A. M., and Hamill R. W. (1995) Glucocorticoid receptor messenger-RNA in Alzheimer's diseased hippocampus. *Brain Res.* **679**, 72–81.

Wighton-Benn W., Vardy E., Heath P. R., and Pearson R. C. A. (1995) Alterations in messenger RNA's encoding major isoforms of amyloid precursor protein in Alzheimer's disease neocortex. *Soc. Neurosci. Abstr.* **21**, 85.4.

Willoughby D. A., Johnson S. A., Pasinetti G. M., Tocco G., Najm I., Baudry M., and Finch C. E. (1992) Amyloid precursor protein mRNA encoding the Kunitz protease inhibitor domain is increased by kainic acid-induced seizures in rat hippocampus. *Exp. Neurol.* **118**, 332–339.

Wilson C. A., Doms R. W., and Lee V. M.-Y. (1999) Intracellular APP processing and A β production in Alzheimer disease. *J. Neuropathol. Exp. Neurol.* **58**, 787–794.

Wisniewski T., Castano E., Ghiso J., and Frangione B. (1993a) Cerebrospinal fluid inhibits Alzheimer β -amyloid fibril formation in vitro. *Ann. Neurol.* **34**, 631–633.

Wisniewski T., Golabek A., Matsubara E., Ghiso J., and Frangione B. (1993b) Apolipoprotein E: binding to soluble Alzheimer's β -amyloid. *Biochem. Biophys. Res. Commun.* **192**, 359–365.

Wolf B. A., Wertkin A. M., Jolly Y. C., Yasuda R. P., Wolfe B. B., Konrad R. J., Manning D., Ravi S., Williamson J. R., and Lee V. M.-Y. (1995) Muscarinic regulation of Alzheimer's disease amyloid precursor protein secretion and amyloid β -protein production in human neuronal NT2N cells. *J. Biol. Chem.* **270**, 4916–4922.

Wolfe M. S., Xia W., Ostaszewski B. L., Diehl T. S., Kimberley W. T., and Selkoe D. J. (1999) Two transmembrane aspartates in presenilin-1 required for presenilin endoproteolysis and γ -secretase activity. *Nature* **398**, 513–517.

Wolozin B., Hirashima N., Luo Y., Li Y. H., Alkon D. L., Etcheberrigaray R., and Sunderland T. (1995) Transforming growth factor β induces a β -responsive calcium fluxes in neurons. *Neuroreport* **6**, 1301–1305.

Wu Y., Gadina M., Tao-Cheng J.-H., and Youle R. J. (1994) Retinoic acid disrupts the Golgi apparatus and increases the cytosolic routing of specific protein toxins. *J. Cell Biol.* **125**, 743–753.

Wyss-Coray T., Feng L., Masliah E., Ruppe M. D., Lee H. S., Toggas S. M., Rockenstein E. M., and Mucke L. (1995) Increased central nervous system production of extracellular matrix components and development of hydrocephalus in transgenic mice overexpressing transforming growth factor- β 1. *Am. J. Pathol.* **147**, 53–67.

Wyss-Coray T., Lin C., Sanan D. A., Mucke L., and Masliah E. (2000) Chronic overproduction of transforming growth factor- β 1 by astrocytes promotes Alzheimer's disease-like microvascular degeneration in transgenic mice. *Am. J. Pathol.* **156**, 139–150.

Wyss-Coray T., Masliah E., Mallory M., McConlogue L., Johnson-Wood K., Lin C., and Mucke L. (1997) Amyloidogenic role of cytokine TGF- β 1 in transgenic mice and in Alzheimer's disease. *Nature* **389**, 603–606.

Yan R., Bienkowski M. J., Shuck M. E., Miao H., Tory M. C., Pauley A. M., Brashler J. R., Stratman N. C., Mathews W. R., Buhl A. E., Carter D. B., Tomasselli A. G., Parodi L. A., Henrikson R. L., and Gurney M. E. (1999) Membrane-anchored aspartyl protease with Alzheimer's disease β -secretase activity. *Nature* **402**, 533–537.

Yan S. D., Fu J., Soto C., Chen X., Zhu H., Al-Mohanna F., Collison K., Zhu A., Stern E., Saido T., Tohyama M., Ogawa S., Roher A., and Stern D. (1997) An intracellular protein that binds amyloid- β peptide and mediates neurotoxicity in Alzheimer's disease. *Nature* **389**, 689–695.

Ye Y., Lukinova N., and Fortini M. E. (1999) Neurogenic phenotypes and altered Notch processing in *Drosophila Presenilin* mutants. *Nature* **398**, 525–529.

Yoshikawa K., Aizawa T., and Hayashi Y. (1992) Degeneration *in vitro* of post-mitotic neurons overexpressing the Alzheimer amyloid protein precursor. *Nature* **359**, 64–67.

Young I. D., Willmer J. P., and Kisilevsky R. (1989) The ultrastructural localization of sulphated proteoglycans is identical in the amyloids of Alzheimer's disease and AA, AL, senile cardiac and medullary carcinoma-associated amyloidosis. *Acta Neuropathologica* **78**, 202–209.

Zambrano N., Buxbaum J. D., Minopoli G., Fiore F., De Candida P., De Renzis S., Faraonio R., Sabo S., Cheetham J., Sudol M., and Russo T. (1997) Interaction of the phosphotyrosine interaction/phosphotyrosine binding-related domains of Fe65 with wild-type and mutant Alzheimer's β -amyloid precursor proteins. *J. Biol. Chem.* **272**, 6399–6405.

Zhan S.-S., Sandbrink R., Beyreuther K., and Schmitt H. P. (1995) APP with Kunitz type protease inhibitor domain (KPI) correlates with neuritic plaque density but not with cortical synaptophysin immunoreactivity in Alzheimer's disease and non-demented aged subjects: a multifactorial analysis. *Clin. Neuropathol.* **14**, 142–149.

Zhao B., and Schwartz J. P. (1998) Involvement of cytokines in normal CNS development and neurological diseases: recent progress and perspectives. *J. Neurosci. Res.* **52**, 7–16.

Zlokovic B. V., Ghiso J., Mackic J. B., McComb J. G., Weiss M. H., and Frangione B. (1993) Blood-brain barrier transport of circulating Alzheimer's amyloid β . *Biochem. Biophys. Res. Commun.* **197**, 1034–1040.